NOTICE

The quality of this microform is heavily dependent upon the quality of the original thesis submitted for microfilming. Every effort has been made to ensure the highest quality of reproduction possible.

If pages are missing, contact the university which granted the degree.

Some pages may have indistinct print especially if the original pages were typed with a poor typewriter ribbon or if the university sent us an inferior photocopy.

Previously copyrighted materials (journal articles, published tests, etc.) are not filmed.

Reproduction in full or in part of this microform is governed by the Canadian Copyright Act, R.S.C. 1970, c. C-30.

AVIS

La qualité de cette microforme dépend grandement de la qualité de la thèse soumise au microfilmage. Nous avons tout fait pour assurer une qualité supérieure de reproduction.

S'il manque des pages, veuillez communiquer avec l'université qui a conféré le grade.

La qualité d'impression de certaines pages peut laisser à désirer, surtout si les pages originales ont été dactylographiées à l'aide d'un ruban usé ou si l'université nous a fait parvenir une photocopie de qualité inférieure.

Les documents qui font déjà l'objet d'un droit d'auteur (articles de revue, tests publiés, etc.) ne sont pas microfilmés.

La reproduction, même partielle, de cette microforme est soumise à la Loi canadienne sur le droit d'auteur, SRC 1970, c. C-30.

Canada

THE UNIVERSITY OF ALBERTA

THE DETERMINATION OF THIOLS AND METABOLIC DISULFIDES OF PENICILLAMINE AND OTHER BIOLOGICAL MERCAPTANS BY HPLC-ED

BY

GARRY TAKASHI YAMASHITA

A THESIS

SUBMITTED TO THE FACULTY OF GRADUATE STUDIES AND RESEARCH

IN PARTIAL FULFILLMENT OF THE REQUIREMENTS FOR THE DEGREE

OF DOCTOR OF PHILOSOPHY

DEPARTMENT OF CHEMISTRY

EDMONTON, ALBERTA

FALL 1988

ISBN 0-315-45718-X

UNIVERSITY OF ALBERTA

RELEASE FORM

NAME OF AUTHOR: GARRY TAKASHI YAMASHITA

TITLE OF THESIS: The Determination of Thiols and Metabolic Disulfides of Penicillamine and Other Biological Mercaptans by HPLC-ED

DEGREE: Ph.D.

YEAR THIS DEGREE GRANTED: 1988

Garry Yamashita

#2 - 380 Bermuda Drive N.W.
Calgary, Alberta
T3K 2B2

Date: October 7, 1988

THE UNIVERSITY OF ALBERTA

FACULTY OF GRADUATE STUDIES AND RESEARCH

The undersigned certify that they have read, and recommend to the Faculty of Graduate Studies and Research for acceptance, a thesis entitled

The Determination of Thiols and Metabolic Disulfides of Penicillamine and Other Biological Mercaptans by HPLC-ED

submitted by Garry Takashi Yamashita

in partial fulfillment of the requirements for the degree of Doctor of Philosophy.

B Krstulovic, for
D.L. Rabenstein
Supervisor

(External Examiner)

Date: October 7/1988

This thesis is dedicated to my parents,
who showed me how to Live;

to my brothers and sisters,
who showed me how to Learn;

to my daughters Erin, Jenna and Heather,
who showed me how to Love;

and especially to my wife, Donna,
who shared with me in all three.

ABSTRACT

A method has been developed for the determination of penicillamine, a therapeutic drug thiol, and other naturally-occurring thiols along with their symmetrical and mixed disulfides using high performance liquid chromatography with electrochemical detection (HPLC-ED). The biological thiols studied included the amino acid, cysteine, its homolog, homocysteine, and the tripeptide, glutathione.

Initial studies examined the electrochemical behaviour of these thiols and disulfides at the surface of the Hg/Au electrodes. From the electrochemical results, the conditions for optimum detection of the thiols and disulfides were determined. The dual electrode detector was operated in the series configuration with reduction of the disulfides at the upstream electrode and oxidation of the thiols at the downstream electrode. During subsequent chromatographic analyses the upstream electrode was held at -1.100 V vs. Ag/AgCl while the downstream electrode was maintained at +0.150 V vs. Ag/AgCl.

The effect of the mobile phase composition on the chromatographic behaviour of the thiols and disulfides was also studied. The three variables examined were the mobile phase pH, the concentration of ion-pairing reagent in the

mobile phase and the concentration of methanol in the mobile phase. Adjustment of the latter two parameters in a pH 3.0 phosphate buffer mobile phase provided the resolution for baseline separations of various thiol and disulfide mixtures.

Based on the electrochemical and chromatographic studies, the methodology for the determination of the thiols and disulfides of penicillamine/glutathione mixtures and for penicillamine/homocysteine mixtures was developed. Standards of the thiols and symmetrical and mixed disulfides were [redacted]ing a thiol/disulfide exchange reaction, and then were calibrated by proton NMR spectroscopy. Samples of human blood and urine were spiked with the standards and analysed for the thiols and disulfides.

ACKNOWLEDGEMENT

Research involves more than just hard work and perseverance. It is a focussed endeavour to increase one's foundation of knowledge guided by wisdom and years of experience. I would therefore like to express my appreciation to Dr. Dallas Rabenstein for his support and guidance throughout the course of my research.

As well, I am extremely grateful to all of my friends and colleagues, past and present, who have shared a fragment of their lives with me, laughing, learning and growing.

I would like to thank my wife, Donna, for enduring the years and being so patient while I was in the lab and in California.

Finally, I would also like to thank Dow Chemical for financial support towards the writing of this thesis.

TABLE OF CONTENTS

LIST OF TABLES

TABLE PAGE

LIST OF FIGURES

CHAPTER I

THE DETERMINATION OF PENICILLAMINE AND ITS METABOLITES

A. Introduction

In living systems, compounds containing thiol groups (RSH) can be oxidized to disulfides (RSSR). The majority of the thiol and disulfide groups that are found in peptides and proteins derive from the amino acid cysteine (I) and its oxidized form, cystine (II).

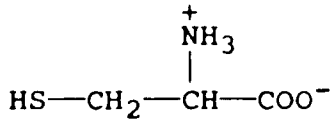

(I)

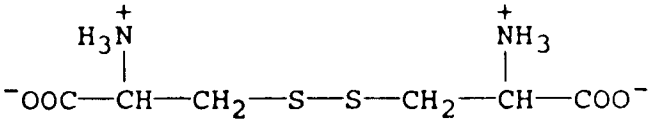

(II)

Historically, of the above sulfur-containing molecules, cystine was the first to be discovered. In 1810, Wollaston [1] isolated the compound from a urinary calculus, but it wasn't until 1902 that its structure was determined [2].

Cysteine was obtained in 1884 by the reduction of cystine [3] and soon afterwards other biological compounds which contain thiol and disulfide groups were discovered.

Both cysteine and cystine are found at measurable levels in the non-protein fraction of human plasma and urine, but generally their non-protein concentrations in mammalian tissues are small, only about 30 - 120 nanomoles/gram of fresh tissue [4]. In extracellular fluids, the concentration of cystine is normally higher than that of cysteine, but this is reversed within the cell where the cysteine is the predominant form [5]. This is thought to be due to reduction of any intracellular cystine by reduced glutathione within the cell.

In cells, the tripeptide, glutathione, GSH, (γ-L-glutamyl-L-cysteinyl-glycine, III) is the most abundant non-protein thiol [6].

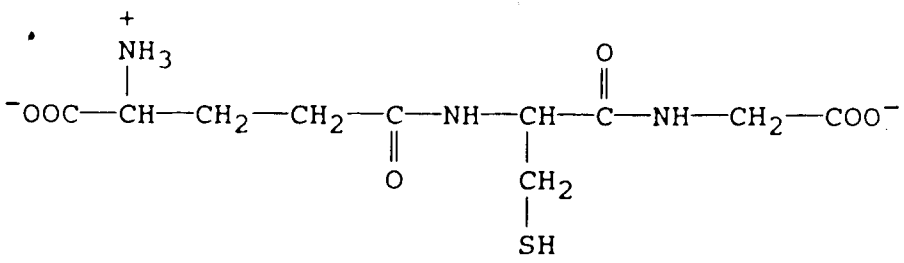

(III)

The bulk of this thiol is kept in the reduced form via the glutathione reductase-catalyzed reduction of oxidized

glutathione by $NADPH_2$ [7]. Reduced glutathione functions as a protective agent and it has been found to reduce several disulfides such as CSSC and HSSH [8,9] via thiol/disulfide exchange reactions, as well as hydrogen peroxide [10]. In the kidney and liver, glutathione participates in a number of enzyme-catalyzed conjugation reactions with a variety of toxins that result in their excretion as urinary mercapturates [11].

As well, a number of therapeutic drug thiols have been developed and are being used extensively for the treatment of a variety of diseases and disorders. These include drugs such as captopril (IV), British Anti-Lewisite or BAL (V), and D-penicillamine (VI).

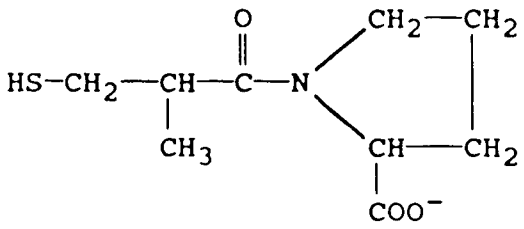

(IV)

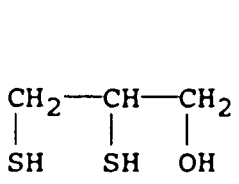

(V)

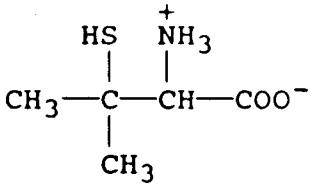

(VI)

Captopril is an orally active agent that inhibits angiotensin I-converting enzyme and is effective in the treatment of hypertension. It also has potential use for the treatment of congestive heart failure. BAL is known for its ability to bind with heavy metals and is used primarily for heavy metal detoxification. The reactivity and the role of these thiol-containing drug molecules, particularly penicillamine, has been the subject of many biochemical and physiological studies [12-28].

B. D-Penicillamine

Penicillamine (β,β-dimethylcysteine or 3-mercaptovaline) was first discovered in vivo by Walshe in the urine of a patient being treated with the antibiotic, penicillin [29]. The therapeutic use of penicillamine was then demonstrated with patients having Wilson's disease [30], a metabolic disorder causing the accumulation of copper ions in various tissues of the body. Based on the structural similarity, Walshe predicted that penicillamine should complex divalent metal ions much like cysteine, thus augmenting urinary metal ion excretions. Not only was this prediction correct, but also the ability of penicillamine to extract copper ions was found to be higher than that of cysteine. This has been explained by the fact that penicillamine does not undergo structural degradation in the

body, while cysteine is largely metabolized to sulphate [31]. Since the penicillamine remains intact, it can chelate more copper than an equivalent dose of cysteine.

Penicillamine has also been used for the removal of other heavy metal ions from the body [17]. Studies have shown that it can increase the urinary excretion of lead [32,33], zinc [17] and, to a limited extent, arsenic [34]. Its efficacy in complexing mercury, gold and cadmium, however, is poor [17].

D-Penicillamine is also used for the treatment of congenital cystinuria [35-37] and cystinosis [38]. In both disorders there is an elevated level of cystine in the body. In cystinuria, there is an increased level of cystine in the urine and precipitation of cystine may result in the formation of renal calculi or "stones" [35]. The solubility of cystine has been reported in the literature to be 7.8 x 10^{-4} moles/liter in pH 6.95 phosphate buffer [39]. Cystinuria is caused by a failure of the cells in the renal tubules and gut to reabsorb the cystine [5].

In cystinosis, the cellular concentration of cystine is raised. This is probably due to a defect in the mechanism within the cells used for the reduction of the disulfide to the thiol [40].

The theory behind D-penicillamine therapy for the

treatment of cystinuria and cystinosis is based on the two-step thiol/disulfide exchange reaction,

$$PSH + CSSC \rightleftharpoons PSSC + CSH \quad (1)$$

$$PSH + PSSC \rightleftharpoons PSSP + CSH \quad (2)$$

Penicillamine reacts with cystine, CSSC, to form a stable intermediate mixed disulfide, PSSC, and cysteine. The mixed disulfide can then react with another penicillamine molecule to form symmetrical penicillamine disulfide and another molecule of cysteine.

The penicillamine-cysteine mixed disulfide formed in the first step of the exchange reaction is more soluble than cystine and is found in both the urine and plasma of cystinuric patients undergoing penicillamine treatment. The higher solubility of the mixed disulfide results in a greater excretion of cystine by conversion to the mixed disulfide and cysteine and thus lowers cystine levels in the urine. Lowering the urinary cystine concentration reduces the chance of formation of kidney stones or calculi.

Similarly, high concentrations of homocystine (HSSH, VII) have been measured in the urine of patients having the disorder known as homocystinuria [41-43].

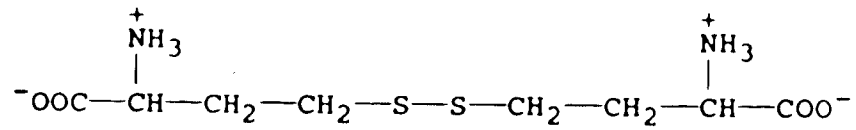

(VII)

In homocystinuria there is a defect in the metabolism of the amino acid homocysteine (HSH, VIII). This results in increased levels of HSH which oxidizes to form homocystine.

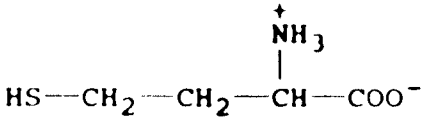

(VIII)

D-penicillamine can react with the homocystine to generate penicillamine-homocysteine mixed disulfide and the symmetrical penicillamine disulfide via the thiol/disulfide exchange reactions:

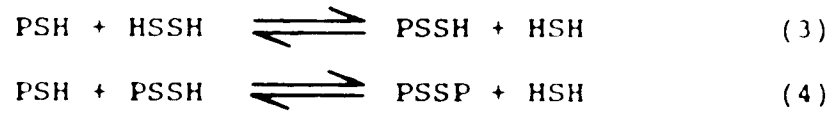

This results in excretion of the mixed disulfide and a lowering of the homocystine concentration in the urine.

In addition, penicillamine has been used extensively for the treatment of certain cases of rheumatoid arthritis that are not responsive to other conventional methods of treatment [22,26,28,44]. The exact mode of action of the drug in this disease has yet to be determined, but current theories suggest that penicillamine interacts with the disulfide bonds present in the rheumatoid factor, possibly by a thiol/disulfide exchange [36].

As well, several other conditions, scleroderma [21, 25,36], primary biliary cirrhosis [36], and certain disorders of the skin [36], have been treated with D-penicillamine. The mode of action in all three disorders appears to be related to the ability of D-penicillamine to affect collagen synthesis, although copper chelation is also an important function of penicillamine in biliary cirrhosis.

More recently, the observation that D-penicillamine selectively inhibits the replication of the AIDS-associated virus, HTLV-III/LAV, suggests that it may have another therapeutic application and this has heightened further the interest in this drug [45].

One major concern with all applications of drug therapy is the possibility of adverse effects, and penicillamine is not without its share of drawbacks. Long term studies have shown that patients undergoing penicillamine treatment for cystinuria or Wilson's disease have a lower incidence of adverse effects than those being treated for rheumatoid arthritis, but several common adverse reactions have been noted [18,36]. The common side effects reported by all groups of patients include gastrointestinal upset, skin rashes and renal complications. The pathways by which penicillamine induces adverse effects are still unknown, although an immune mechanism has been postulated for the renal and dermatological side effects.

Because of the widespread use of penicillamine in medicine and its adverse effects, it is essential that sensitive methods be developed for the determination of penicillamine and its metabolites. With such methods it should be possible not only to characterize more completely the metabolites of penicillamine, but also to monitor the levels of penicillamine and its metabolites in the fluids of patients being treated with the drug.

Penicillamine Analysis

Early methods of analysis for penicillamine were derived from techniques used to determine aminothiols, i.e. compounds having both an amino and a sulfhydryl group. The best methods involved a chromatographic separation with colorimetric detection of the eluting analytes. However, many of the original colorimetric methods lacked the sensitivity and specificity needed for the analysis of thiols at physiological concentrations [46].

One method for the determination of aminothiols is by an amino acid analyzer utilizing an ion-exchange column with ninhydrin (IX) detection [47].

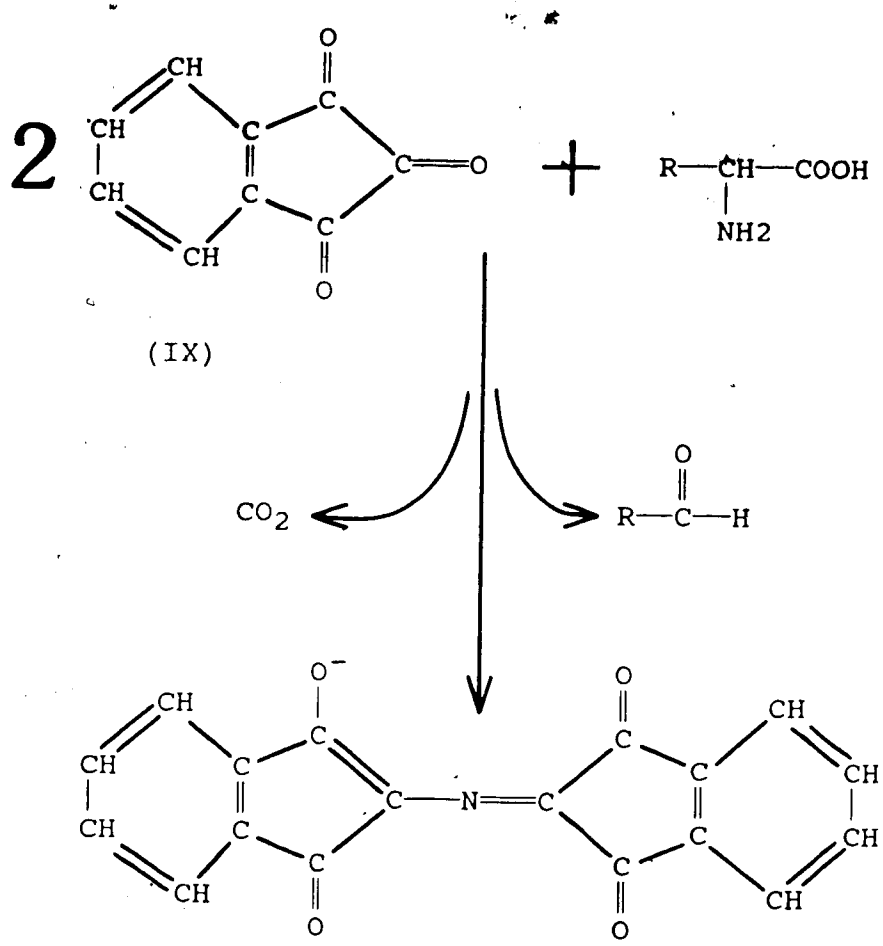

(IX)

(X)

Ninhydrin utilizes the amino functional group to form the coloured conjugated complex (X). Prior to the chromatographic analysis, aminothiols are reacted with iodoacetic acid to form the S-carboxymethyl derivative. This enhances the ninhydrin reactivity of the aminothiols, and as well, protects the thiol group from oxidation. Since ninhydrin reacts nonselectively with amino compounds, aminothiols must be separated from all other ninhydrin-

sensitive compounds by chromatography. This results in extremely long analysis times, often as long as several hours. Despite this disadvantage, the technique became popular because it provided simultaneous determination of a large number of thiols and disulfides [48-53].

More selective reactions have been developed with the sulfhydryl group being the target. Beutler et al [54] showed that the disulfide, 5,5'-dithio-bis(2-nitrobenzoic acid), or DTNB (XI), would react with thiols by a thiol/disulfide exchange reaction to form stable coloured compounds.

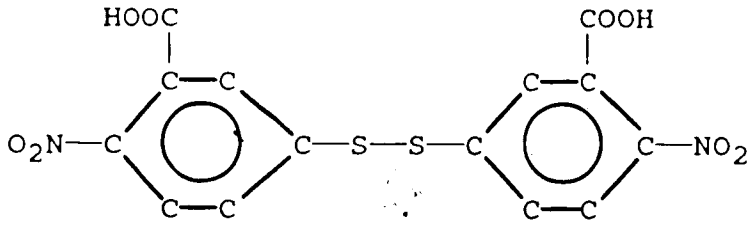

(XI)

These coloured compounds result from the cleavage of the disulfide bond in the DTNB to release the highly coloured thiol, 2-nitro-5-thiobenzoic acid. Absorbance of this compound is monitored at 412 nm since DTNB does not absorb at this wavelength. DTNB will react with any thiol, and thus the DTNB method gives total thiol content if more than one thiol is present. The method has become the most commonly used method for the determination of glutathione in biological assays [55-57]. The addition of DTNB as a post-

column reagent has been used for the analysis of penicillamine in human urine [58]. Although the conditions needed for the measurement of penicillamine disulfide were not completely developed, use of a second column inserted between the analytical column and the post-column reactor for the reduction of the disulfide, appeared to show promise.

The compound 6,6'-dithiodinicotinic acid is another spectrophotometric reagent developed for thiol detection following separation by high performance liquid chromatography [59]. Its main advantages over DTNB are that it can form a stable product at a lower pH and can be detected at a wavelength where the interferences from impurities are minimized.

Several chromatographic methods have been developed for the analysis of thiols using pre-column or post-column reactions to form derivatives which can be detected fluorometrically. Lankmayr et al [60] measured D-penicillamine in serum by reacting it with 5-dimethylaminonaphthaline-1-sulfonylaziridine prior to analysis. The derivatization reaction required 60 minutes and a temperature of 60°C. Similarly, the fluorogenic reagent ammonium 7-fluorobenzo-2-oxa-1,3-diazole-4-sulphonate (SBD-F) has also been used to react with thiols and also takes 60 minutes at 60°C to obtain complete

derivatization [61]. During this latter study total thiol (ie. thiol plus reduced disulfide) as well as the thiol alone were determined. The procedure for the determination of total thiol content involved addition of tributyl phosphine, a reagent known to reduce disulfides to thiols, to a second aliquot of the sample before derivatization with SBD-F.

The determination of thiols, disulfides and S-sulfonates in biological samples by pre- and post-column formation of o-phthalaldehyde derivatives with fluorescence detection has also been reported [62,63]. The reaction is rapid and no interfering reagent or reagent byproduct signals have been observed.

Organosulphur compounds have been separated by column chromatography and detected by a post-column ligand-exchange reaction with a palladium(II)-calcein complex [64]. Fluorescence of the calcein is quenched by complexation with palladium in the post-column reagent. As the sulphur-containing compounds elute, they react with the palladium to release the fluorescent calcein. The reactor for this system consisted of glass coils thermostatted in an oil bath and the reagent was added in air-segmented streams. Glutathione, cysteine, penicillamine, methionine, cystine and several thioureas were studied. The determination of

penicillamine which had been added to serum and urine was demonstrated using this method.

Penicillamine has also been detected by fluorescence using N-[p-(2-benzoxazolyl)-phenyl]maleimide derivatization [65]. This reagent is specific for the sulfhydryl group and the fluorescent derivative is stable for at least 24 hours.

Overall, the fluorescence methods display high sensitivity with detection limits for penicillamine and other biological thiols in the picomole range. Table 1.1 lists some of the reported detection limits for the above methods. The disadvantages of the fluorescence mode of detection include long reaction times for some of the derivatization steps, difficult reaction procedures, and the addition of complex post-column reactors.

The development and use of the mercury-based electrochemical detector was the catalyst for the determination of thiols by HPLC with electrochemical detection. Saetre and Rabenstein [66,67] designed a detector cell having a small mercury pool working electrode, a saturated calomel reference electrode, and a platinum wire counter electrode. The calomel reference electrode was positioned immediately downstream from the mercury pool, while the platinum wire was located in an overflow beaker at the outlet of the detector cell. Separation was achieved by

Table 1.1 Detection limits for the determination of biological thiols by reverse-phase HPLC with fluorescence detection.

Derivatization Reagent	Analytes	Detection Limit[1]	Reference
dimethylaminonaphthaline-1-sulfonylaziridine	penicillamine	85 pmol	60
N-[p-(2-benzoxazolyl)-phenyl]maleimide	penicillamine	12 pmol	65
pyrene maleimide	N-acetylcysteine	10 pmol	85
o-phthalaldehyde	glutathione	25 pmol	62
o-phthalaldehyde	glutathione	10 pmol	63
	oxidized glutathione	10 pmol	
	glutathione-S-sulfonate	50 pmol	
	cysteine-S-sulfonate	200 pmol	
Pd-calcein complex	penicillamine	300 pmol	64
	glutathione	16 pmol	
	cysteine	4 pmol	
	cystine	12 pmol	
ammonium 7-fluorobenzo-2-oxa-1,3-diazole-4-sulphonate	homocysteine	0.23 pmol	61
	glutathione	0.45 pmol	
	cysteine	0.6 pmol	
	N-acetylcysteine	1.1 pmol	

1Reported as the amount injected onto the column.

ion-exchange chromatography and was extremely rapid compared to analyses by ion-exchange with an amino acid analyzer. For thiol analysis, the technique did not require derivatization. However, determination of disulfides required analysis of the sample before and after an electrochemical reduction step [68,69].

Since that time, a number of electrode materials have been used for thiol determinations. Carbon paste electrodes have been used for electroactive substances such as catechols and hydroxyindoles, but they do not provide the sensitivity for the detection of thiols that are obtained with mercury-based electrodes [70]. The kinetics of the oxidation of thiols at carbon electrodes is usually slow compared to mercury-based ones.

Recently, a method by Imai and co-workers [71] derivatized thiols to catechol adducts prior to analysis by HPLC with electrochemical detection at a glassy carbon electrode. The procedure involved reaction of thiol with 3,5-di-tert-butyl-1,2-benzoquinone followed by three washings with hexane to extract any unreacted benzoquinone. Although tedious, the method has made carbon paste electrodes a feasible means of electrochemical detection for sulfhydryl compounds.

Halbert and Baldwin [72] have used a chemically modified carbon paste electrode to monitor glutathione and

cysteine directly. Cobalt phthalocyanine is mixed with graphite powder and Nujol to make the modified electrode. This electrode is reported to have the advantage of being able to produce optimum responses at a potential setting much lower than that required by conventional carbon paste electrodes.

The majority of thiol determinations by high performance liquid chromatography with electrochemical detection use the mercury-gold electrode. The extremely low electrode potential required for thiol detection on mercury-based electrodes provides a low background current and improves the detection limits compared to other electrode materials. Applications include whole blood [67,73-76,80], blood plasma [68,74-76,80], urine [68,69,76], bile [74], liver and kidney tissue samples [74,75,77-79,81], and fruits and plant tissue [73,75,83].

Early methods for the determination of both thiols and disulfides by HPLC required the measurement of thiols before and after reduction of the sample, where the difference in the amount of thiol measured was assumed to be due to the disulfides in solution. The reduction of the disulfides was performed by a chemical reaction of the sample with reducing agents like tributyl phosphine [84] or dithiothreitol [85], or by electrochemical reduction at a mercury electrode [68,69]. Since these methods require a second analysis of

the sample, the determination of thiols and disulfides becomes time-consuming.

Eggli and Asper [86] demonstrated that on-line electrolytic reduction of disulfides using a post-column reactor was a feasible method for the simultaneous determination of thiols and disulfides. A second column containing amalgamated silver particles was inserted between the analytical column and the detector and performed the reduction of the disulfides. The concept of on-line reduction was adapted by Allison and Shoup [73] who incorporated the post-column reactor into the detector cell. Two mercury-gold electrodes were placed in series within the detector cell to monitor thiols and disulfides. In this detection scheme, reduction of disulfides occurs at the upstream electrode while measurement of thiols, initially present in the sample or those generated at the upstream electrode, is performed at the downstream electrode. The dual electrode detector has been used for the analysis of thiols and their symmetrical disulfides, but only a few papers have examined its use for the determination of mixed disulfides.

HPLC methods for the determination of penicillamine with electrochemical detection have detection limits in the picomole range, similar to the fluorescence methods of detection. Unlike the fluorescence techniques, however,

dual mercury-gold electrodes with amperometric detection permit the simultaneous determination of both thiols and disulfides with minimal workup.

To date, very few methods have been developed for the determination of symmetrical and mixed disulfide metabolites of penicillamine. Both symmetrical and mixed disulfides of penicillamine can be detected by amino acid analyzer methods, however the long analysis times make it impractical for routine use or clinical research.

D. This thesis

The extensive use of penicillamine in medicine, along with the lack of knowledge about its function and metabolism in the body make it an important target compound to analyze. The therapeutic and adverse effects of penicillamine need to be thoroughly examined and characterized. The thiol/disulfide exchange reaction is one of the important metabolic pathways for the drug and results in the production of the symmetrical and mixed disulfides of penicillamine. Analytical methods are needed to monitor and measure these metabolites under physiological conditions.

In the research described in this thesis, the determination of penicillamine and several other thiols and their symmetrical and mixed disulfides with penicillamine by high performance liquid chromatography with electrochemical

detection has been investigated. First, the electrochemical behaviour of the thiols and disulfides at the mercury-gold electrode was characterized. Then the reverse phase ion-paired chromatography of the various thiols and disulfides was investigated.

The information obtained from these studies was used to determine the optimum chromatographic conditions for the analysis of biological fluids containing penicillamine, its major symmetrical and mixed disulfide metabolites and other biologically significant thiols and disulfides.

CHAPTER II

EXPERIMENTAL

A. Chemicals

Reduced and oxidized glutathione (GSH and GSSG, respectively), D-penicillamine and its oxidized form (PSH and PSSP, respectively), sodium octyl sulfate (SOS), and L-homocystine (HSSH) were used as received from Sigma Chemical Company. The oxidized glutathione was labelled as being acid-free and essentially ethanol-free. D,L-cysteine (CSH), D,L-cystine (CSSC), and D,L-homocystine (HSSH) were obtained from ICN Pharmaceuticals, Inc. As well, D,L-homocysteine (HSH) came from Nutritional Biochemicals Corporation. Tert-butyl alcohol (TBA) from BDH Chemicals was used as the chemical shift internal reference for the NMR analyses after about a 500-fold dilution with D_2O.

The water used in the chromatographic mobile phase was doubly distilled and then deionized with a mixed bed resin in a Barnstead water purification system. Reagent grade methanol was obtained from AnaChemia and was distilled in glass prior to use. All other chemicals were of reagent grade and were used as received. All samples and solutions including the mobile phases were filtered through 0.2 μm

Nylon 66 membrane filters obtained from Schleicher & Schuell.

B. Preparation of Solutions

Stock solutions of the individual thiols and disulfides were prepared by weighing out appropriate amounts of the solid chemicals into volumetric flasks and filling them with 0.1 M phosphate buffer fixed at pH 3.0 and containing 0.001 M Na_2H_2EDTA. The concentrations of the stock solutions were calculated on the basis of the measured weights and, generally, were in the 0.001 to 0.010 M range. All stock solutions were kept a maximum of two weeks. Care is needed during sample preparation since changes in the thiol and disulfide concentrations can occur by oxidation.

Thiols can be readily oxidized to disulfides by dissolved oxygen in solution [87]. This process is known as autoxidation and its rate is dependent on a number of conditions, some of these being pH, the presence of catalytic trace metals, and the presence of dissolved oxygen. To minimize autoxidation of the thiol samples, the solutions used to prepare all samples were buffered to pH 3.0 using disodium hydrogen phosphate and phosphoric acid. The rate of thiol oxidation increases with pH and the thiolate anion, RS^-, has been found to be the reactive species. The maximum rate of thiol oxidation appears to

occur at pH 7.5 and diminishes as the pH is lowered or raised above this value [88]. Use of a pH 3.0 phosphate buffer ensures that the sulfhydryl group is not deprotonated, thus reducing the chance of thiol oxidation. As well, it is fully compatible with the mobile phase used for the chromatography.

The oxidation of thiols to disulfides is catalyzed by trace metal impurities in solution [89]. Dissolving Na_2H_2EDTA into the buffer prior to the addition of the thiols effectively complexes any metal ions in solution and prevents variation in the thiol concentration by metal-catalyzed oxidation.

Also, to minimize air oxidation of the samples, the buffer was deoxygenated before use by bubbling nitrogen into the solution and by refluxing at 40-50°C for fifteen minutes, then reducing the temperature to about 30°C. The nitrogen used for deoxygenation was bubbled into an oxygen scrubber solution made of acidified ammonium meta-vanadate and then was passed through a water solution to prevent any contamination by the aerosol from the vanadium solution. Degassing with the nitrogen took place during the refluxing and while the buffer was cooling before being used.

Since mixed disulfides of penicillamine were not commercially available, a thiol/disulfide exchange reaction was used to prepare solutions having PSSR as one of its

reaction products, where the RS moiety is cysteine, glutathione, or homocysteine. The reaction steps for the exchange are

$$PS^- + RSSR \rightleftharpoons PSSR + RS^- \quad (5)$$

$$PS^- + PSSR \rightleftharpoons PSSP + RS^- \quad (6)$$

$$2\ PS^- + RSSR \rightleftharpoons PSSP + 2\ RS^- \quad (7)$$

where PS- is deprotonated penicillamine, RSSR is the symmetrical disulfide of cysteine, glutathione, or homocysteine, PSSR is the mixed disulfide and RS- is the deprotonated cysteine, glutathione, or homocysteine. As with autoxidation reactions, it is the thiolate anion that is the reactive species [90]. In the first step of the reaction, the penicillamine anion, PS^-, exchanges with one thiol moiety of the disulfide to generate the mixed disulfide. In the second step, a second PS^- anion reacts with the mixed disulfide and displaces a second thiol fragment of the original disulfide while forming the penicillamine symmetrical disulfide. Since the autoxidation of the penicillamine would be a competing reaction, the thiol/disulfide exchange was performed under nitrogen.

Individual reactant solutions of PSH and symmetrical disulfide, RSSR, were prepared in pH 3.0 phosphate/D_2O buffer containing 0.001 M Na_2H_2EDTA. Both reactant solutions were in the 0.050-0.100 M range. One milliliter of each solution was pipetted into a 5 or 10 mL volumetric

flask and the mixture was raised to pH 11 using sodium hydroxide. At pH 11, the penicillamine is in the reactive PS- form. During the reaction period, the reaction mixture was bubbled with nitrogen to prevent oxidation of the PSH. After a reaction time of 20 minutes the mixture was acidified with 50:50 H_3PO_4:D_2O to a pH value of 3.0 or less to protonate the penicillamine and prevent further generation of the PSSR mixed disulfide. The flask was then filled to volume with the pH 3.0 phosphate/D_2O buffer and a 0.5 mL aliquot was placed in an NMR tube for subsequent analysis by ^1H NMR. The remainder of the solution was diluted and used for calibration standards or sample spiking.

Studies on the air oxidation of penicillamine have shown that the initial rate of oxidation decreases as the pH is lowered below a value of 7 or raised above a value of 8 [88]. Often, due to the high reactant concentrations, short reaction time, and constant deoxygenation, no PSSP was observed in the NMR spectra of the above mixtures or in the chromatograms for the diluted reaction mixtures. In these instances PSSP from a stock solution was added during the dilution step before spiking the biological samples.

C. Preparation of Samples

Whole blood was drawn into vacutainers containing K_3HEDTA and the tubes were shaken to ensure complete mixing. The EDTA-containing tubes were chosen over vacutainers with heparin because of the added complexing ability of the EDTA towards trace metal ions that may be present in the sample and which could catalyze thiol oxidation. The blood was transferred to centrifuge tubes and centrifuged at 2500 rpm for 10 minutes. Two milliliters of the plasma were pipetted into a second centrifuge tube and diluted volumetrically with an equal amount of cold 5% (w/v) trichloroacetic acid (TCA) solution. The plasma and TCA were mixed well and left for about 5 minutes to allow complete precipitation of the plasma proteins. The sample was again centrifuged at 2500 rpm for 10 minutes. The supernatant was collected and filtered through a 0.2 [illegible] membrane filter before being spiked with the reaction mixture. It is essential that the proteins be removed prior to the addition of the spike to the plasma since the thiols in the standard mixture would bind to the proteins and consequently be lost during the precipitation step.

For the red blood cell study [91,92], whole blood was centrifuged and the plasma and white blood cells removed by aspiration. The cells were washed four times using a N-2-hydroxyethylpiperazine-N'-2-ethanesulphonic acid (HEPES,

Sigma Chemical Company) buffered saline solution containing 150 mM NaCl, 2% (w/v) glucose and 15 mM HEPES at pH 7.5. Washing was performed by adding saline solution to the cells, capping and shaking the tubes, centrifuging the solution and then aspirating off the supernatant. The cells were diluted about 20:80 (v/v) cells/saline solution and the % hematocrit was measured. Typically 0.3 mL of the cells/saline suspension was pipetted into a 1.5 mL microcentrifuge tube containing 0.3 mL of a stock PSH solution. A set of stock PSH solutions was prepared with the HEPES buffered saline solution which had a range of concentrations that would produce an extracellular PSH concentration in the 1.0-10.0 mM range for the incubated samples. The samples were kept on ice until incubated. Previous experiments by Ellory and Young have shown that no transport occurs at this temperature [91].

For incubation, the samples were mixed and mounted onto a thermostatted heater set at 37°C. When incubation was completed, the samples were returned to the ice to stop any further transport. The samples were centrifuged and the external PSH solution was removed by aspiration. The remaining cells were washed four times with a 106 mM $MgCl_2$ solution. Penicillamine transport has been found to be mediated by sodium ions in solution so this secondary saline wash solution was composed of $MgCl_2$ rather than NaCl to help

prevent further transport of PSH into or out of the cells. The lower concentration for the $MgCl_2$ solution is to compensate for the increased number of ions per salt molecule and thus maintains the same osmotic pressure on the cells. Each wash entailed using a volumetric dispenser to add 0.5 mL of saline to the cells, capping the tubes, vortexing them briefly, centrifuging at 15000 g for ten seconds and then aspirating off the supernatant. After the final aspiration, 0.5 mL of 0.5% (v/v) Triton X-100/water was added to each tube to lyse the cells. This was followed by 0.5 mL cold 5% (v/v) TCA solution which was used to precipitate the proteins in the sample. Each tube was centrifuged and the supernatant was filtered through a 0.2 μm membrane filter into clean vials which were promptly capped. All samples were volumetrically diluted prior to analysis.

For the urine samples, about 25 milliliters of urine was collected in a beaker containing 5 mL cold 10% (v/v) TCA solution. Upon arrival in the laboratory 2 mL of the specimen was pipetted into a 25 mL volumetric flask and diluted to the mark with cold 10% TCA solution. The sample was transferred to a centrifuge tube and the tube tightly capped. The tube was kept on ice for 5-10 minutes to allow complete deproteinization and then was centrifuged at 2500 rpm for 10 minutes. The supernatant was filtered with a

0.2 μm membrane filter and spiked with the reaction mixture just prior to analysis.

D. NMR Analysis

The concentrations of the various thiols and disulfides in the thiol/disulfide exchange reaction mixtures were determined by ^1H NMR analysis. NMR spectra for the reaction mixtures were obtained with a Bruker WH-400 spectrometer using the pulse/Fourier transform method. All measurements were made at ambient temperature and processing was performed using standard Bruker software on the Aspect 2000 system. All chemical shifts were measured with respect to the methyl resonance of the internal tert-butyl alcohol reference. This resonance was set to a chemical shift of 1.2397 ppm versus sodium 2,2-dimethyl-2-silapentane-5-sulfonate (DSS).

Figure 2.1 shows a typical ^1H NMR spectrum for a reaction mixture containing penicillamine, glutathione, oxidized penicillamine, oxidized glutathione and the penicillamine-glutathione mixed disulfide. The excessive overlap of the resonances between 2 and 4 ppm makes it difficult to get any quantitative measures of these peak areas. However, the methyl resonances for the PSH,PSSP and PSSG are well resolved from each other and therefore they

Figure 2.1. A 400 MHz ^1H NMR spectrum of a mixture

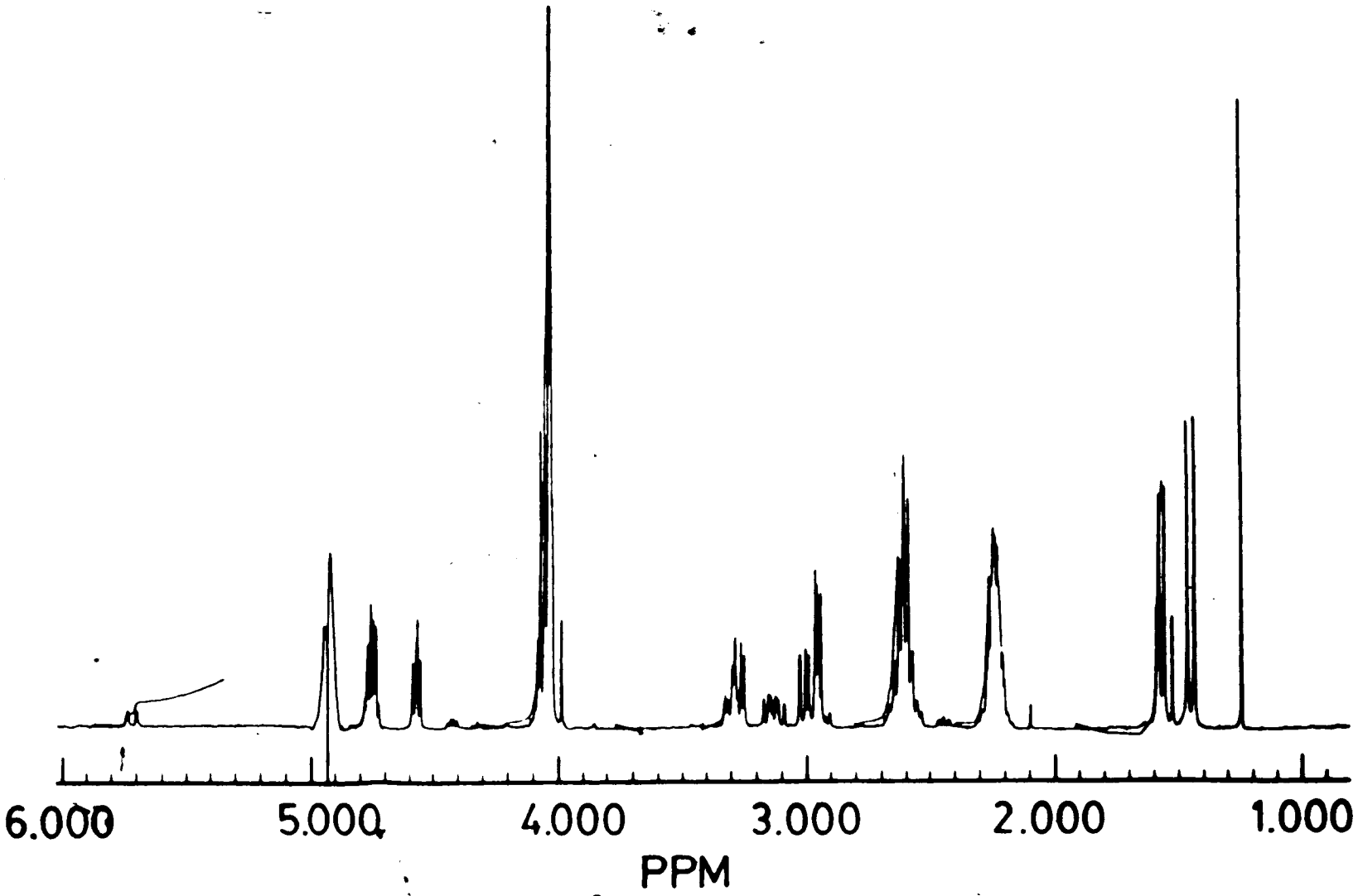

Figure 2.1. A 400 MHz ^1H NMR spectrum of a mixture containing GSH, PSH, GSSG, PSSG and PSSP in pH 3.0 phosphate:D_2O buffer.

were used to determine the composition of the reaction mixture. The two methyl groups in each of these molecules give separate ^1H resonances because of the asymmetric center at the α-carbon [93]. An expanded view of the methyl region is shown in Figure 2.2 together with the corresponding integral traces as determined by the spectrometer software. Peak assignments for each of the resonances have been previously determined [94] and are labelled on the spectrum.

The peak areas for the methyl resonances of the various penicillamine-containing compounds were measured by the vertical displacement of the integral traces. For each compound, the measured displacements for the two methyl resonances were added together to get a net area. The ratio of the net area over the sum of all the areas gives the fraction of the total penicillamine in each of the three forms within the mixture.

In the sample spectrum in Figure 2.2, the peaks X, Y, and Z represent the methyl resonances for the PSH, PSSR, and PSSP, respectively, where the PSSR is the mixed disulfide resulting from the thiol/disulfide exchange reaction, ie. PSSG in this case. The areas of the methyl resonances for the PSH, PSSR, and PSSP are labelled as I_X, I_Y, and I_Z, respectively, in equations 8 - 10. These three equations give the fraction of the total penicillamine in each of the penicillamine-containing compounds in solution.

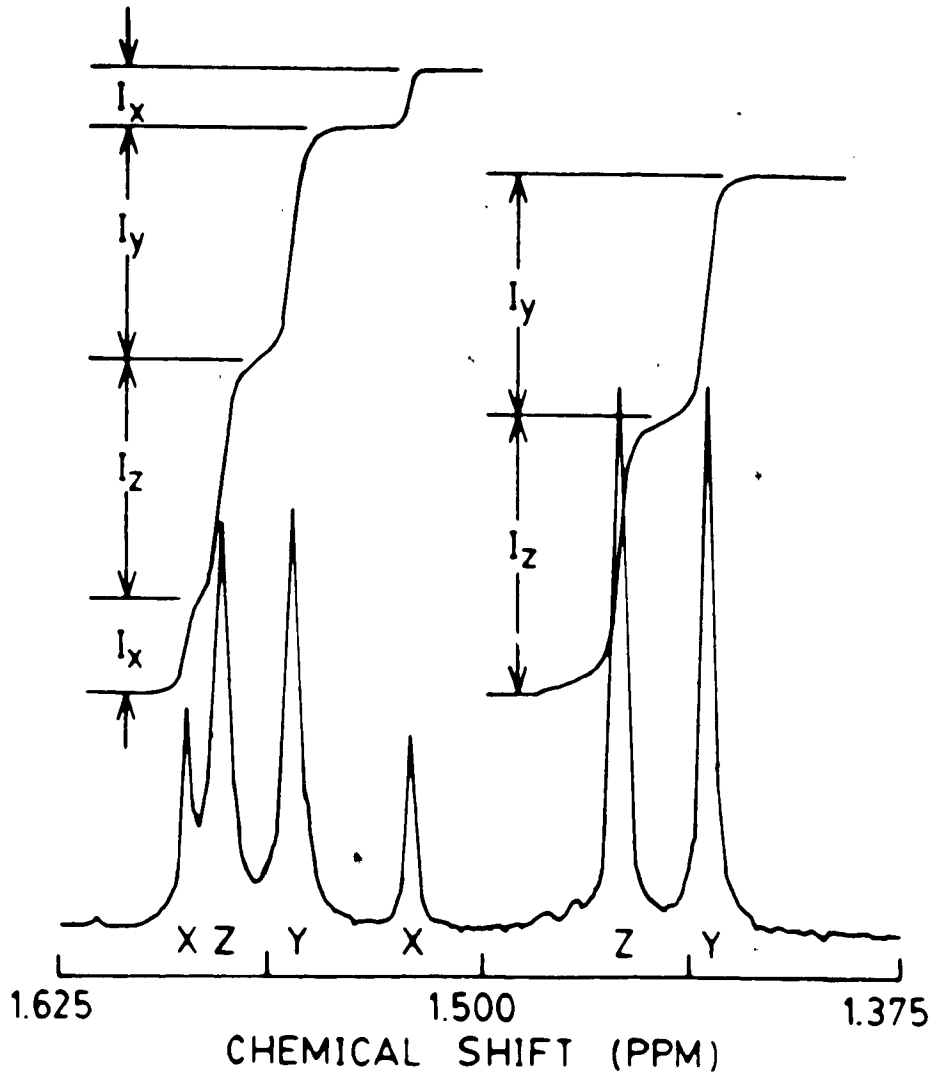

Figure 2.2. An expanded view of the methyl region of the ^1H NMR spectrum in Figure 2.1. The resonances X, Y and Z correspond to the methyl protons on the penicillamine of PSH, PSSG and PSSP, respectively. The integrated areas of these resonances are labelled as I_X, I_Y and I_Z.

$$f(PSH) = \frac{\Sigma I_x}{(\Sigma I_x + \Sigma I_y + \Sigma I_z)} \qquad (8)$$

$$f(PSSR) = \frac{\Sigma I_y}{(\Sigma I_x + \Sigma I_y + \Sigma I_z)} \qquad (9)$$

$$f(PSSP) = \frac{\Sigma I_z}{(\Sigma I_x + \Sigma I_y + \Sigma I_z)} \qquad (10)$$

Since all three compounds derive from the initial PSH, $[PSH]_0$, their concentrations are calculated using $[PSH]_0$ and equations 11, 12, and 13.

$$[PSH] = [PSH]_0 * f(PSH) \qquad (11)$$

$$[PSSR] = [PSH]_0 * f(PSSR) \qquad (12)$$

$$[PSSP] = [PSH]_0 * f(PSSP)/2 \qquad (13)$$

The denominator of 2 in equation 13 takes into account the fact that there are two penicillamine moieties per PSSP molecule. The concentrations of RSH and RSSR were then calculated from these concentrations and $[RSSR]_0$ and $[PSH]_0$ using equations 14 and 15.

$$[RSH] = [PSH]_0 - [PSH] \qquad (14)$$

$$[RSSR] = [RSSR]_0 - ([RSH]+[PSSR])/2 \qquad (15)$$

Frequently, the reactions were performed for such short durations that no PSSP was observed. The ^1H NMR spectrum and expanded methyl region of such a reaction mixture is

shown in Figure 2.3 for penicillamine reacted with oxidized homocysteine. The fractions of the PSH and PSSR in the mixture were calculated from the relative areas for the methyl resonances. Equations 16 and 17 illustrate this calculation; all the terms have the same definitions described previously.

$$f(PSH) = \frac{\Sigma I_x}{(\Sigma I_x + \Sigma I_y)} \qquad (16)$$

$$f(PSSR) = \frac{\Sigma I_y}{(\Sigma I_x + \Sigma I_y)} \qquad (17)$$

Equations 11 and 12 are still used to determine the concentrations of the PSH and PSSR, but the calculation of [RSH] is now simplified. Substituting equation 11 into equation 14 and factoring out the term $[PSH]_0$ gives,

$$[RSH] = [PSH]_0 * (1 - f(PSH)) \qquad (18)$$

From equations 16 and 17,

$$f(PSSR) = 1 - f(PSH) \qquad (19)$$

therefore,

$$[RSH] = [PSH]_0 * f(PSSR) = [PSSR] \qquad (20)$$

This also simplifies the calculation for the concentration of RSSR to,

$$[RSSR] = [RSSR]_0 - [PSSR] \qquad (21)$$

After determining the concentrations of all the components in the stock reaction mixture, the appropriate

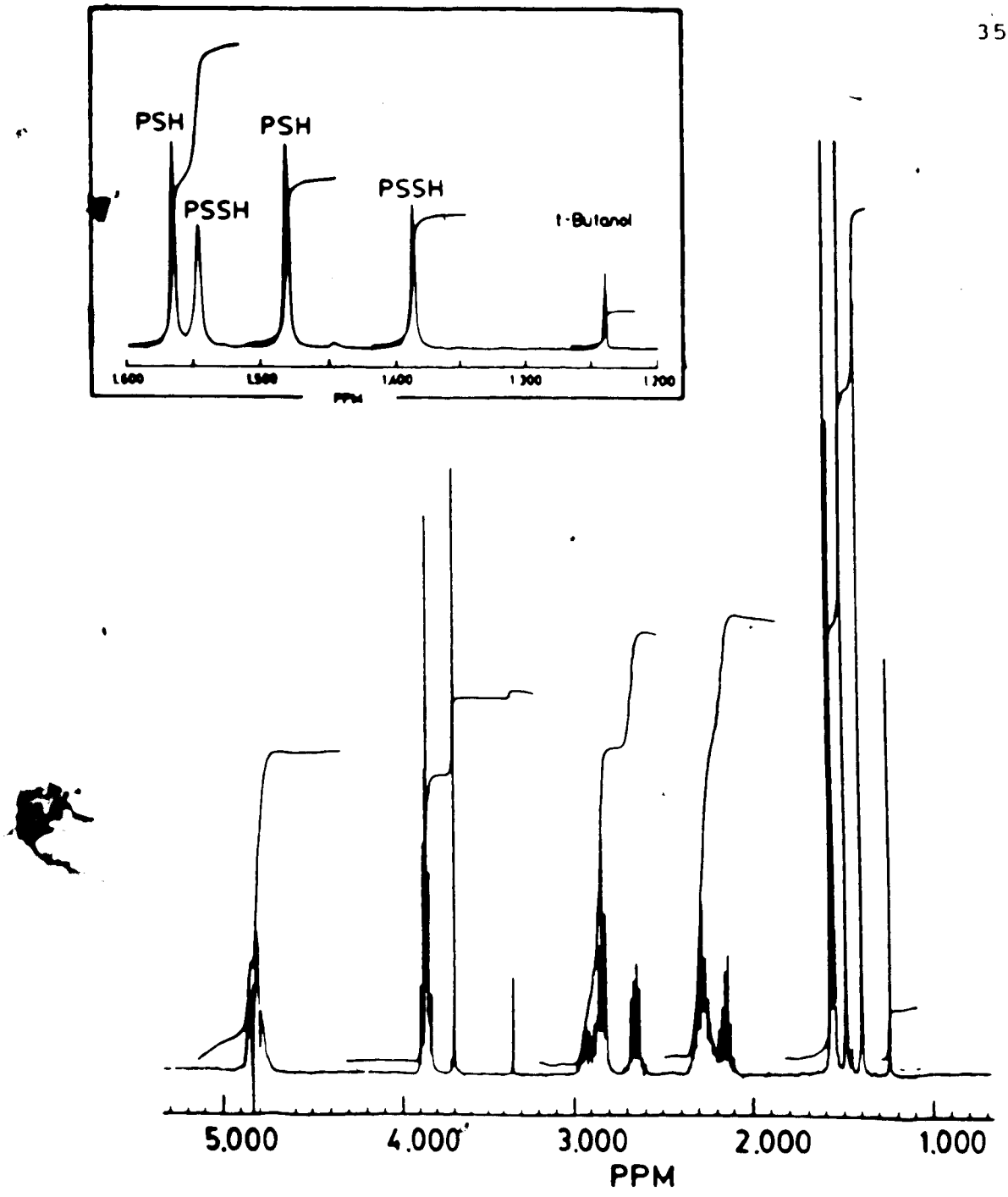

Figure 2.3 A 400 MHZ ^{1}H NMR spectrum for a mixture containing HSH, PSH, HSSH and PSSH. The inset is an expanded view of the methyl region. The resonances seen in the inset correspond to the methyl protons on the penicillamine and on the penicillamine moiety of the penicillamine-homocysteine mixed disulfide.

dilution factors were then used to calculate the concentrations of all the compounds in the standards used for the HPLC calibrations.

E. Chromatography

The separation and measurement of the thiols and disulfides was performed using a Bioanalytical System LC 154 chromatograph with dual mercury-gold electrodes in the series configuration. To prepare the gold electrodes for amalgamation, a three step polishing process was followed. The first step gave a coarse polish and often left deep scratches on the soft gold surface and on the plexiglas. Therefore it was used only when the electrode surface was severely pitted or discoloured and could not be cleaned by the milder polishing steps. The coarse polish was performed with a 600 grit silicon carbide polishing pad attached to a glass plate having water as the lubricant. The electrode block was placed face down on the wetted carbide pad and manually moved in a circular motion with gentle pressure. The gold electrodes should have a matte finish and be thoroughly rinsed with water before proceeding to the second stage.

The second or medium polishing step was done on a Texmet (Buehler Ltd) pad with 6 μm diamond polishing compound. A small amount of this polishing compound was

added to the pad with an equal amount of water and again the electrodes were rubbed over the pad with light pressure. This process can often be used directly without the coarse polishing step if the electrodes are not badly worn. It is important at this stage that the electrodes be carefully cleaned of any particles and residual diamond polishing compound. The final surface finish can be marred by the abrasive particles from this step. An ultra-sonic bath filled with distilled and deionized water was used to remove the old particles before going to the third and final polishing step.

Fine polishing was accomplished using a Microcloth (Buehler Ltd) pad and several drops of a slurry made from water and 0.05 μm gamma alumina polishing compound (Buehler Ltd). After several minutes of circular polishing and rinsing with water, the gold electrodes have a high lustre. The electrodes were carefully cleaned with a soft tissue to prevent scratches from occurring.

The electrode block was placed in a petri dish during the application of the mercury to contain any accidental spillage. Triple distilled mercury was deposited onto the electrodes and left for 3 - 4 minutes. After that time, the excess mercury was knocked directly into a waste jar with the edge of an index card using a slicing motion. The stock mercury container and the waste jar were kept tightly sealed

when not being used. When no more mercury could be removed, the electrodes were gently smoothed with a soft tissue to get a shiny finish. This slowly turns to a dull sheen. The electrodes were left overnight to allow the amalgam to equilibrate.

The analytical columns used in this research included a Bioanalytical Systems Biophase 5μm octadecyl silane (ODS) 4.6 X 250 mm column and Whatman Partisil 5μm ODS-3 columns of the same dimensions. The Partisil ODS-3 packing has 9% carbon load by weight and is 95% endcapped, ie 95% of the free silanols are bound. A 4.0 cm guard column packed with 10 μm Partisil ODS-3 was attached to the system between the injector and the analytical column to trap any strongly adsorbing substances from the biological samples so as to prolong the life of the analytical column.

A mobile phase consisting of phosphate buffer was used in all the studies. Generally the total phosphate concentration was 0.1 M. The buffer was prepared by weighing out appropriate amounts of solid $NaH_2PO_4 \cdot H_2O$, adding it to doubly distilled and deionized water, adjusting to pH 3.0 with H_3PO_4 and diluting to volume. If sodium octyl sulfate was required, it was added to the buffer prior to the pH adjustment. Any addition of methanol was made after the buffer was prepared and all mobile phases

containing methanol are reported as volume/volume ratios of methanol to buffer.

The mobile phase was refluxed under nitrogen at an elevated temperature of about 30°C with a water-filled bubbler attached to the top of the condenser to prevent oxygen from entering the mobile phase. A flow rate of 1.0 mL/min. was used and all injections were made with a 20 μL sample loop. The column was usually left at ambient temperature except when the room temperature rose above 25°C. When that occurred, the column was thermostatically set to 25°C and the column holder was wrapped with tygon tubing that had cold water running through it. This coil of tubing acted as a cooling jacket.

To find the optimum separation conditions, the effect of several mobile phase parameters on retention times were studied, these being the mobile phase pH, ion-pairing reagent concentration, and organic modifier content. To identify the best mobile phase pH, each analyte was chromatographed using 0.1 M phosphate buffers at various pH values over the range of 2.5 to 5.5. To minimize variations in the composition of the mobile phases, a large 16-liter beaker was used to make the buffer solution. Sodium dihydrogen phosphate was weighed and mixed with about 11 liters of doubly distilled and deionized water. Phosphoric acid was added to reach a pH of 2.5 and the volume was made

to 12 liters. Two liters were removed and stored in an opaque glass bottle. The buffer in the beaker was adjusted to the next pH value with sodium hydroxide pellets and another two liters were removed and stored. This was repeated until all the required mobile phase buffers were made. All buffers were tightly capped and stored at 5°C until used. This procedure maintains a fairly constant phosphate concentration since the sodium hydroxide pellets add only a negligible amount to the buffer volume.

The second parameter that was examined was the concentration of the ion-pairing reagent in the buffer. Each compound was chromatographed with mobile phases containing pH 3.0 phosphate buffer (0.1 M) and sodium octyl sulfate at concentrations covering the range of 0.00 - 1.10 mM. Finally the effect of an organic modifier in the mobile phase on the capacity factor of each analyte was investigated. Methanol was selected as the modifier and was added to the phosphate buffer. The methanol content covered the 0-10% (v/v) range.

F. Hydrodynamic Voltammograms and Polarograms

Polarographic experiments were performed using a Princeton Applied Research (PAR) SMDE model 303 polarograph with a PAR model 174A polarographic analyzer. Thiol solutions were prepared in pH 3.0 phosphate buffer and were bubbled with nitrogen for 10 minutes before each analysis.

The polarographic cell was kept under nitrogen throughout the polarographic experiments. All scans were done at a scan rate of 5 mV/sec. with a filter of 0.3 second and a drop time of 1 second.

The electrochemical behaviour of all the analytes was also studied at the mercury-gold electrodes of the detector to determine the optimum detector settings. Hydrodynamic voltammograms were measured by making replicate injections of each individual compound at stepped potential settings. All potentials were measured with respect to a Ag/AgCl reference electrode. For the thiols, the downstream electrode potential was varied while the upstream electrode potential was held constant. For the disulfides, the potential at the upstream electrode was varied while the downstream electrode potential was fixed. Peak currents were calculated from the measured peak heights. The hydrodynamic voltammogram of the mobile phase was made by measuring the background current at stepped potentials of the downstream electrode without any offset current being applied.

CHAPTER III

ELECTROCHEMICAL DETECTION

A. HPLC with Electrochemical Detection

The demands of trace determinations in biological samples require that the analytical method provide high sensitivity, a high degree of selectivity, and low detection limits. For pharmaceutical assays of sulfhydryl-containing drugs, where there are few interfering compounds and the thiol concentrations are higher, non-chromatographic methods are adequate [95,96]. However, for thiol and disulfide analyses in biological samples, non-chromatographic methods suffer from low sensitivity and often cannot selectively distinguish between drug thiols and endogenous thiols. Although chromatographic techniques have provided the desired selectivity by separating the analytes prior to analysis, sensitive and specific detection schemes have yet to be fully developed. Detection of thiols and disulfides by methods such as reaction with ninhydrin followed by UV absorption measurements or fluorometric derivatization usually are tedious and time-consuming, are nonspecific for both thiols and disulfides, or lack the sensitivity required for physiological applications. The use of electrochemical detection for liquid chromatography is not new [97,98], but its more recent success in biochemical applications [99,100]

has stimulated research in this area, especially for thiol and disulfide analysis [66,68,69,73,99].

A wide variety of electrode materials have been used for electrochemical detectors, but the advantages of mercury are that it has a wide working potential range, it can be operated at a lower potential for thiol oxidation and it responds more rapidly to thiol redox reactions than other materials [99,100,101]. The mercury pool electrode developed by Saetre and Rabenstein [66] displayed high sensitivity with low detection limits and had a wide dynamic range for the analysis of thiols. MacCrehan and coworkers [102] and Kissinger [99] have designed thin-layer gold disk electrodes with mercury amalgamation and these have been applied to thiol analyses by Allison and Shoup [73].

These thin-layer electrodes offer small detector volumes and are therefore suitable for modern liquid chromatographic separations. As well, for the amalgamated electrodes, the gold surface adds mechanical stability. All of these electrodes, the mercury pool and the two thin-layer models, were operated as amperometric detectors. That is, the current across the working electrode and the auxiliary electrode is measured while a fixed potential difference is applied between the working and reference electrodes. In general, less than ten percent of the analyte passing through an amperometric detector undergoes oxidation (or

reduction, as the case may be), and thus the current flow through the detector is kept small. This results in little change to the electrode potential (IR drop) due to the measurement process.

In coulometric detection complete electrochemical conversion of the analyte is required. This is achieved by using slow flow rates and electrodes with surface areas that are large. Not only are coulometric processes more destructive, but also they are acutely affected by the cell resistance and tend to have lower sensitivity [99] compared to amperometric methods. This last point is due to increased noise and residual background current resulting from the large electrode surface area needed to get complete electrolysis.

B. Electrochemistry

The principles of amperometric detection can be derived from Faraday's Law which states:

$$Q = nFN \qquad (22)$$

where Q is the charge generated in coulombs, n is the number of moles of electrons transferred in the electrochemical process per mole of reactant, F is the Faraday constant, ie. 96,487 coulombs/mole of electrons, and N is the number of moles of reactant undergoing the electrochemical change. The derivative of this equation with respect to time, given

by Equation 23, shows that the current, i, from the electrochemical reaction at the electrode surface is proportional to the rate of the electrochemical process occurring.

$$i = \frac{\delta Q}{\delta t} = nF \frac{\delta N}{\delta t} \qquad (23)$$

Initially, as the potential is set across the reference and working electrodes, there is a non-Faradaic charging current observed. Once this non-Faradaic charging current has diminished to a negligible level, the main contributing factor to the remaining background current will be due to the Faradaic response of the detector to electroactive species in the mobile phase. Since only electroactive species are detected, the background current can be kept low by careful selection of the mobile phase components. If the electrode reaction is limited only by the mass transport of electroactive species to the electrode surface, then the current will be proportional to the electrode surface area and the flux, as described by Equation (24).

$$i_{lim} = nFAJ \qquad (24)$$

where i_{lim} is the diffusion-limited current, n and F are the same as defined for Faraday's Law, A is the electrode surface area, and J is the flux.

For hydrodynamic systems, the flux can be defined in terms of various detector and analyte parameters and the

expression for current for the thin-layer detector used in this research expands to the following: [103]

$$i_{lim} = 1.467\ nFAC_0\ (D/h)^{2/3}\ (U/d)^{1/3} \qquad (25)$$

The term C_0 is the bulk analyte concentration in the eluent, D is the diffusion coefficient for the analyte, h is the detector channel thickness, U is the volume flow rate and d is the detector channel width. From this equation it is evident that the cell geometry plays an important part in the detector response.

The electrochemical detector used in this work is illustrated in Figure 3.1. It consists of a lower Kel-F block having two pressure-fitted cylindrical gold electrodes, two thin teflon gaskets, and an upper stainless steel block with machined holes for the cell inlet and outlet. The upper block is made from 316 type stainless steel and acts as the auxiliary electrode with connection via the pin located on the top. This planar auxiliary electrode is separated from the working electrodes by two teflon gaskets, each having a thickness of 127 μm. The detector channel is determined by the oval cut out of the center of the gaskets. The dimensions of the oval define the cell volume, but the detection volume is calculated by the volume of the cell that is directly over each electrode, which has been determined to be less than 2 μL. The Ag/AgCl

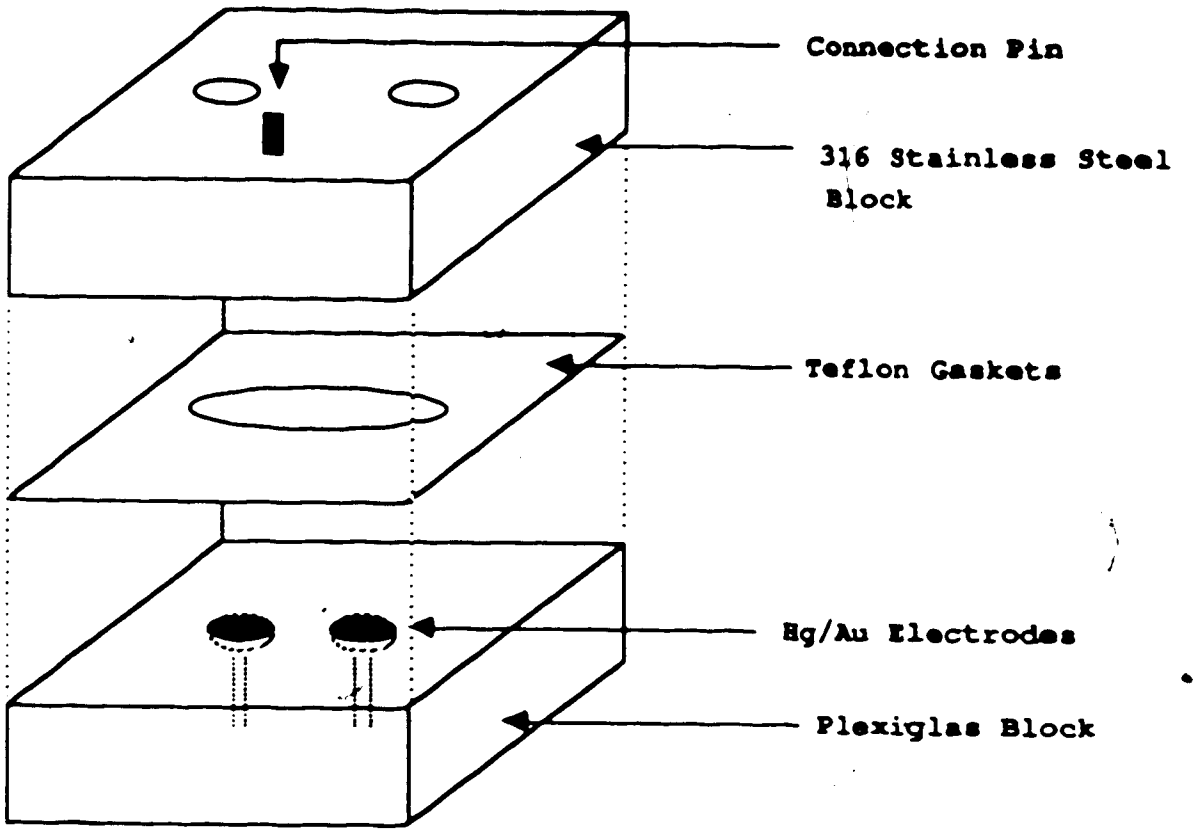

Figure 3.1 Schematic diagram of the dual Hg/Au electrochemical detector cell. The reference electode is located downstream from the cell and is not shown.

reference electrode was located downstream from the detector cell in a reference chamber.

Since the small dimensions of the detector cell places the working electrode very close to the auxiliary electrode, and because of the low impedance produced by the mobile phase, there is a negligible potential drop (IR drop) between the working electrode and the reference electrode during the measurement of the current. As well, the current is measured across the cell width rather than along the cell length towards the reference electrode so the effect of IR drop is further minimized. This stable potential control provides increased precision in measurements made with electrochemical detection.

For the analysis of thiols and disulfides, the dual electrode detector was used in the series configuration illustrated in Figure 3.2. The effluent from the column flows sequentially over the two electrodes, each being poised at different potentials. The upstream electrode, located nearest the detector inlet, was operated in the reductive mode while the downstream electrode was used for oxidation. As disulfides eluting from the column enter the detector, they will be reduced to the corresponding thiol moieties. This proceeds according to a simple reduction reaction.

$$RSSR + 2H^+ + 2e^- \longrightarrow 2RSH \qquad (26)$$

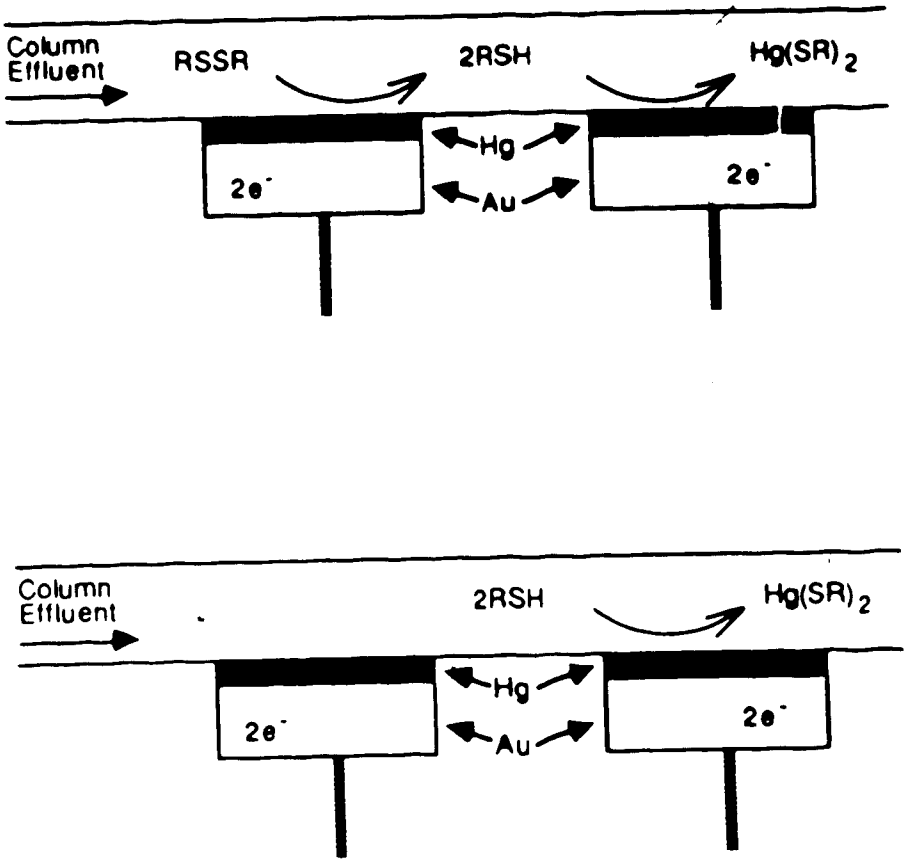

Figure 3.2 Illustration of series mode detection of (a) disulfides and (b) thiols with the dual Hg/Au electrodes.

As this chromatographic zone reaches the second electrode, the freshly generated thiols will participate in the oxidation at the mercury surface if a suitable electrode potential is applied. The reaction for this oxidation is

$$2\ RSH + Hg \longrightarrow Hg(SR)_2 + 2H^+ + 2e^- \qquad (27)$$

and the liberated electrons give rise to the measured current.

When thiols elute from the column there will be no reduction occurring at the upstream electrode since they are already in the reduced form. As the thiols flow over the second electrode they will be detected by the same mercury oxidation reaction described above. The upstream electrode acts only as a post-column reactor while the downstream electrode performs the measurement step. Thus, both thiols and disulfides can be monitored from a single injection, provided they are chromatographically resolved from each other and provided that the electrode potentials are appropriate for the disulfide reduction and the mercury oxidation reactions.

C. Polarography

In order to achieve the optimum operating conditions for any given analysis by HPLC-ED, the electrode potentials must be selected so as to provide adequate and reproducible oxidation or reduction of the analytes without excessive

background noise, high background currents, or rapid electrode degradation. Information on the electrochemical behaviour of each analyte is needed to make optimum choices of electrode potentials. Kissinger [99] notes that the potential needed for amperometry is often greater than that expected from theory and that electrode material, choice of electrolyte and the electrode kinetics of the analyte play major roles in the selection of practical operating potentials.

To determine the oxidation potentials for the various thiols under investigation, sampled DC polarography was initially used. Figures 3.3 - 3.6 display the polarograms for all of the thiols. The polarogram for 60 μM HSH, Figure 3.3, will be used to illustrate the general features that are significant to the discussions in this chapter. The potential was scanned from +0.200 V to -0.600 V versus a Ag/AgCl reference electrode at a rate of 5 mV/sec. and the current range was set to 0.5 μA full scale. In the figure, there are four regions, labelled I - IV, which define the overall polarogram. Region I is the breakdown zone where the mercury electrode undergoes direct oxidation and it is characterized by excessively high currents at the more positive potentials. Potentials in this region are unsuitable since the mercury would be quickly depleted and variations in the measured currents would arise. As well,

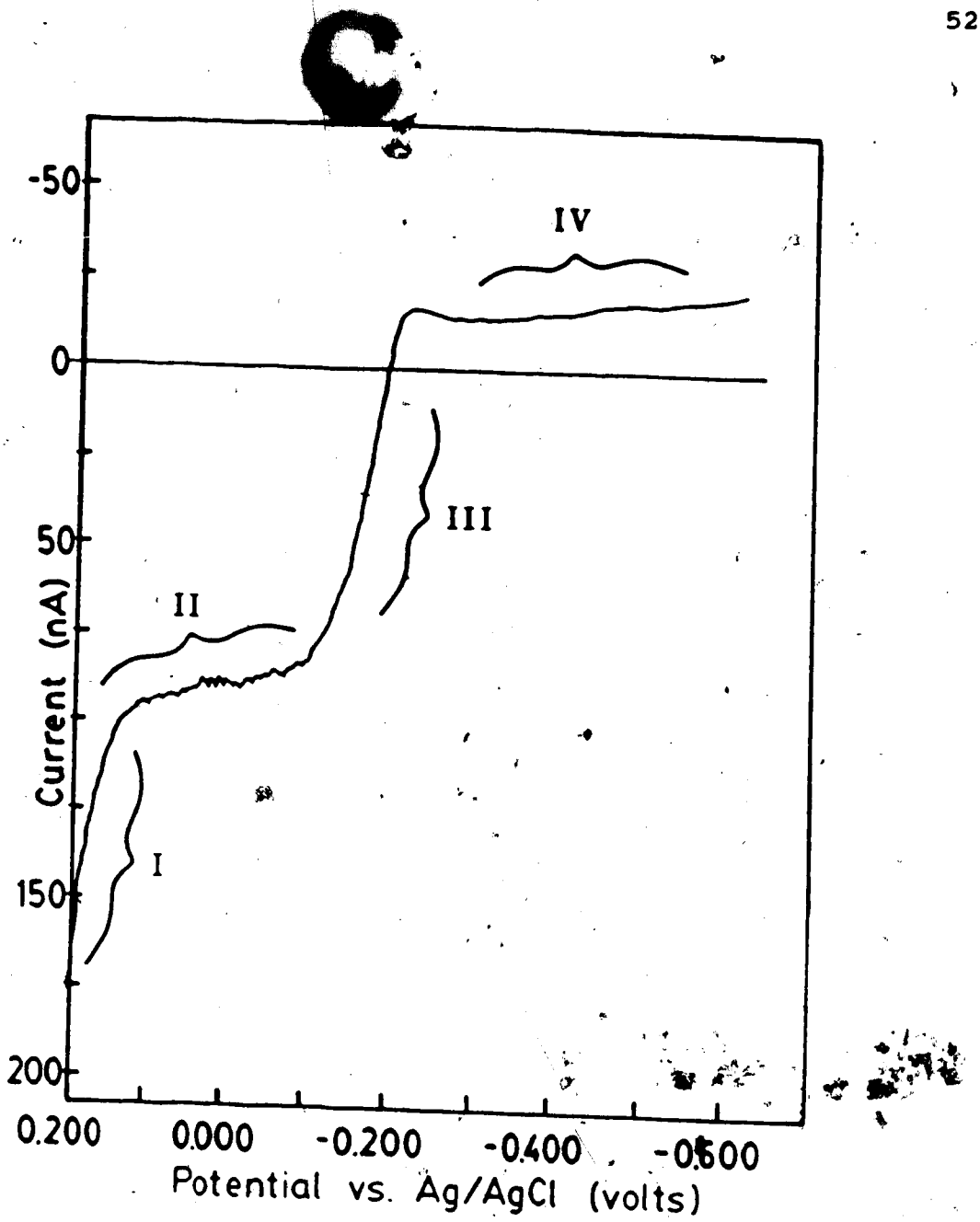

Figure 3.3 DC-sampled polarogram of 60 μM HSH in pH 3.0 phosphate buffer. The scan rate was 5 mV/sec. and the drop time was 1 sec. A filtering time constant of 0.3 seconds was used.

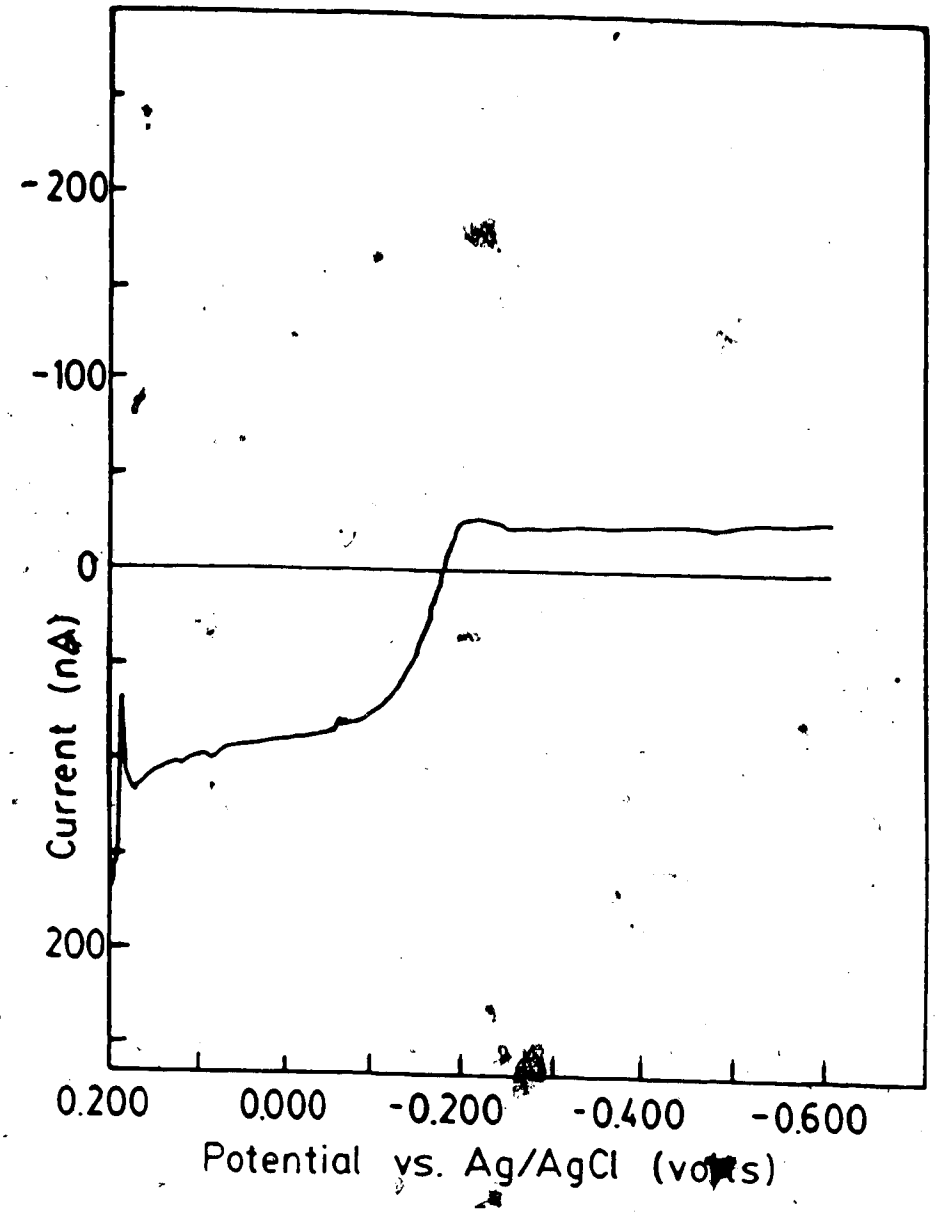

Figure 3.4. DC-sampled polarogram for 60 μM CSH in pH 3.0 phosphate buffer. The drop time was 1 second and the scan rate was 5 mV/sec. A 0.3 second filtering time constant was used.

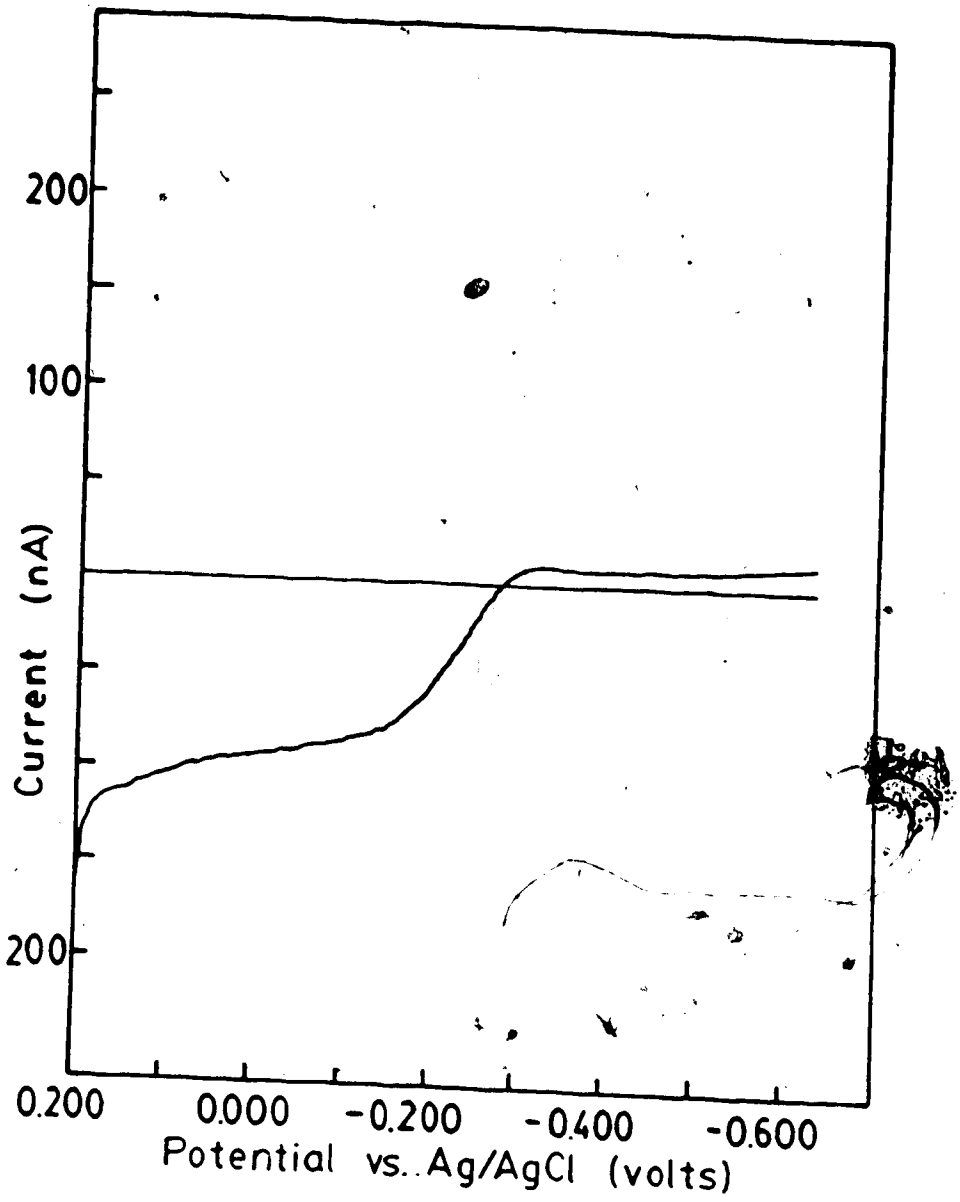

Figure 3.5 DC-sampled polarogram for 68 μM GSH in pH 3.0 phosphate buffer. The drop time was 1 second and the scan rate was 5 mV/sec. A filtering time of 0.3 second constant was used.

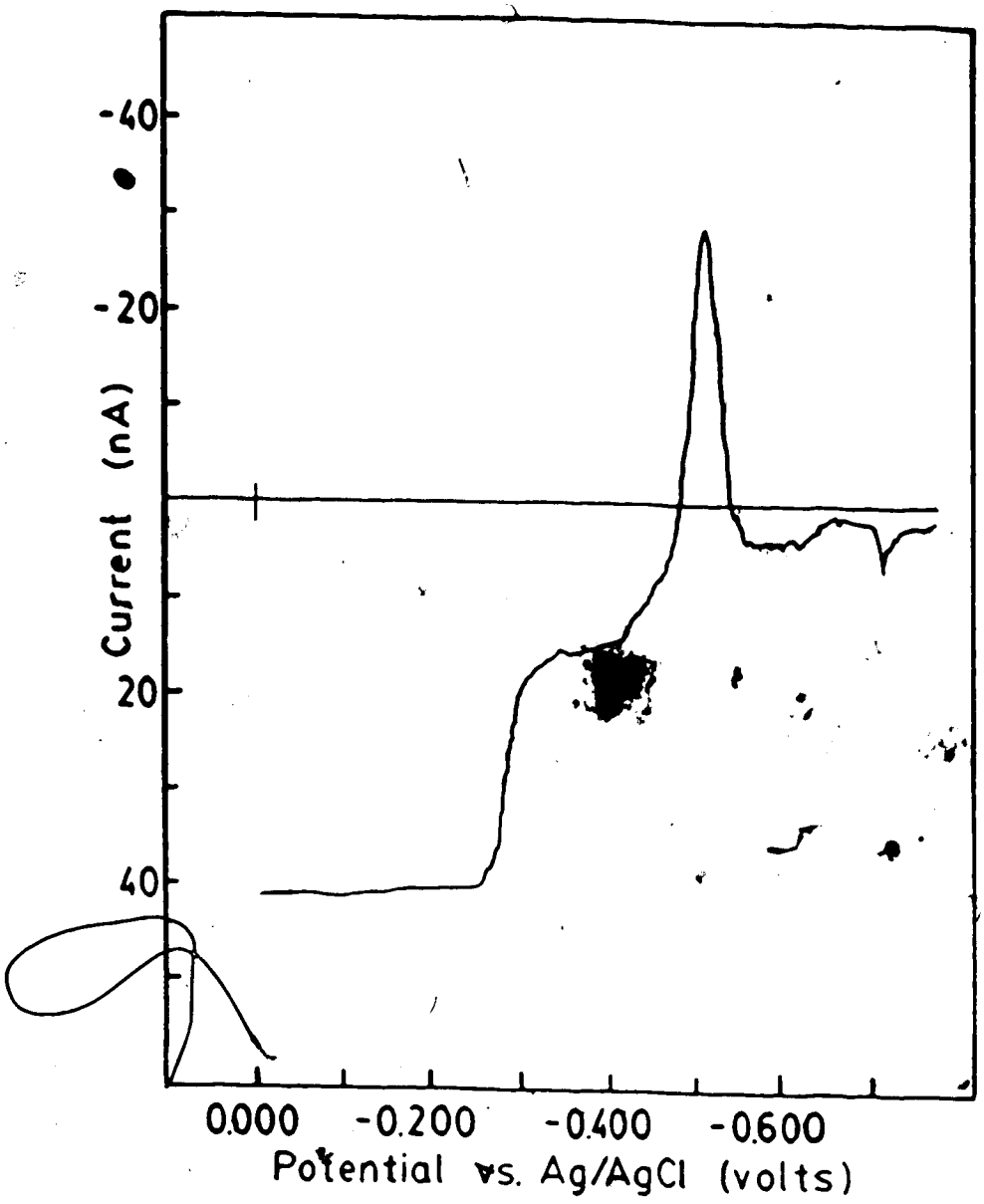

Figure 3.6 DC-sampled polarogram for 77 μM PSH in pH 3.0 phosphate buffer. The drop time was 1 second and the scan rate was 5 mV/sec. A filtering time of 0.3 second constant was used.

high background currents usually are accompanied by high background noise and therefore there would be a loss in detector sensitivity.

Region II is the oxidative plateau. Here the current is the sum of both the background current and the anodic current from the oxidation of mercury in the presence of the thiol. There is little change in the current as a function of potential and diffusion of the analyte to the electrode surface is the governing factor. Region III is an intermediate or transition phase. The observed anodic current decreases as the potential is made more negative. Finally, region IV is where the electrode potential is insufficient for the oxidation of mercury in the presence a thiol. This current corresponds to the background current.

Figure 3.7 shows a polarogram of the pH 3.0 phosphate buffer used to prepare the thiol solutions. Note that regions II and III are no longer present due to the absence of the thiols and that region IV now is observed over the full potential range until it reaches the electrode breakdown zone at +0.200 V.

An unusual peak was seen in region IV for penicillamine, but appears to be an artifact since a differential pulse polarogram of the penicillamine did not show any signal in that region.

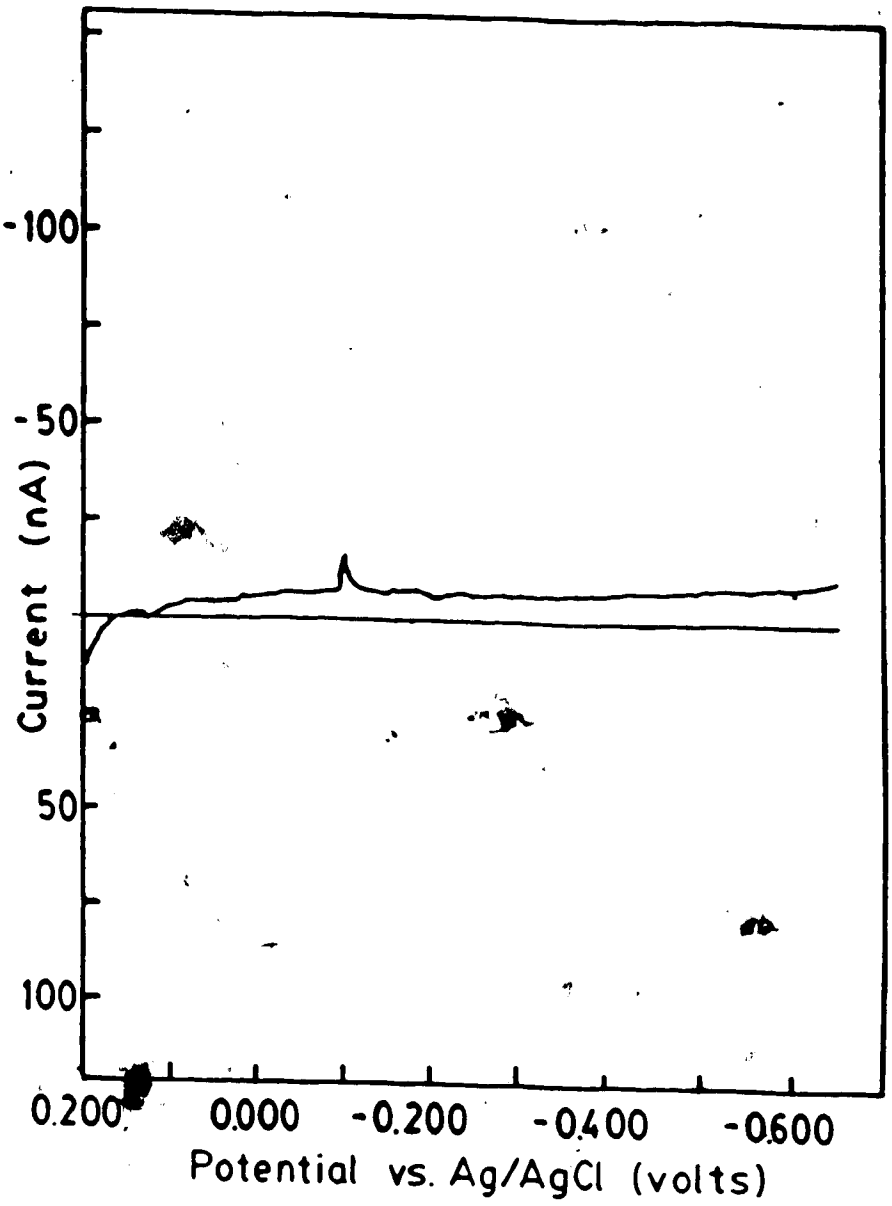

Figure 3.7 DC-sampled polarogram for pH 3.0 phosphate buffer without any thiol. The conditions were identical to those listed for the thiol solutions.

Table 3.1 lists the measured potentials defining the oxidative plateau and the potential on the polarographic wave where the measured current is half that found on the plateau. The onset potentials are determined by the intersection of the lines that define region II and region III in Figure 3.3. The potentials for the onset of the oxidative plateau range from -0.275 V for penicillamine to -0.129 V for homocysteine. All of the polarograms show direct electrode oxidation occurring at about +0.200 V, which is consistent with that seen in the background current profile for the phosphate buffer by itself.

D. Hydrodynamic Voltammetry Studies

Hydrodynamic voltammograms measured using high performance liquid chromatography with mercury-gold electrochemical detectors resemble polarograms since both are based on the same electrochemical processes. However, in polarography the analyte solution is stationary and the dropping mercury electrode is the moving phase, while in hydrodynamic voltammetry the electrode is fixed and the solution is the transient phase. This difference is important since the current measured at the dropping mercury electrode has both a Faradaic and a non-Faradaic component while the measured chromatographic peak is essentially Faradaic. The non-Faradaic current in the polarography

Table 3.1. Potentials defining the half-wave potential and the oxidative plateau for HSH, CSH, GSH and PSH from the polarograms shown in Figures 3.3 - 3.6, respectively. All potentials were measured with respect to Ag/AgCl.

Thiol	Half-wave Potential	Oxidative Plateau
HSH	-0.160 V	-0.129 to +0.200 V
CSH	-0.165 V	-0.130 to +0.200 V
GSH	-0.222 V	-0.158 to +0.200 V
PSH	-0.275 V	-0.215 to +0.200 V

arises from the charging of the growing mercury drop.

In hydrodynamic voltammetry a non-Faradaic current initially occurs as the electrode is brought to the set potential. Once the potential has been achieved, the non-Faradaic component of the current diminishes and the background current results from the electrochemical oxidation or reduction of electroactive impurities in the mobile phase. After a sample has been injected, the solutes are retained by the column as the sample solvent travels through it, unretained. When the interface of the mobile phase and the injected sample solvent passes over the electrode, a non-Faradaic charging or discharging current is observed and then the current returns to the normal background levels. This charging/discharging phenomenon is the result of the differences in the composition of the sample solvent compared to that of the mobile phase. Because the chromatography separates the analyte from this interface, the current measured as the analyte passes over the electrode is essentially a Faradaic current.

Furthermore, since the peak current is measured with the background current as the baseline, the peak current will be due to the electrochemical reaction of the eluting compound only. Figure 3.8 shows a typical chromatogram of a mixture of thiols and disulfides. The elution of the interface between the mobile phase and the injected sample

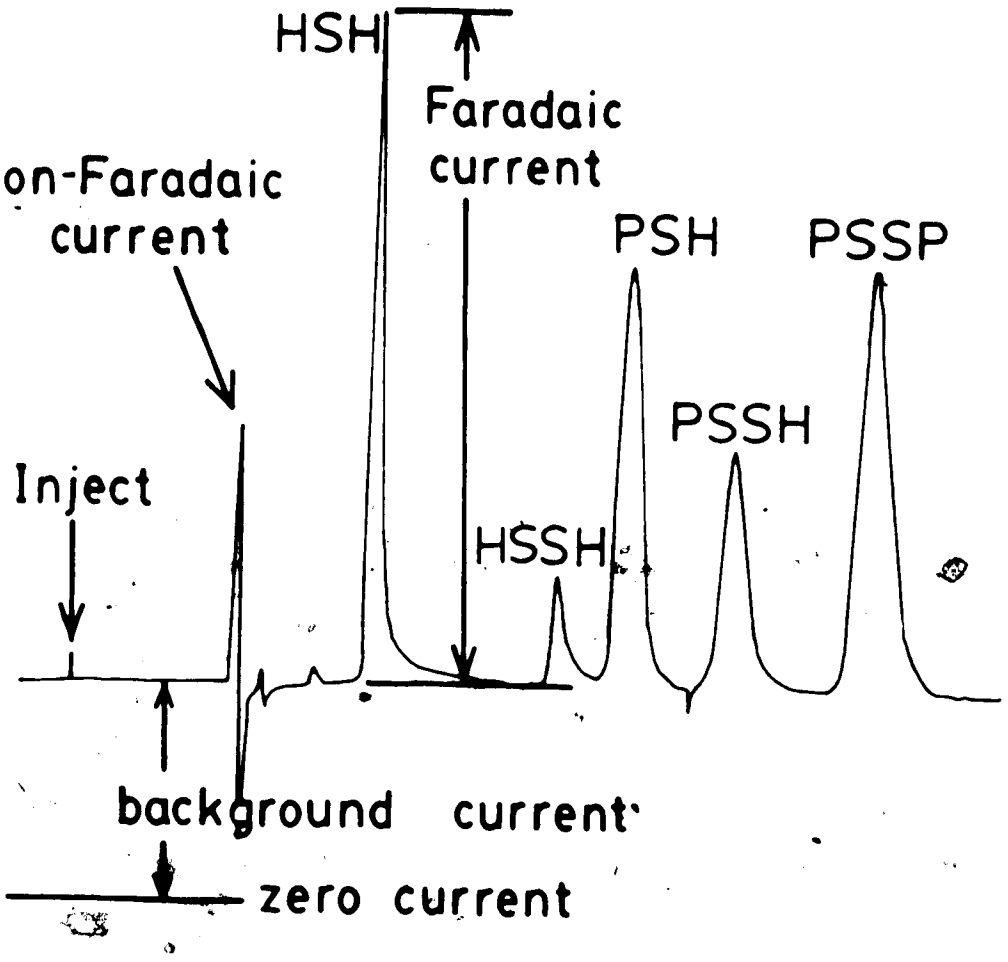

Figure 3.8 Typical chromatogram for a mixture of PSH, HSH, HSSH, PSSH and PSSP using pH 3.0 phosphate buffer as the mobile phase.

solvent into the detector is noted on the chromatogram by the charging/discharging current observed at about 2.8 minutes. The five peaks represent the five solutes HSH, PSH, HSSH, PSSH and PSSP and the Faradaic peak current for the HSH is measured by the peak height, as illustrated in the figure.

Hydrodynamic voltammograms measured for the thiols, HSH, CSH, GSH, and PSH with the Hg/Au electrochemical detector are presented in Figures 3.9 - 3.12. The height of the thiol peak in each chromatogram was measured, converted to a peak current and then plotted as a function of the applied potential setting. The hydrodynamic voltammograms consist of the same four regions described above for the polarograms for these same compounds. The important feature of the hydrodynamic voltammograms, with respect to the selection of the operating potential for detection of thiols at the downstream electrode, is the oxidative plateau. The potential ranges defining this plateau for the thiols are listed in Table 3.2. By setting the downstream electrode to a potential on the plateau, there is maximum oxidation of mercury in the presence of the thiol with little variation in the peak current due to small variations in applied potential. In this work, the electrode potential was set slightly more positive than the potential at the onset of the plateau so that the peak current would be independent of

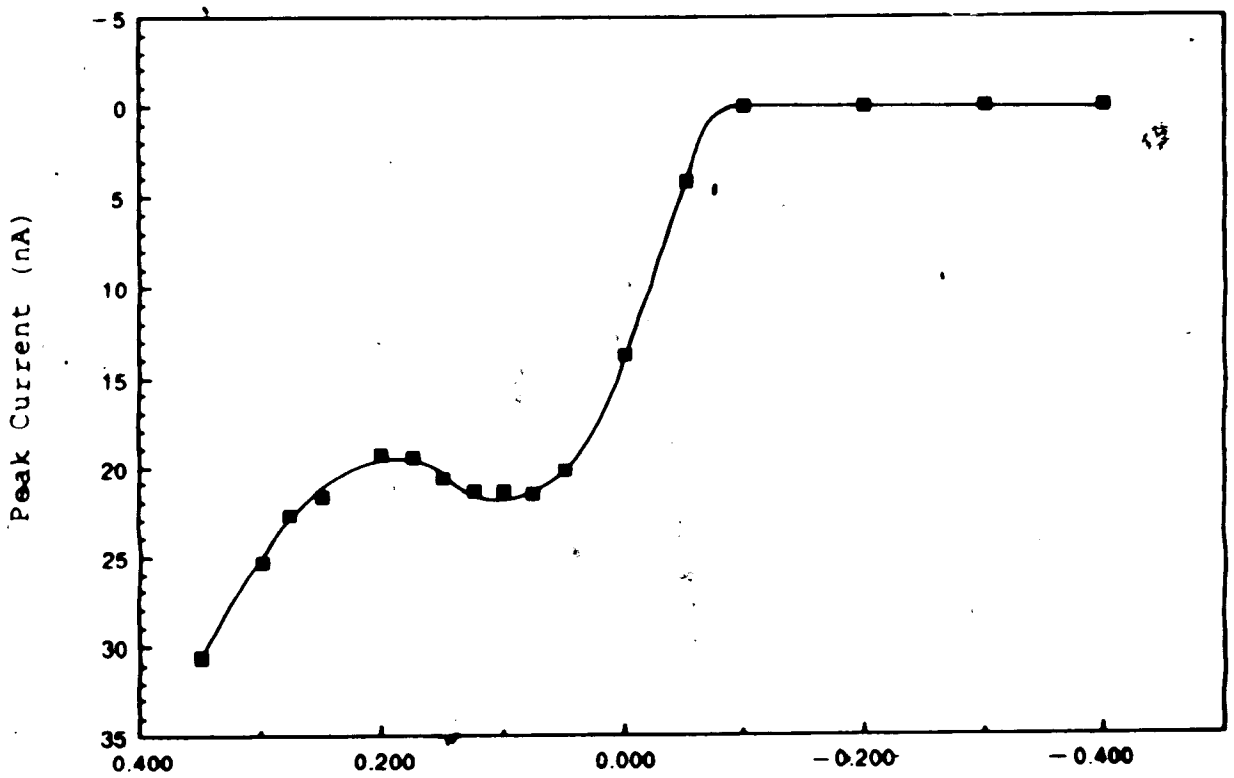

Figure 3.9 Hydrodynamic voltammogram for HSH. The upstream electrode potential was held constant at -1.000 V vs. Ag/AgCl while the downstream electrode potential was varied.

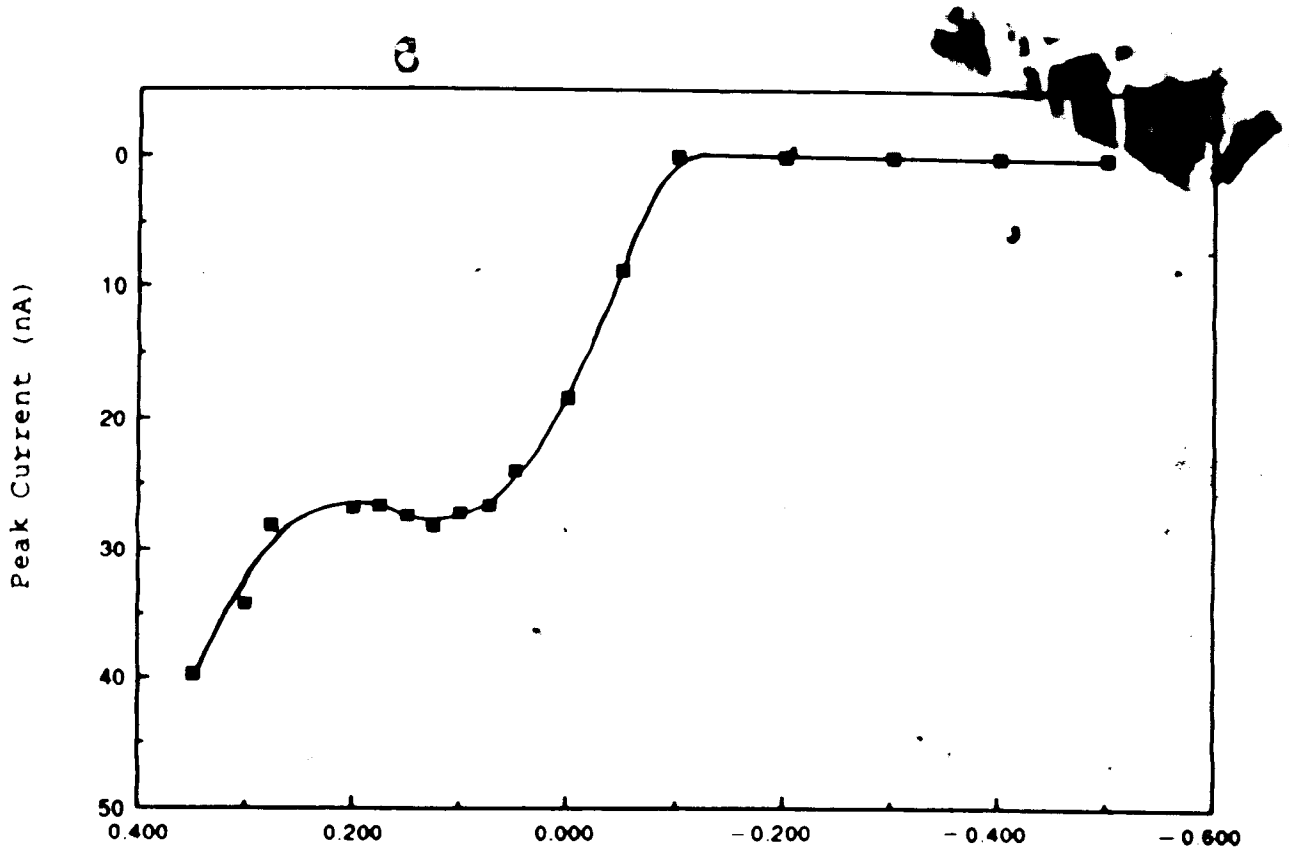

Figure 3.10 Hydrodynamic voltammogram for CSH using an upstream electrode potential of -1.000 V vs. Ag/AgCl.

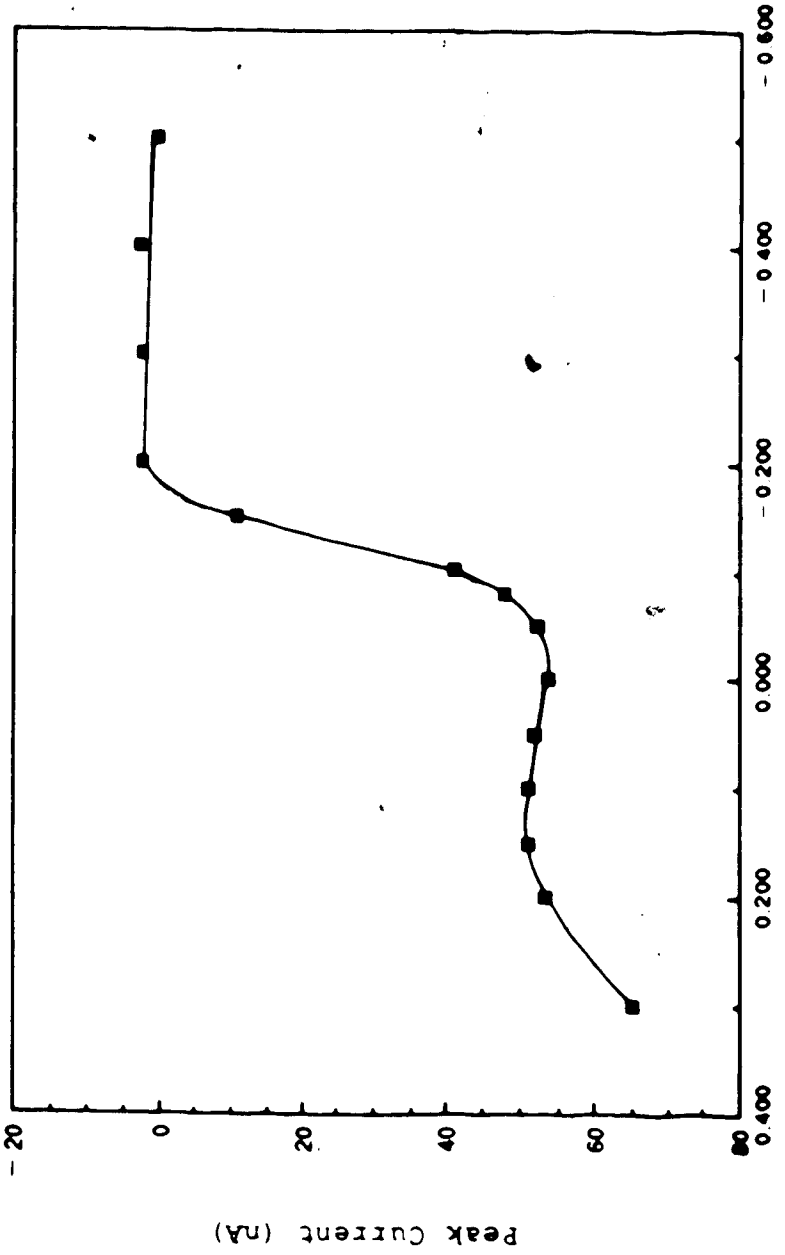

Figure 3.11 Hydrodynamic voltammogram for GSH. The upstream electrode potential was set to -1.000 V vs. Ag/AgCl.

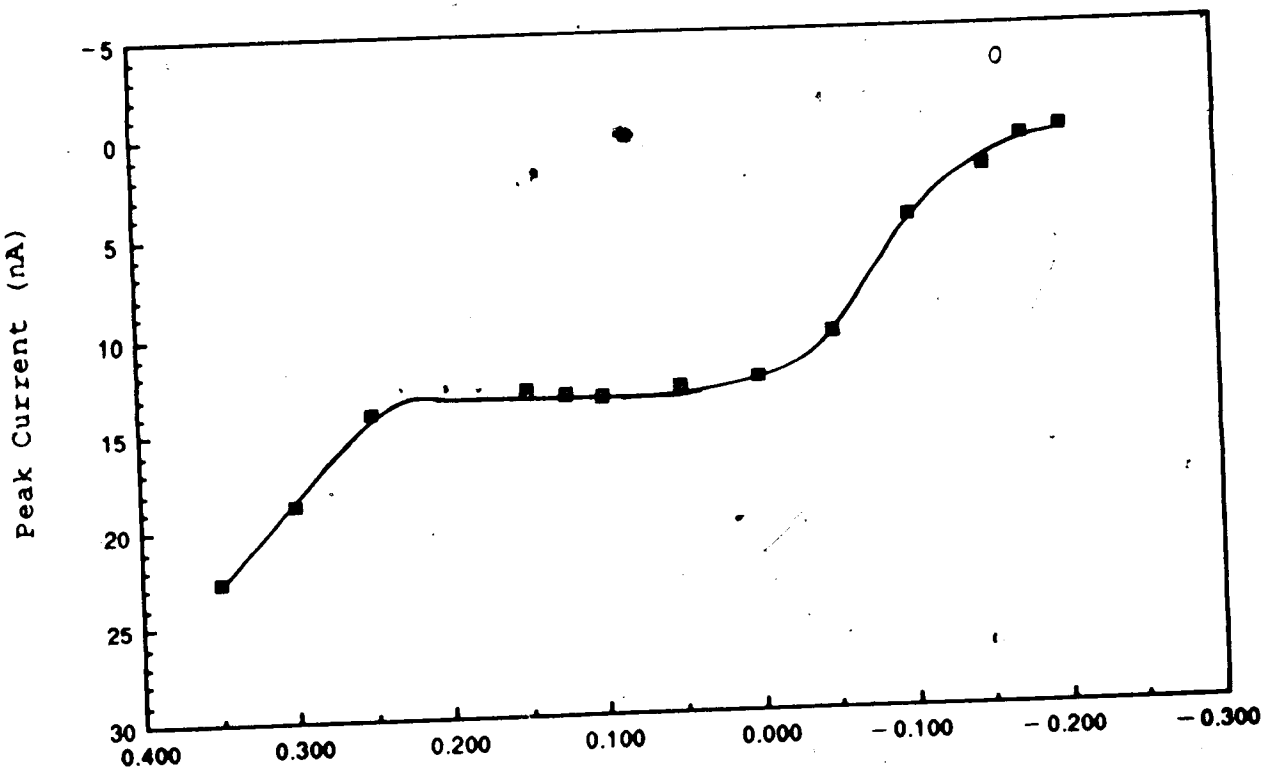

Figure 3.12 Hydrodynamic voltammogram for PSH. The upstream electrode potential was held at -1.000 V.

any fluctuations in the potential, e.g. due to any IR drop.

With homocysteine, oxidation begins around -0.100 volts versus Ag/AgCl and reaches its plateau around +0.029 volts. The oxidative plateau ends near +0.250 volts where the current begins to increase again. A similar trend is observed in the voltammogram for cysteine with the oxidative plateau occurring in the range of +0.039 to +0.250 volts. Mercury oxidation in the presence of glutathione begins near -0.186 volts and levels off at a potential of -0.086 volts. The plateau reaches as far as +0.200 volts, and an increase in the anodic current is seen at +0.300 volts. The location of the end of the plateau is not well defined since the background current became too high to measure the peak current at a potential setting of +0.400 volts. Oxidation with penicillamine begins around -0.150 volts and reaches a plateau near -0.025 volts. The plateau extends to about +0.240 volts.

The hydrodynamic voltammograms show a general shift in the onset of the oxidation plateau to a more positive potential compared to the corresponding polarograms. The reference electrode used in both the polarograms and the hydrodynamic voltammograms was a Ag/AgCl electrode. The differences between the results from the polarograms and the hydrodynamic voltammograms are as little as 0.043 V, in the case of penicillamine to 0.215 V, as observed for cysteine.

Table 3.2. Potentials measured vs. Ag/AgCl defining the half-wave potential and the oxidative plateau for HSH, CSH, GSH and PSH from their hydrodynamic voltammograms shown in Figures 3.9 - 3.12.

Thiol	Half-wave Potential	Oxidative Plateau
HSH	-0.013 V	+0.029 to +0.250 V
CSH	-0.027 V	+0.039 to +0.267 V
GSH	-0.128 V	-0.086 to +0.200 V
PSH	-0.080 V	-0.025 to +0.240 V

As a result of the observations from the hydrodynamic voltammograms for the thiols, the downstream electrode was set to a potential of +0.150 V versus the Ag/AgCl electrode for all subsequent studies. This potential is near the middle of the oxidative plateau for all four thiols and therefore will exhibit little change in the peak current even if small changes in the electrode potential occur.

Correspondingly, the selected potential for the upstream electrode should be based on the hydrodynamic voltammograms for the disulfides to be studied. The hydrodynamic voltammograms for the disulfides are plotted as peak currents measured at the downstream electrode versus the applied potential at the upstream electrode. Although the actual current that is measured is due to an oxidation process, the species that give rise to the signal are derived from the reduction of the disulfides and therefore the current is plotted as a cathodic one. This format will display the hydrodynamic voltammograms in a fashion that resembles standard polarographic convention.

In a typical hydrodynamic voltammogram for a disulfide, there are three regions observed. These regions are complementary to some of the regions observed in the voltammograms for the thiols. The hydrodynamic voltammogram for homocystine, shown in Figure 3.13, will be used to illustrate the features of these plots. The current in

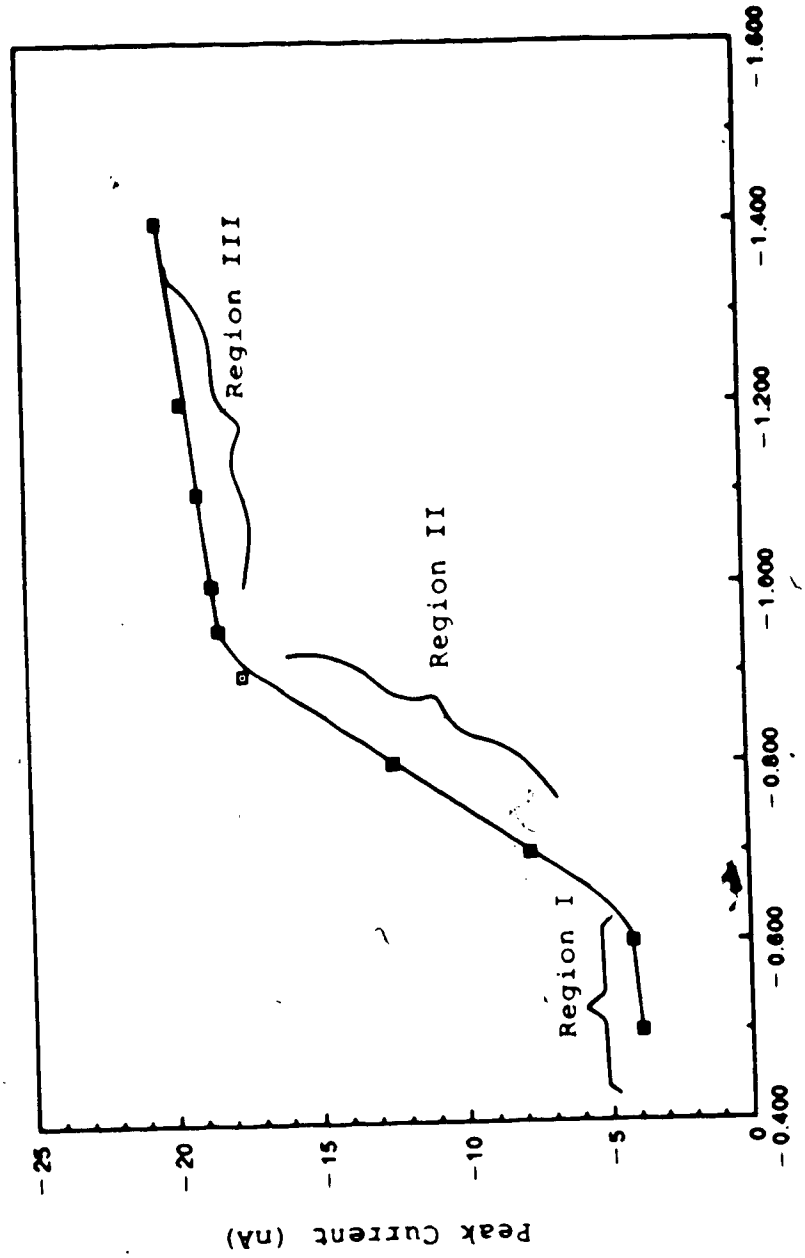

Figure 3.13. Hydrodynamic voltammogram for HSSH. The downstream electrode potential was held at +0.150 V vs. Ag/AgCl while the upstream electrode potential was varied.

region I is due to the residual or background current. This is similar to region IV on the thiol voltammograms. Over this potential range there is no reduction of the disulfide at the upstream electrode and hence no signal is measured at the downstream electrode except for the background current. Region II in Figure 3.13 shows the current increasing as the potential is made more negative. Over this potential range, the upstream electrode reduces a fraction of the disulfide at the electrode surface and the resulting thiols are then measured at the downstream electrode by the chromatographic peak for the oxidation of the mercury in the presence of the thiol. Finally, region III corresponds to the reductive plateau where the measured current is relatively constant as the upstream potential becomes more negative. In this potential region the reduction of disulfide to thiols is rate-limited by the mass transport of the analyte to the electrode surface and thus a maximum peak current is observed.

In polarography, a fourth region having an increasing background current is usually observed at high negative potentials. This high current is due to reduction of water at the surface of the electrode and is analogous to the high current observed for the direct oxidation of the mercury electrode in the polarograms or voltammograms for the thiols. With the HPLC-ED system, a high background current

was observed at the upstream electrode when its potential was set more negative than -1.000 volts versus Ag/AgCl. This does not create a problem in the dual electrode detection scheme, however, because the reduction of the disulfide at the upstream electrode is indirectly monitored at the downstream electrode by the oxidation of the mercury in the presence of the generated thiols. Since the downstream electrode is not affected by the current at the upstream electrode, the measured anodic current at the downstream electrode does not display any change once the plateau for the reduction of the disulfide has been reached. This is the reason why there are only three regions observed on the hydrodynamic voltammograms for the disulfides, even though the upstream electrode potential is set more negative than -1.000 volts.

The hydrodynamic voltammograms for HSSH, CSSC, GSSG, and PSSP are presented in Figures 3.13 - 3.16. Table 3.3 lists the half-wave potential and the potential range defining the reduction plateau for each of the disulfides. For optimum sensitivity and precision, the upstream electrode potential should be selected from the potential range defining the reduction plateau for the disulfide under study. Ideally, if two or more disulfides are to be monitored, the upstream electrode potential should be on the reductive plateau for all the disulfides of interest.

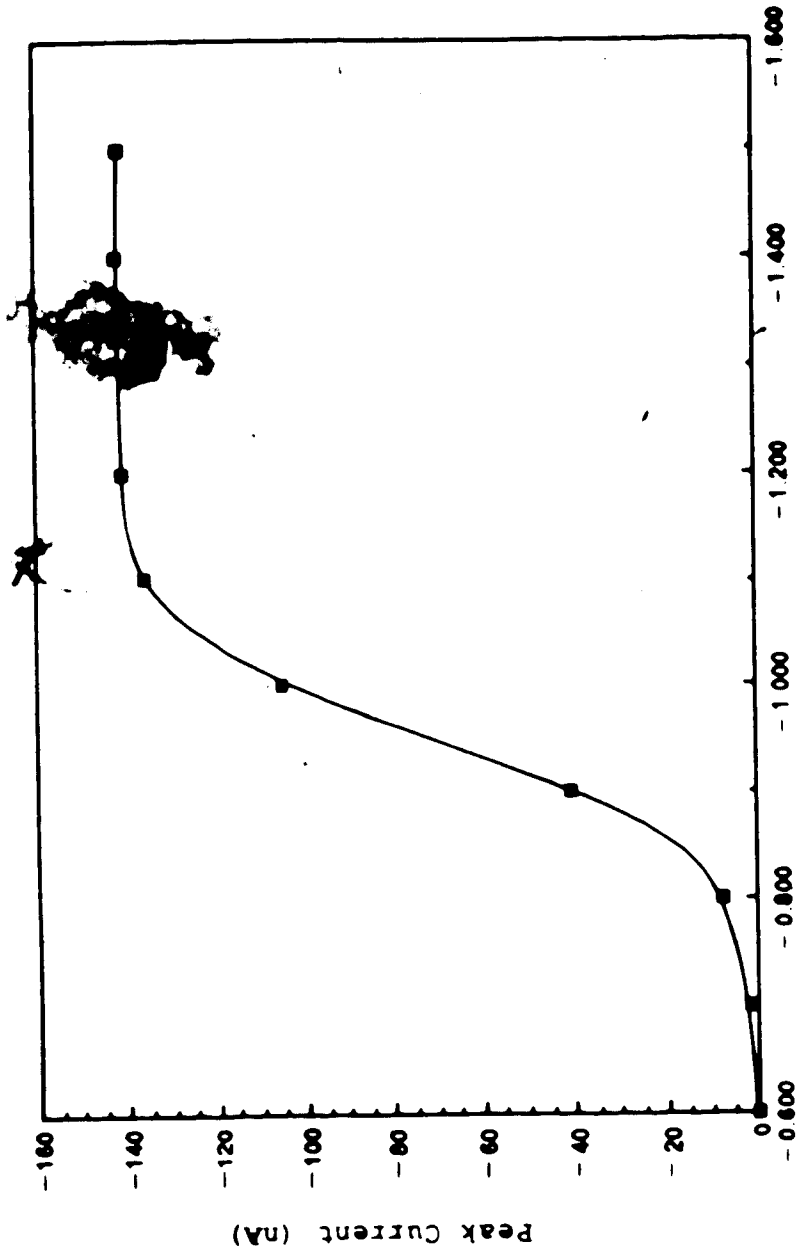

Figure 3.14 Hydrodynamic voltammogram for CSSC. The downstream electrode potential was constant at +0.150 V vs. Ag/AgCl.

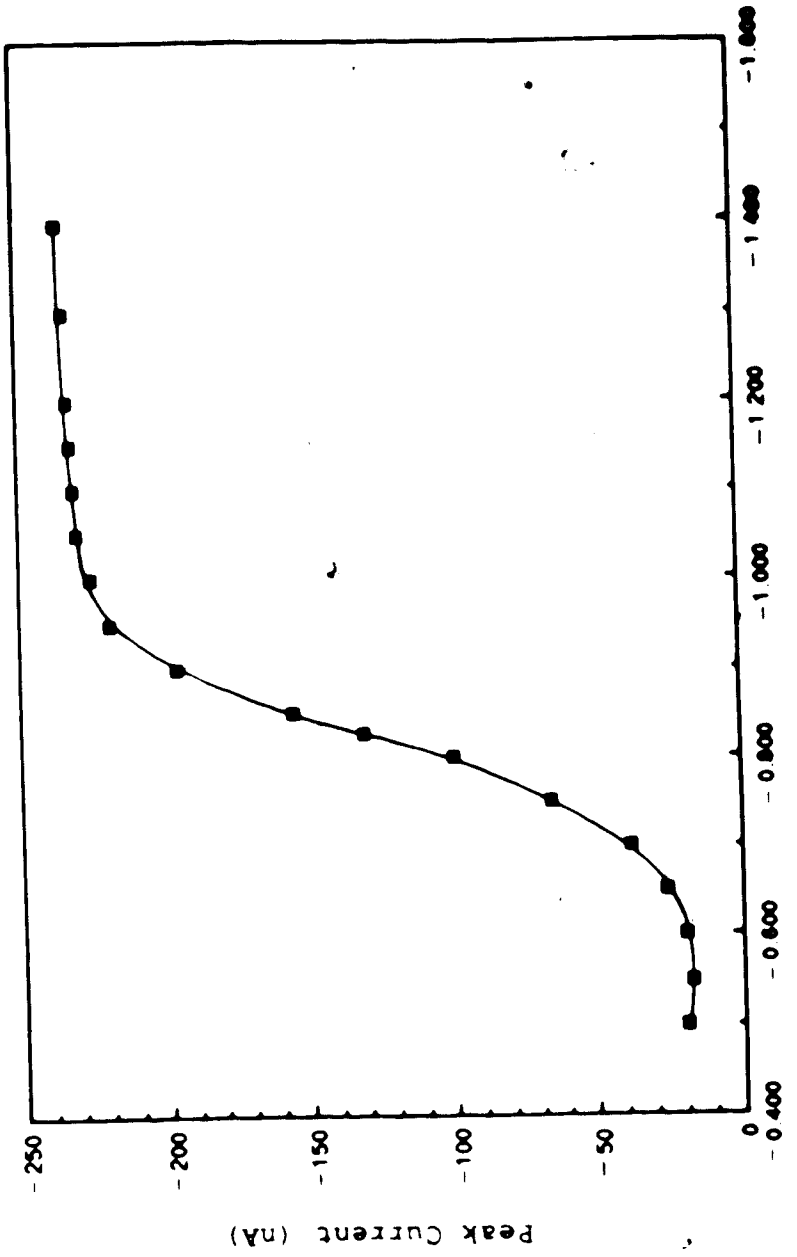

Figure 3.15 Hydrodynamic voltammogram for GSSG using a downstream electrode potential of +0.150 V vs. Ag/AgCl.

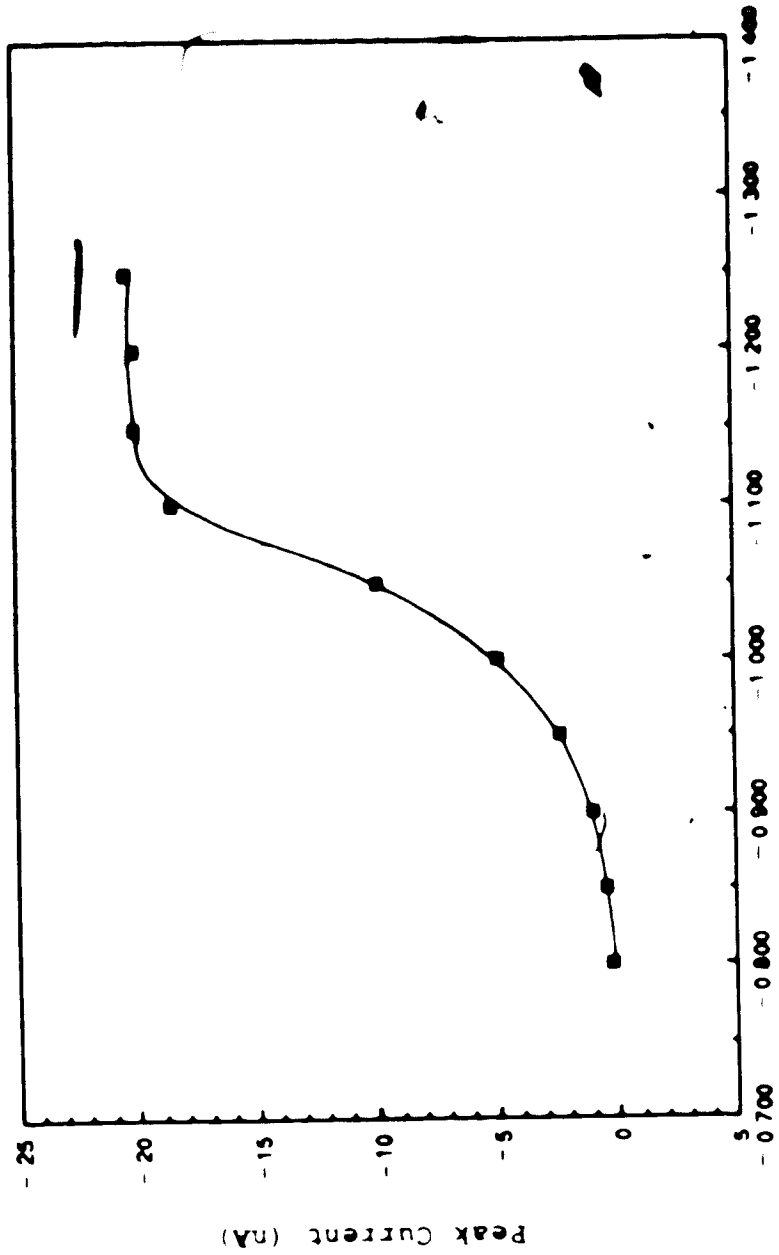

Figure 3.16 Hydrodynamic voltammogram for PSSP. A downstream electrode potential of +0.150 V vs. Ag/AgCl was used.

Table 3.3. Potentials measured vs. Ag/AgCl defining the half-wave potential and the reduction plateau from the hydrodynamic voltammograms for the symmetrical disulfides shown in Figures 3.13 - 3.16.

Thiol	Half-wave Potential	Reduction Plateau
HSSH	-0.757 V	-0.900 to -1.400 V
CSSC	-0.950 V	-1.200 to -1.500 V
GSSG	-0.820 V	-1.050 to -1.400 V
PSSP	-1.050 V	-1.150 to -1.250 V

Hence, the disulfide for which the reductive plateau begins at the most negative potential will determine the appropriate potential for the upstream reduction electrode.

Table 3.3 shows that oxidized penicillamine has the most negative potential for the onset of its reduction plateau. Thus, for a mixture containing oxidized penicillamine and any of the other disulfides, the upstream electrode potential should be set to a potential in the reductive plateau region of the hydrodynamic voltammogram for PSSP. Generally, the electrode potential selected for the upstream electrode should be 50 - 100 mV more negative than the potential at the onset of the plateau. For oxidized penicillamine then, the upstream electrode should be set at -1.200 volts versus Ag/AgCl. Unfortunately, rapid deterioration of the surface of the upstream electrode was observed with this potential setting. A compromise between detector sensitivity and electrode lifetime was made by using a potential of -1.100 volts at the upstream electrode when running analyses of samples containing PSSP.

Others [73,102] have reported fast electrode degradation at high potentials and therefore use an upstream potential of -1.000 volts. However, the hydrodynamic voltammogram of PSSP indicates that, if the potential of the upstream electrode is set to -1.000 V, peak currents will only be about 25% of the maximum current measured when the

potential of the upstream electrode is set to a potential in the plateau region. This potential will not provide high sensitivity for the oxidized penicillamine. PSSP does not undergo a facile reduction at -1.000 volts, but use of the -1.100 V setting with freshly prepared electrodes produced a significantly higher response for PSSP without excessive electrode deterioration. Under these conditions a peak current of about 88% of the maximum current at the plateau was achieved.

The average lifetime of the upstream electrode was about one week with continual use, although this was reduced somewhat when the mobile phase contained a high (ie. > 1.0 mM) concentration of sodium octyl sulfate. With the ion pairing reagent present, the upstream electrode was the first to lose its mercury. It could however, be re-amalgamated on its own since its only function is to generate the thiols. For re-amalgamation the electrodes were rinsed with 98% ethanol, air-dried, and a single drop of mercury was placed on only the upstream electrode. After several minutes the excess mercury was removed as described in the experimental section of Chapter II being careful to prevent the mercury from coming in contact with the downstream electrode. If there was any uncertainty in the condition of either electrode both were polished and amalgamated.

The hydrodynamic voltammograms for the mixed disulfides, PSSG, PSSH, and PSSC are shown in Figures 3.17 - 3.19. Figure 3.20 shows the structures of these three mixed disulfides while Table 3.4 lists the half-wave potential and the potentials defining the reduction plateau for each mixed disulfide. All three voltammograms are shifted to more positive potentials compared to the voltammogram for the oxidized penicillamine. The $E_{\frac{1}{2}}$ value for each mixed disulfide, PSSR, is between the $E_{\frac{1}{2}}$ values for the oxidized penicillamine, PSSP, and the corresponding symmetrical disulfide, RSSR. This seems reasonable since the mixed disulfide is a composite of the two symmetrical disulfides, PSSP and RSSR, and therefore would most likely have an intermediate behaviour. This is illustrated in Figure 3.21 which shows the overlay of the hydrodynamic voltammograms for GSSG, PSSG and PSSP. Here the data are normalized by plotting the percent reduction versus the applied potential, where 100% reduction is taken to be the current measured at the reduction plateau.

E. Discussion

The electrochemical behaviour of thiols and disulfides at mercury electrodes has been studied for many years. Kolthoff and co-workers [107-109] investigated the reduction

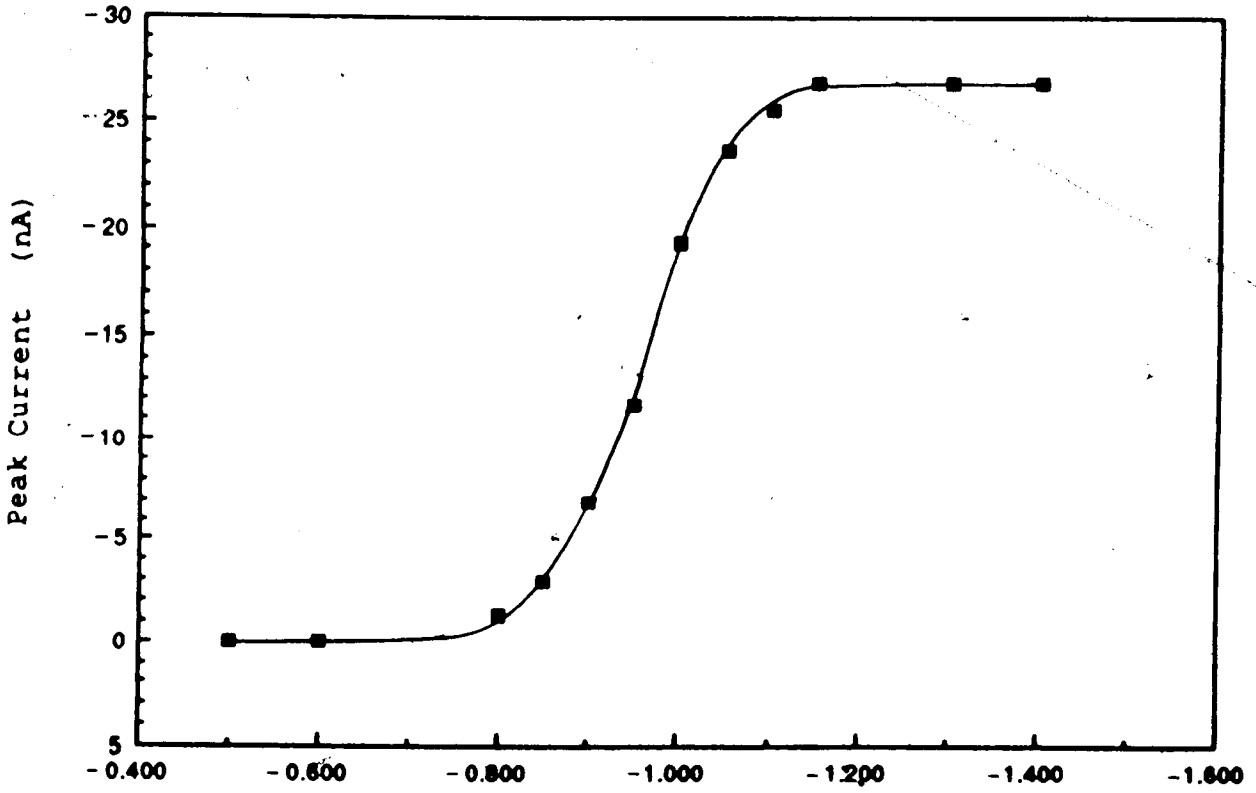

Figure 3.17 Hydrodynamic voltammogram for PSSG. The downstream electrode potential was held constant at +0.150 V vs. Ag/AgCl. Typical reaction conditions used to prepare the mixed disulfide are given in Chapter V.

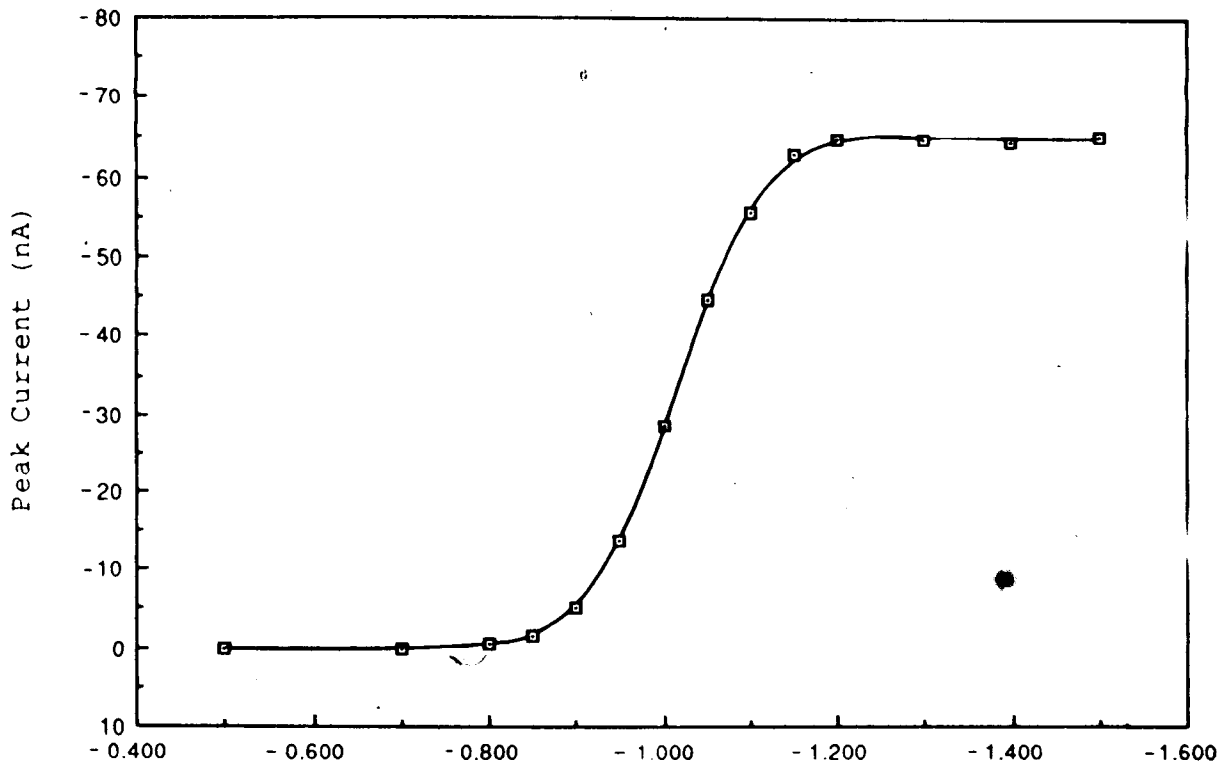

Figure 3.18 Hydrodynamic voltammogram for PSSH using a downstream electrode potential of +0.150 V. Synthesis of the mixed disulfide is described in Chapter VI.

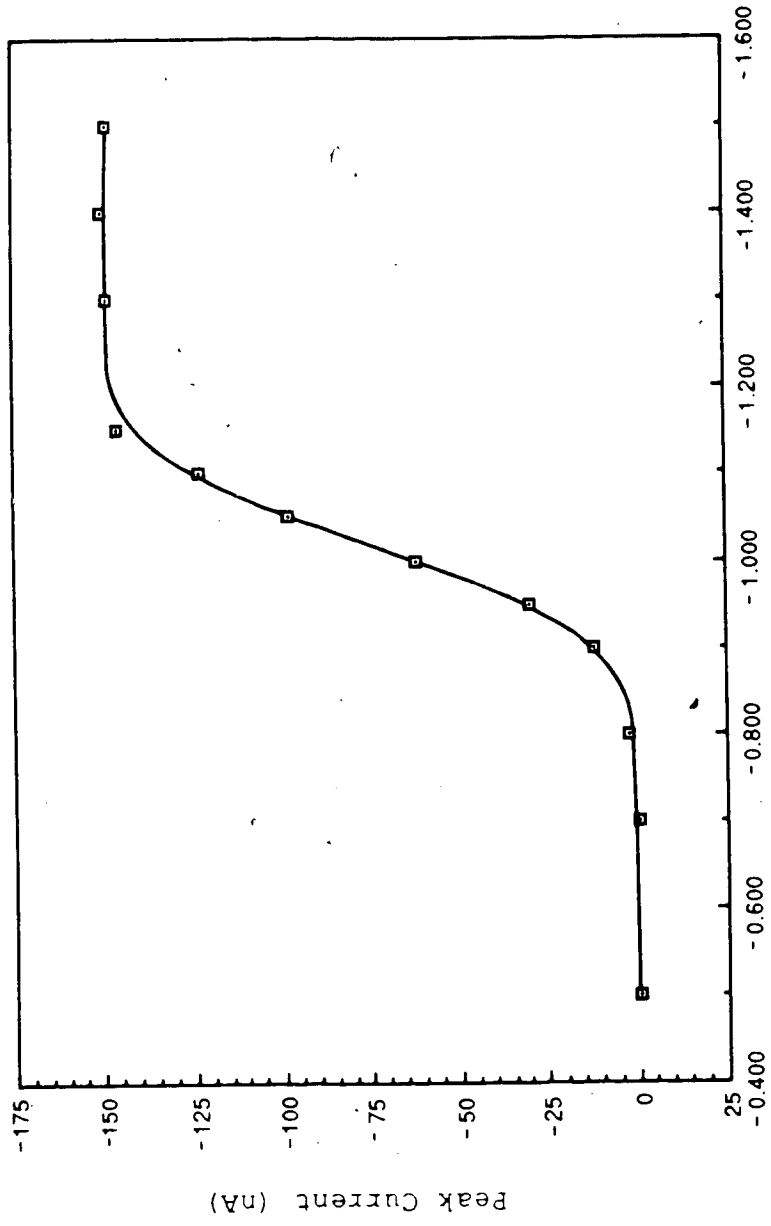

Figure 3.19 Hydrodynamic voltammogram for PSSC. The downstream electrode potential was held at +0.150 V vs. Ag/AgCl.

a) PSSG

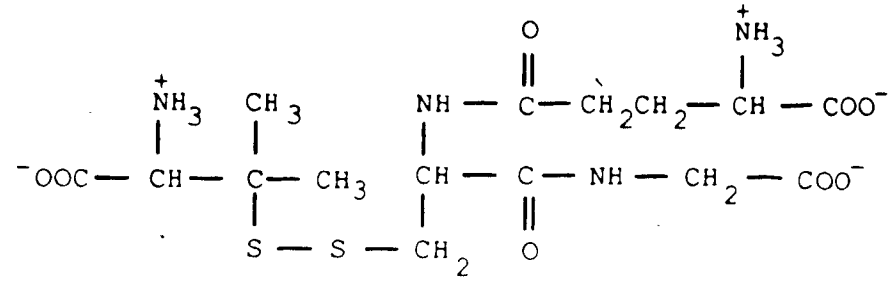

b) PSSH

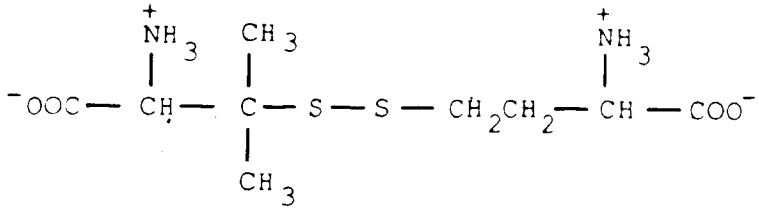

c) PSSC

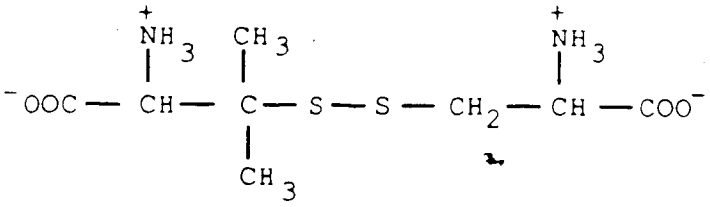

Figure 3.20 Stuctural formulae of the mixed disulfides, PSSG, PSSH and PSSC.

Table 3.4. Potentials defining the half-wave potential and the reduction plateau for the mixed disulfides PSSG, PSSH and PSSC as seen in Figures 3.17 - 3.19.

Mixed Disulfide	Half-wave Potential	Reduction Plateau
PSSG	-0.957 V.	-1.054 to -1.400 V.
PSSH	-1.067 V.	-1.127 to -1.500 V.
PSSC	-1.013 V.	-1.127 to -1.500 V.

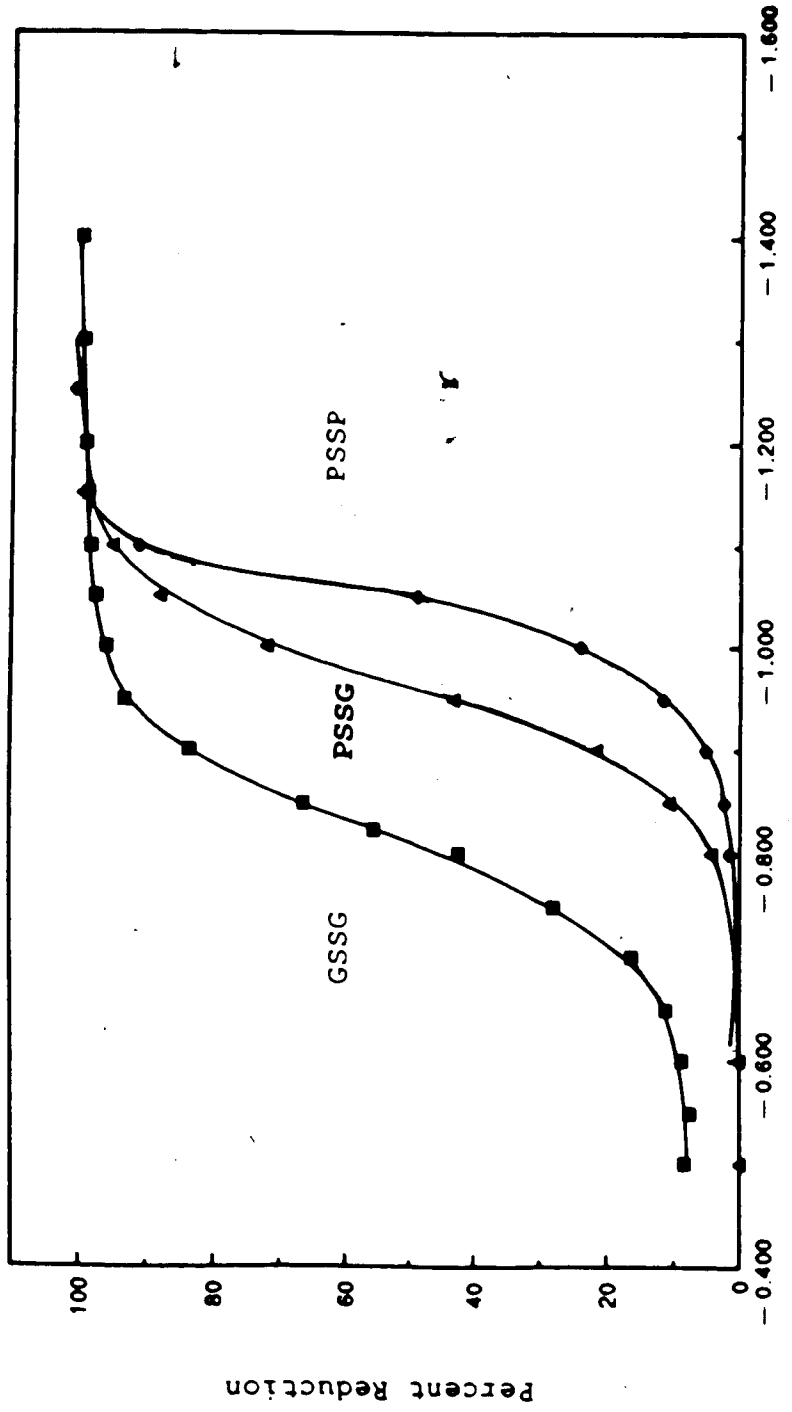

Figure 3.21. Superimposed hydrodynamic voltammograms for GSSG, PSSG and PSSP. All voltammograms were normalized with respect to the peak current on their respective plateaux.

of cystine and oxidized glutathione at the dropping mercury electrode. They showed that the reduction of a disulfide at a mercury electrode follows the reaction sequence,

$$RSSR + e^- + H^+ \rightleftharpoons RS^\cdot + RSH \qquad (28)$$

$$RS^\cdot + e^- + H^+ \rightleftharpoons RSH \qquad (29)$$

$$RSSR + 2e^- + 2H^+ \rightleftharpoons 2\ RSH \qquad (30)$$

They also showed that if the breakage of the disulfide bond in reaction (28) were the rate-determining step, then at 25°C the potential at any point along the polarographic wave would be expressed by

$$E = E_0 + 0.059\log \frac{[RSSR]^\circ [H^+]^\circ}{[RS^\cdot]^\circ [RSH]^\circ} \qquad (31)$$

where E_0 is the standard potential of reaction (28) and the superscripted terms are concentrations of the species involved at 25°C. Since $[RSSR]^\circ$ is proportional to $(i_d - i)$ while $[RS^\cdot]^\circ$ and $[RSH]^\circ$ are proportional to i, the expression becomes:

$$E = E' + 0.059\log([H^+]+K) + 0.059\log \frac{(i_d - i)}{(i^2)} \qquad (32)$$

where K is a constant that accounts for dissociation of the sulfhydryl group in RSH and E' is a constant relating to the standard potential of reaction (28) and the diffusion coefficients for the three species, RSSR, $RS^\cdot$ and RSH. The term i_d is the current at the mass transport limited plateau

while i is the current at a given point on the polarographic wave. At a fixed pH then, the graph of potential versus $\log((i_d-i)/i^2)$ should yield a straight line with a slope of 0.059. The intercept is the summation of the first two terms on the right hand side of Equation (32). Furthermore, the results indicate that in the presence of sufficient thiol, RSH, the potential is no longer proportional to $\log((i_d-i)/i^2)$, but rather $\log((i_d-i)/i)$.

A similar graphical analysis for the mixed disulfides PSSG, PSSC and PSSH can be made from the hydrodynamic voltammograms obtained by HPLC-ED. Using the voltammograms in Figures 3.17 - 3.19, the values for $\log((i_d-i)/i^2)$ and for $\log((i_d-i)/i)$ were calculated as a function of potential. The plots of potential versus the $\log((i_d-i)/i^2)$ as well as versus $\log((i_d-i)/i)$ for the mixed disulfides are shown in Figure 3.22. Since the chromatography separates the analytes before detection, there should be no interference by the thiols with the electrochemical reduction of the disulfides at the electrode. As expected, the plots of potential as a function of $\log((i_d-i)/i)$ for the mixed disulfides were not linear. Plots of potential versus $\log((i_d-i)/i^2)$ displayed straight lines with slopes of 0.073, 0.062 and 0.067, for the PSSG, PSSH and PSSC, respectively.

Figure 3.22 Comparison of $\log((i_d-i)/(i^2)))$ to $\log((i$ i)/i) as a function of applied potential from the hydrodynamic voltammograms for a) PSSG, b) PSSC and c) PSSH in Figures 3.17 - 3.19.

a)

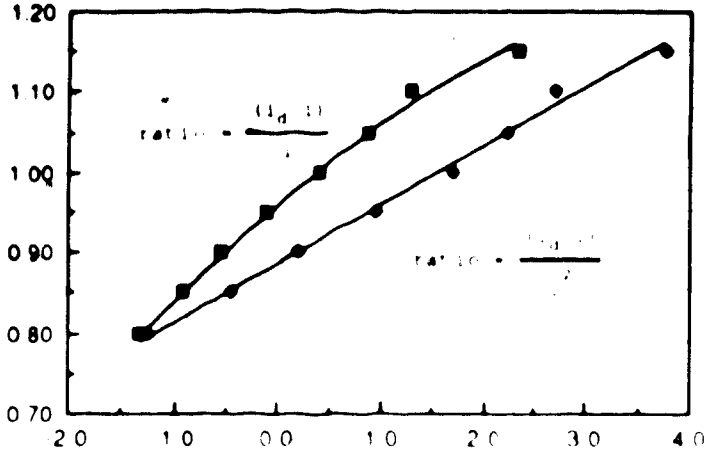
1.20
1.10
1.00
0.90
0.80
0.70
-20
-10
00
10
20
30
40

b)

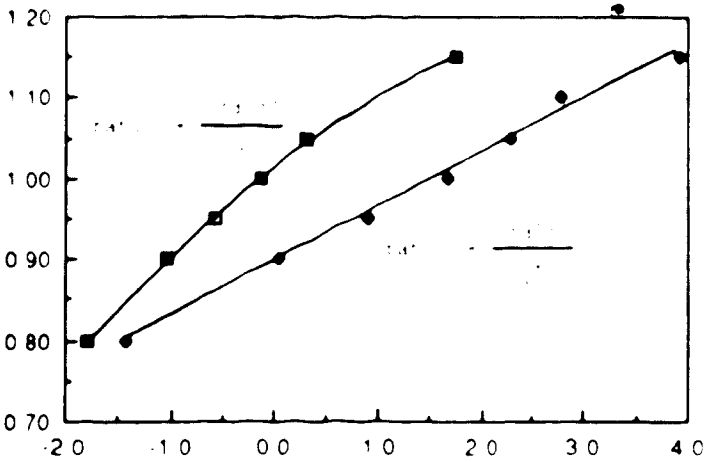
Applied Potential (volts)
1.20
1.10
1.00
0.90
0.80
0.70
-20
-10
00
10
20
30
40

c)

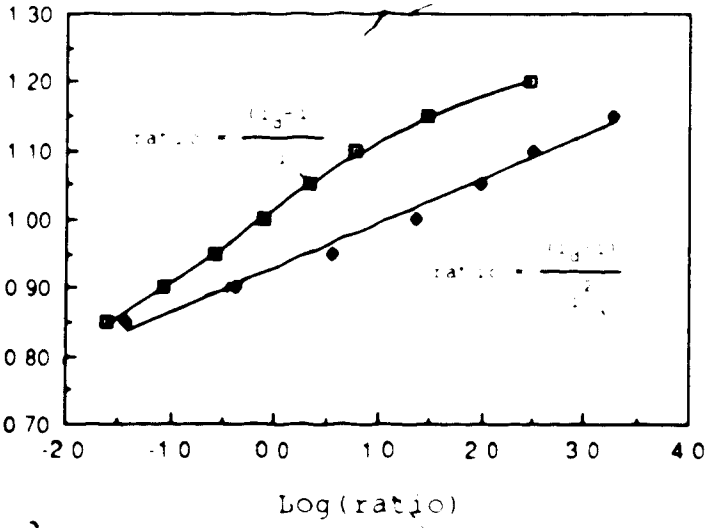
1.30
1.20
1.10
1.00
0.90
0.80
0.70
-20
-10
00
10
20
30
40
Log(ratio)

A rapid procedure has been outlined by Dahl, Selberg, and Lott [110] to obtain hydrodynamic voltammetry data, but it may not be readily applicable to the analysis of thiols and disulfides using the mercury-gold electrodes. The procedure was performed on a glassy carbon electrode for detection of diphenylamines and called for the direct flow of the analyte solution into the detector cell. Continual exposure of a mercury-gold electrode to thiols, especially at potentials where oxidation occurs, would lead to rapid loss of mercury resulting in deterioration of the electrode and a change in the electrode sensitivity. As well, Allison and Shoup [73] have shown that the high negative potentials required for disulfide cleavage are accompanied by high background currents, making direct detection of the reduction potential difficult. Use of the dual electrode scheme might reduce the problem, but the deterioration of the downstream electrode would still remain as the limiting factor in this method.

Typically the selected electrode potentials are 50 - 100 mV past the onset of the oxidation or reduction. The variations observed between the onset potentials determined by polarography and the onset potentials determined by hydrodynamic voltammetry suggest that, although the routine use of replicate injections may be time-consuming, it is perhaps the best method for

determining the electrode potentials for HPLC-ED. Other techniques, like cyclic voltammetry, may indicate the feasibility of electrochemical detection for various target molecules, but the practical operating settings for electrode potentials will still need to be determined by direct experimentation.

CHAPTER IV

CHROMATOGRAPHY OF THIOLS AND DISULFIDES

A. Introduction

As mentioned in Chapter III, the sensitivity of electrochemical detection for thiols and disulfides can only be fully utilized if the analyte peaks are chromatographically resolved from one another. Therefore a knowledge of their chromatographic behaviour under various chromatographic conditions is necessary for the selection of optimum operating conditions. This chapter will examine the effect of various mobile phase parameters on the reversed-phase chromatographic behaviour of several thiols and disulfides. The mobile phase variables investigated were the pH, the ion-pairing reagent concentration, and the organic modifier content. In Chapters V and VI, the results presented in this chapter are used to optimize the separation of several mixtures of thiols and disulfides in biological fluids to permit quantitative measurement of each component.

B. Chromatography of Thiols and Disulfides

Since most of the sulfur-containing compounds encountered in living organisms derive from the amino acid

cysteine [113], techniques that were designed for amino acid analysis have been applied to the determination of biologically significant thiols. The separation of biological thiols and disulfides has been achieved on an amino acid analyzer using ion-exchange chromatography [114,115]. Although this method has been automated, it still suffers from long analysis times and requires long columns to obtain adequate resolution for a mixture of compounds. Furthermore, ion-exchange columns tend to have lower efficiencies, are less stable and are less reproducible compared to columns used in other LC techniques [116].

The development of reversed-phase high performance liquid chromatography has caused the replacement of many ion-exchange methods with reversed-phase ones. In reversed-phase chromatography, retention is dependent on the hydrophobic nature of the sample while the selectivity of the separation occurs by interactions between the solute molecules and the mobile phase. Increases in the retention of ionic or ionizable solutes can be obtained by the addition of ion-pairing reagents to the mobile phase while alterations in selectivity of the separation can be made with the addition of an organic modifier to the mobile phase. This control on the chromatography makes it

especially suited to the determination of complex mixtures of thiols and disulfides in biological samples.

In reversed-phase chromatography the stationary phase consists of a silica-based porous support with covalently bonded hydrocarbon chains. The two most common types of packing in a reversed-phase column are octyl and octadecyl silanes. The mobile phase used with this technique is generally an aqueous solution which may contain buffer salts and/or an organic modifier. The mobile phase is often buffered since the resolution in many separations is pH dependent.

C. Precision

To study the precision of the measurement system, replicate injections of GSH, CSH, HSH, and PSH, as well as their symmetrical disulfides were performed. From the reproducibility of the measured results, the precision of the measurement step can be evaluated. Figure 4.1 shows a chromatogram for a typical GSH sample and will be used to define some of the chromatographic terms and to indicate the quantities measured on the chromatogram.

Since the injected sample solvent has a slightly different composition compared to the mobile phase, there will be a charging and discharging of the electrode surface as the sample solvent plug passes over it. Assuming the

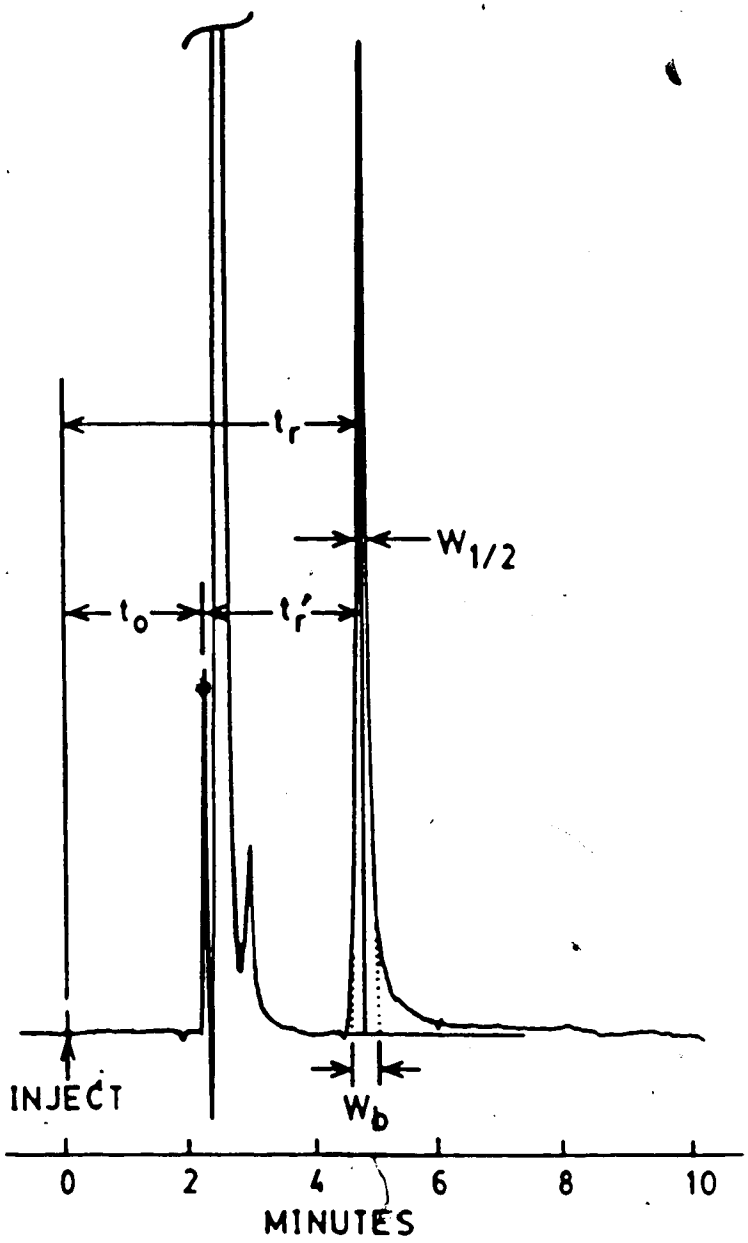

Figure 4.1. A typical chromatogram of a GSH sample. The chromatographic terms t_0, t_r and t_r' are illustrated as defined in the text. As well, the peak width at the base, W_b, and peak width at half the peak height, $W_{\frac{1}{2}}$, are labelled.

sample solvent does not interact with the column packing material, then the discharging and charging currents observed in the chromatogram will be a measure of the column dead time or void volume. This is assigned the term t_0 in Figure 4.1, and is the time it takes the sample solvent front to travel from the injector, through the column, and to the detector electrodes.

Similarly, the solute should require the same amount of time to get to the detector, but, because of interactions involving the solute, the mobile phase and the column, it is retarded and elutes at a later time. This time is called the solute retention time, labelled as t_r in Figure 4.1, and is measured with respect to the point of injection. The adjusted retention time, t_r', is the amount of time that the solute spends sorbed on the column and therefore is calculated by subtracting the column dead time from the solute retention time.

$$t_r' = t_r - t_0 \qquad (33)$$

Because of differences in column dimensions and packing, the absolute retention time is not a unique characteristic measure of the solute retention. A more useful measure of solute retention is the ratio of the time the solute spends in the stationary phase to the time it spends in the mobile phase. This is called the capacity factor, k', and is the

ratio of the adjusted retention time to the column dead time, as shown in Equation 34.

$$k' = \frac{t_r'}{t_0} = \frac{(t_r - t_0)}{t_0} \qquad (34)$$

Table 4.1 lists the column dead time, the solute retention time and the calculated capacity factor for HSH, CSH, GSH, and PSH chromatographed with a mobile phase consisting of pH 3.0 phosphate buffer containing 0.75 mM SOS and 5% methanol. All measurements were made in centimeters and were converted to minutes by dividing the distance by the chart speed setting. More measurements were taken for the cysteine due to its short retention time. As well, half of the cysteine runs were made with a faster chart speed to get more precise measurements for t_0 and t_r. The relative standard deviation of k' for the thiols was 1.9% for the CSH, 2.0% for the GSH, 1.8% for the HSH, and 1.3% for the PSH. The CSH has the shortest retention time while the PSH has the longest retention time. The lower percent deviation for the PSH is probably due to the higher precision in measuring the longer retention time. A capacity factor between 2 and 5 is considered ideal. However, for the analysis of multiple components the range may extend from 1 to 15 [117] or 1 to 10 [118]. Of the four thiols studied, only the penicillamine had a k' value between 2 and 5.

Table 4.1. Retention times and calculated capacity factors for the thiols CSH, HSH, GSH and PSH. All samples were run on a Partisil 5 ODS-3 column using a pH 3.0 phosphate buffer as the mobile phase.

Compound	Speed cm/min	t_0 cm	t_r cm	k'	average (std. dev.)
CSH	1.0	2.29	3.15	0.376	0.387
		2.28	3.15	0.382	(0.007)
		2.28	3.18	0.395	
		2.30	3.20	0.391	
		2.29	3.18	0.389	
		2.29	3.18	0.389	
	2.0	4.59	6.30	0.372	
		4.52	6.29	0.392	
		4.55	6.30	0.385	
		4.55	6.28	0.380	
		4.49	6.26	0.394	
		4.50	6.28	0.396	
		4.49	6.23	0.388	
HSH	2.0	4.43	9.49	1.14	1.15
		4.40	9.49	1.16	(0.01)
		4.41	9.43	1.14	
		4.40	9.52	1.16	
		4.39	9.49	1.16	
		4.41	9.53	1.16	
		4.40	9.42	1.14	
GSH	2.0	4.57	9.12	1.00	1.01
		4.52	9.03	1.00	(0.02)
		4.41	9.01	1.04	
		4.48	9.07	1.02	
		4.51	9.00	1.00	
PSH	2.0	4.60	15.29	2.32	2.32
		4.61	15.28	2.31	(0.03)
		4.60	15.32	2.33	
		4.51	15.17	2.36	
		4.68	15.35	2.28	

Table 4.2 gives the k' values for the symmetrical disulfides of homocysteine, cysteine, glutathione, and penicillamine. With the exception of the cystine, all of the disulfides displayed a k' value between 2 and 7. For this reason the relative standard deviations of the capacity factors for the disulfides tend to be lower than those calculated for the thiols. The relative standard deviations of the capacity factors for GSSG, HSSH, and PSSP are 0.7%, 1.0% and 1.4%, respectively. The short retention time for the cystine makes the measurement of its capacity factor less precise, and this is reflected in the slightly larger relative standard deviation of 2.0%.

The method used to quantify the size of a chromatographic peak can affect the accuracy and precision of the overall analysis. The two most common methods of quantifying peak size is by measuring peak area and peak height. To manually measure the peak area, several techniques may be employed [119]. Table 4.3 lists the various manual methods for measuring peak areas along with estimates for the precision of each technique. The first two methods assume the chromatographic peak to be a triangle [120]. In method one, the peak width at half peak height is measured and then multiplied by the peak height. In the second method the tangents to the sides of the peak are drawn and the peak width at the base is multiplied by the

Table 4.2. Retention times and calculated capacity factors for the symmetrical disulfides CSSC, HSSH, GSSG and PSSP. All samples were run on a Partisil 5 ODS-3 column using a pH 3.0 phosphate buffer as the mobile phase.

Compound	Speed cm/min	t_0 cm	t_r cm	k'	average (std. dev.)
CSSC	1.0	2.71	3.92	0.446	0.441
		2.72	3.94	0.448	(0.009)
		2.72	3.93	0.445	
		2.71	3.91	0.443	
		2.72	3.92	0.441	
		2.75	3.92	0.426	
		2.72	3.94	0.448	
		2.72	3.94	0.448	
		2.72	3.92	0.441	
		2.78	3.96	0.425	
		2.79	4.00	0.434	
HSSH	0.5	1.12	8.92	6.96	6.98
		1.13	8.98	6.95	(0.07)
		1.14	9.00	6.90	
		1.13	8.94	7.05	
		1.11	8.94	7.05	
		1.11	8.98	7.09	
		1.13	9.01	6.97	
GSSG	1.0	2.22	8.57	2.86	2.90
		2.21	8.58	2.88	(0.02)
		2.20	8.59	2.90	
		2.20	8.62	2.92	
		2.22	8.68	2.91	
		2.21	8.56	2.87	
		2.20	8.62	2.92	
		2.20	8.60	2.91	
		2.20	8.61	2.91	
		2.20	8.61	2.91	
		2.19	8.63	2.94	

Table 4.2 continued.

Compound	Speed cm/min	t_0 cm	t_r cm	k'	average (std. dev.)
PSSP	0.5	1.14	5.67	3.97	4.09
		1.13	5.67	4.02	(0.08)
		1.14	5.70	4.00	
		1.10	5.71	4.19	
		1.12	5.70	4.09	
		1.10	5.67	4.15	
		1.09	5.68	4.21	
		1.12	5.69	4.08	
		1.11	5.71	4.14	
		1.12	5.70	4.09	
		1.12	5.69	4.08	

Table 4.3 Manual methods of measuring chromatographic peak areas.

Method	Equation or technique	Estimate of precision[116]
1. triangular I	$H' * (W_{\frac{1}{2}})$	3%
2. triangular II	$H * (W_b)/2$	4%
3. trapezoidal	$H' * (W_{0.15} + W_{0.85})/2$	
4. planimetry	trace peak with planimeter	4%
5. cut and weigh	cut out peak and weigh	2%

H = peak height after drawing tangent lines to the two sides of the peak.

$W_{\frac{1}{2}}$ = peak width measured at half the peak height.

W_b = peak width at the base of the peak.

H' = peak height of the actual peak.

$W_{0.15}$ = peak width measured at 0.15 of the peak height.

$W_{0.85}$ = peak width measured at 0.85 of the peak height.

peak height of the extrapolated triangle. Methods using a triangular approximation are not reliable for asymmetric peaks or overlapping peaks. Although the disulfides showed symmetrical peak shapes, peak tailing was commonly observed for the thiols so these methods of quantifying peak size were inappropriate for thiol determinations.

In the cut and weigh method, the chromatogram is first photocopied, the baseline is then drawn in by pencil and each chromatographic peak is cut out and weighed. The precision of the method depends on the uniformity of the weight of the paper and on the care used in cutting out the peaks. Planimetry is a nondestructive alternative to the cut and weigh method. With planimetry, the peaks are traced using a planimeter, making this method rather tedious. Increased precision of the peak measurement can be obtained by repeated tracings over the chromatographic peak. However, this makes the measurement step even more time-consuming. As well, considerable skill in using the planimeter is required and the capabilities of the operator will determine the precision of the method.

The trapezoidal method, which involves calculating the average of the peak widths at 15% and 85% of the peak height and then multiplying by the peak height, is reported to give an accurate measure of the peak size, even for asymmetric peaks. Similarly, both the cut and weigh technique and

planimetry give excellent quantitative measurements for asymmetric peaks, but all three require tedious and time-consuming measurement or cutting steps.

) The peak height measurement method is simpler and faster than manual methods for peak area measurement. Peak heights are measured from the baseline to the peak maximum using a ruler or the marked divisions on the chart paper. Peak heights are less prone to interference by adjacent overlapping peaks so peak height measurements are preferred when peaks are not completely resolved from each other. Furthermore the precision of peak height measurements is no worse than those for peak area measurements and have a precision of 1-4% [121]. Peak area methods are used when the composition of the mobile phase is changing, eg. in gradient elution, while peak height measurements are made when the composition of the mobile phase is relatively constant and there is some variation in the flow rate. In general, the accuracy and simplicity of peak height measurement makes it the more versatile method of quantifying the size of chromatographic peaks.

Throughout this research peak heights were used to quantify the peak sizes. Before running quantitative analyses, it was necessary to verify that the use of peak heights would give a good measure of peak size for any asymmetric thiol peak. Since the cut and weigh method gives

a precise measure of peak size for asymmetric peaks, a comparison of peak height measurements to peak weights was performed. A set of calibration standards was chromatographed and the peak responses were measured by the peak height method and by the cut and weigh procedure. Figure 4.2 shows a typical chromatogram for one of the calibration standards. Plots of peak heights versus peak weights for PSH, GSH, PSSP, and GSSG are displayed in Figure 4.3. Even with the tailing observed for the PSH peak there is a good linear correlation between the peak height and the peak weight implying that the peak height will be an adequate measure of the peak size, even if the peak is asymmetric.

The precision of peak height measurements was evaluated by determining the standard deviation for a peak heights obtained from replicate injections of a solution having a fixed analyte concentration. Table 4.4 gives the results for a series of chromatographic runs of a solution containing 25 μM GSH and 275 μM GSSG. The samples were run using a mobile phase of pH 3.0 phosphate buffer. The measured peak heights were converted to peak currents and averaged. The glutathione had an average peak current of 69.7 nA with a standard deviation of 0.4 nA while the GSSG had an average peak current of 115.2 nA with a standard deviation of 1.0 nA. These correspond to relative standard

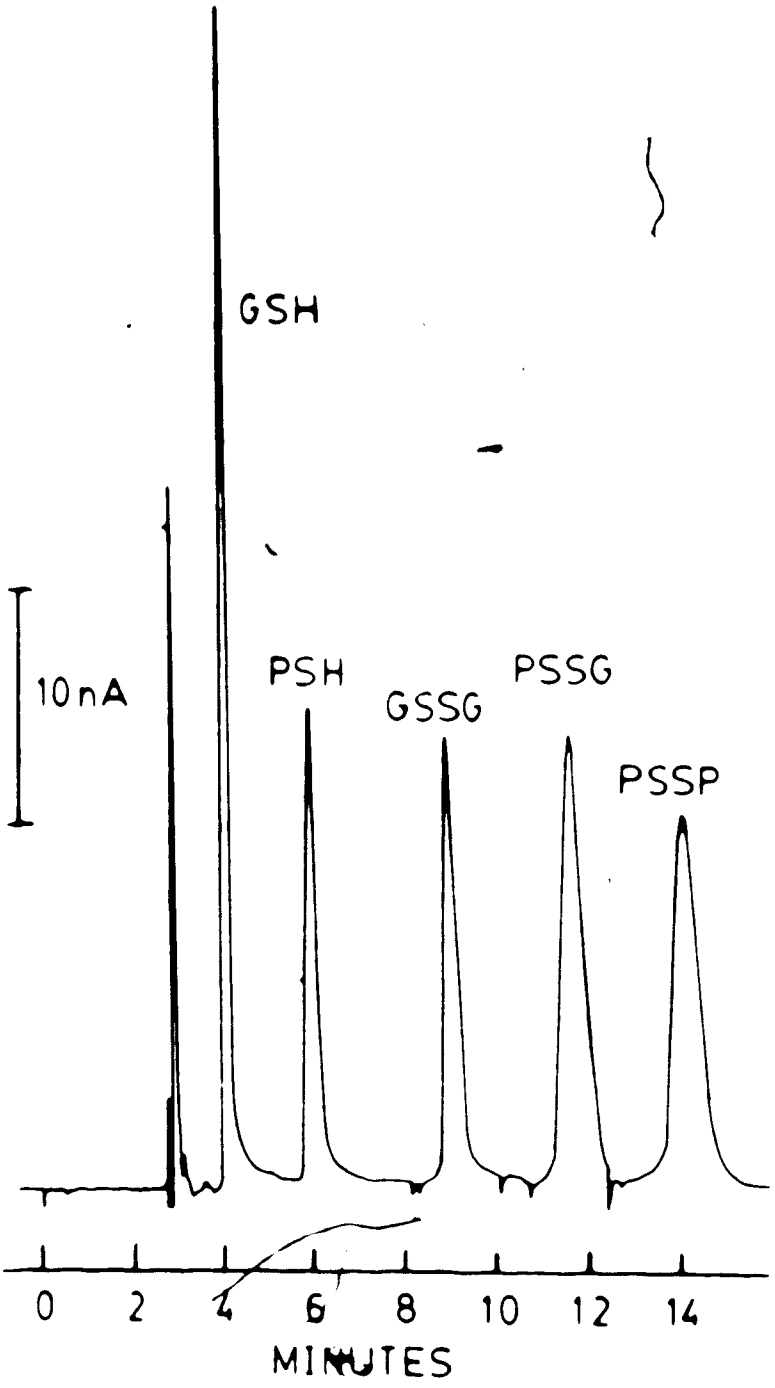

Figure 4.2. A typical chromatogram of a mixture containing PSH, GSH, GSSG, PSSG and PSSP used to compare peak height with peak weight measurements. The mobile phase used for the separation was a pH 3.0 phosphate buffer (0.1 M) with 0.80 mM sodium octyl sulphate and 3% methanol.

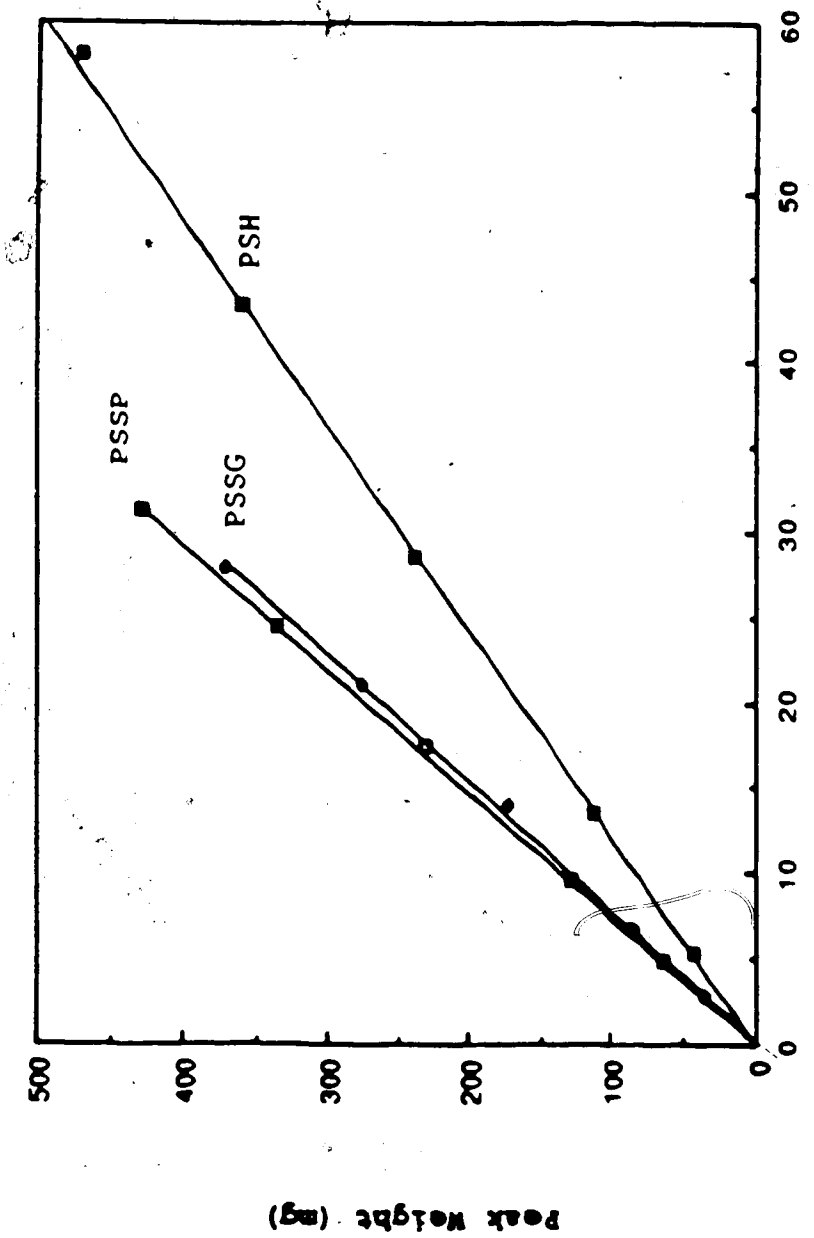

Figure 4.3. Plots of peak height versus peak weight measurements for PSH, PSSG and PSSP from a calibration series of chromatograms.

Table 4.4. Precision of peak height measurements for GSH and GSSG using a pH 3.0 phosphate buffer as the mobile phase and having an upstream electrode potential of -1.000 V. and downstream electrode potential of +0.150 V. versus Ag/AgCl.

	25μM GSH			275μM GSSG		
	Peak Height	Range	Peak Current	Peak Height	Range	Peak Current
1.	3.45	500	69.00	14.62	200	116.96
2.	3.45	500	69.00	14.55	200	116.40
3.	3.48	500	69.60	14.40	200	115.20
4.	3.50	500	70.00	14.31	200	114.48
5.	3.50	500	70.00	14.31	200	114.48
6.	3.50	500	70.00	14.21	200	113.68
7.	3.50	500	70.00	14.42	200	115.36
8.	3.48	500	69.60			
9.	3.46	500	69.20			
10.	3.50	500	70.00			
11.	3.47	500	69.40			
12.	3.51	500	70.20			
Average			69.70			115.22
(std. dev.)			0.62			0.99

deviations of 0.6% for the reduced glutathione and 1.0% for the oxidized glutathione. Even with the small peak heights measured for the glutathione the precision of the measurement is high.

D. Retention Studies

The precision of the retention time and peak height measured for any peak will depend, in part, on the resolution of that peak from any adjacent peaks. By observing the retention behaviour of thiols and disulfides when the mobile phase parameters are varied, appropriate conditions can be selected to optimize the separation of a mixture and thereby maximize the precision of the measurements.

In reverse phase chromatography it is thought that solute molecules are adsorbed onto the stationary phase because of hydrophobic interactions involving the nonpolar sites on the solute molecules, the nonpolar ligands on the stationary phase and the polar mobile phase [122,123]. The selectivity of a separation, however, is chiefly due to specific solute interactions with the mobile phase. The exact mechanism of this retention is not completely understood and a detailed explanation of current theory is beyond the scope of this thesis. It suffices to say that

selectivity of the separation of ionic molecules can be controlled by changes in the mobile phase composition.

The retention characteristics of the thiols, HSH, CSH, GSH, and PSH, and their symmetrical disulfides, HSSH, CSSC, GSSG, and PSSP, were studied to determine the chromatographic conditions needed to achieve the desired separation for the analysis of a mixture of some of these components. The retention behaviour of the analytes, as measured by their capacity factor, was observed as a function of three parameters; the mobile phase pH, the concentration of ion-pairing reagent in the mobile phase, and the organic modifier content of the mobile phase. Each of these will be discussed individually with an overview of their effects being reserved for the final discussion section in this chapter.

i) Mobile Phase pH

First, the effect of mobile phase pH on the retention characteristics of HSH, CSH, GSH, PSH and their symmetrical disulfides was studied. The procedure involved making multiple injections of thiols and disulfides into mobile phases having pH values in the range 2.5 to 5.5. This pH range was used since it is within the working range of the reverse phase octadecyl silane column [124] and because the rate of thiol oxidation decreases significantly below pH 5.5

Figure 4.4 shows the retention behaviour of homocysteine, cysteine, glutathione, and penicillamine as a function of the mobile phase pH. The mobile phase was composed of 0.1 M sodium phosphate/phosphoric acid buffer set at the various pH values by the addition of sodium hydroxide.

In general, all four thiols showed a decrease in capacity factor with an increase in mobile phase pH, although the extent of the effect was different for each compound. Since each compound is composed of carboxylic acid, ammonium and sulfhydryl groups, the differences in the ionization of these acidic functional groups will lead to differences in the molecular species present in solution at the various pH settings. These different species will have different charges which will therefore affect the retention of the compound.

The macroscopic ionization scheme for cysteine, homocysteine and penicillamine is:

$$H_3A^+ \overset{K_1}{\rightleftharpoons} H_2A \overset{K_2}{\rightleftharpoons} HA^- \overset{K_3}{\rightleftharpoons} A^{2-} \qquad (35)$$

while the macroscopic ionization scheme for glutathione is:

$$H_4A^+ \overset{K_1}{\rightleftharpoons} H_3A \overset{K_2}{\rightleftharpoons} H_2A^- \overset{K_3}{\rightleftharpoons} HA^{2-} \overset{K_4}{\rightleftharpoons} A^{3-} \qquad (36)$$

The macroscopic deprotonation constants for HSH [125], CSH, PSH and GSH [126] are listed in Table 4.5. Using these

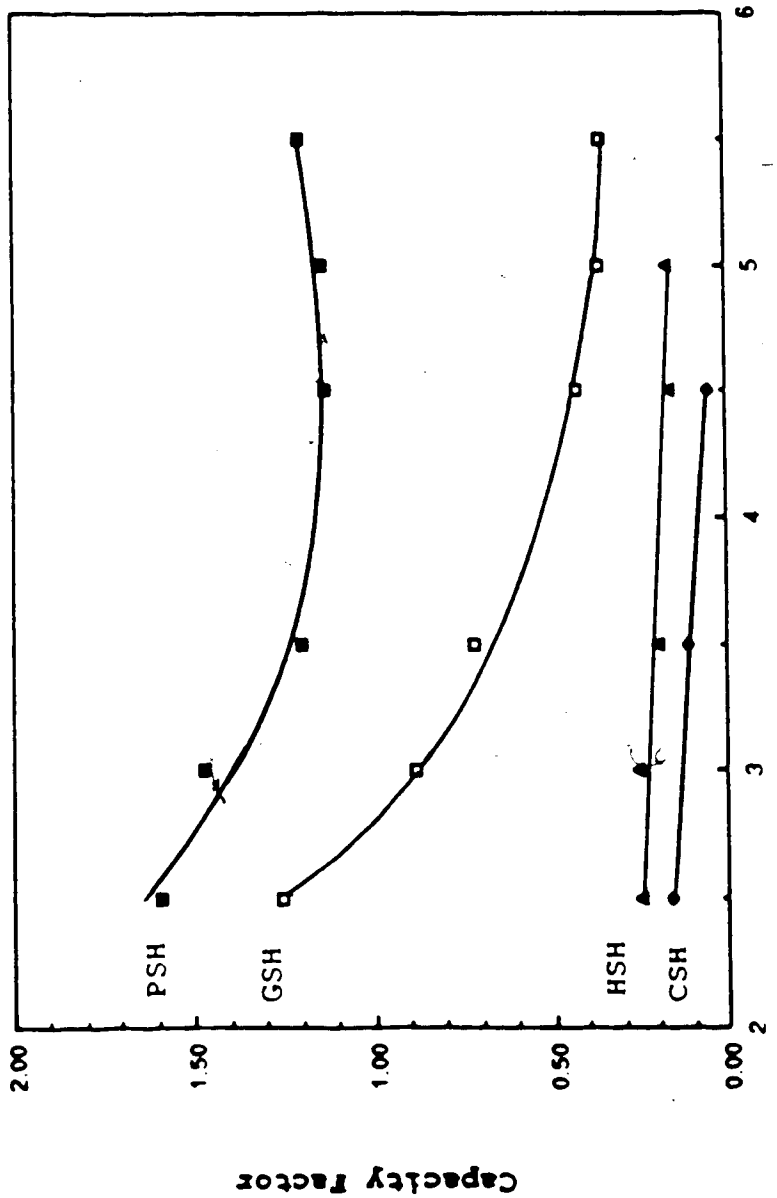

Figure 4.4. A plot of the capacity factor for HSH, CSH, PSH, and GSH as a function of the mobile phase pH. All mobile phases contained 0.1 M phosphate buffer.

Table 4.5. Macroscopic dissociation constants for CSH, HSH, GSH and PSH.

Compound	K_1	K_2	K_3	K_4	Reference
CSH	1.87	8.19	10.29		126
HSH	2.27	8.66	10.55		125
GSH	2.05	3.47	8.67	9.49	126
PSH	2.47	7.93	10.41		126

constants, the fractional concentration of the various ionized species of each molecule was calculated as a function of pH. Since the macroscopic ionization scheme is identical for cysteine, homocysteine and penicillamine, the distribution diagrams for these three thiols will be similar. Figures 4.5 to 4.7 show the species distribution diagrams for HSH, CSH, and PSH, respectively, over the pH range 0 to 5.5. Over this pH range, these thiols are present in two molecular forms. At low pH the dominant species is the fully protonated thiol which carries a net charge of +1 while the doubly charged (one positive and one negative) zwitterion becomes dominant at the higher pH values plotted. As the pH is raised from 2.5 to 5.5 the dominant species changes from the more strongly sorbed +1 form to the less strongly sorbed zwitterion. Hence, a decrease in capacity factor is observed for an increase in the mobile phase pH.

The small k' values for the cysteine and homocysteine made it difficult to observe any significant changes as a function of the mobile phase pH. However, the capacity factor for homocysteine was larger than that for cysteine over the entire pH range investigated. Studies on homologous compounds have shown that increasing the number of repeating groups e.g. the number of aliphatic carbon atoms for a series of compounds, corresponds to increases in

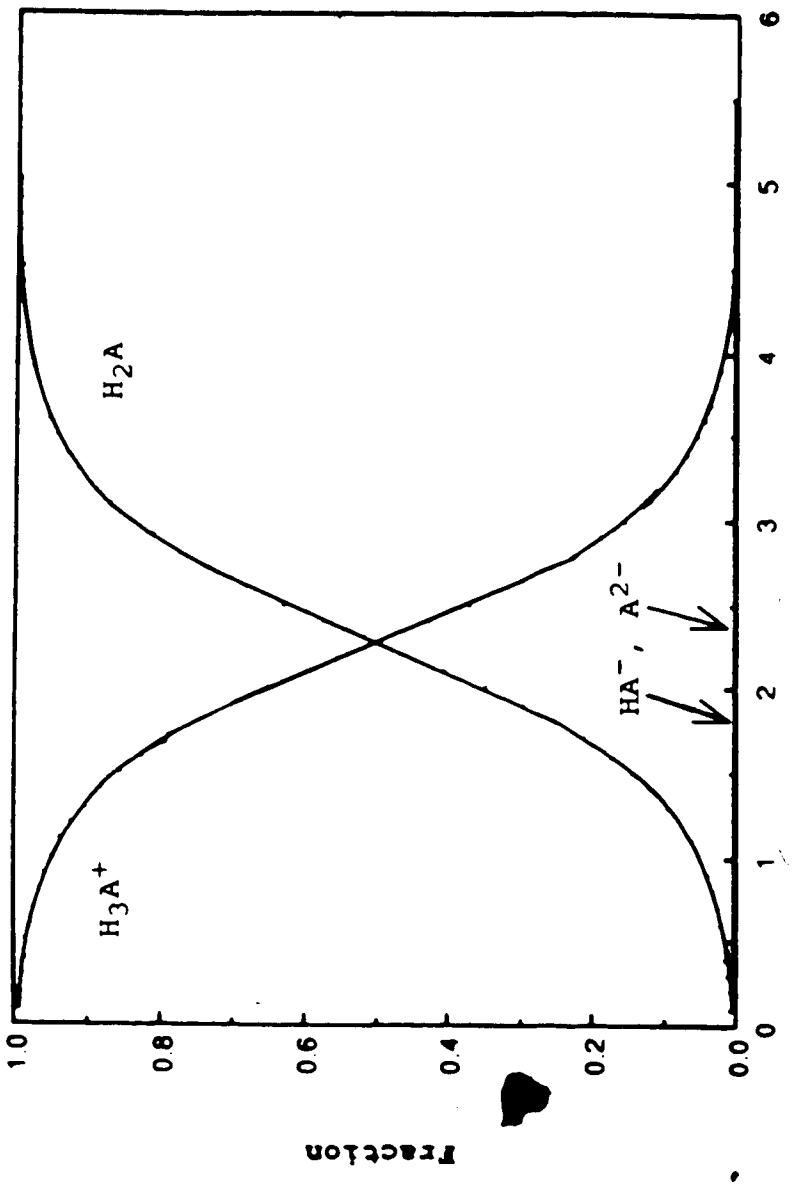

Figure 4.5. Species distribution diagram for homocysteine as calculated using the dissociation constants listed in Table 4.5.

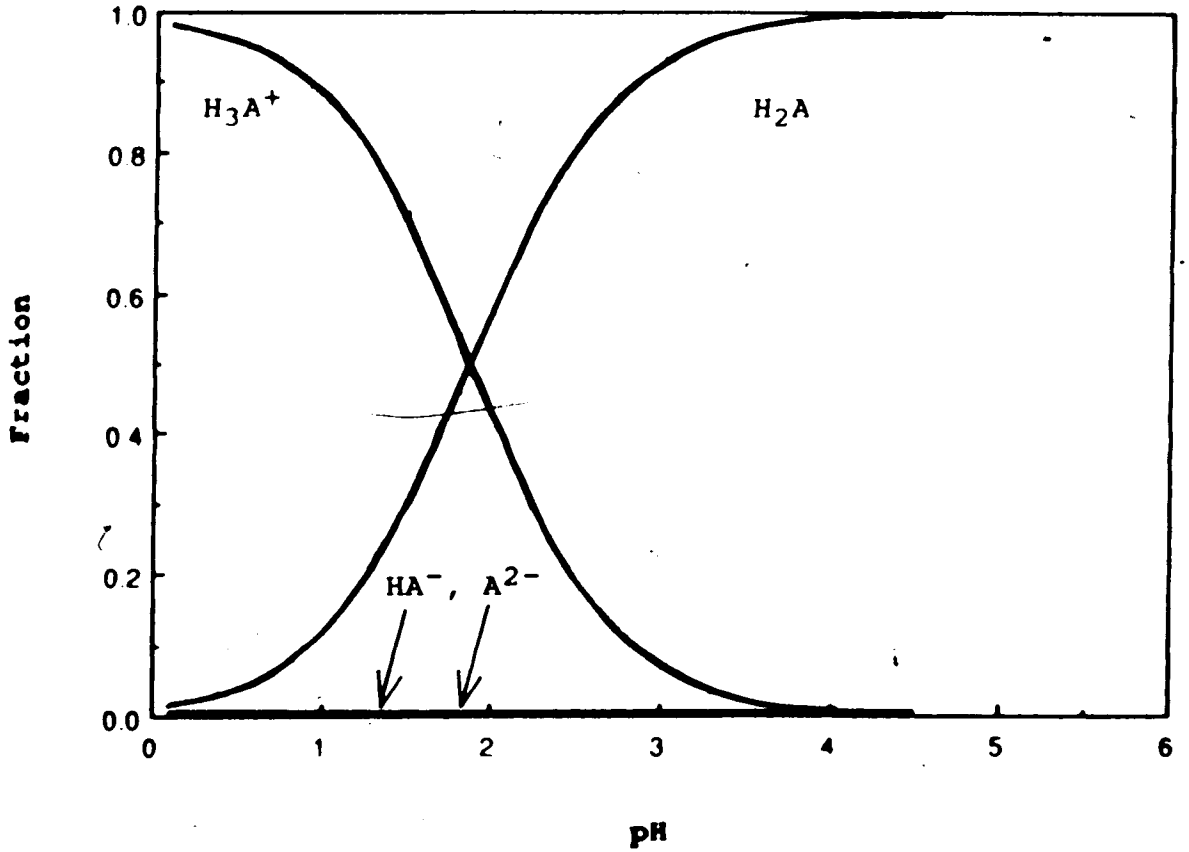

Figure 4.6. Species distribution diagram for cysteine as calculated using the dissociation constants listed in Table 4.5.

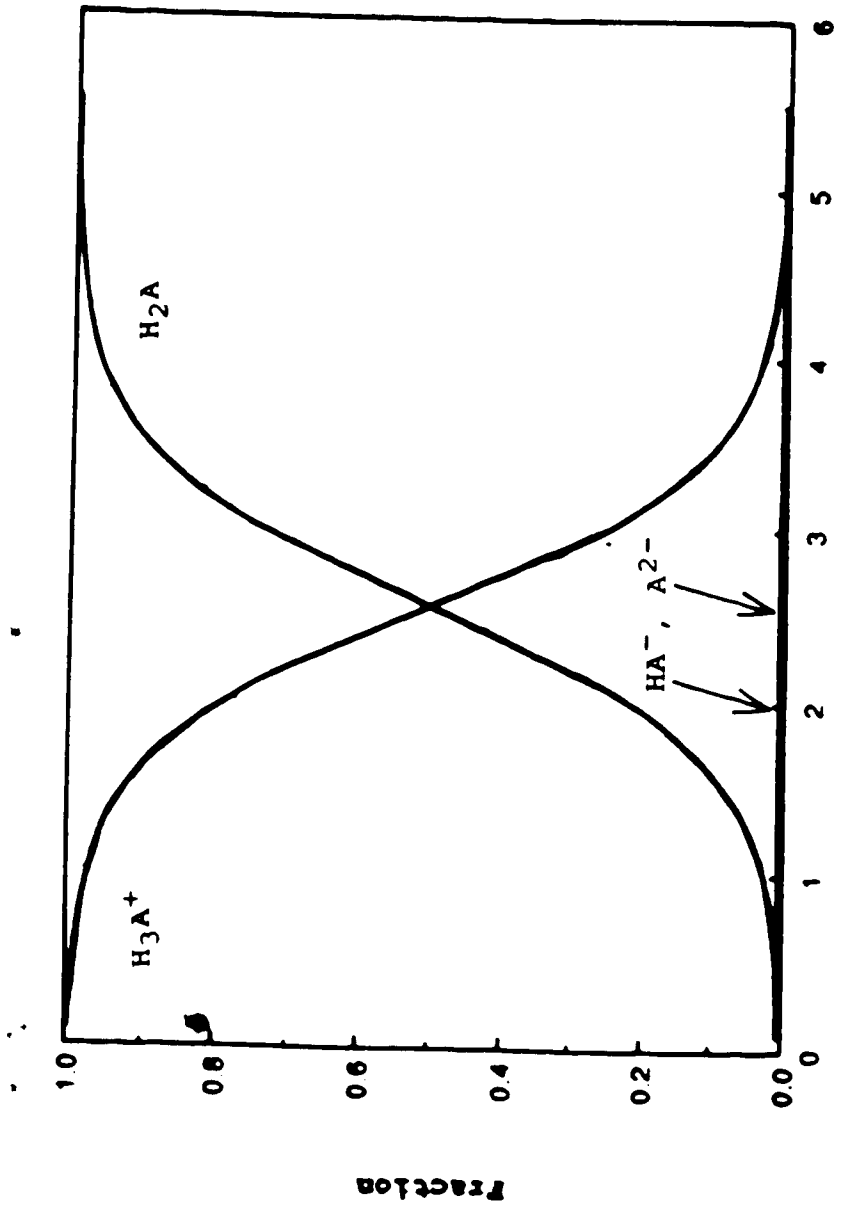

Figure 4.7. Species distribution diagram for penicillamine as calculated using the dissociation constants listed in Table 4.5.

the capacity factor and has been generalized by the Martin rule:

$$\log k' = A + Bn \qquad (37)$$

where A and B are constants for a given homologous series and a given LC system under isocratic elution. The term n is the number of repeating groups within the sample molecule [127].

Furthermore, any changes in the carbon skeleton which increase the hydrophobic nature of the compound should increase the capacity factor for that compound since it will be more readily retained by the nonpolar stationary phase. Penicillamine is a β,β-dimethyl analog of cysteine and therefore has an increased carbon length compared to cysteine, and increased branching of the carbon chain. Increasing the branching of the carbon skeleton increases the nonpolar nature of the molecule. As expected, the capacity factor for penicillamine, seen in Figure 4.4, is much greater than that for cysteine and homocysteine at all monitored pH values.

The species distribution diagram for glutathione in Figure 4.8 was constructed from the calculated fractional concentrations of the various ionized species. Three molecular species are present over the pH range plotted: the fully protonated form, which has a net charge of +1, the neutral zwitterion, and the doubly deprotonated form which

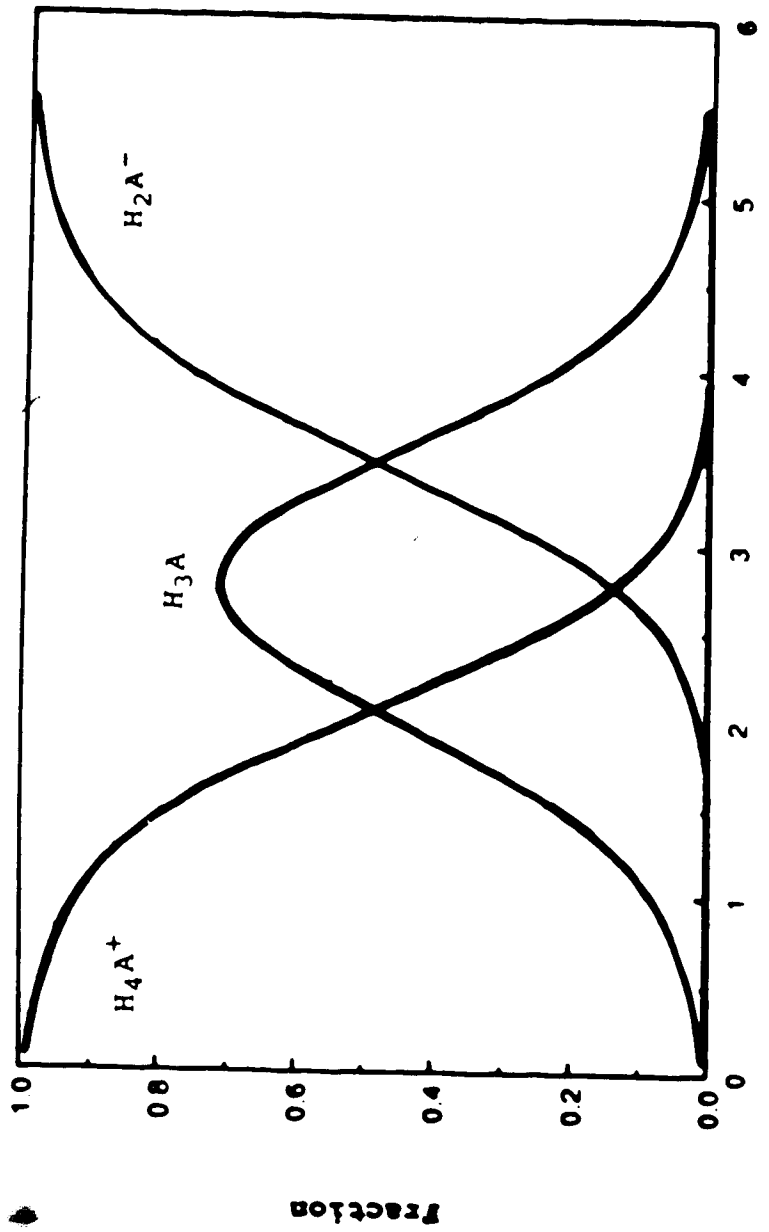

Figure 4.8. Species distribution diagram for glutathione as calculated using the dissociation constants listed in Table 4.5.

decline in the fraction of glutathione in the doubly charged zwitterionic form which is accompanied by an increase of glutathione in the doubly deprotonated form. The glutathione in the doubly deprotonated form is more hydrophilic than that in the zwitterionic form and therefore at higher pH, more of the glutathione will spend more time in the mobile phase and thus it will elute faster. This is in agreement with the observed retention behaviour for glutathione shown in Figure 4.8.

The effect of mobile phase pH on the retention behaviour of the disulfides HSSH, CSSC, PSSP, and GSSG is shown in Figure 4.9. The disulfides have larger capacity factors than their corresponding thiols at the same pH values. This is due to the increased size of the disulfide relative to the thiols. The cystine, homocystine and oxidized penicillamine show little change in capacity factor as a function of the pH. The macroscopic ionization scheme for these compounds is:

$$H_4A^{2+} \underset{}{\overset{K_1}{\rightleftharpoons}} H_3A^{+} \overset{K_2}{\rightleftharpoons} H_2A \overset{K_3}{\rightleftharpoons} HA^{-} \overset{K_4}{\rightleftharpoons} A^{2-} \qquad (38)$$

and the corresponding ionization constants for these compounds, along with the constants for oxidized glutathione, are listed in Table 4.6. Figures 4.10 to 4.12 show the species distribution diagrams for homocystine, cystine and oxidized penicillamine, respectively. The three

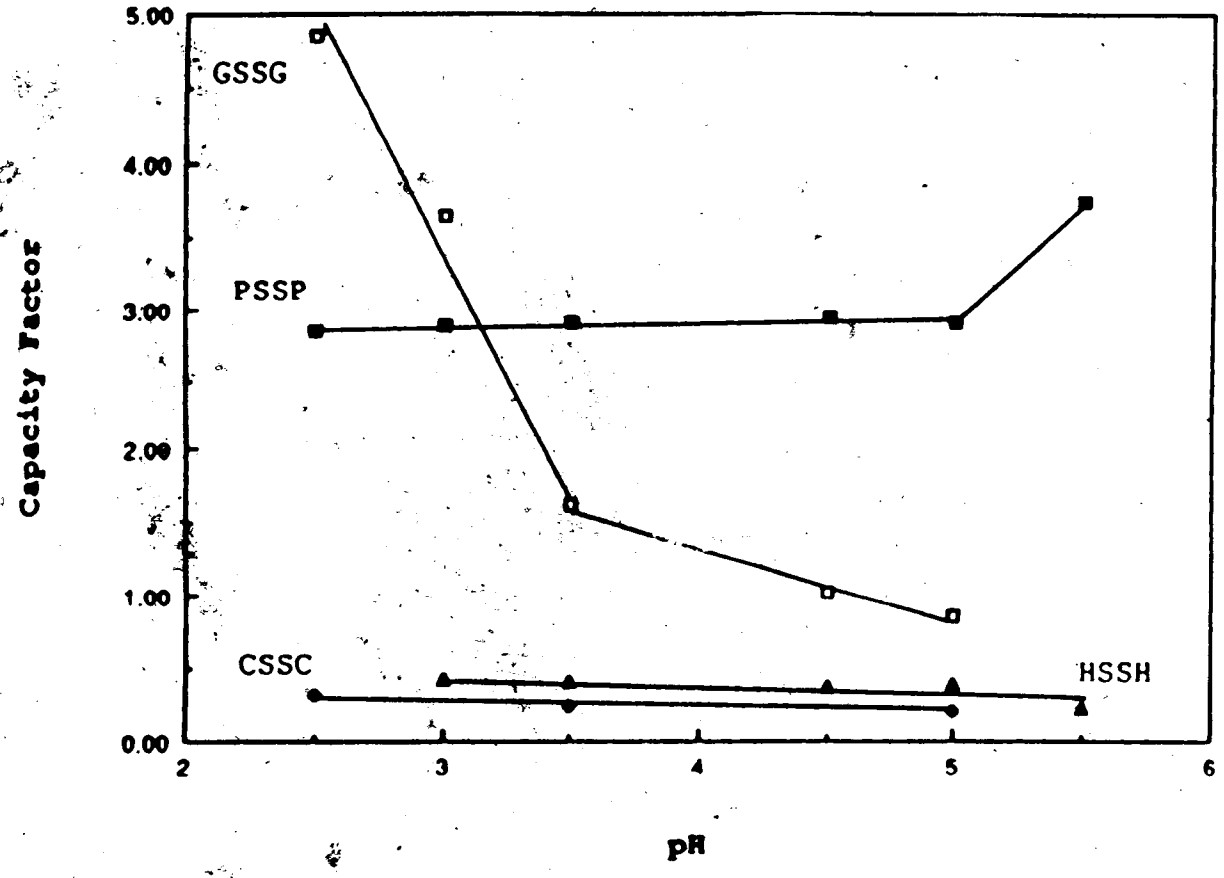

Figure 4.9. The capacity factors for HSSH, CSSC, GSSG and PSSP as a function of mobile phase pH. A 0.1 M phosphate buffer was used for the mobile phase with pH adjustment by the addition of sodium hydroxide.

Table 4.6. Macroscopic dissociation constants for CSSC, HSSH, GSSG and PSSP.

Compound	K_1	K_2	K_3	K_4	Reference
CSSC	1.51	2.21	7.88	9.30	126
HSSH	1.59	2.54	8.52	9.44	128
GSSG	1.58	2.41	3.08	4.00	126
PSSP	1.40	2.05	7.52	8.55	126

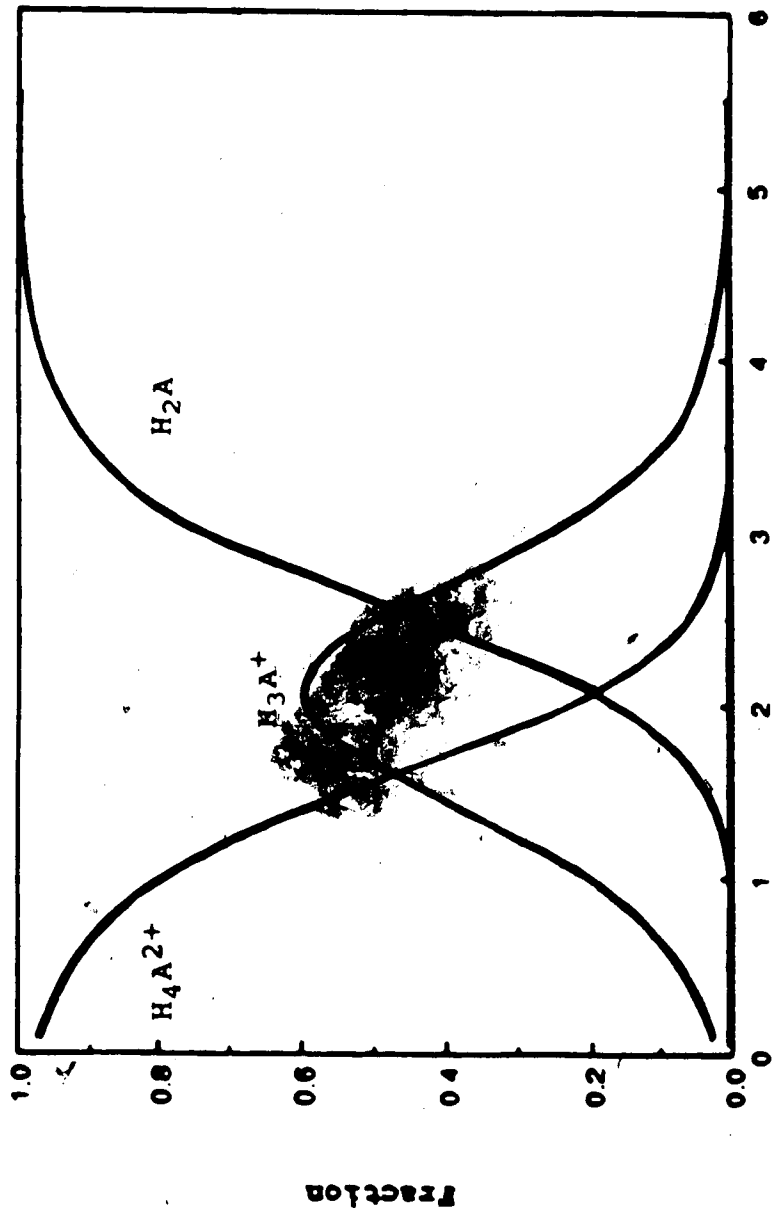

Figure 4.10. Species distribution diagram for homocystine as calculated using the dissociation constants listed in Table 4.6.

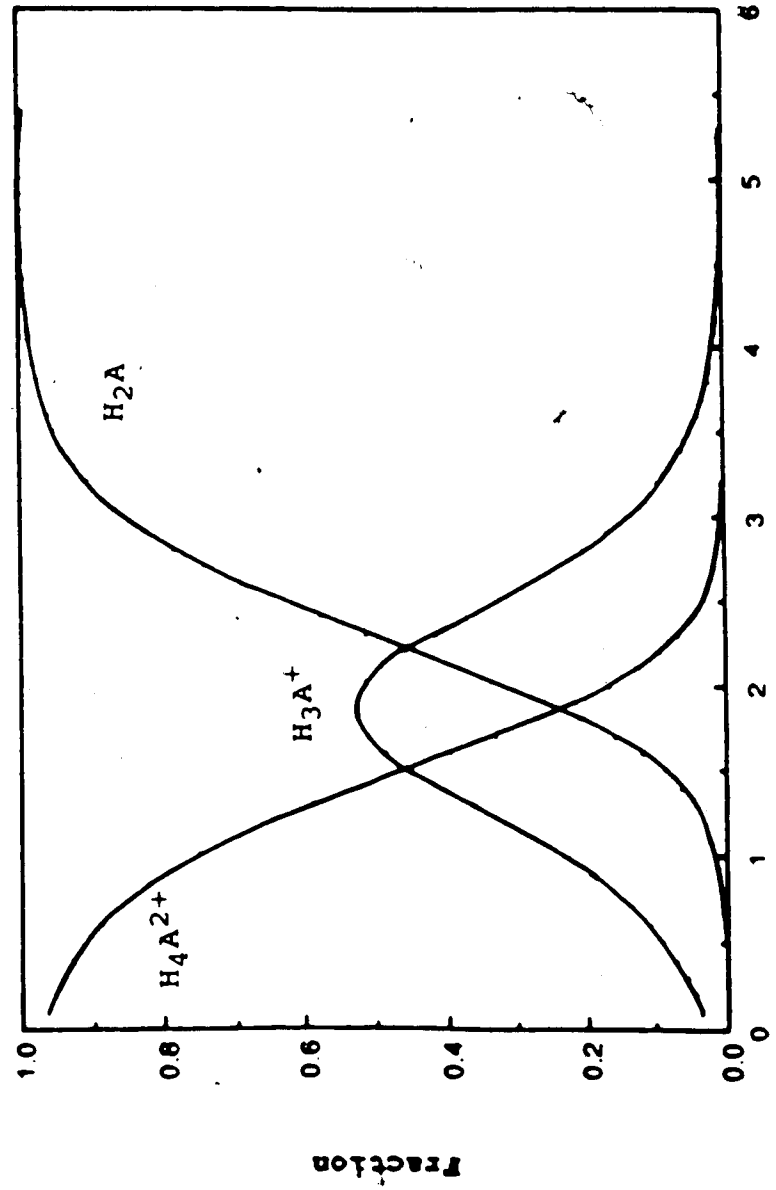

Figure 4.11. Species distribution diagram for cystine as calculated using the dissociation constants listed in Table 4.6.

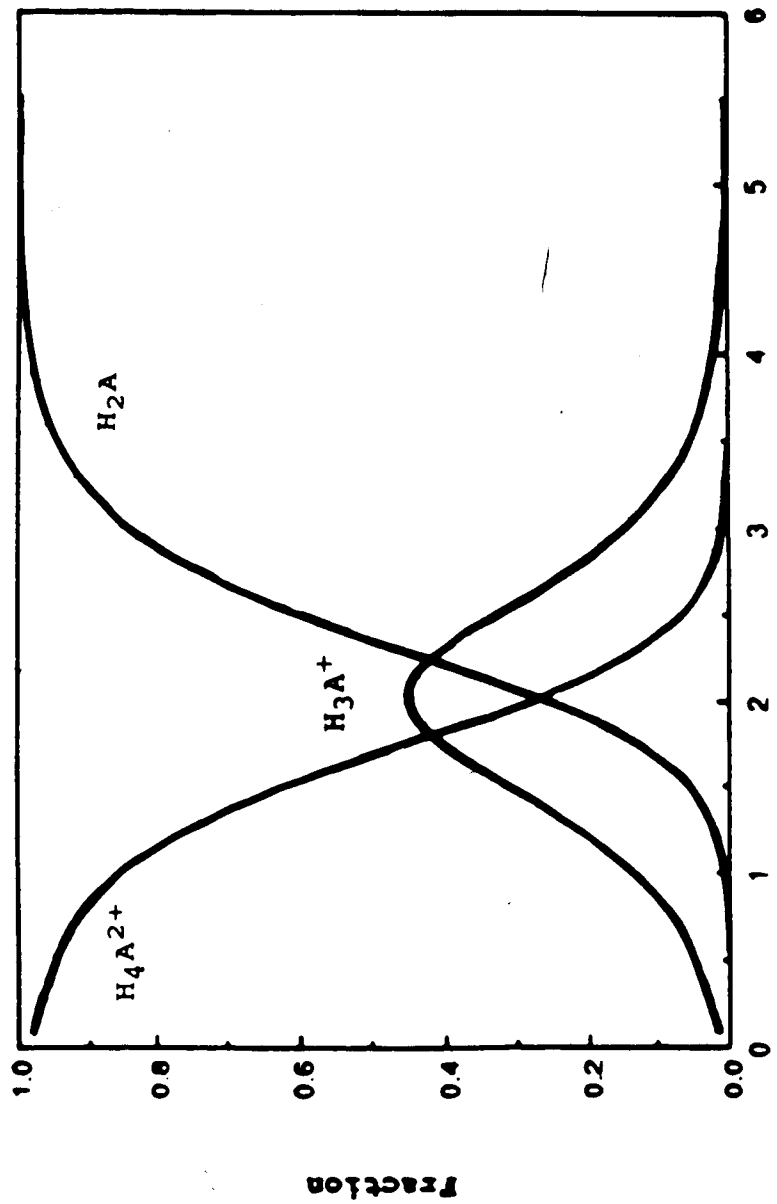

Figure 4.12. Species distribution diagram for oxidized penicillamine as calculated using the dissociation constants listed in Table 4.6.

molecular species observed in the plots correspond to the fully protonated form, which has a net charge of +2, the singly deprotonated +1 form, and the zwitterionic form which has no net charge. The major species for the disulfides of cysteine, homocysteine, and penicillamine is the zwitterionic form. Since this species dominates over the entire pH range examined there is little change in the retention behaviour of these three disulfides over the pH range studied.

Oxidized glutathione displays a significant decrease in capacity factor as the mobile phase pH is increased. The macroscopic ionization scheme for GSSG is:

$$H_6A^{2+} \overset{K_1}{\rightleftharpoons} H_5A^{+} \overset{K_2}{\rightleftharpoons} H_4A \overset{K_3}{\rightleftharpoons} H_3A^{-} \overset{K_4}{\rightleftharpoons} H_2A^{2-} \overset{K_5}{\rightleftharpoons} HA^{3-} \overset{K_6}{\rightleftharpoons} A^{4-} \qquad (39)$$

The species distribution diagram for oxidized glutathione is shown in Figure 4.13. As the pH is increased from 2.5 to 5.5, three molecular species, in turn, become dominant. At low pH the doubly charged zwitterion species is the major form of oxidized glutathione. As the pH is increased, the concentration of the -1 charged species reaches a maximum and finally at higher pH values the -2 charged species rises to a maximum. The decrease in the capacity factor for the oxidized glutathione correlates well with the increase in the negatively charged species in solution. Between pH 2.5

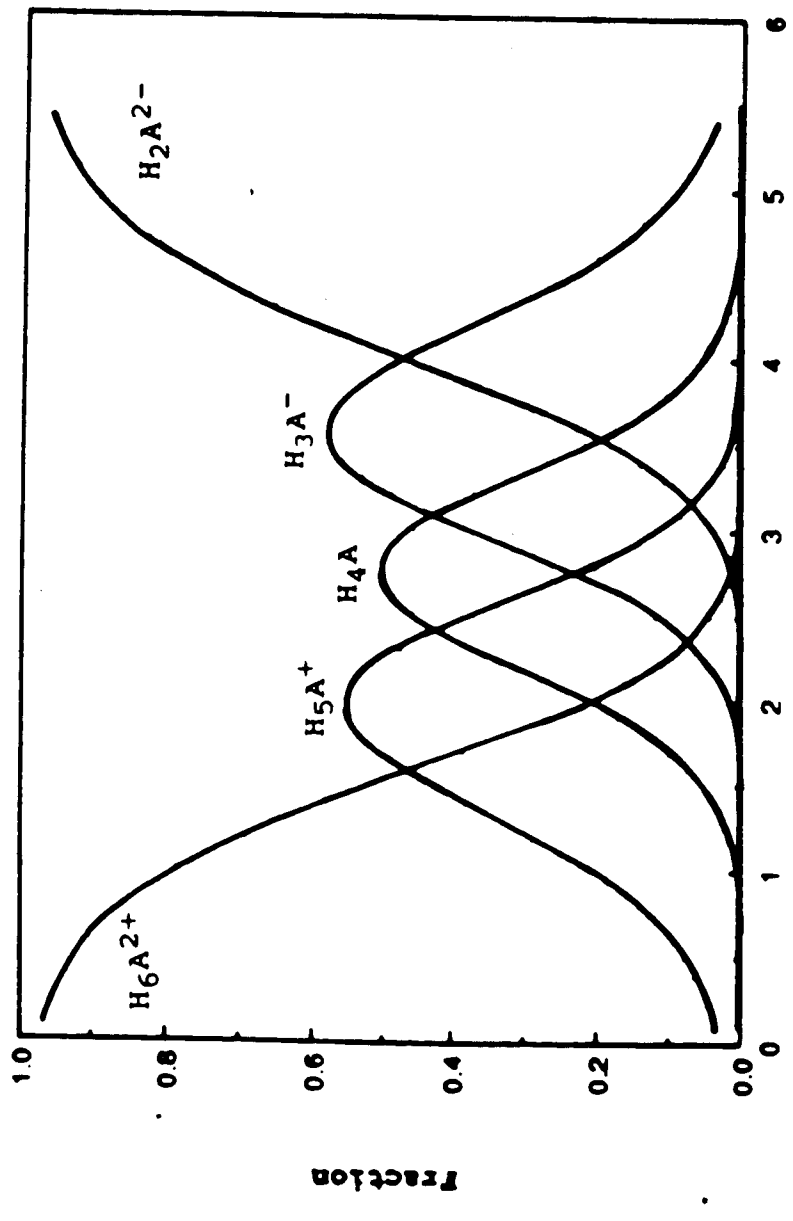

Figure 4.13. Species distribution diagram for oxidized glutathione as calculated using the dissociation constants listed in Table 4.6.

and 3.5 the capacity factor for oxidized glutathione decreases rapidly. Over this same pH region, the fraction of the GSSG in the zwitterionic form decreases while the fractions of both the -1 and the -2 charged species increase. At about pH 3.5 the fraction of GSSG in the -1 charged form reaches a maximum and begins to decline at higher pH values. Similarly, at pH values above 3.5 the rate of the decrease in the capacity factor of the oxidized glutathione diminishes.

For all subsequent studies a mobile phase pH of 3.0 was used. At this pH, the major fraction of all of the thiols and disulfides studied are present as non-ionic species. As well, at this pH the rate of thiol autoxidation is minimized.

ii) Concentration of Ion-pairing Reagent

Because of the short retention times for cysteine, homocysteine, cystine, and homocystine over the entire pH range studied in the above section, it was necessary to further modify the mobile phase to get adequate separation of these compounds from the solvent front. One method for increasing the retention times of ionic solute molecules is to add ion-pairing reagents to the mobile phase [129]. Use of ion-pairing reagents is not uncommon in reversed-phase chromatography and many anionic and cationic ion-pairing reagents are readily available.

From the species distribution diagrams, the two species which are common to all of the thiols are the neutral, non-ionic form and the charged +1 or fully protonated form. Only the charged species will be capable of forming an ion-pair and since it has a net +1 charge, an anionic ion-pairing reagent will be required. Sodium octyl sulfate was selected as the ion-pairing reagent since previous studies [72,73,77,78,130] have demonstrated that this reagent is suitable for the determination of thiols and disulfides. The use of other reagents such as the sodium salt of heptane sulfonic acid has also been reported [74,75].

The dependence of the capacity factor on the concentration of sodium octyl sulfate in the mobile phase for cysteine, homocysteine, penicillamine, and glutathione is shown in Figure 4.14. The mobile phase was composed of 0.1 M phosphate buffer at pH 3.0 and contained sodium octyl sulfate in the concentration range of 0.000 to 0.001 M.

Since positively charged species form ion-pairs with the sodium octyl sulfate, and since these ion-pairs are responsible for the increased retention time of the compound, the fraction of the compound in the positively charged state will determine the extent of the increase in the capacity factor. From the species distribution diagrams, the fraction of each thiol in the fully

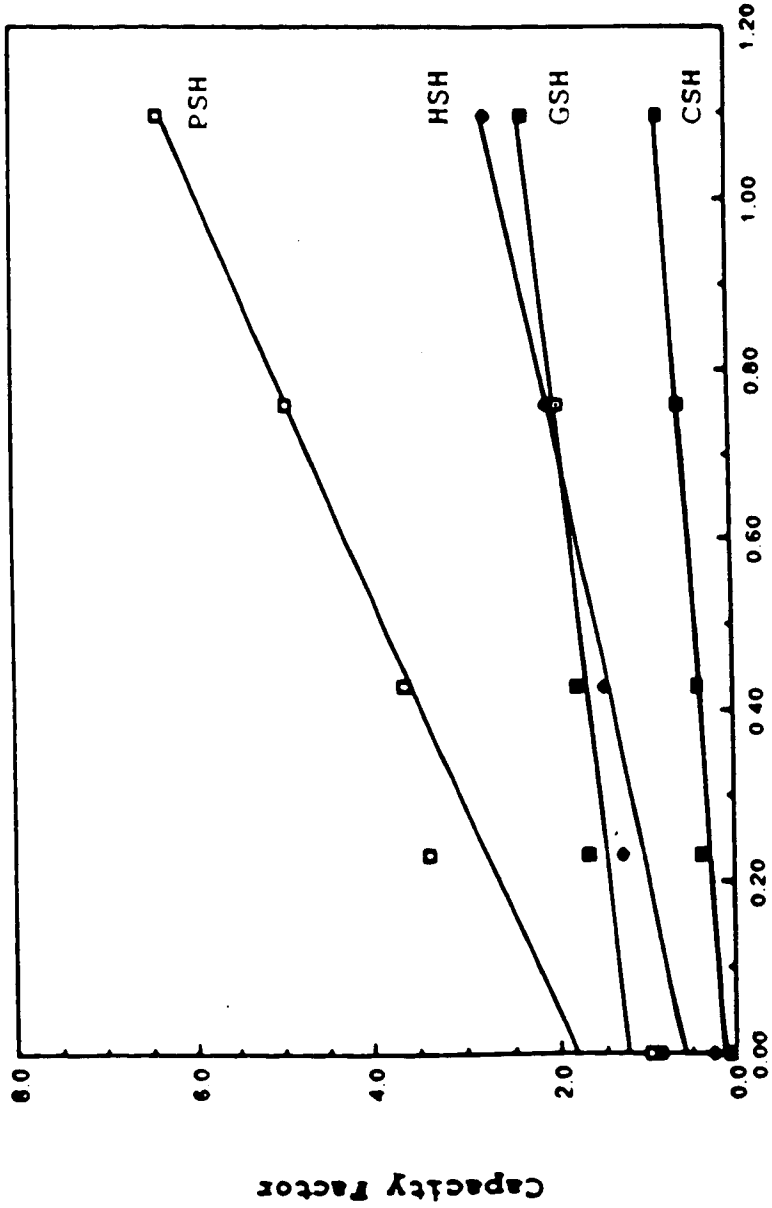

Figure 4.14. The capacity factors for HSH, CSH, GSH and PSH as a function of the concentration of sodium octyl sulphate in the mobile phase. The mobile phase consisted of pH 3.0 phosphate buffer with varying amounts of sodium octyl sulphate.

protonated form, ie. having a +1 charge at pH 3.0, is 0.069 for cysteine, 0.077 for glutathione, 0.157 for homocysteine, and 0.257 for penicillamine. These fractions predict that the effect of the concentration of the ion-pairing reagent on the capacity factor will be smallest for cysteine and greatest for penicillamine. The results in Figure 4.14 indicate that the capacity factor for each of the thiols increases linearly with an increase in the concentration of the ion-pairing reagent. Also, the magnitude of this effect increases in the order CSH ≈ GSH < HSH < PSH, in agreement with the above prediction.

Figure 4.15 shows the capacity factor as a function of the concentration of the sodium octyl sulfate in the mobile phase for CSSC, HSSH, GSSG, and PSSP. With the exception of cystine, the effect of the concentration of the ion-pairing reagent on the capacity factor was greater for the disulfides than for any of the thiols.

The species distribution diagrams for the disulfides, Figures 4.10 - 4.13, show that the fully protonated form carries a +2 charge and the first deprotonated species has a +1 charge. For cystine, homocystine and oxidized penicillamine, the major species in solution at pH 3.0 would be the zwitterionic species. As well, there will be a small fraction of the compounds having a single charge and an even smaller amount having the +2 charge. Assuming that the

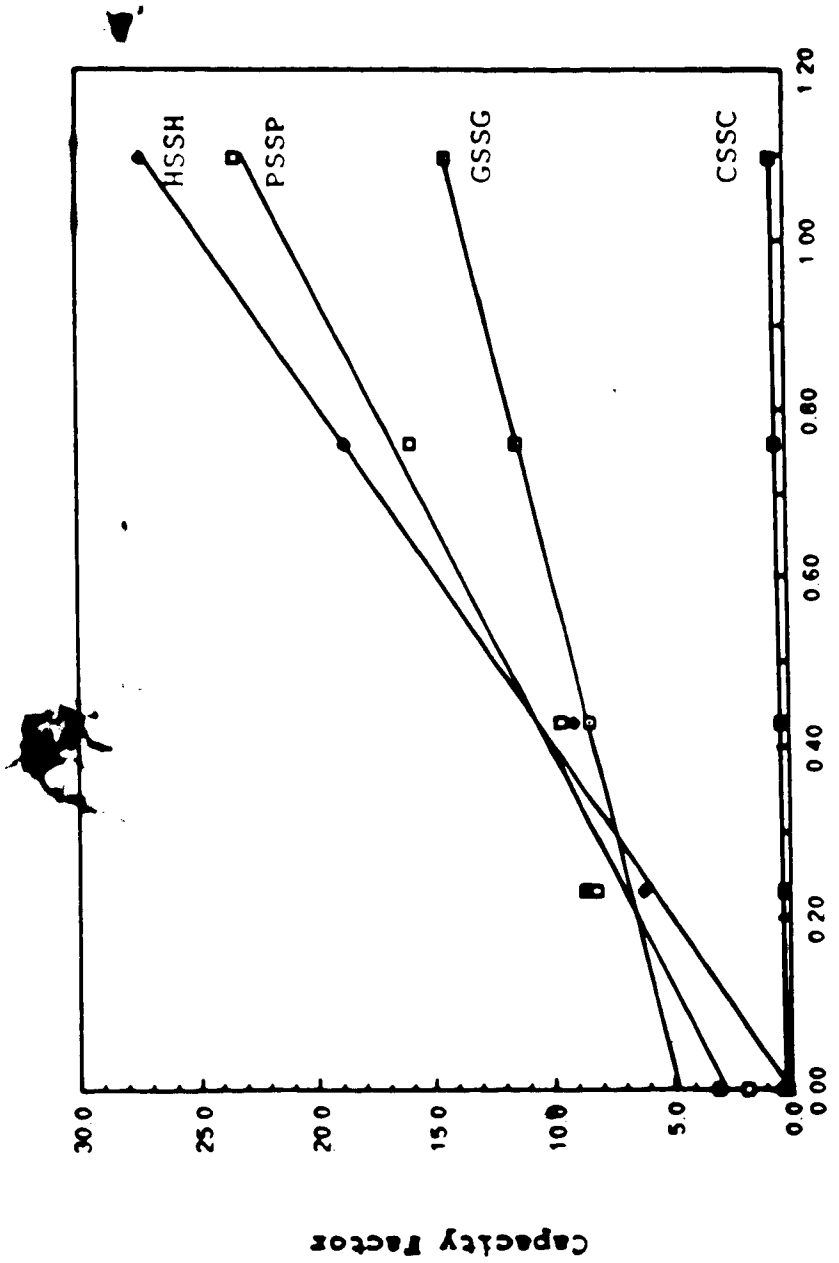

Figure 4.15. The capacity factors for HSSH, CSSC, GSSG and PSSP as a function of the concentration of sodium octyl sulphate in the mobile phase. The mobile phase consisted of pH 3.0 phosphate buffer with varying amounts of sodium octyl sulphate.

species with the +2 charge will form ion-pairs more readily than the species with the +1 charge, then the greater influence of the concentration of the sodium octyl sulfate on the capacity factor for the disulfides over the thiols may be explained, in part, by the presence of more highly charged species.

Since, at pH 3.0, the fraction of the cystine, homocystine, oxidized glutathione and oxidized penicillamine in the +1 and +2 charged species are very similar, the differences in the effect of the concentration of the ion-pairing reagent on the capacity factor cannot be due only to the charge characteristics of the molecules. Compared to cystine, both the oxidized penicillamine and the homocystine show increased hydrophobicity and therefore are expected to have greater capacity factors than the cystine. For oxidized penicillamine, the four methylene protons of cystine are replaced by methyl groups and this increases the hydrophobic nature of the molecule. Homocystine incorporates two more methylene groups into the overall length of the cystine molecule which also causes an increase in its hydrophobic nature. Both the oxidized penicillamine and the homocystine display larger slopes than the cystine for the relationship between capacity factor and concentration of the sodium octyl sulfate in the mobile phase.

Since oxidized glutathione has an increased chain length compared to cystine, it would be expected to have a longer retention time compared to cystine. However, from the species distribution diagram for GSSG in Figure 4.13, a considerable fraction of the oxidized glutathione will be in the anionic form at pH 3.0 . This would imply that a significant fraction of the GSSG will reside in the mobile phase which would reduce the retention time of the oxidized glutathione. The net result observed is that oxidized glutathione has a retention behaviour intermediate between cystine and homocystine.

iii) Concentration of Methanol

From the studies on the effect of ion-pairing reagent on the capacity factors for the thiols and disulfides, it was seen that long retention times would arise for the disulfides when enough sodium octyl sulfate was added to the mobile phase to get adequate resolution of the thiols. Addition of an organic modifier to the mobile phase will make the mobile phase less polar and thus increase the time spent by nonpolar molecules in the mobile phase [122,129]. This will result in shorter retention times for the analytes that are mainly in the nonpolar form.

To study the effect of an organic modifier on the retention behaviour of thiols and disulfides, methanol was

added to the mobile phase to cover a 0 - 10 percent range. The mobile phase was a pH 3.0 phosphate buffer and the percent methanol was calculated as the ratio of the volume of methanol to the total nominal volume of the mixed mobile phase. Figure 4.16 shows the capacity factor values for the thiols as a function of the percent methanol in the mobile phase. The trends observed here are similar to those seen in Figure 4.4 when the pH of the mobile phase was varied. The addition of methanol increases the solvent strength of the mobile phase, ie. it increases the ability of the mobile phase to solvate the nonpolar solute molecules thereby increasing the residence time of the solute molecules in the mobile phase and causing them to elute faster. The extent of the effect will, of course, depend on the specific solutes involved.

A similar trend is observed for the disulfides, as seen in Figure 4.17. The oxidized glutathione and the oxidized penicillamine show significant decreases in retention time as methanol content of the mobile phase is increased while the short retention times for cystine and homocystine make it difficult to say if any changes are occurri due to the increased methanol content.

These experiments were repeated with a mobile phase containing pH 3.0 phosphate buffer and 0.75 mM sodium octyl sulphate and varying amounts of methanol. Addition of the

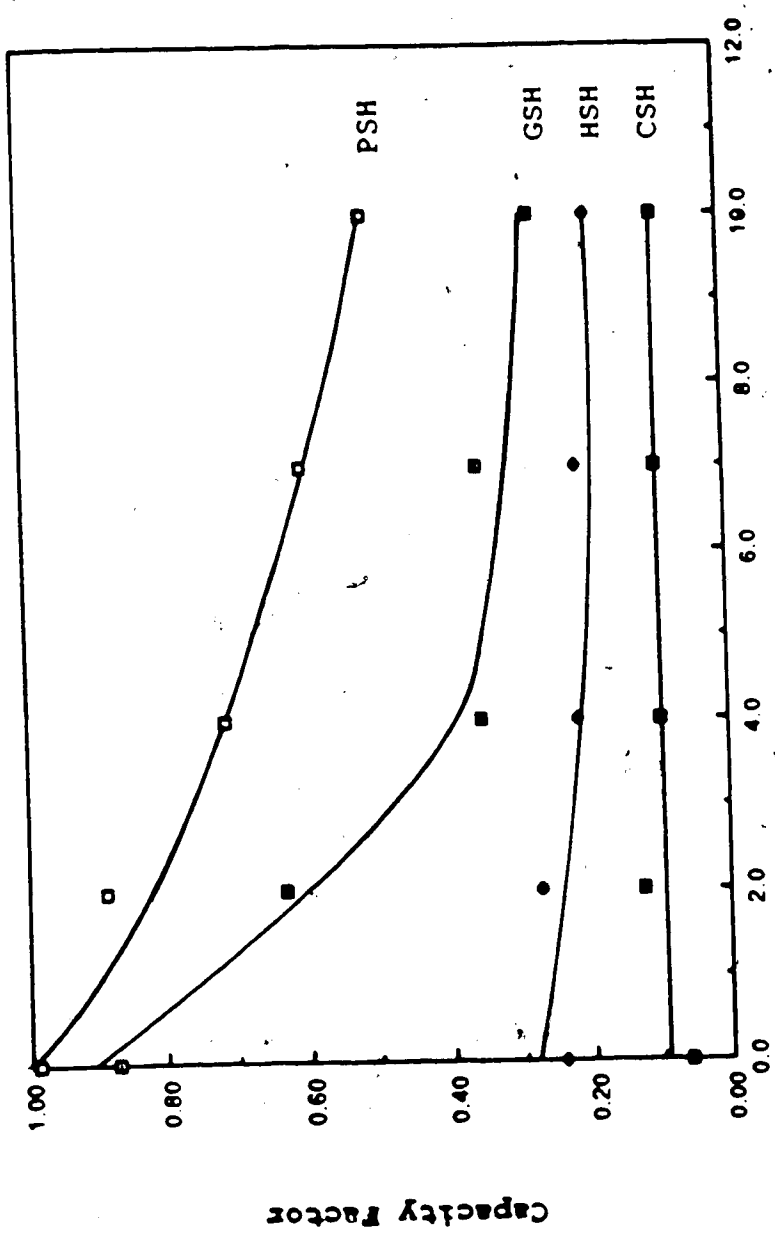

Figure 4.16. A plot of the capacity factors for HSH, CSH, GSH and PSH as a function of the percent methanol in the mobile phase. The mobile phase consisted of pH 3.0 phosphate buffer with various percentages of methanol as calculated by volumes.

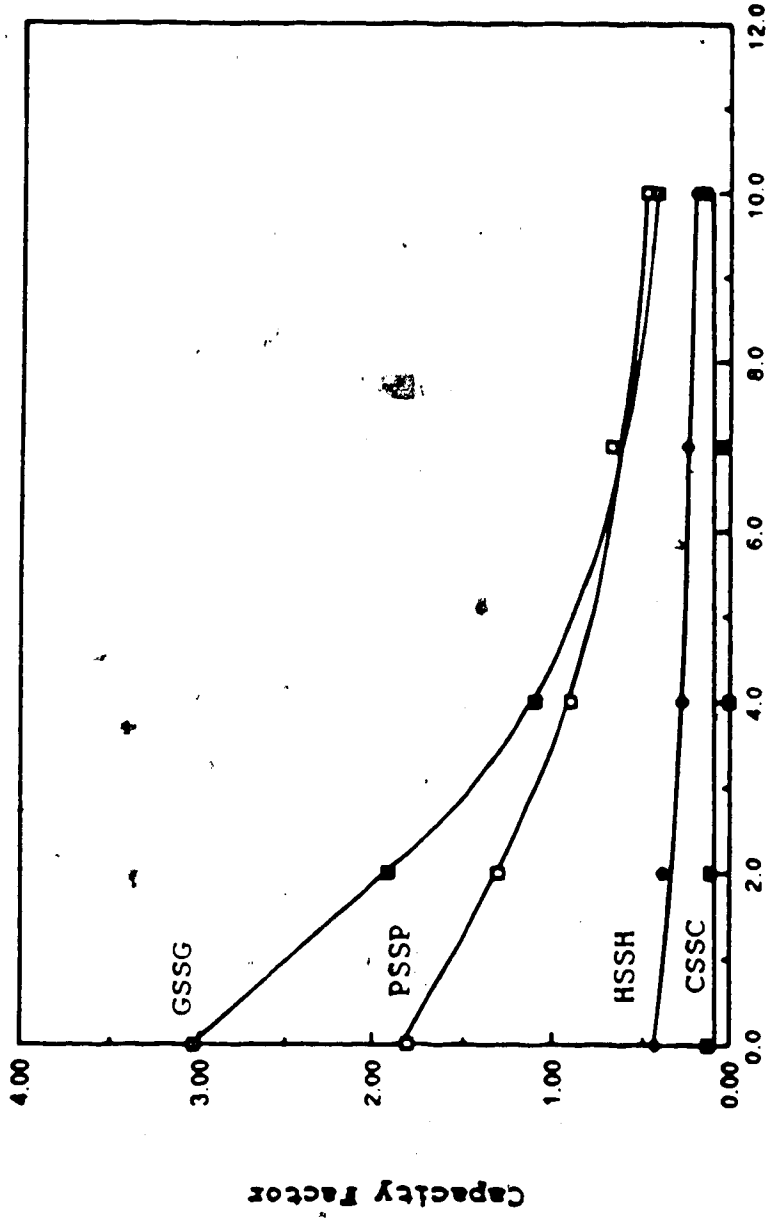

Figure 4.17. A plot of the capacity factors for HSSH, CSSC, GSSG and PSSP as a function of the percent methanol in the mobile phase. The mobile phase consisted of pH 3.0 phosphate buffer with various percentages of methanol as calculated by volumes.

ion-pairing reagent was expected to increase the retention times of all the compounds and reveal the effect of the methanol on the retention behaviour of the cysteine and homocysteine. The thiol capacity factors are plotted versus the percent methanol in the mobile phase in Figure 4.18.

Figure 4.19 is a plot of the disulfide capacity factors as a function of the concentration of methanol in the mobile phase containing sodium octyl sulfate. From solvophobic theory [122,129], there should be an approximately linear relationship between the log of the capacity factor and the percent organic modifier in the mobile phase. The log k' values for the thiols and the disulfides are plotted as a function of the percent methanol in the mobile phase in Figures 4.20 and 4.21, respectively. As expected the plots are generally linear.

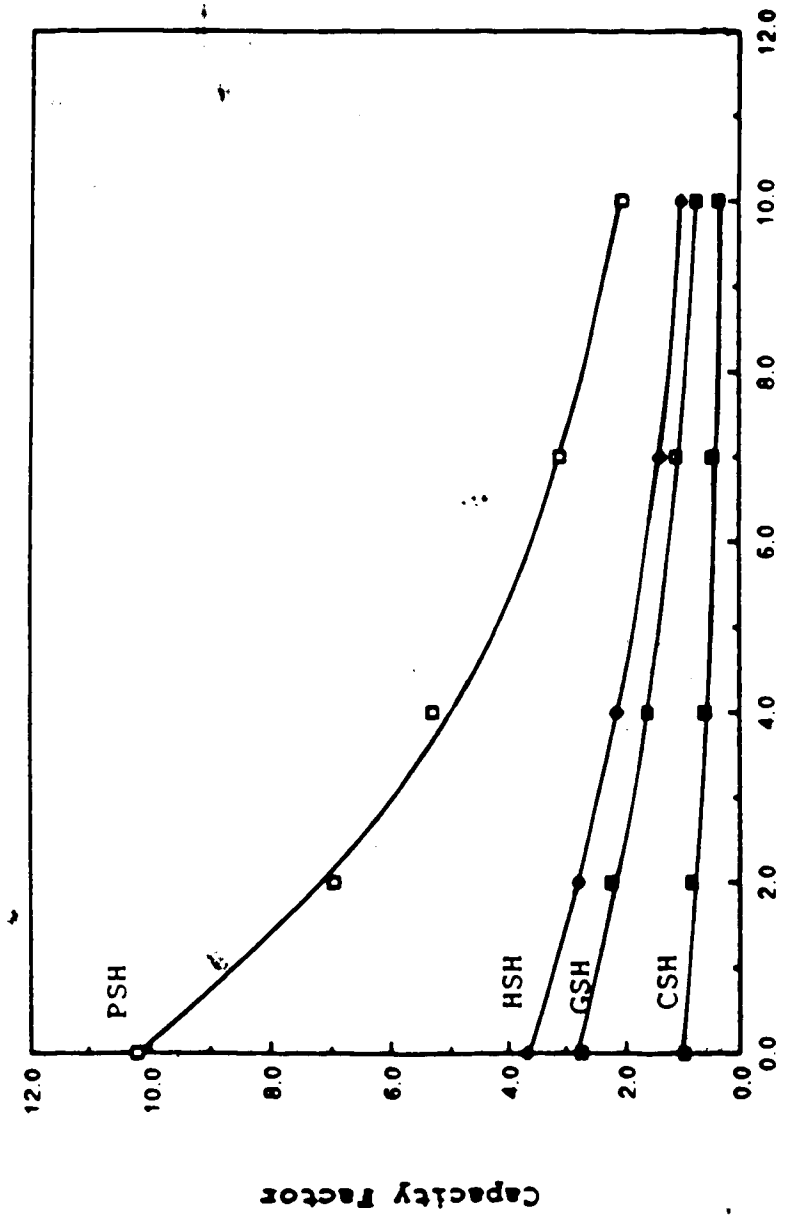

Figure 4.18. A plot of the capacity factors for HSH, CSH, GSH and PSH as a function of the percent methanol in the mobile phase. The mobile phase consisted of pH 3.0 phosphate buffer with 0.75 mM sodium octyl sulphate and varying amounts of methanol.

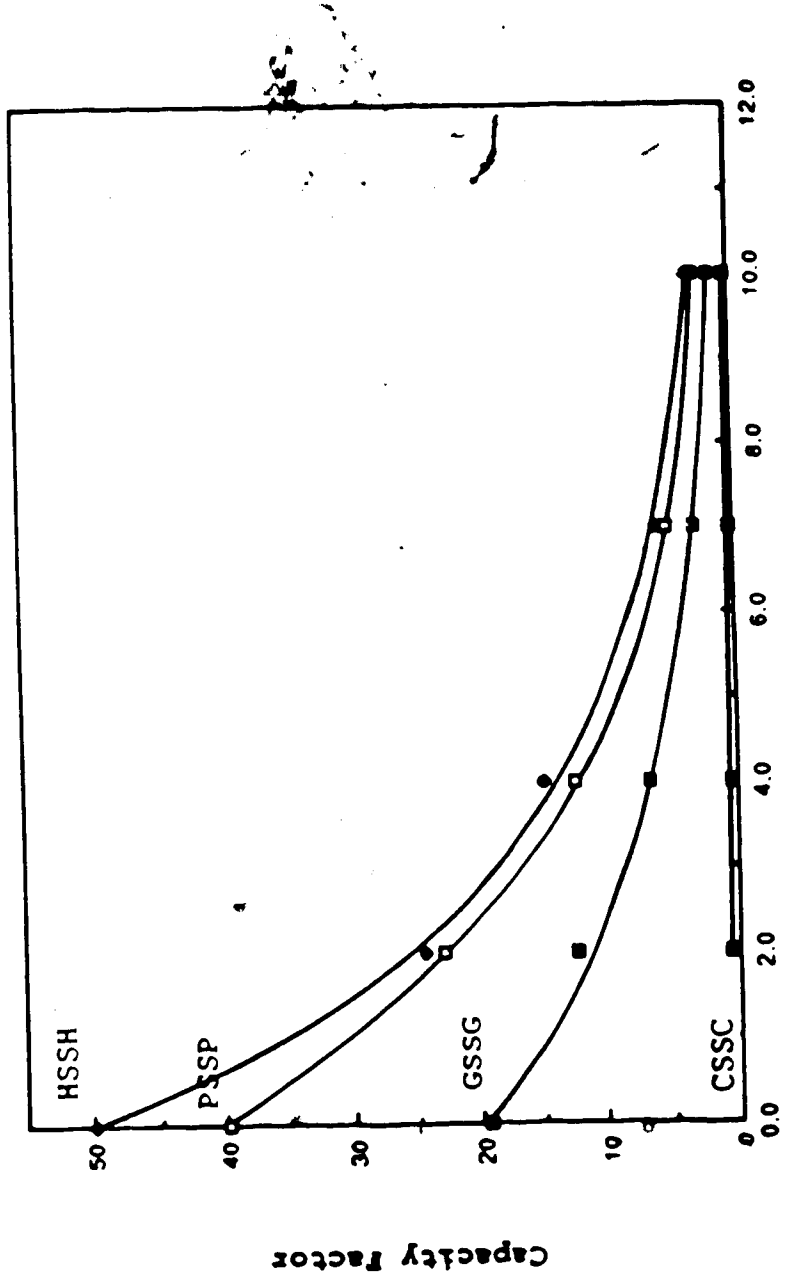

Figure 4.19. A plot of the capacity factors for HSSH, CSSC, GSSG and PSSP as a function of the percent methanol in the mobile phase. The mobile phase consisted of pH 3.0 phosphate buffer with 0.75 mM sodium octyl sulphate and varying amounts of methanol.

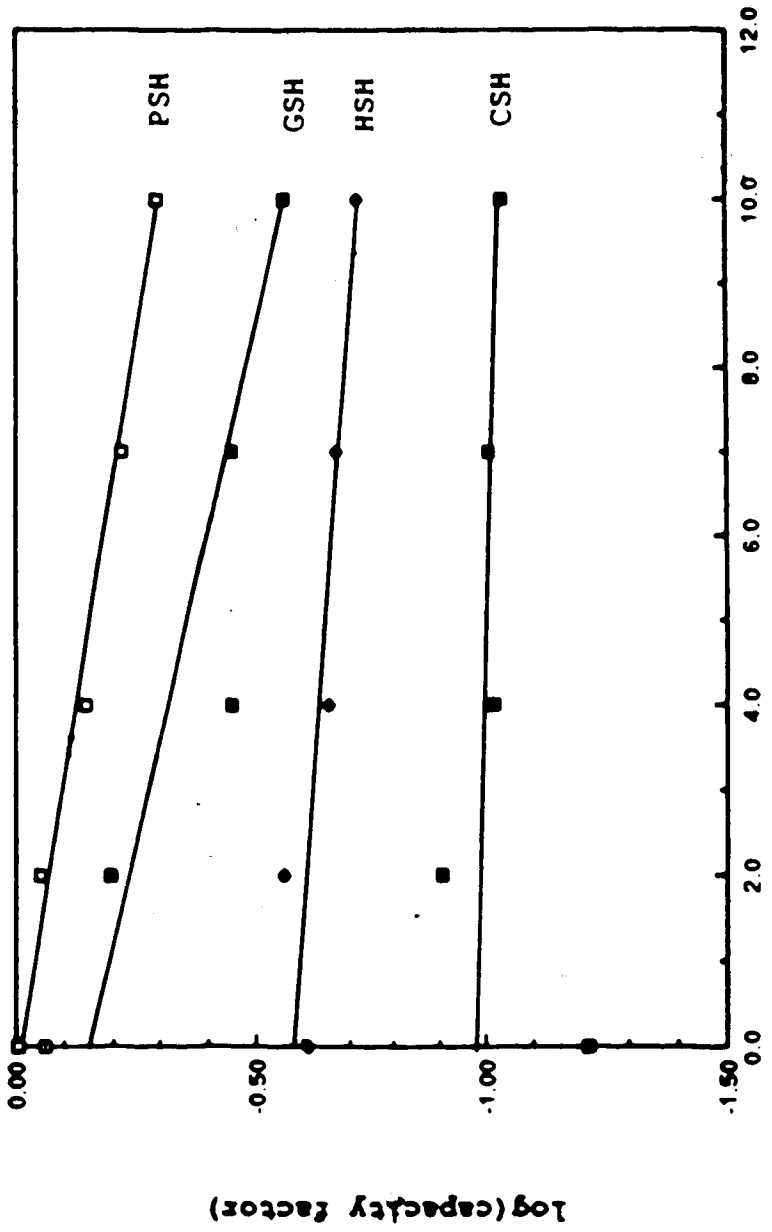

Figure 4.20. A plot of the log of the capacity factors for HSH, CSH, GSH and PSH as a function of the percent methanol in the mobile phase. The mobile phase consisted of pH 3.0 phosphate buffer with 0.75 mM sodium octyl sulphate and varying amounts of methanol.

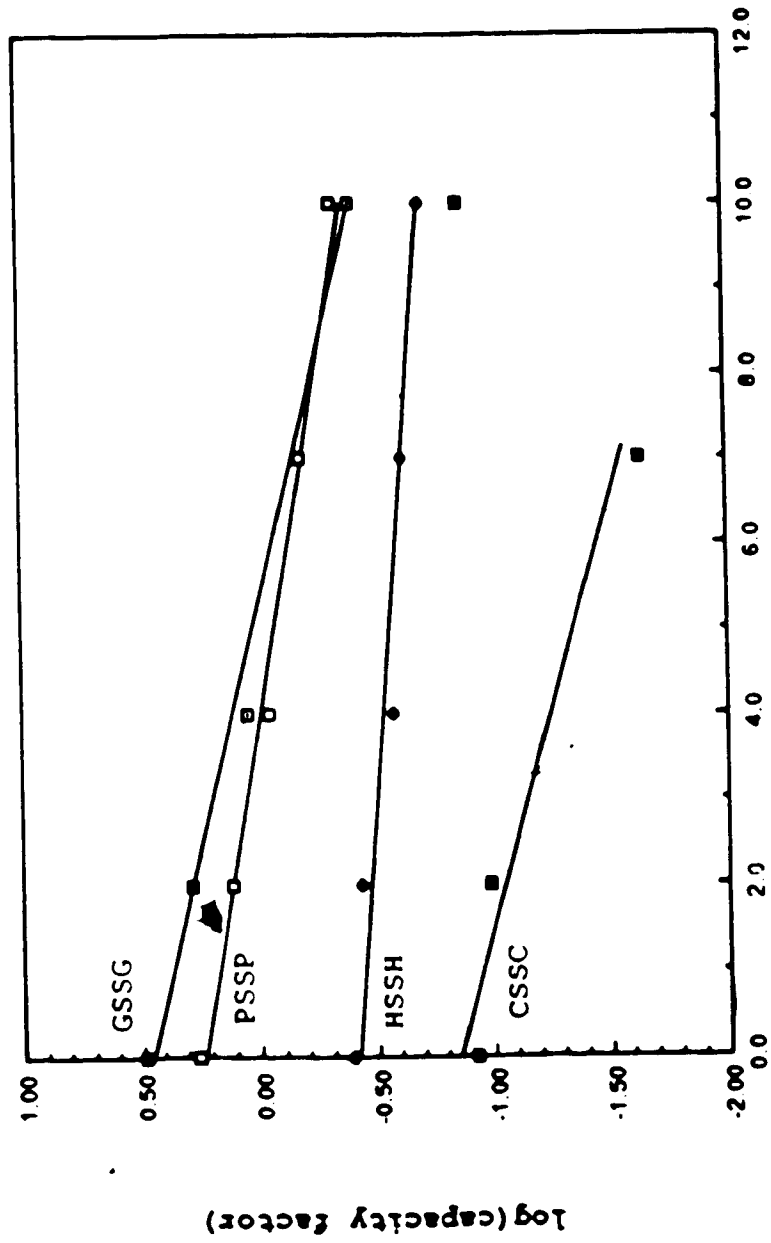

Figure 4.21. A plot of the log of the capacity factors for HSSH, CSSC, GSSG and PSSP as a function of the percent methanol in the mobile phase. The mobile phase consisted of pH 3.0 phosphate buffer with 0.75 mM sodium octyl sulphate and varying amounts of methanol.

E. Discussion

The use of mobile phase modifications has been shown to alter the retention characteristics of cysteine, homocysteine, glutathione, penicillamine, and their symmetrical disulfides. Addition of the ion-pairing reagent, sodium octyl sulfate, to the mobile phase increases the capacity factor for both thiols and disulfides in a linear fashion. Increased methanol content in the mobile phase decreases the capacity factor of the thiols and disulfides.

By combining both the ion-pairing reagent with methanol in the buffered mobile phase, selective separations of a mixture of thiols and disulfides should be possible. Thus far, only the chromatography of thiols and symmetrical disulfides has been studied. The retention behaviour of the mixed disulfides of penicillamine, PSSR, is presumed to be intermediate between the behaviour of the symmetrical disulfide, RSSR, and that of the oxidized penicillamine, PSSP. The composition of the mobile phase in the following two chapters will be based on the findings in the above sections and will be designed to optimize the separation of both the thiols and the disulfides, including the mixed disulfides of penicillamine.

CHAPTER V

THE DETERMINATION OF PENICILLAMINE, GLUTATHIONE AND THEIR DISULFIDES

A. Introduction

Penicillamine is widely used in medicine and is known to be metabolised via thiol/disulfide exchange reactions to mixed disulfides, PSSR, and to the symmetrical disulfide, PSSP [36]. Although methods have been developed for the analysis of penicillamine by HPLC, few provide a direct measure of the disulfide metabolites. Quantitative methods for the determination of these penicillamine metabolites will be essential for monitoring patients on penicillamine therapy as well as for physiological and pharmacological studies of this drug.

Since the formation of the penicillamine-glutathione mixed disulfide has been reported to be involved in the metabolism of penicillamine [130], methodology was developed for the determination of penicillamine, glutathione and their symmetrical and mixed disulfides by HPLC with electrochemical detection. The determination of reduced and oxidized glutathione by HPLC with electrochemical detection has been established [73] and the determination of reduced and oxidized penicillamine has been demonstrated, but to

date, there have been no reports of the determination of the penicillamine-glutathione mixed disulfide by HPLC-ED.

Data on the electrochemical and chromatographic behaviour of the different compounds involved in this system were presented in Chapters III and IV and references to the appropriate sections in those chapters will be included, where possible, throughout this chapter.

B. Penicillamine-Glutathione Mixed Disulfide

The mixed disulfide of penicillamine and glutathione is not commercially available. To produce a solution containing the penicillamine-glutathione mixed disulfide (Figure 3.20), a thiol/disulfide exchange reaction of PSH with GSSG was used. The five possible compounds contained in a solution resulting from this reaction are reduced penicillamine, reduced glutathione, oxidized penicillamine, oxidized glutathione, and penicillamine-glutathione mixed disulfide. The reaction sequence is expressed by the two-step process,

$$PS^- + GSSG \rightleftharpoons PSSG + GS^- \qquad (40)$$

$$PS^- + PSSG \rightleftharpoons PSSP + GS^- \qquad (41)$$

The kinetics of this exchange reaction have been characterized by Theriault and Rabenstein [88] using NMR spectroscopy. The results of those studies showed that the rate of the reaction is dependent on the pH of the reaction mixture and that the PS^- anion is the reactive species. It

was reported that less than 1% of the PSH in solution at a pH of 9 will be oxidized to PSSP during a 30 minute period while the penicillamine-glutathione mixed disulfide reached its equilibrium concentration in 15 minutes. This means that the second step is the slow or rate-determining step.

Typically, stock solutions of 127 mM PSH and 106 mM GSSG were prepared in a pH 3.0 phosphate/D_2O buffer containing 0.003 M Na_2H_2EDTA. The reaction procedure outlined in Chapter II was followed and the final dilution of the reactants was 1:10 in the reaction mixture. ^1H NMR analysis of a 0.5 mL sample of the reaction mixture was performed as described in Chapter II.

Figure 5.1 shows the ^1H NMR spectrum for the reaction mixture of PSH with GSSG and the expanded methyl region is presented in Figure 5.2. The three pairs of resonances observed correspond to the methyl resonances for the three forms of penicillamine in solution, namely PSH, PSSP, and PSSG. The chemical shifts were measured with respect to the internal reference tert-butyl alcohol resonance set at 1.2397 ppm. The PSH resonances occur at 1.5877 ppm and 1.5220 ppm. The two resonances for PSSP appear at 1.5767 ppm and 1.4607 ppm while the resonances at 1.5549 ppm and 1.4333 ppm are for PSSG. Table 5.1 lists the chemical shift data and the measured vertical displacements of the integral traces for each of the peaks. From the measured peak

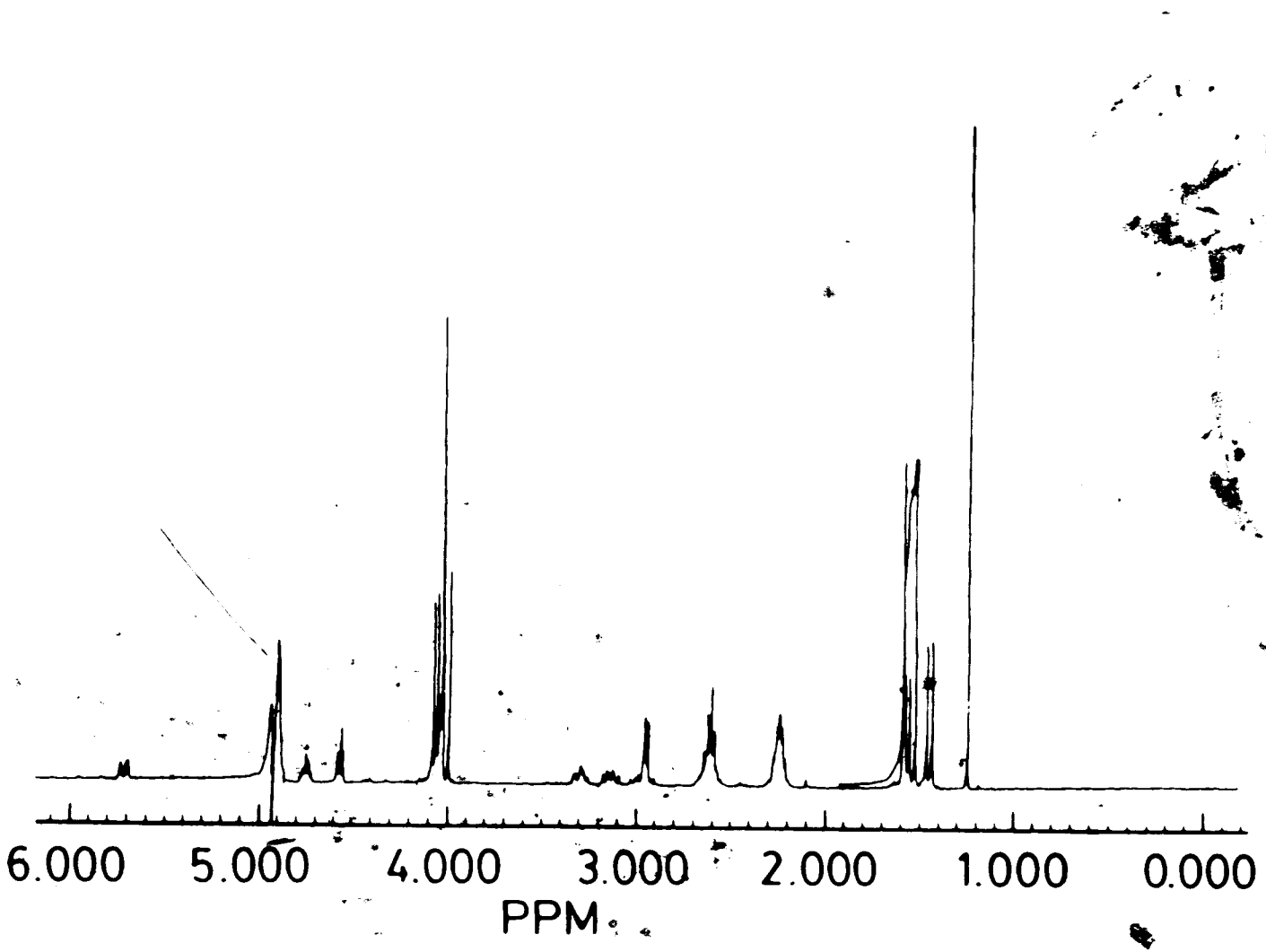

Figure 5.1. A 400 MHz ^1H NMR spectrum of a mixture containing GSH, PSH, GSSG, PSSG, and PSSP. The mixture was generated by a thiol/disulfide exchange reaction in a phosphate buffer:D_2O solution.

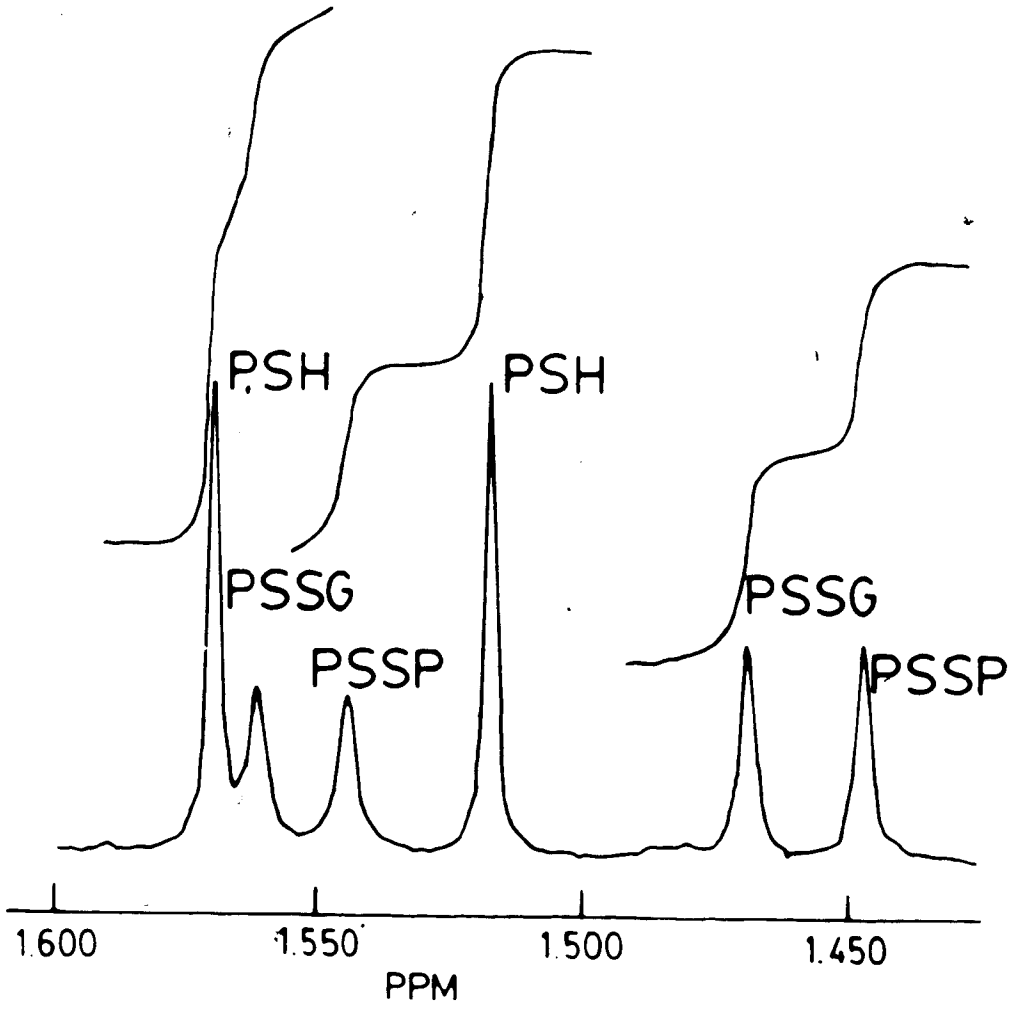

Figure 5.2. An expansion of the methyl region of the 400 MHz spectrum seen in Figure 5.1. The six peaks correspond to signals from PSH, PSSG and PSSP.

Table 5.1. Chemical shift data and measured amplitudes of the integrals for the peak areas of the methyl resonances in Figure 5.2.

Methyl Resonance Assignment	Chemical Shift (ppm)	Amplitude of Peak Integral (height in mm)
PSH	1.588	60.6 ± 0.3
PSSP	1.577	34.3 ± 0.3
PSSG	1.555	33.2 ± 0.3
PSH	1.522	57.0 ± 0.3
PSSP	1.461	35.8 ± 0.3
PSSG	1.433	35.9 ± 0.3
	Total	256.8 ± 0.7

f(PSH) = (60.6+57.0)/256.8 = 0.458 ± 0.003

f(PSSP) = (34.3+35.8)/256.8 = 0.273 ± 0.002

f(PSSG) = (33.2+35.9)/256.8 = 0.269 ± 0.002

integral traces the fraction of each penicillamine-containing species in solution was calculated using Equations 8 - 10 in Chapter II. With these calculated fractions and the initial reactant concentrations, the concentrations of the various components in solution were calculated according to Equations 11 - 13 in Chapter II.

Once the concentrations of all five components were determined, the stock solution was diluted using volumetric pipettes and flasks to make calibration standards. The concentration range for the thiols was generally 0 - 50 μM while the concentration of PSSG and of GSSG was in the 0 - 150 μM range. Since oxidized penicillamine is not easily reduced at the upstream electrode the concentration of PSSP was kept in the 0 - 1.5 mM range.

To select the potentials for the upstream and downstream electrodes the hydrodynamic voltammograms from Chapter III were examined. Based on the hydrodynamic voltammograms for oxidized glutathione and oxidized penicillamine, Figures 3.15 and 3.16 in Chapter III, the upstream electrode potential was set to -1.100 V versus a Ag/AgCl reference electrode. At this potential the penicillamine, although not at its maximum level of reduction, gave the best response and the background current was of an acceptable level. Also, this potential setting is on the reduction plateau of the hydrodynamic voltammogram

for glutathione so small variations in the electrode potential will not cause any significant change in the glutathione peak currents.

The downstream electrode potential was set at +0.150 volts versus a Ag/AgCl reference electrode. This potential is on the oxidation plateau of the hydrodynamic voltammograms for both the reduced penicillamine and the reduced glutathione, as seen in Figures 3.11 and 3.12.

The composition of the mobile phase required for a given separation was determined by preliminary studies of the type described in Chapter IV. The results in Chapter IV demonstrate that the main mobile phase parameters that affect the chromatographic behaviour of the analytes are its pH, the concentration of any ion-pairing reagent, and the concentration of any added organic modifier.

The selected mobile phase pH must be suitable for the solutes as well as be appropriate for the chromatography. Studies on the autoxidation of penicillamine show that the initial rate of oxidation increases as the pH is increased above pH 5.0 and reaches a maximum near pH 7.5 [88]. Consequently, to minimize the possibility of thiol oxidation during the separation, the mobile phase was kept at a pH less than 5 and was sparged with inert gas to reduce the amount of dissolved oxygen in the system. The lower limit to the mobile phase pH is determined by the column packing

material. Octadecyl silane begins to hydrolyse at pH 2, so to avoid column degeneration the lowest mobile phase pH used was 2.5.

From the plots of the capacity factor for GSH, PSH, GSSG, and PSSP as a function of mobile phase pH in Figures 4.4 and 4.9, the highest degree of separation appears to be at pH 2.5, however, at this pH tailing is a problem for the thiols. Two chromatograms for a mixture of 30 μM GSH and 30 μM PSH are presented in Figure 5.3. Chromatogram i) was run using a mobile phase composed of 0.1 M phosphate buffer at pH 2.5 and chromatogram ii) was run using a similar mobile phase but having a pH of 3.0. A measure of the selectivity of a chromatographic system for two adjacent peaks is the separation factor, α. The separation factor for two peaks labelled A and B is given by the equation:

$$\alpha(B,A) = k'(B)/k'(A) \qquad (42)$$

where k'(B) is the capacity factor for the later eluting peak and k'(A) is that for the earlier eluting peak. Thus, all separation factors will be greater than 1. A second term which is often used in evaluating peak separation is resolution, R_S. Resolution is defined as the ratio of twice the difference between the peak retention times over the sum of the peak widths at the baseline.

$$R_S = \frac{2\ (t_r(B) - t_r(A))}{(W(B) + W(A))} \qquad (43)$$

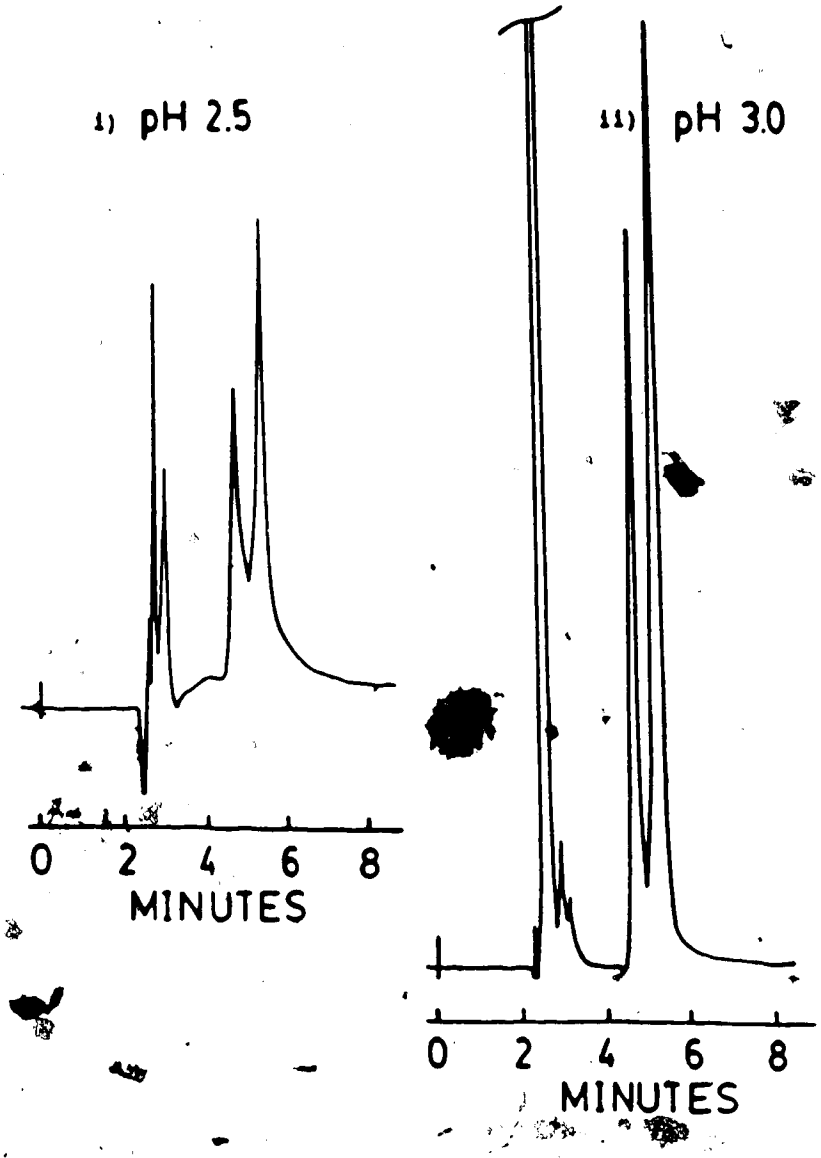

Figure 5.3 Chromatograms of a mixture of 30 μM GSH and 30 μM PSH using a mobile phase of phosphate buffer at i) pH 2.5 and ii) pH 3.0.

The terms $t_r(A)$ and $t_r(B)$ are the retention times for peaks A and B, respectively, while W(A) and W(B) are the peak widths of peaks A and B measured in the same units of time as the retention times. Table 5.2 lists the measured chromatographic parameters and the calculated separation factor and resolution for the two chromatograms in Figure 5.3.

Although greater separation exists between the GSH and PSH at the lower pH, shown by the larger separation factor of 1.30, tailing is observed and considerable overlap occurs. At pH 3.0 the glutathione and penicillamine peaks are narrower and although they exhibit a lesser degree of separation, they are better resolved. The species distribution diagrams for PSH and for GSH (Figures 4.9 and 4.10, respectively) indicate that the fraction of both of these compounds in the ionic form having a +1 charge increases as the pH goes from 3.0 to 2.5. It might be that the increased amount of tailing at the lower pH is due to greater interaction of these ionic species with silanol groups on the column.

From the above results, a phosphate buffer at pH 3.0 seems to be the best mobile phase for the analysis of reduced and oxidized glutathione, and reduced and oxidized penicillamine. The chromatographic behaviour of the mixed disulfide, PSSG, would be expected to be similar to that of

Table 5.2. Measured and calculated values for various chromatographic terms for GSH and PSH using a mobile phase at pH 2.5 and at 3.0 as seen in Figure 5.3.

(i) at pH 2.5

Compound	t0 (min.)	tr (min.)	k'	width (min.)	α	Resolution
GSH	2.30	4.60	1.00	0.58		
					1.30	1.20
PSH	2.30	5.28	1.30	0.55		

(ii) at pH 3.0

Compound	t0 (min.)	tr (min.)	k'	width (min.)	α	Resolution
GSH	2.30	4.70	1.04	0.32		
					1.21	1.56
PSH	2.30	5.20	1.26	0.32		

the symmetrical disulfides, with PSSG eluting at some intermediate time between PSSP and GSSG since it has structural and chemical similarities to both of these compounds. Figure 5.4 shows a chromatogram of a four-component mixture containing PSH, GSH, PSSP, and GSSG using a pH 3.0 phosphate buffer for the mobile phase. The flow rate was 1.0 mL/min. and the chart speed was set to 1.0 cm/min. In Figure 5.5, the same chromatographic conditions were used to chromatograph a five-component mixture containing the above four components plus PSSG. As expected the elution time of the mixed disulfide was intermediate between those of PSSP and GSSG.

To improve the separation of PSH and GSH use of an ion-pairing reagent appeared to be a logical approach. In chapter IV it was shown that the ion-pairing reagent, sodium octyl sulfate, caused increased retention times for GSH, PSH, GSSG, and PSSP. The capacity factors for these compounds are presented as a function of the concentration of the sodium octyl sulfate in Figures 4.12 and 4.14. Addition of the ion-pairing reagent to the mobile phase will increase the separation between the two overlapping thiols. At the same time, the disulfides will also experience the effects of the sodium octyl sulfate and their retention times may become excessively long. This can be counteracted by the addition of an organic modifier to the mobile phase.

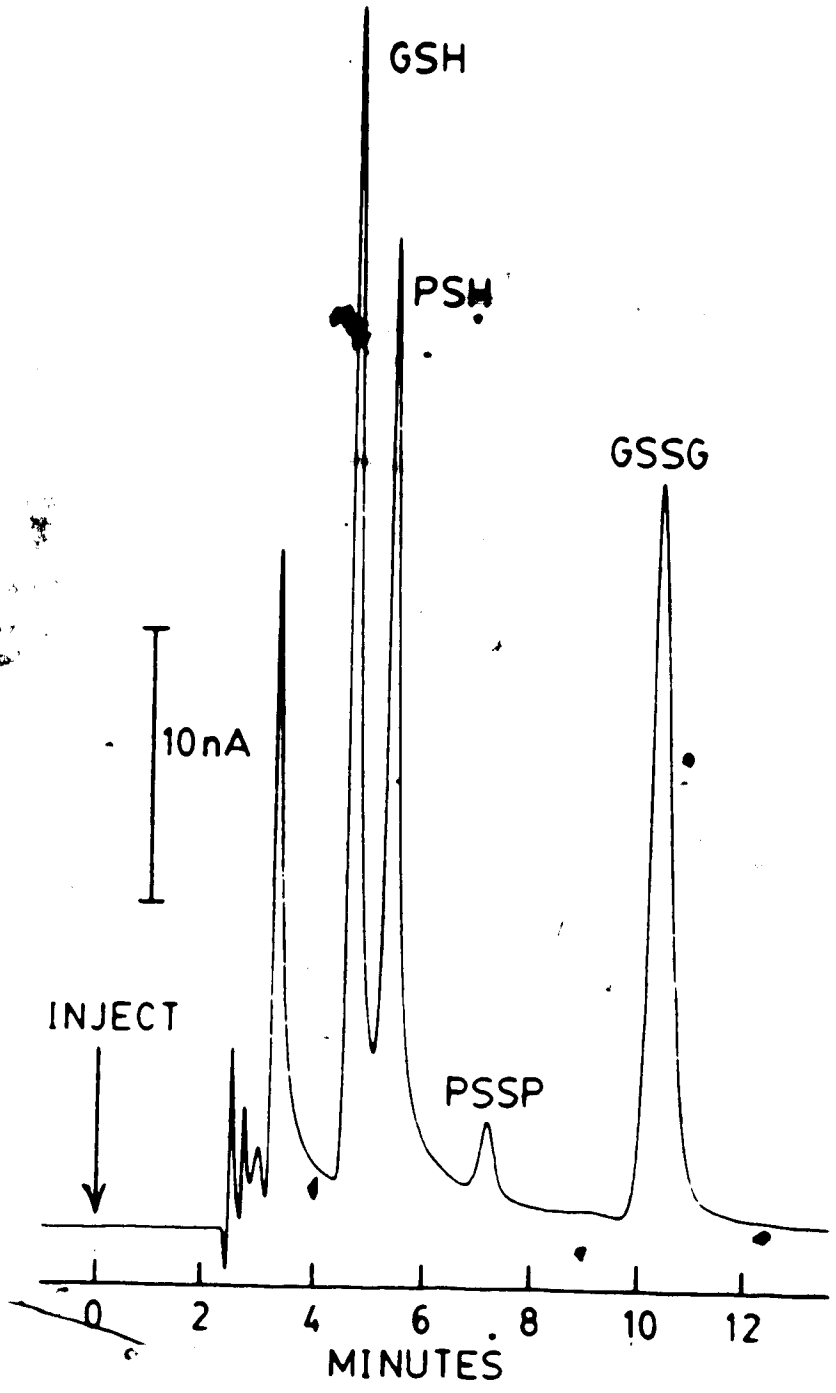

Figure 5.4. Chromatogram of a four-component mixture containing GSH, PSH, GSSG and PSSP. The mobile phase was a pH 3.0 phosphate buffer and the flow rate was set to 1.0 mL/min. The chart speed was 1.0 cm/min. and the detector was set to -1.100 V at the upstream electrode and +0.150 V at the downstream electrode.

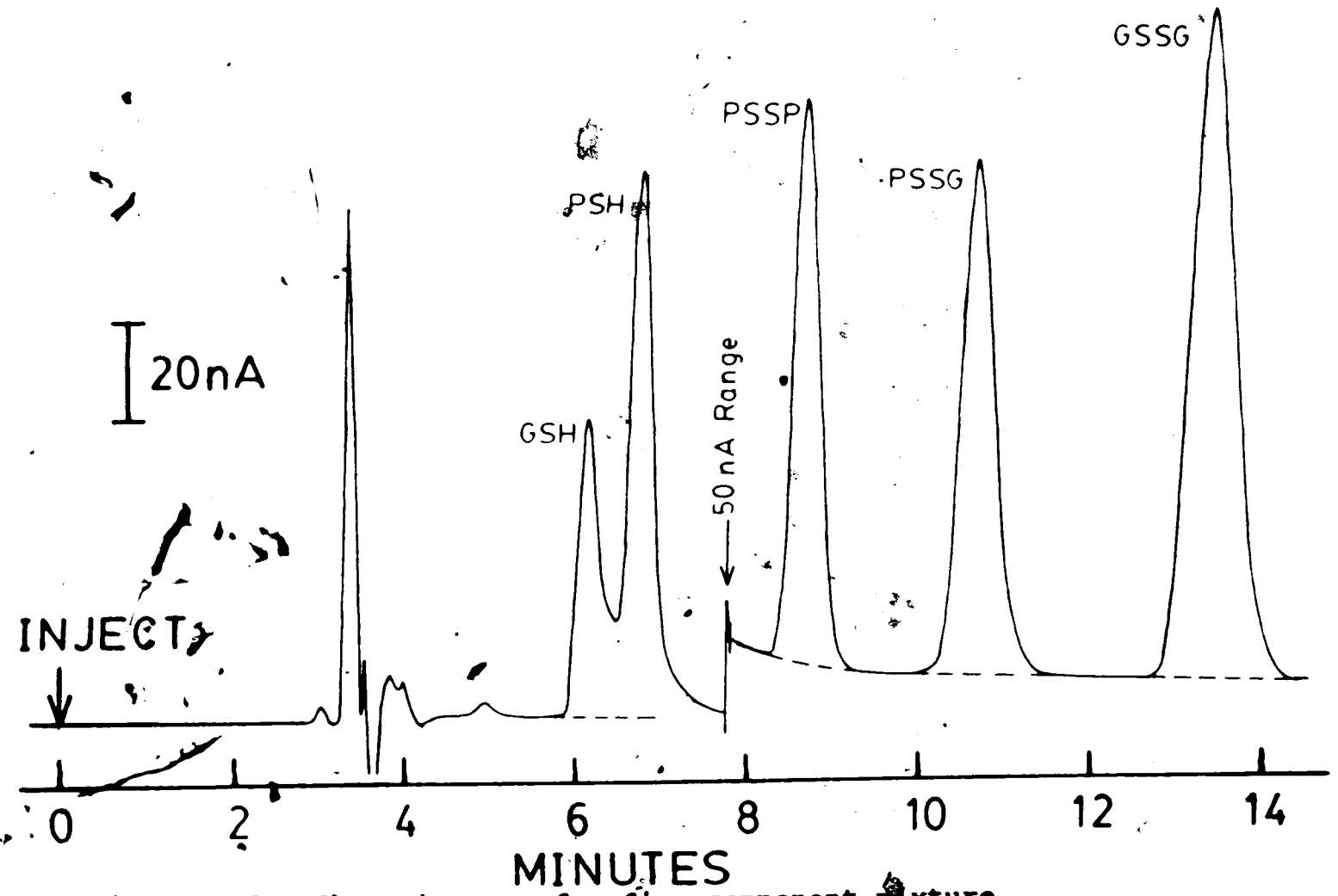

Figure 5.5. Chromatogram of a five-component mixture containing GSH, PSH, GSSG, PSSG and PSSP. The chromatographic conditions were the same as those listed in Figure 5.5, but the chart speed was set to 2.0 cm/min.

Addition of methanol to the mobile phase was observed to reduce the retention times for thiols and disulfides as illustrated in Figures 4.15 and 4.16. Since this effect is more prominent for the disulfides than the thiols, the combined effect of the ion-pairing reagent and the methanol will be to increase the separation of the thiols while preventing the retention times for the disulfides from becoming too long.

From Figure 4.18, overlap of the GSSG and PSSP peaks is predicted at a sodium octyl sulfate (SOS) concentration of 0.30 mM. Increased separation of PSSP and GSSG occurs as the concentration of the ion-pairing reagent is decreased below or raised above this level. Initially, a mobile phase of pH 3.0 phosphate buffer containing 0.03 mM SOS without any methanol was tried. By using a low concentration of ion-pairing reagent, the thiols might be sufficiently resolved without the disulfides becoming too strongly retained on the column. Adequate resolution was achieved for calibration solutions prepared in buffer, however this study was discontinued because of overlap of the GSH peak with a peak from a plasma constituent.

To achieve the desired separation, both ion-pairing reagent and methanol were added to the buffered mobile phase. Figure 5.6 shows the effect of methanol on the capacity factors for GSH, PSH, GSSG and PSSP when 0.75 mM

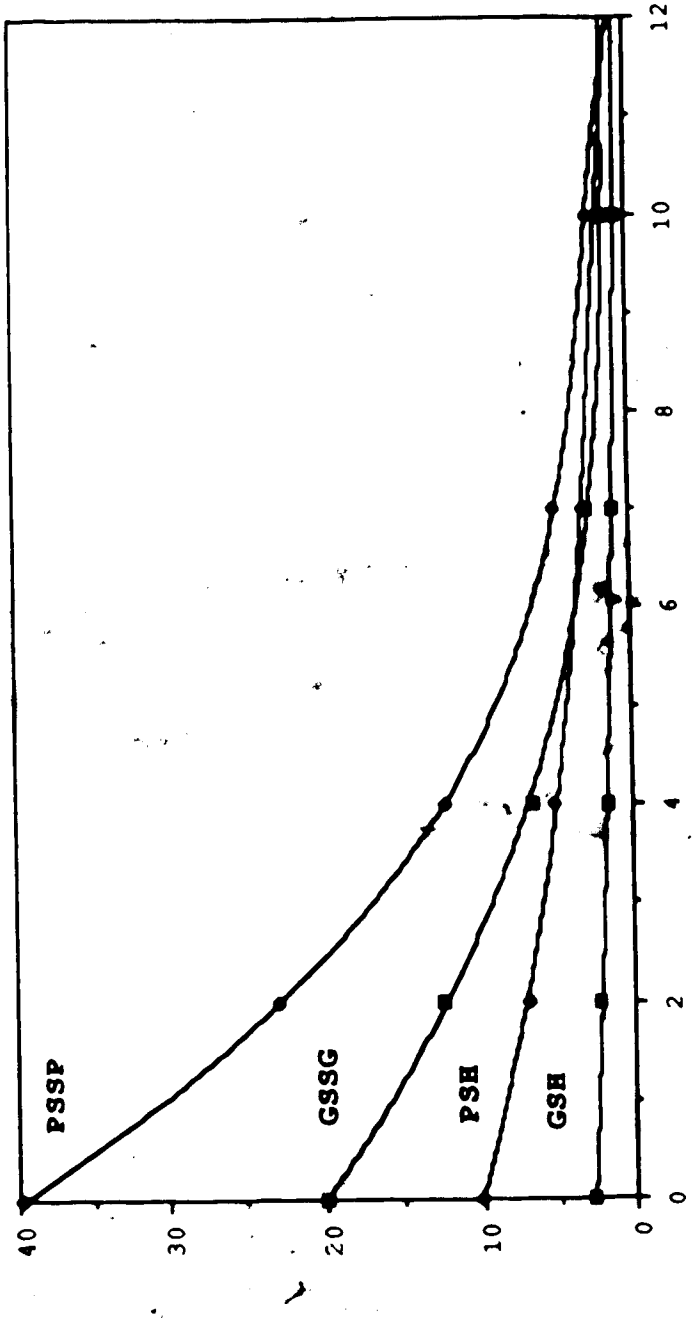

Figure 5.6. The capacity factors for GSH, PSH, GSSG and PSSP as a function of percent methanol in a mobile phase of pH 3.0 phosphate buffer containing 0.75 mM sodium octyl sulphate.

sodium octyl sulfate was present in the mobile phase. From these data and the linear relationship between capacity factors and the concentration of the sodium octyl sulfate in phosphate buffer, separation was attempted using a mobile phase composition of pH 3.0 phosphate buffer containing 0.43 mM SOS with 4% methanol. However, this mobile phase did not provide adequate separation between the disulfide peaks, so the ion-pairing concentration was increased to 0.65 mM SOS while the methanol content was decreased to 3%. With this mobile phase the thiol peaks were overlapping so the concentration of SOS was increased to 0.80 mM SOS while the methanol content was kept at 3%. This mobile phase gave good separation of all five compounds. A chromatogram of a five-component mixture of GSH, PSH, GSSG, PSSG and PSSP spiked with CSH using the above mobile phase is shown in Figure 5.7. The peak observed four minutes after injection corresponds to cysteine. Cysteine was added to the mixture to condition the upstream mercury electrode and prevent the loss of the penicillamine and glutathione. This will be described in the following section.

C. Calibrations

A series of calibration standards for GSH, PSH, and GSSG were chromatographed repeatedly over a four day period

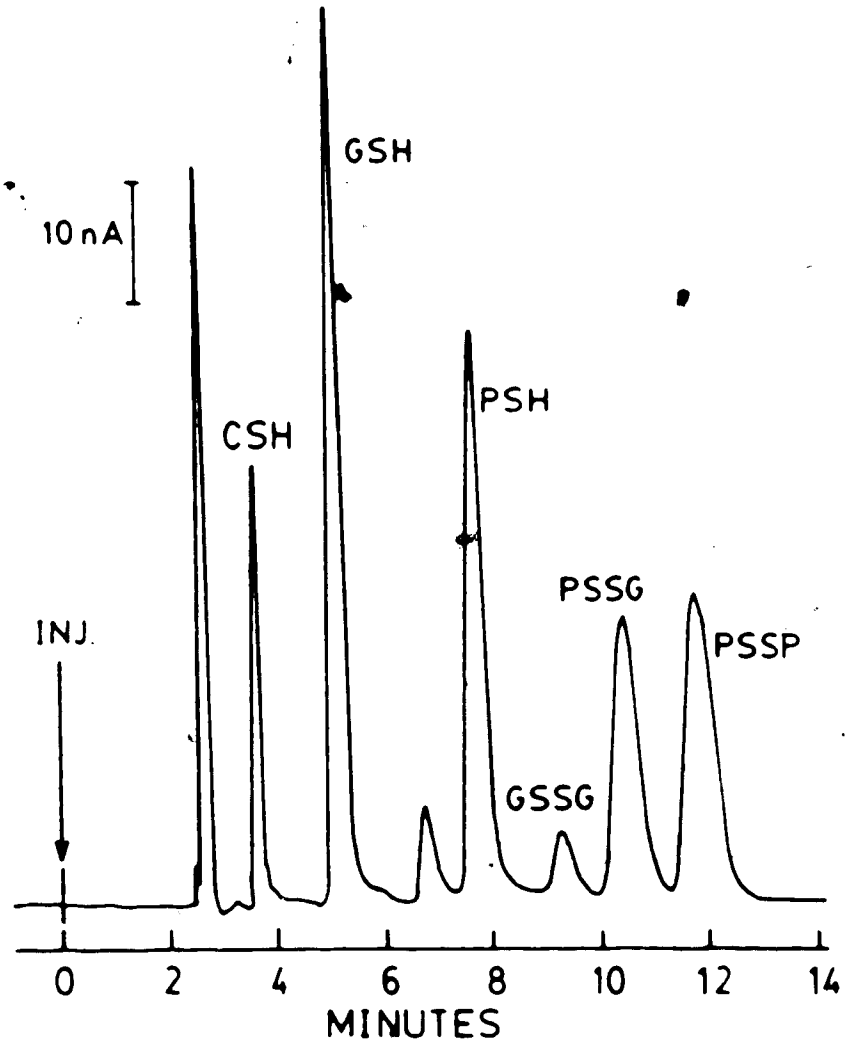

Figure 5.7. A chromatogram of a five-component mixture containing GSH, PSH, GSSG, PSSG and PSSP that had been spiked with CSH to precondition the upstream electrode. The mobile phase consisted of a pH 3.0 phosphate buffer containing 0.80 mM sodium octyl sulphate and 3% (v/v) methanol.

to observe the change in the electrode response and to evaluate the lifetime of the electrodes. The mobile phase used consisted of pH 3.0 phosphate buffer containing 0.03 mM sodium octyl sulfate. The electrodes were not polished or resurfaced with mercury during the four day period. The electrodes were prepared two days before use and the detector block was attached to the chromatograph with mobile phase running through it for those two days. At the end of each day the detector cell was opened to check for any visible signs of electrode deterioration.

The slope of the line defining the calibration curve for a given analyte gives a measure of the sensitivity of the detector for that compound. Figure 5.8 is a plot of the slopes for the different compounds over the four days. Although there is a decrease in the slope of the electrode response, the detector still responds reproducibly and linearly versus the sample concentration up until the fourth day. On the last day the detector showed loss of linearity for the disulfides. Upon inspection, the upstream electrode was found to have a gold tinge signifying a loss of mercury from the electrode surface. Samples should therefore be run in the same time frame as the calibration curve and for analyses requiring high sensitivity a freshly prepared electrode surface should be employed. The results for the calibration standards of GSH, PSH, PSSP, PSSG and GSSG using

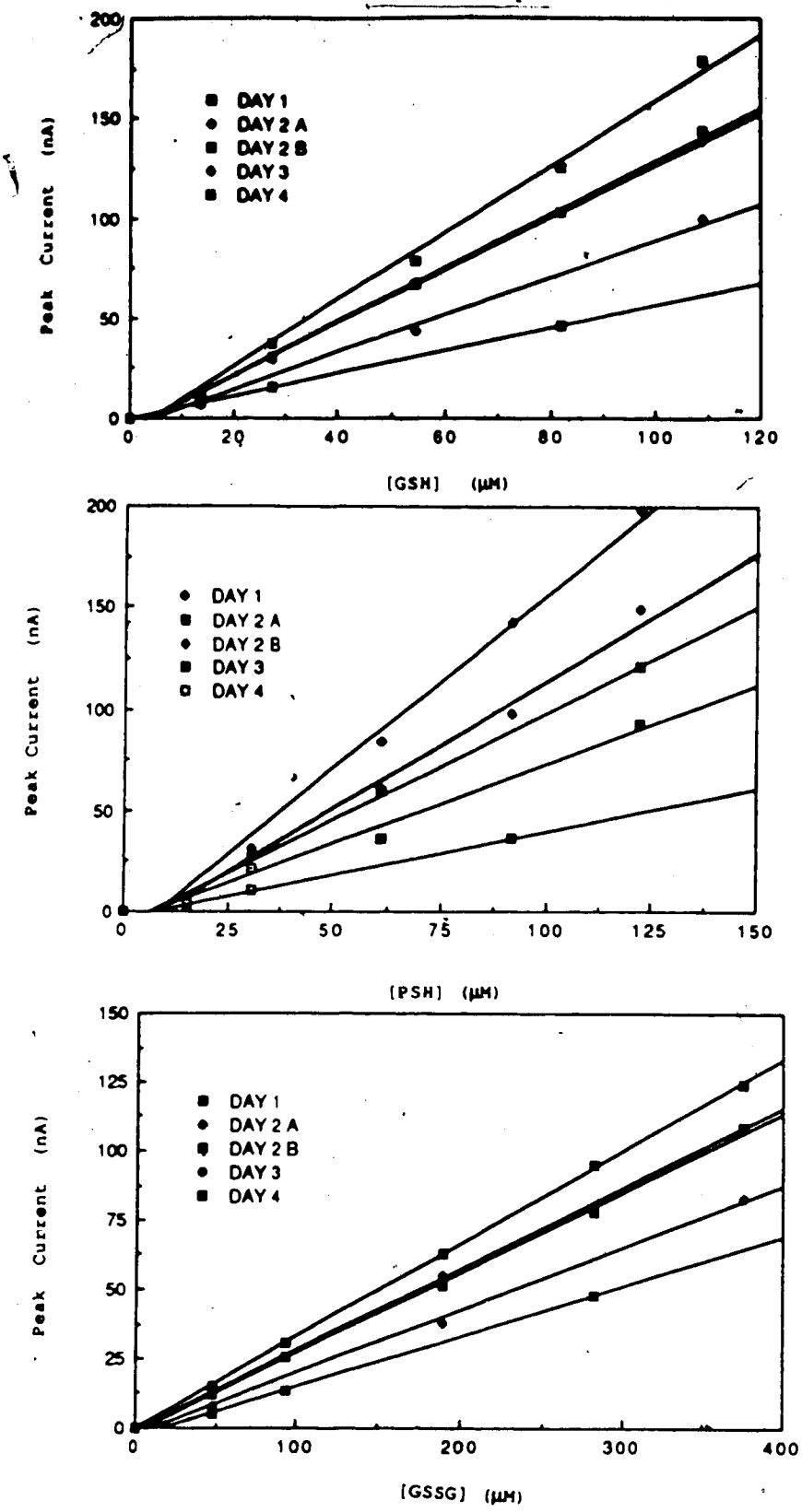

Figure 5.8. Calibration curves for GSH, PSH, and GSSG over a four day period. Two separate series of calibration standards were run on the second day and are labelled as 2A and 2B.

freshly prepared electrodes with pH 3.0 phosphate buffer containing 0.03 mM sodium octyl sulfate as the mobile phase, are given in Figure 5.9. The calibration curves for the disulfides show good linearity. However, the plots of peak current versus concentration for the thiols display a negative y-intercept. It was thought that there might be some loss of thiol, perhaps by adsorption onto the mercury of the upstream electrode, before it gets detected at the downstream electrode. Addition of another, less retained thiol, cysteine in this case, was found to prevent the loss of the GSH and PSH. Figure 5.10 shows the calibration curves for standards prepared with about 10 μM CSH present. The mobile phase used for these calibrations contained pH 3.0 phosphate buffer with 0.80 mM sodium octyl sulfate and 3% methanol. The detection limits, as defined by twice the background noise, were found to be 0.3 μM for GSH and PSSG, 0.1 μM, 0.4 μM, and 30 μM, for PSH, GSSG and PSSP, respectively.

D. Penicillamine and Glutathione in Blood and Urine

The penicillamine-glutathione mixed disulfide can be formed by reaction of PSH with GSSG. Traces of GSSG have been found in blood plasma, but none has been detected within erythrocytes [132]. For this reason the metabolic product, PSSG, will most likely appear in the plasma rather

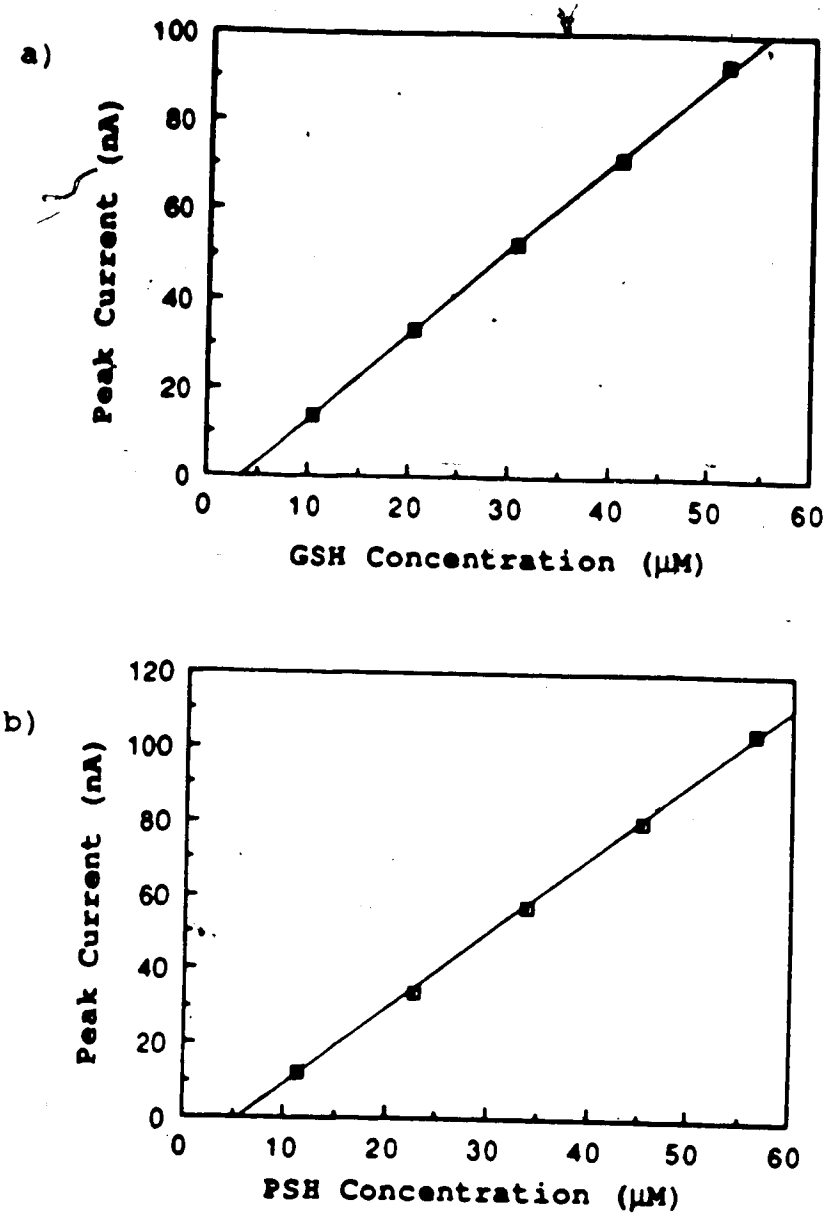

Figure 5.9. Calibration curves for GSH, PSH, GSSG, PSSG and PSSP from a series of solutions containing the five-component mixture.

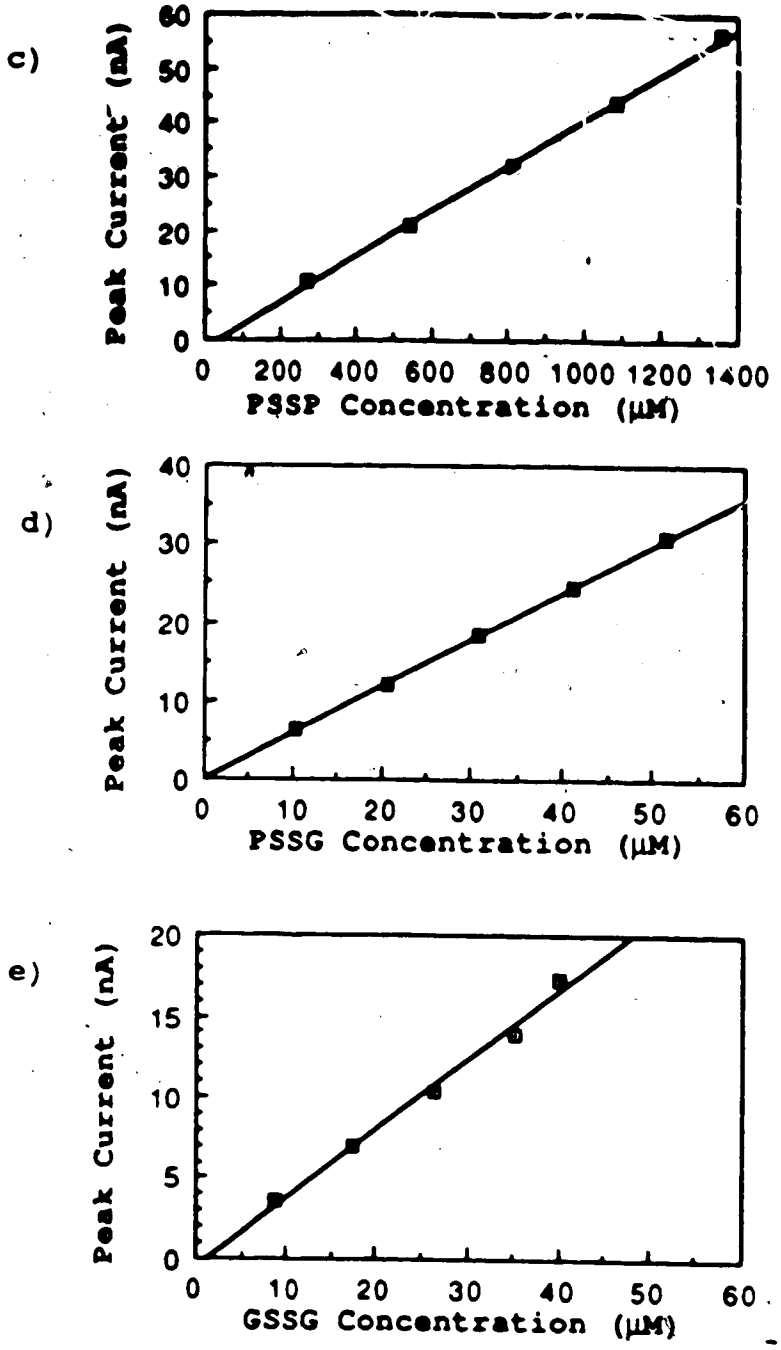

Figure 5.9 continued. Calibration curves for GSH, PSH, GSSG, PSSG and PSSP from a series of solutions containing the five-component mixture.

a)

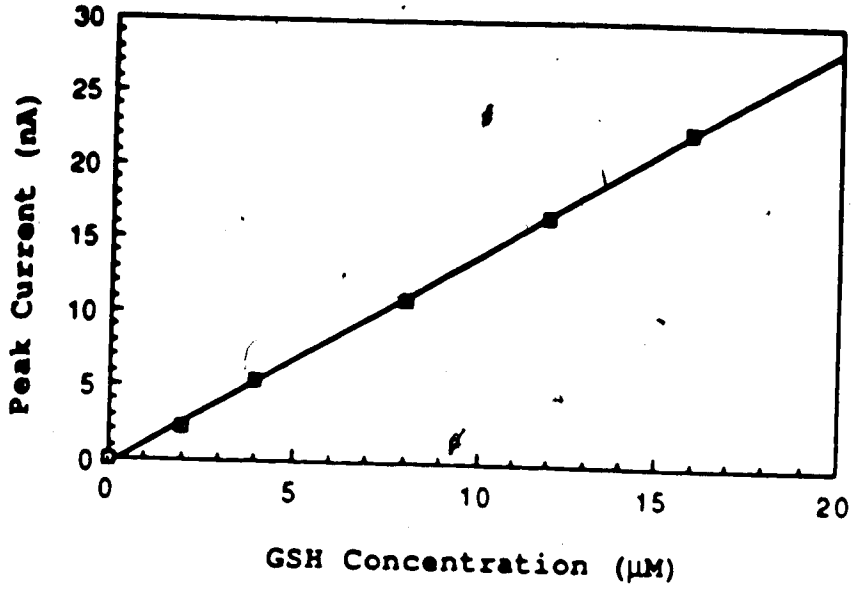

b)

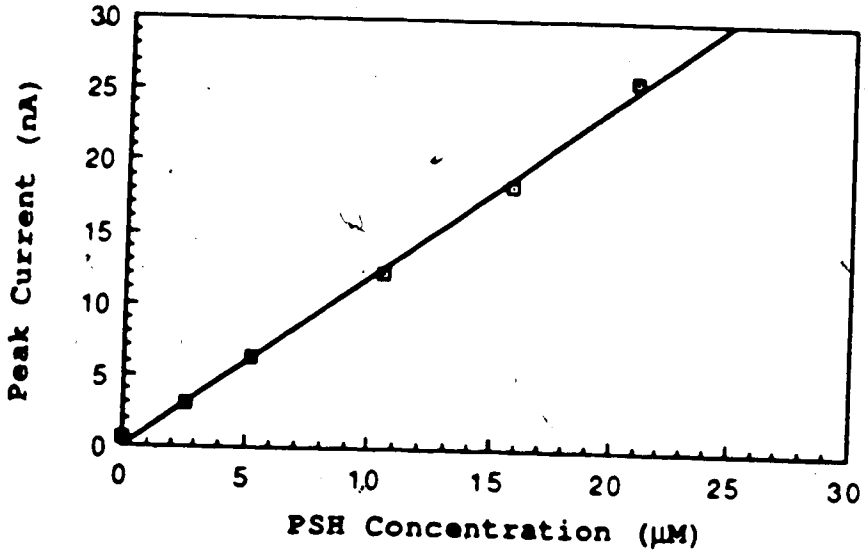

Figure 5.10. Calibration curves for GSH and PSH after the addition of CSH to the calibration standards.

than in the red blood cells of patients undergoing penicillamine therapy. As well, since penicillamine and the penicillamine-cysteine metabolite have been found in the urine of patients on penicillamine treatment [36], excretion of other metabolic products in the urine would be expected. The ability of the chromatographic system to handle biological samples with adequate resolution and sensitivity will be important if this methodology is to be useful for measuring penicillamine and it metabolites in biological fluids. The detection and quantitative measurement of PSH, GSH, PSSP, GSSG and PSSG in plasma and urine will now be presented.

i) PSH, GSH, GSSG, PSSP and PSSG in Plasma

A mobile phase of pH 3.0 phosphate buffer containing 0.80 mM SOS and 3% methanol was used for the analysis of GSH, PSH, GSSG, PSSG, and PSSP in blood plasma. Calibration standards were prepared in buffer and the plasma was worked up as described in the sample preparation section of Chapter II. Plasma was spiked with a standard mixture of PSH, GSH, GSSG, PSSP and PSSG. After running the calibration standards, the plasma samples were deoxygenated and a 20 μL sample was subjected to analysis. Figure 5.11 is a typical chromatogram for a spiked plasma sample. The three peaks preceding the GSH peak belong to electroactive impurities in

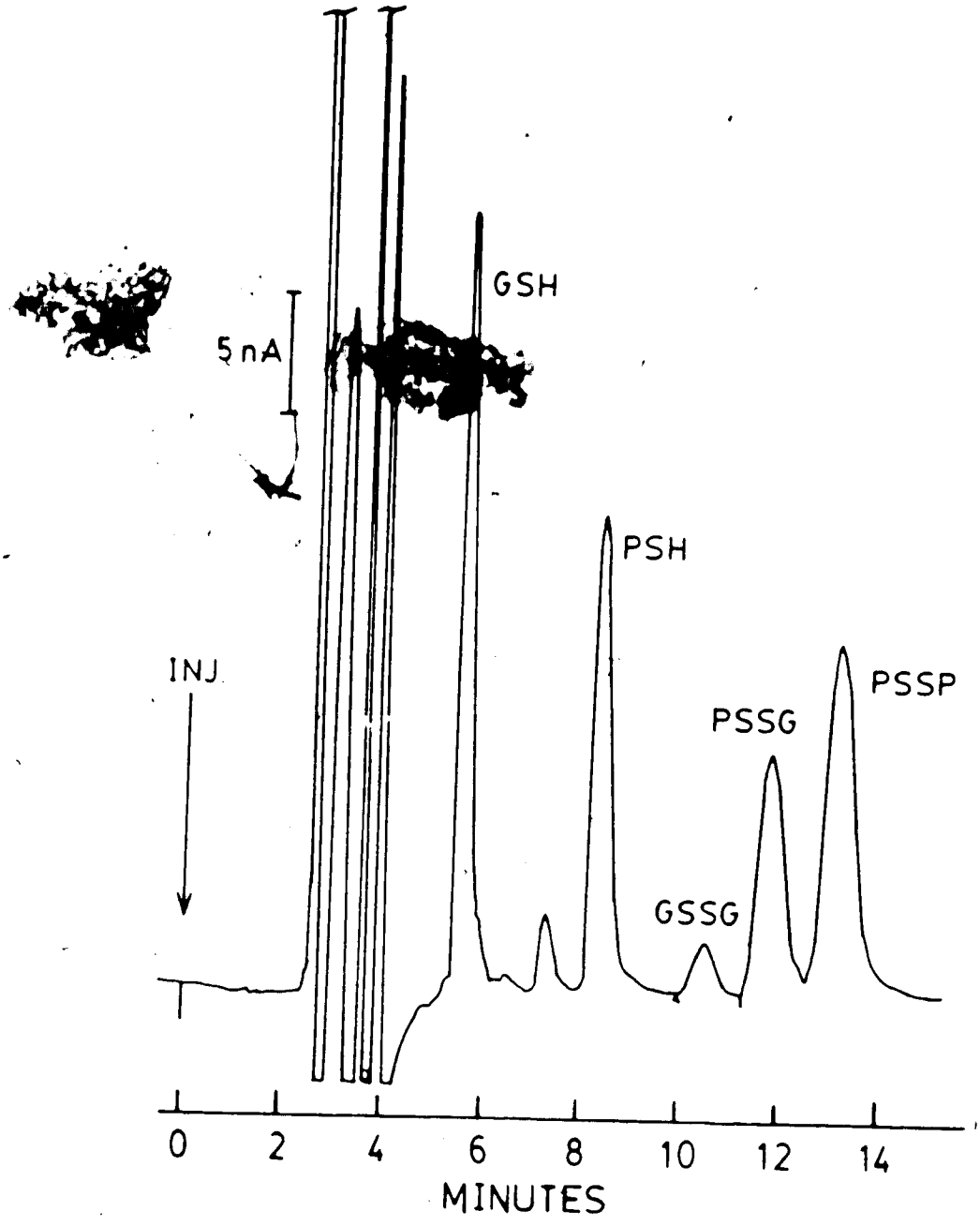

Figure 5.11. A typical chromatogram of a plasma sample spiked with GSH, PSH, GSSG, PSSG and PSSP. The mobile phase was a pH 3.0 phosphate buffer containing 0.80 mM sodium octyl sulphate with 3% methanol. The flow rate was set to 1.0 mL/min. and the chart speed was 1.0 cm/min.

the trichloroacetic acid used to precipitate the proteins in the plasma during sample workup and to the added cysteine. The recovery of PSH, GSH, GSSG, PSSP and PSSG added to plasma was calculated as a percent of the expected nominal concentration for each component; the results are listed in Table 5.3.

The percent recoveries for samples that were spiked with a second aliquot of the thiol/disulfide mixture are listed in Table 5.3 as the percent of the total analyte content and are marked with an asterisk. The percent recovery of the second spike by itself was also determined and is listed separately in Table 5.4. The procedure for calculating this percentage is described below with PSH as an example.

For a sample that was initially spiked by taking X_1 mL of a standard PSH solution, having a concentration $[PSH]_{std}$, and diluting to Y_1 mL, the concentration of PSH in the solution, $[PSH]_1$, will be equivalent to

$$[PSH]_1 = [PSH]_{std} (X_1/Y_1) \qquad (44)$$

If X_2 mL of this solution were then diluted with a volume of Y_2 mL of the standard solution, then the final net concentration in this second solution, $[PSH]_2$ can be calculated by

$$[PSH]_2 = \frac{(X_2)([PSH]_1) + (Y_2)([PSH]_{std})}{(X_2 + Y_2)} \qquad (45)$$

Table 5.3 Percent Recovery of GSH, PSH, GSSG, PSSG and PSSP in plasma samples. Concentrations are in μM units.

Compound	Run No.[a]	Observed Concentration	Expected Concentration	Percent Recovery
GSH	1.	8.8 ± 0.1	8.6	102 ± 1
	2.*	16.5 ± 0.1	17.1	96 ± 1
	3.	10.7 ± 0.1	10.8	99 ± 1
	4.	12.4 ± 0.2	12.8	97 ± 1
	5.	6.1 ± 0.1	6.8	90 ± 1
	6.	12.0 ± 0.1	12.8	94 ± 1
	7.*	23.0 ± 0.1	23.6	97 ± 1
	8.	16.5 ± 0.1	17.1	96 ± 1
PSH	1.	7.8 ± 0.1	9.4	83 ± 1
	2.*	15.2 ± 0.1	18.9	81 ± 1
	3.	9.3 ± 0.1	11.9	78 ± 1
	4.	18.3 ± 0.2	21.9	83 ± 1
	5.	7.3 ± 0.1	11.7	64 ± 1
	6.	21.0 ± 0.3	21.9	96 ± 1
	7.*	40.6 ± 0.3	40.1	101 ± 1
	8.	28.9 ± 0.1	29.1	99 ± 1
GSSG	1.	6.6 ± 0.1	6.7	98 ± 1
	2.*	13.2 ± 0.1	13.4	99 ± 1
	3.	8.7 ± 0.1	8.4	103 ± 1
	4.	27.3 ± 0.9	27.1	101 ± 4
	5.	13.5 ± 0.6	14.4	93 ± 4
	6.	25.7 ± 0.5	27.1	95 ± 2
	7.*	49.7 ± 0.3	49.7	100 ± 6
	8.	37.8 ± 0.3	36.1	105 ± 1
PSSG	1.	8.6 ± 0.1	8.8	98 ± 1
	2.*	16.5 ± 0.2	16.5	100 ± 2
	3.	11.0 ± 0.1	10.7	103 ± 1
	4.	13.0 ± 0.6	12.8	101 ± 4
	5.	6.4 ± 0.1	6.8	93 ± 1
	6.	11.9 ± 0.3	12.8	93 ± 2
	7.*	23.4 ± 0.3	23.6	100 ± 1
	8.	17.2 ± 0.1	17.1	100 ± 1

[a]Runs 1-3 were performed in one experiment, runs 4 and 5 in a second, and runs 6-8 in a third.
*Runs 2 and 7 are samples 1 and 6 with a second spike.

Table 5.3 Continued. Percent Recovery of GSH, PSH, GSSG, PSSG and PSSP in plasma samples. Concentrations are in μM units.

Compound	Run No.[a]	Observed Concentration	Expected Concentration	Percent Recovery
PSSP	1.	71 ± 4	45	159 ± 9
	2.*	133 ± 1	90	148 ± 1
	3.	107 ± 6	57	190 ± 10
	4.	580 ± 30	430	135 ± 6
	5.	318 ± 6	229	139 ± 3
	6.	397 ± 1	359	111 ± 1
	7.*	750 ± 10	660	113 ± 2
	8.	551 ± 3	478	115 ± 1

[a]Runs 1-3 were performed in one experiment, runs 4 and 5 in a second, and runs 6-8 in a third.
*Runs 2 and 7 are samples 1 and 6 with a second spike.

Table 5.4. Percent recovery of second spike for GSH, PSH, GSSG, PSSG and PSSP in plasma samples.

Compound	Run No.	Observed Concentration (μM)	Expected Concentration (μM)	Percent Recovery
GSH	1.	9.4 ± 0.1	10.3	91 ± 1
	2.	17.0 ± 0.1	17.1	99 ± 1
PSH	1.	8.9 ± 0.1	11.3	79 ± 1
	2.	30.1 ± 0.3	29.2	103 ± 1
GSSG	1.	7.9 ± 0.1	8.0	99 ± 2
	2.	36.8 ± 0.5	36.1	102 ± 2
PSSG	1.	9.6 ± 0.1	10.3	93 ± 1
	2.	17.5 ± 0.3	17.1	102 ± 2
PSSP	1.	76 ± 4	54	122 ± 23
	2.	550 ± 10	480	115 ± 3

Run No. 1. corresponds to sample 2* on Table 5.3.
Run No. 2. corresponds to sample 7* on Table 5.3.

where $(X_2)([PSH]_1)$ equals the number of moles of PSH contributed by sample 1 and $(Y_2)([PSH]_{std})$ equals the number of moles of PSH contributed by the second spike. By rearrangement of this expression, the number of moles recovered in the second spike, n, can be calculated from Equation 46.

$$n = ([PSH]_2)(X_2 + Y_2) - (X_2 * [PSH]_1) \qquad (46)$$

Using the measured concentrations of $[PSH]_1$ and $[PSH]_2$ and the appropriate volumes of dilution, the measured number of moles from the second spike that are recovered can be determined. This value is compared to the theoretical number of moles added, $(Y_2)([PSH]_{std})$, and multiplied by 100 to find the percent recovery of the spike.

$$\% = \frac{\text{recovered moles of spike}}{\text{moles of spike added}} * 100 \qquad (47)$$

The data presented in Table 5.3 covers three individual experiments. Runs 1-3 were performed during the first experiment, runs 4 and 5 were made during a second experiment and finally runs 6-8 were obtained in a third experiment. Addition of a second spike was used in only the first and last experiment.

In the first experiment a poor recovery was seen for PSH, averaging only 81%. Even the second spike of PSH, as seen in Table 5.4, showed only a 79% recovery. In the

second experiment a low recovery for PSH was again observed. From both experiments, the low recovery of PSH coupled with the rather high recovery of PSSP suggested that oxidation of the PSH might be occurring.

In the final study care was taken to ensure that the plasma and the standard PSH/GSSG mixture were kept thoroughly deoxygenated by bubbling nitrogen into each solution during the spiking process. Recoveries of the PSH were quantitative for all three runs, but the PSSP still showed an elevated percent recovery. No explanation for the high recoveries of PSSP can be given at this time. It is suggested here that a matrix effect of the plasma constituents or of the TCA is the cause, since quantitative recoveries were observed for PSSP when a solution of phosphate buffer was spiked with the standard PSH/GSSG mixture.

Since the effect only alters the recoveries of the PSSP, it may be due to co-elution of a non-electroactive compound in the matrix that enhances the reduction of the PSSP at the upstream electrode. Recall from Chapter III that only a small fraction of the analyte passing over the electrode surface is oxidized or reduced when using amperometric detection. Therefore any variable or compound which increases the fraction of analyte oxidized or reduced can cause increases in the percent recovery. Since no

extraneous peaks were observed in the blank solutions which contained all of the matrix components except the thiols and disulfides, the component that affects the reduction of the PSSP is believed to be non-electroactive.

ii) PSH, GSH, GSSG, PSSP and PSSG in Urine

Urine from a healthy volunteer not on any drug treatment was used for all the urine studies and was spiked in a similar fashion to the plasma experiments. The sample was prepared by diluting human urine by half with a 5% TCA solution. It was then kept on ice for several minutes to ensure complete precipitation of proteins by the TCA, followed by centrifugation and filtration with a 0.2 μm membrane. The supernatant was then spiked with the PSH/GSSG reaction mixture. Figure 5.12 shows a chromatogram of a urine sample that contains 12.9μM GSH, 22.4μM PSH, 20.5μM GSSG, 12.4μM PSSG, and 429.9μM PSSP. The results of the recoveries for spiked samples are listed in Table 5.5.

Recoveries for reduced glutathione and reduced penicillamine were quantitative for all samples analysed. The average recovery for glutathione was 98 ± 4% while that for penicillamine was 95 ± 7%. Determination of the penicillamine-glutathione mixed disulfide was quantitative for all samples studied. Recoveries of PSSG were in the

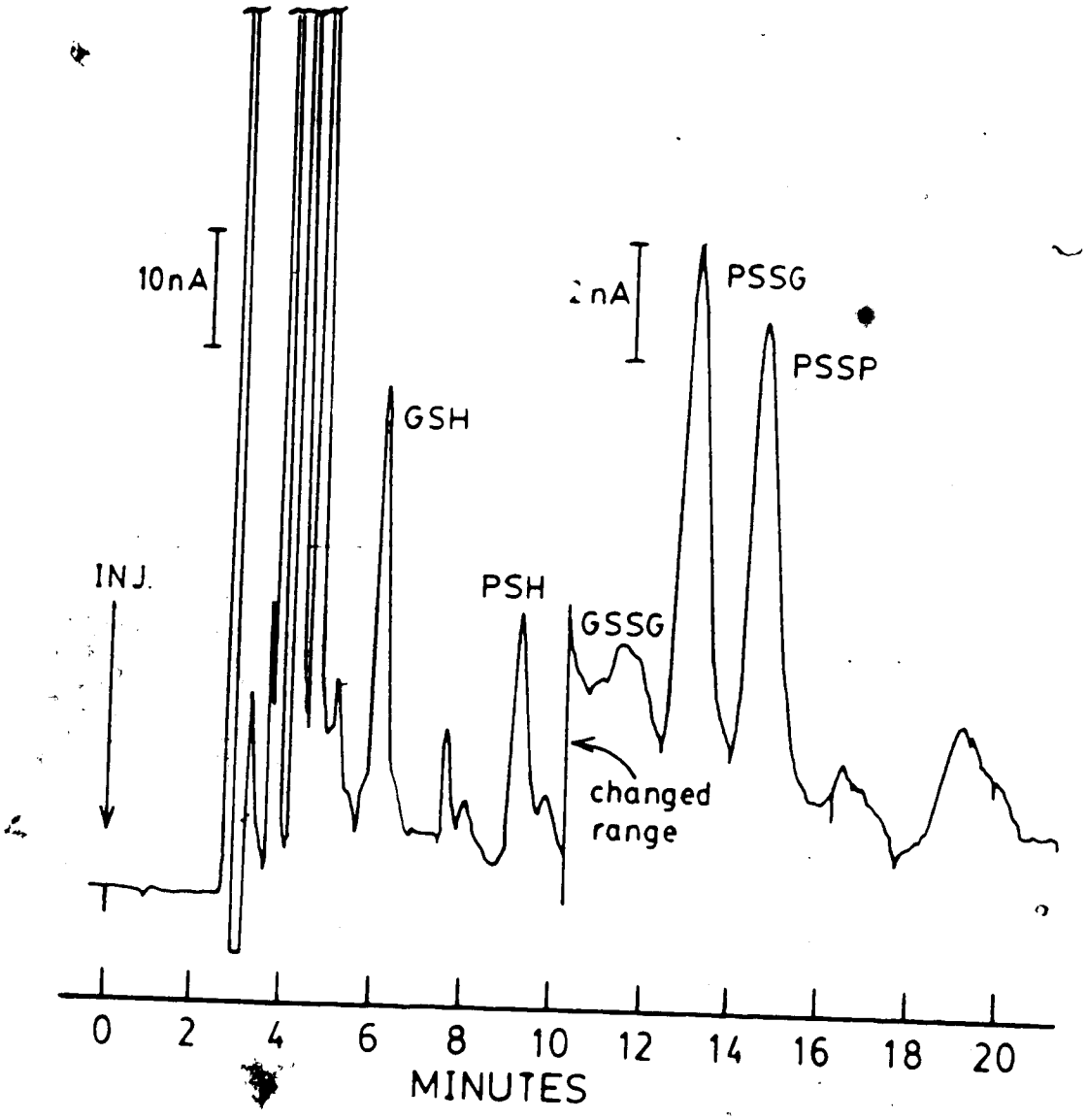

Figure 5.12. A typical chromatogram of urine spiked with 12.85 μM GSH, 21.87 μM PSH, 27.10 μM GSSG, 12.85 μM PSSG and 429.00 μM PSSP. The mobile phase was a pH 3.0 phosphate buffer containing 0.80 mM sodium octyl sulphate with 3% methanol. The flow rate was set to 1.0 mL/min. and the chart speed was 1.0 cm/min.

Table 5.5 Percent Recovery of GSH, PSH, GSSG, PSSG and PSSP in urine samples.

Compound	No.	Observed Concentration	Expected Concentration	Percent Recovery
GSH	1.	11.8 ± 0.2	12.8	92 ± 1
	2.	39.4 ± 0.3	38.6	102 ± 1
	3.	25.2 ± 0.6	25.9	98 ± 3
	4.	17.8 ± 0.6	18.1	99 ± 5
	5.	12.6 ± 0.4	12.9	97 ± 4
	6.	8.0 ± 0.2	7.8	103 ± 4
PSH	1.	22.4 ± 0.3	21.9	102 ± 1
	2.	42.4 ± 0.4	42.4	100 ± 1
	3.	35.8 ± 0.7	36.8	97 ± 3
	4.	24.8 ± 0.2	25.8	96 ± 1
	5.	16.8 ± 0.1	18.4	91 ± 1
	6.	9.2 ± 0.2	11.0	83 ± 3
GSSG	1.	20.5 ± 0.3	27.1	76 ± 2
	2.	30.6 ± 0.3	33.0	93 ± 1
	3.	7.5 ± 0.1	8.1	92 ± 2
	4.	5.3 ± 0.1	5.7	94 ± 2
	5.	3.7 ± 0.1	4.1	92 ± 3
	6.	2.3 ± 0.1	2.4	95 ± 6
PSSG	1.	12.4 ± 0.2	12.8	96 ± 1
	2.	36.5 ± 0.3	38.6	95 ± 1
	3.	10.5 ± 0.2	11.5	92 ± 2
	4.	7.7 ± 0.4	8.0	96 ± 7
	5.	5.3 ± 0.1	5.7	93 ± 3
	6.	3.2 ± 0.1	3.4	94 ± 4
PSSP	1.	430 ± 17	429	100 ± 6
	2.	479 ± 18	528	91 ± 5
	3.	580 ± 41	585	99 ± 9
	4.	599 ± 24	410	146 ± 9
	5.	413 ± 17	293	141 ± 8
	6.	242 ± 14	176	138 ± 11

range of 92 to 96 percent. Similarly, the percent recovery for GSSG was 93 ± 1%.

As was found in the blood plasma recovery studies, high recoveries were obtained for oxidized penicillamine in some of the urine samples (runs 4-6 in Table 5.5). However, the second sample in this table had only a 91% recovery for PSSP. This sample was run after eight injections of other plasma and buffer solutions had been chromatographed. It is possible that oxidation of the mercury electrode had decreased the sensitivity of the electrodes at this time.

The last four spiked urine samples were run in sequence during one experiment. It is interesting to note that the recovery of PSSP in the first spiked urine sample of this set of four was quantitative (99%) while all subsequent samples displayed a high recovery. The average recovery for the last three urine samples was 142%. At the present time no definitive explanations can be given for the variable recovery of PSSP. Evidently the types of matrices being injected into the chromatograph appear to affect the recoveries of the PSSP.

iii) PSH, GSH, GSSG, PSSP and PSSG in Red Blood Cells

Several red blood cell studies have been conducted by Wolowyk and coworkers to try to characterize the amino acid transport system of red blood cell membranes using

penicillamine [133]. In these studies the white blood cells and plasma are drawn off the top of a centrifuged sample of blood. The red blood cells are washed with a saline solution and incubated in a penicillamine solution. After some of the penicillamine has been transported into the cells the extracellular penicillamine is washed away and the cells are ruptured. The membrane residue and intracellular proteins are precipitated with TCA and separated from the intracellular solution by centrifugation. The resulting supernatant is filtered and analysed for penicillamine by HPLC with electrochemical detection.

In these experiments the measured signal was for the free penicillamine only. Since no precautions were made to prevent the possible admission of oxygen to the cells, some of the intracellular penicillamine may undergo either autoxidation or a thiol/disulfide exchange with any intracellular disulfide. In order to investigate this possibility, incubations were carried out according to the procedure outlined in Chapter II.

Table 5.6 lists results from a study in which red blood cells were incubated in a solution of 10 mM penicillamine. Incubation times of 30, 60 and 90 minutes were used. It was observed that, the longer the incubation time, the greater the concentration of penicillamine in the red blood cells. The profile of the uptake of penicillamine by red blood

Table 5.6. Measured concentrations of GSH, PSH, GSSG, PSSG and PSSP in red blood cells after incubation. The samples incubated in 10 mM PSH were freshly prepared samples while those with lower concentrations of PSH had been stored for several months.

Incubation [PSH]	Incubation Time	[GSH] (μM)	[PSH] (μM)	[GSSG] (μM)	[PSSG] (μM)	[PSSP] (μM)
10 mM	30 min.	35.9 ± 0.7	132 ± 2	4.7 ± 0.1	3.4 ± 0.2	0
10 mM	60 min.	38.2 ± 0.1	217 ± 2	4.8 ± 0.3	3.3 ± 0.3	0
10 mM	90 min.	34.7 ± 0.7	239 ± 1	2.0 ± 0.5	3.7 ± 0.5	0
1.0 mM	60 min.	13.4 ± 0.5	6.5 ± 0.2	74.7 ± 0.2	3.1 ± 0.3	0
1.0 mM	20 min.	12.8 ± 0.6	6.5 ± 0.3	74.8 ± 0.4	3.2 ± 0.4	0
1.5 mM	20 min.	19.4 ± 0.8	7.8 ± 0.2	80.6 ± 0.5	2.4 ± 0.4	0
2.0 mM	20 min.	19.4 ± 0.7	n/a	70.7 ± 0.5	2.1 ± 0.3	0

cells is similar to the profile for alanine uptake by human erythrocytes observed by Young et al [134]. The concentration of glutathione measured in the samples remained fairly constant regardless of incubation time. This is expected since the intracellular concentration of glutathione is normally constant and is not affected by washing the cells or by anaerobic incubation in isotonic media [135]. The slight variation in the measured results could be caused by small differences in the hematocrit of the sampled blood suspension. Both GSSG and PSSG were observed in all of the samples, but at much lower levels than their corresponding thiols.

As well, measurements of the thiols and disulfides present in the freshly incubated samples, were compared to measurements for samples that were incubated in 1-2 mM penicillamine and then stored at 4°C for several months. The penicillamine concentration used for incubating the stored samples is so low that any oxidized penicillamine will not be detectable. This accounts for the absence of PSSP in these samples. The concentration of the PSSG for these samples was similar to that measured in the fresh samples, ie. 2 - 3 μM. However, significantly lower GSH concentrations and higher GSSG concentrations were seen in the old samples. Presumably, this is the result of oxidation of GSH to GSSG. The stability of the PSSG

concentration over the long storage period suggests that it was not generated after sample preparation. The presence of the PSSG mixed disulfide in all of the samples indicates that this side reaction of penicillamine must be examined thoroughly if uptake studies are to be completely accurate.

CHAPTER VI

PENICILLAMINE AND HOMOCYSTEINE

A. Introduction

Homocysteine is a naturally-occurring thiol that is a structural homolog of the amino acid cysteine. In animals, homocysteine is produced as an intermediate compound during the conversion of methionine to cysteine, while in plants it is formed during the metabolism of cysteine to methionine. A generalized outline of biological reactions involving homocysteine for cysteine synthesis is shown in Figure 6.1 [136].

From the figure it is evident that there are three possible pathways by which the homocysteine may react. The first is a condensation reaction with serine in the presence of the enzyme cystathionine β-synthetase to form cystathionine. This compound goes on to generate cysteine. The second is conversion back to methionine via a methyl transferase catalyzed reaction with a methyl donating compound. Both of these processes are rapid and thus there is usually little homocysteine present in the cycle. The third possible reaction is oxidation, either to the symmetrical disulfide, homocystine, or to a mixed disulfide, e.g. cysteine-homocysteine mixed disulfide.

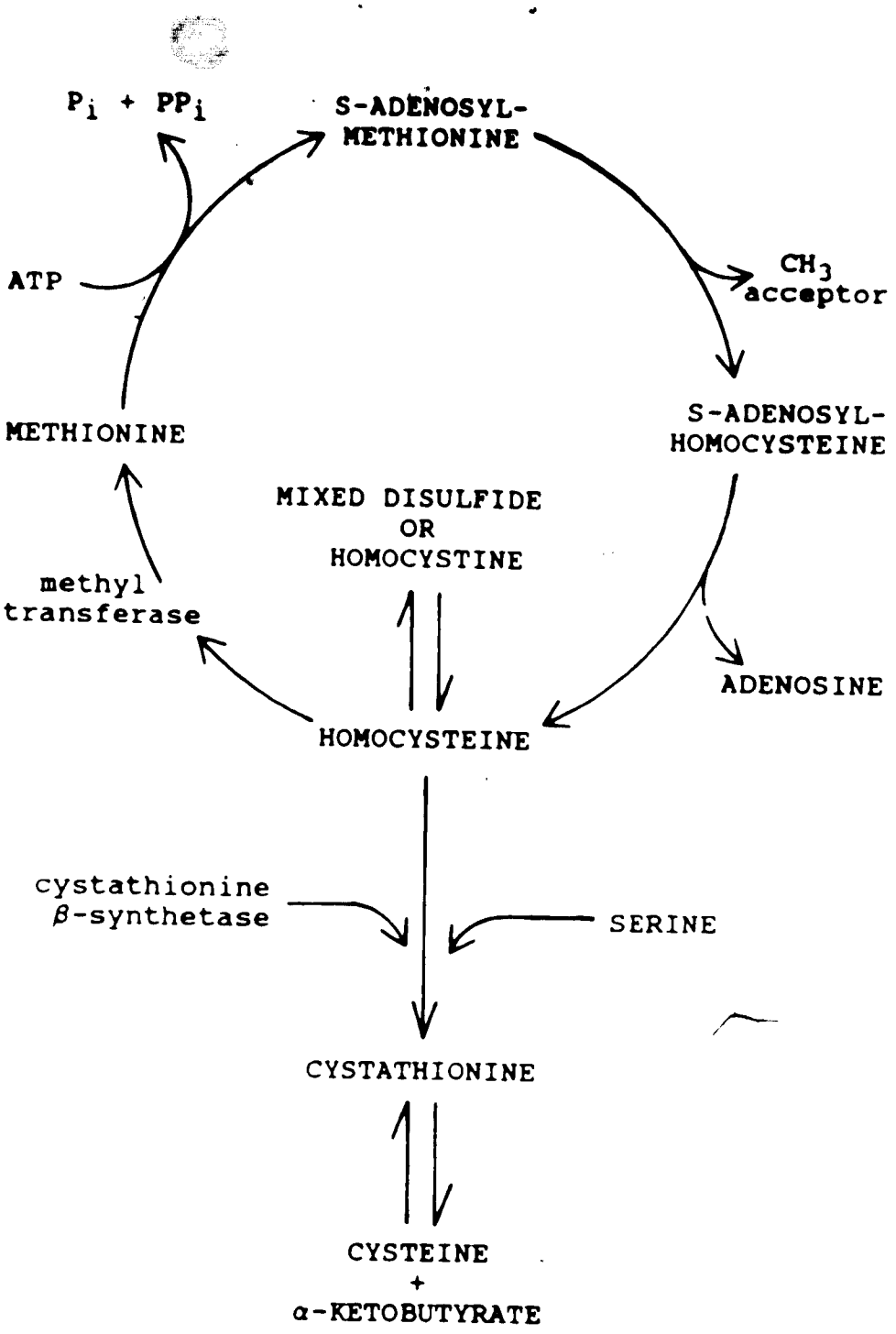

Figure 6.1. Outline of the methionine/homocysteine cycle and its participation in cysteine synthesis.

This last compound has been found in the plasma of fasting subjects and in the urine of patients suffering from Wilson's disease or cystinuria, but to date, no homocysteine or homocystine has been detected in the plasma or urine of normal, healthy subjects [18,41].

In patients having the congenital disorder, homocystinuria, there is a deficiency in one of the enzymes required for the metabolism of homocysteine, resulting in elevated levels of homocysteine and its oxidized form, homocystine. Much of the homocysteine and homocystine appears to be bound to plasma proteins, but significant levels of homocystine in the free form have been detected in the blood plasma of homocystinuric patients.

Administration of D-penicillamine to homocystinuric patients has been found to decrease the concentrations of free homocystine in both the plasma and urine, while increasing the urinary excretion of homocysteine as the penicillamine-homocysteine mixed disulfide [42]. Sensitive and selective methods have not been developed for the determination of this important penicillamine metabolite.

This chapter describes the development of a rapid method for the simultaneous determination of penicillamine homocysteine and their symmetrical and mixed disulfides by high performance liquid chromatography with electrochemical detection.

B. Electrochemical Detection of PSH, HSH, PSSP, HSSH, and PSSH

As with the penicillamine/glutathione system discussed in the previous chapter, the electrochemical and chromatographic operating parameters must be carefully selected for the quantitative analysis of penicillamine, homocysteine and their symmetrical and mixed disulfides.

The results of a study of the electrochemical behaviour of homocysteine, homocystine, penicillamine, penicillamine disulfide, and the penicillamine-homocysteine mixed disulfide at the Hg/Au electrodes of the electrochemical detector were reported in Chapter III. To determine the appropriate potential for the upstream electrode, the hydrodynamic voltammograms for all of the disulfides of interest were examined. Figures 3.13, 3.16, and 3.18 show the voltammograms for homocystine, penicillamine disulfide, and penicillamine-homocysteine mixed disulfide. The hydrodynamic voltammogram for homocystine shows an increasing peak current over the potential range of -0.6 to -1.4 volts versus a Ag/AgCl reference electrode. The slope of the current-potential plot is greatest between -0.6 and -0.950 volts vs Ag/AgCl. At potentials more negative than -0.950 volts the slope drops to only 3.3 nA/V and maximum current responses were observed for the homocystine peak at these potentials. Potential settings in this range are

suitable for quantitative determinations since the peak current is relatively independent of small variations in the electrode potential and still provides maximum reduction of the disulfide.

The hydrodynamic voltammograms for penicillamine disulfide and penicillamine-homocysteine mixed disulfide are very similar. The reduction plateau for both of them occurs at potentials more negative than -1.150 volts vs Ag/AgCl. Unfortunately there is a rapid loss of mercury at the upstream electrode in this potential range. Others have used a potential setting of -1.000 volts vs Ag/AgCl, but they also reported low penicillamine disulfide sensitivity [131]. The hydrodynamic voltammogram for penicillamine disulfide shows that a potential setting of -1.000 volts generates less than 25% of the maximum peak current for PSSP reduction. Use of a potential setting of -1.100 volts vs Ag/AgCl produces a current response that is about 88% of the maximum peak current and use of fresh mobile phase that has been thoroughly deoxygenated reduces the rate at which the mercury on the electrode is lost.

The potential for the downstream electrode was selected by considering the hydrodynamic voltammograms for homocysteine and penicillamine in Figures 3.9 and 3.12. At potentials more negative than -0.200 volts vs Ag/AgCl there is no mercury oxidation occurring as the penicillamine

passes through the detector. Between -0.200 and 0.000 there is an increase in the current for the penicillamine peak as the potential becomes more positive. The oxidative plateau is reached at about 0.000 volts and remains relatively constant until a potential of +0.250 volts. At potentials more positive than +0.250 volts the mercury on the electrode surface is lost by oxidation and an elevated background current is observed. The peak current of the penicillamine begins to increase with potential in this range.

For homocysteine, no peak current is detected at potentials more negative than -0.080 volts. As the potential is made more positive than -0.080 volt there is an increase in the homocysteine peak current with the oxidative plateau occurring between +0.050 and +0.250 volts. The peak current for the homocysteine begins to increase at potentials more positive than +0.250 volts.

From these observations a potential setting of +0.150 volts vs Ag/AgCl was chosen for the downstream electrode. It is located in the central region of the oxidative plateau in both voltammograms, indicating that it will not be significantly affected by any potential fluctuations, e.g. IR drop. The background current with this potential setting was normally between 0.0 and -10.0 nA, the typical operating range suggested by the manufacturer.

C. Chromatographic Conditions

The retention characteristics of homocysteine, homocystine, penicillamine, and penicillamine disulfide were reported in Chapter IV. Figure 4.4 shows a plot of the capacity factors for the thiols as a function of the mobile phase pH while the results for the disulfides appear in Figure 4.9. Both homocysteine and homocystine had low capacity factors over the full pH range studied and showed only a slight decrease in k' as the pH was increased. The capacity factor for the symmetrical penicillamine disulfide was relatively constant over the pH range of 2.0 to 5.0 and had a value just under 3. A small rise in k' for the PSSP was noted at pH 5.5. At pH 2.5 the reduced penicillamine had a capacity factor of about 1.5 which decreased to about 1.1 at pH 3.5 and remained at this value to pH 5.5. Although there is adequate resolution between the reduced penicillamine, the oxidized penicillamine and the reduced or oxidized homocysteine, the short retention times for the latter two compounds made it necessary to add some ion-pairing reagent to the mobile phase.

The effect of the ion-pairing reagent, sodium octyl sulfate, on the homocysteine and penicillamine was shown in Figure 4.14 while homocystine and penicillamine disulfide results were displayed in Figure 4.15. The linear relationships between the capacity factor and the ion-

pairing reagent concentration for each of these compounds are given by the equations in Table 6.1. From the slopes of the lines defined in these equations, it can be seen that the ion-pairing reagent exerts the greatest effect on homocystine and that this effect is some ten times greater than the effect observed for homocysteine. Sodium octyl sulfate can be added to the mobile phase to separate the homocysteine peak from the solvent front peaks, but may result in very long retention times for the homocystine. Careful choice of the sodium octyl sulfate concentration will be required to avoid long analysis times.

The graph of capacity factor for the disulfides versus the concentration of ion-pairing reagent in the mobile phase was presented in Figure 4.15. The graph shows that penicillamine disulfide and homocystine elute at the same time when a mobile phase containing 0.34 millimolar sodium octyl sulfate is used. They can be separated by using a larger or smaller ion-pairing reagent concentration. To prevent the analysis time from getting too long, sodium octyl sulfate concentrations less than 0.34 mM were examined first. Table 6.2 lists the capacity factors for penicillamine, homocysteine and their disulfides as a function of the sodium octyl sulfate concentration in the mobile phase. These theoretical k' values were calculated using the equations in Table 6.1 and cover the concentration

Table 6.1. Equations defining the capacity factor for HSH, PSH, PSSP and HSSH as a function of the concentration of sodium octyl sulphate in the mobile phase.

$$k'(HSH) = 0.010 * [S.O.S.] + 0.37$$

$$k'(PSH) = 0.0210 * [S.O.S.] + 1.21$$

$$k'(PSSP) = 0.084 * [S.O.S.] + 1.53$$

$$k'(HSSH) = 0.107 * [S.O.S.] - 0.306$$

Table 6.2 Calculated capacity factor for HSH, PSH, PSSP and HSSH for various sodium octyl sulphate concentrations.

	[SOS] (mM)	HSH	PSH	PSSP	HSSH
1.	0.042	0.47	1.4	2.4	0.76
2.	0.085	0.56	1.6	3.2	1.8
3.	0.128	0.66	1.8	4.1	2.9
4.	0.170	0.75	2.05	4.9	4.0
5.	0.212	0.85	2.26	5.7	5.1
6.	0.265	0.95	2.47	6.6	6.1
7.	0.308	1.04	2.68	7.4	7.2
8.	0.340	1.14	2.89	8.3	8.3

range of 0.00 mM to 0.34 mM sodium octyl sulfate. Since homocystine was not well resolved from the solvent peaks when a mobile phase with no ion-pairing reagent was used and since it would elute simultaneously with penicillamine disulfide when a concentration of 0.34 mM sodium octyl sulfate was present in the mobile phase, the intermediate concentration of 0.17 mM sodium octyl sulfate was initially selected. The calculated k' values in Table 6.2 show that at this sodium octyl sulfate concentration the homocystine should have a capacity factor of 3.98 while the penicillamine disulfide is predicted to have a capacity factor of 4.89. This corresponds to about 2.5 minutes between these two peaks. Presumably the penicillamine-homocysteine mixed disulfide will also elute in this region.

To verify these predictions a solution containing homocysteine, homocystine, penicillamine, penicillamine disulfide and penicillamine-homocysteine mixed disulfide was prepared as outlined in the experimental section of Chapter II. Typically 1.0 mL of a 30 mM solution of penicillamine was pipetted into a volumetric flask containing 1.0 mL of 30 mM homocystine. Both solutions were prepared in a pH 3.0 phosphate buffer made with D_2O so that a sample of the final mixture could be taken for NMR analysis. The solution pH was elevated to 11.5 with solid NaOH and the mixture was allowed to react under nitrogen for about 30 minutes.

Termination of the reaction was performed by decreasing the pH to 3.0 with 50:50 H_3PO_4:D_2O. Since the PS^- anion is the reactive penicillamine species in the thiol/disulfide exchange reaction (Chapter II), the penicillamine will cease to react with the disulfides at pH 3.0 because the sulfhydryl group will be protonated. Once the reaction was stopped, the volumetric flask was diluted to volume using pH 3.0 phosphate/D_2O buffer. A 0.5 mL aliquot was then taken for ^1H NMR analysis.

Figure 6.2 shows a ^1H NMR spectrum for a PSH/HSSH reaction mixture with an expanded view of the methyl region in Figure 6.3. Four distinct methyl resonances are observed in the expanded spectrum and the area under each resonance is represented by the height of the integral trace. The resonances at 1.48 and 1.57 ppm belong to the two sets of methyl protons of penicillamine while the signals at 1.39 and 1.55 ppm are due to the two sets of methyl protons of the penicillamine fragment of the penicillamine-homocysteine disulfide. The fraction of the total penicillamine in each of these forms was calculated from the relative areas using equations 12 and 13 in Chapter II. The concentrations of penicillamine, penicillamine-homocysteine mixed disulfide, homocysteine, and homocystine were determined from these fractions and the initial penicillamine concentration, $[PSH]_0$, using the equations 7, 8, 16 and 17 in Chapter II.

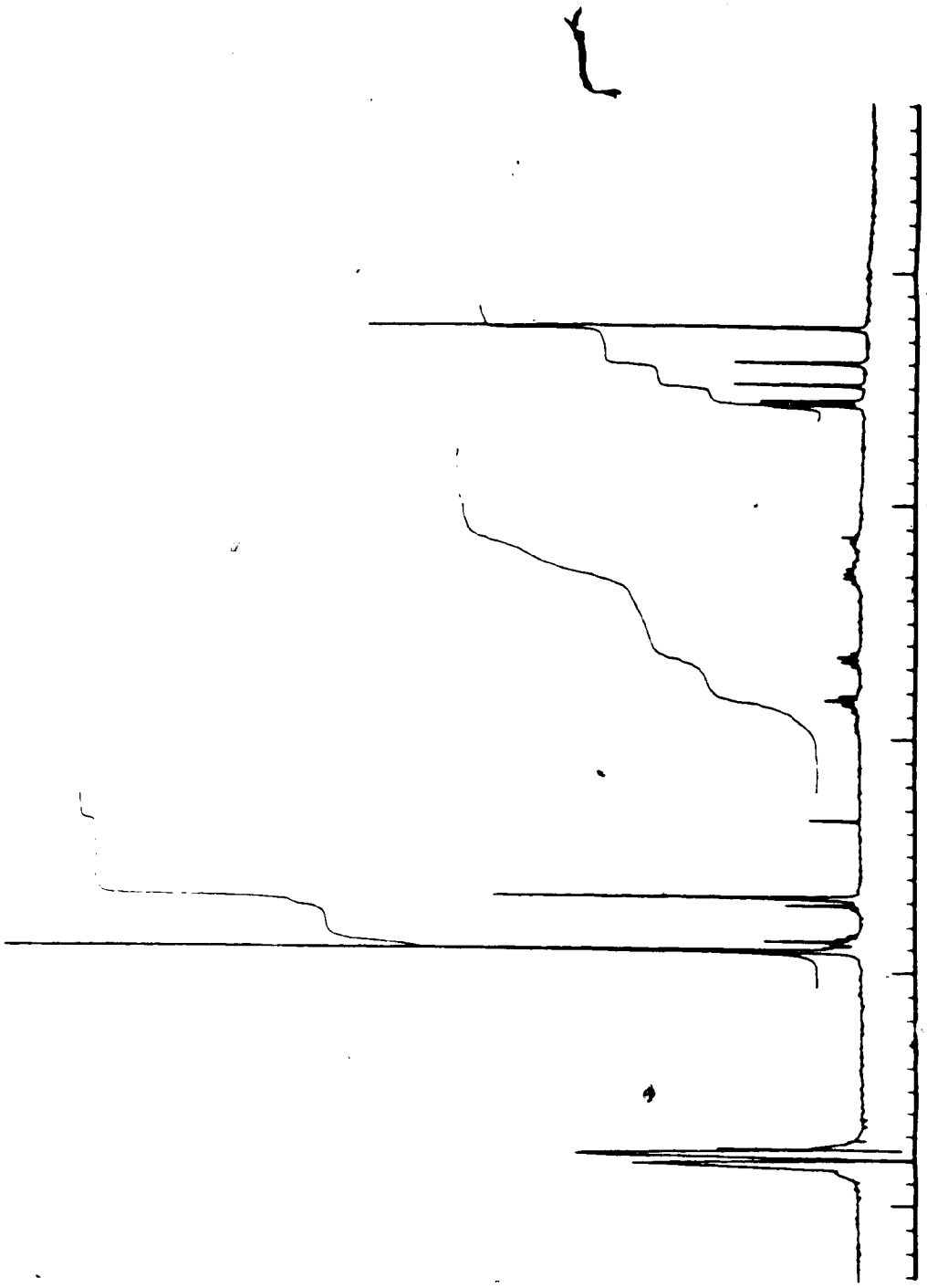

Figure 6.2. A 400 MHz ^{1}H NMR spectrum of a mixture of HSH, PSH, HSSH and PSSH.

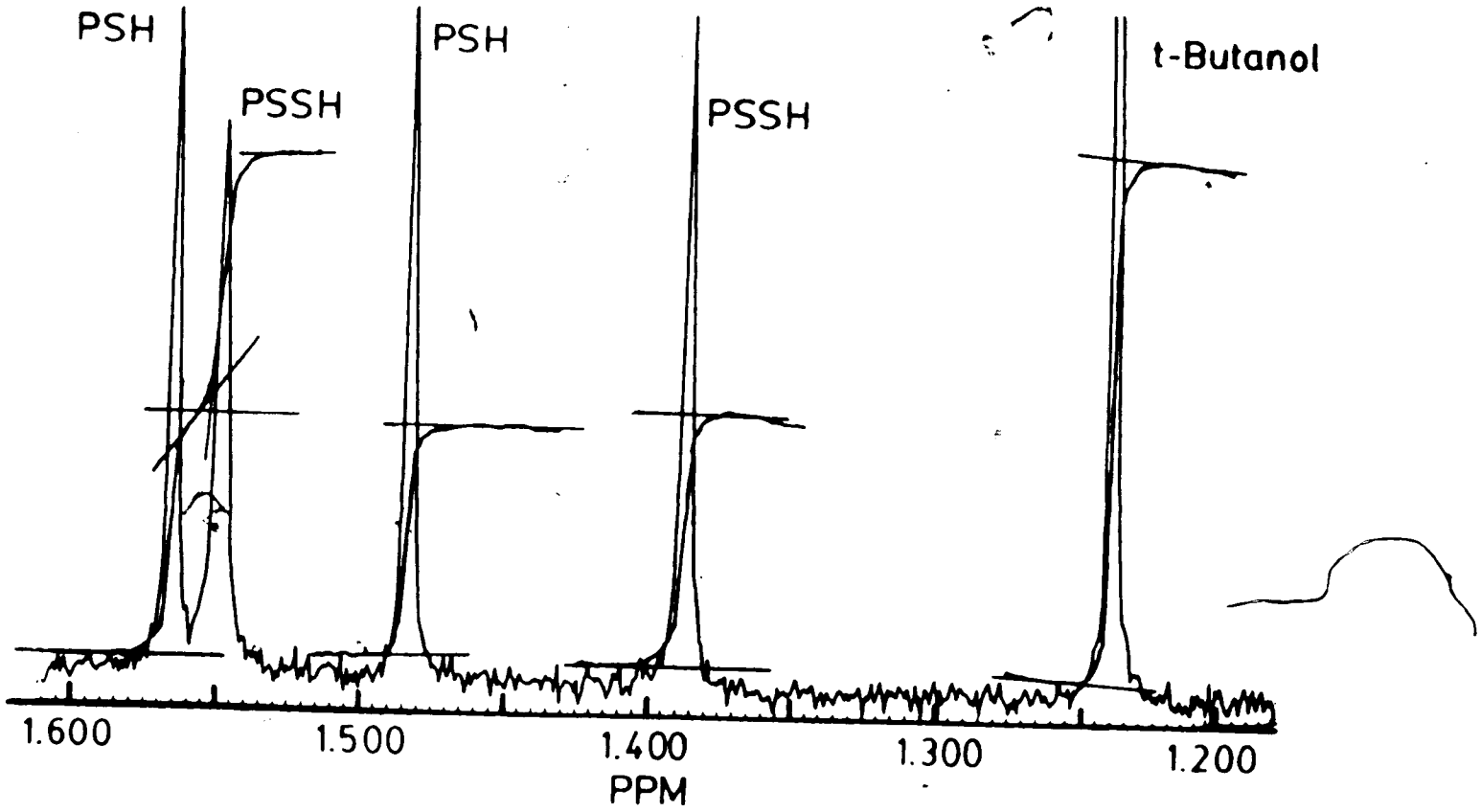

Figure 6.3. An expanded view of the methyl region of the spectrum in Figure 6.2. The resonances at 1.57 and 1.48 ppm correspond to methyl protons on penicillamine while the resonances at 1.55 and 1.39 ppm correspond to methyl protons on the penicillamine moiety of the PSSH. The resonance at the right is due to the t-butanol internal reference and was set to 1.2397 ppm vs DSS.

With nitrogen constantly flushing the reaction vessel, no PSSP was observed in the these reaction mixtures by the NMR analysis. To make the standard solutions for the calibration of the detector response, the reaction mixture was usually diluted 10-fold and an aliquot of PSSP was added during the dilution to make a five-component mixture.

Figure 6.4 shows a chromatogram of a five-component mixture containing homocysteine, penicillamine, homocystine, penicillamine disulfide and penicillamine-homocysteine mixed disulfide using a pH 3.0 phosphate buffer with 0.17 mM sodium octyl sulfate as the mobile phase. All five peaks showed adequate resolution although some overlap of the penicillamine and homocystine peaks was observed. The retention times for the disulfides were quite short, and hence the capacity factors were small than the expected values. This is because the retention studies were performed on a Bioanalytical Systems Biophase ODS column while a Whatman Partisil ODS-3 column was used in this analysis. The difference in the manufacturer, no doubt, produces differences in the stationary phase composition which most likely accounts for the differences in the observed retention times.

Although the above mobile phase gave good resolution for all five peaks, analysis of plasma or urine samples showed additional peaks that interfered with the

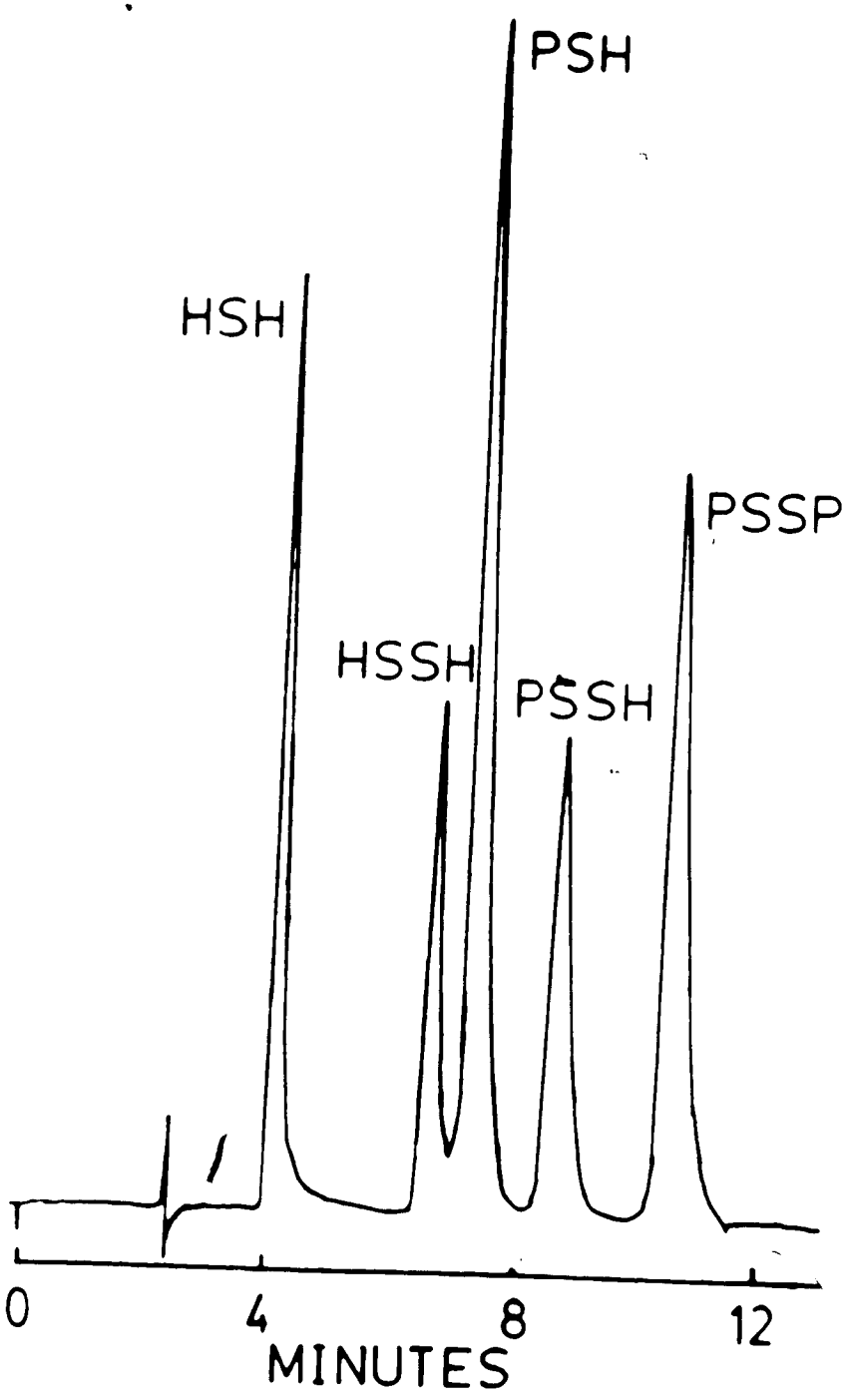

Figure 6.4. Chromatogram of a five-component mixture containing HSH, PSH, HSSH, PSSH, and PSSP in pH 3.0 phosphate buffer. The mobile phase was a pH 3.0 phosphate buffer containing 0.17 mM sodium octyl sulphate. A flow rate of 1.0 mL/min. was used.

homocysteine peak measurement. These additional peaks are due to the trichloroacetic acid used to precipitate proteins in the plasma and urine samples. To separate the homocysteine from these interfering peaks, a capacity factor of about 1.0 would be required. A sodium octyl sulfate concentration of about 0.34 mM would produce a capacity factor of about 1.1 for homocysteine.

Figure 6.5 shows a chromatogram of a plasma sample spiked with a five-component mixture of homocysteine, penicillamine, homocystine, penicillamine disulfide, and penicillamine-homocysteine mixed disulfide. The mobile phase consisted of a pH 3.0 phosphate buffer with 0.34 mM sodium octyl sulfate. Excellent resolution was obtained for all five peaks and there was no interference for the measurement of the homocysteine peak.

D. Recovery Studies

The ability of the chromatographic system to give quantitative results for the analysis of homocysteine, homocystine, penicillamine, penicillamine disulfide, and penicillamine-homocysteine disulfide in biological fluids was studied by recovery experiments. Blood and urine specimens were obtained from a healthy volunteer and were worked up according to the procedure outlined in the Preparation of Samples section of Chapter II. Aliquots of a standard stock solution containing the oxidized and reduced

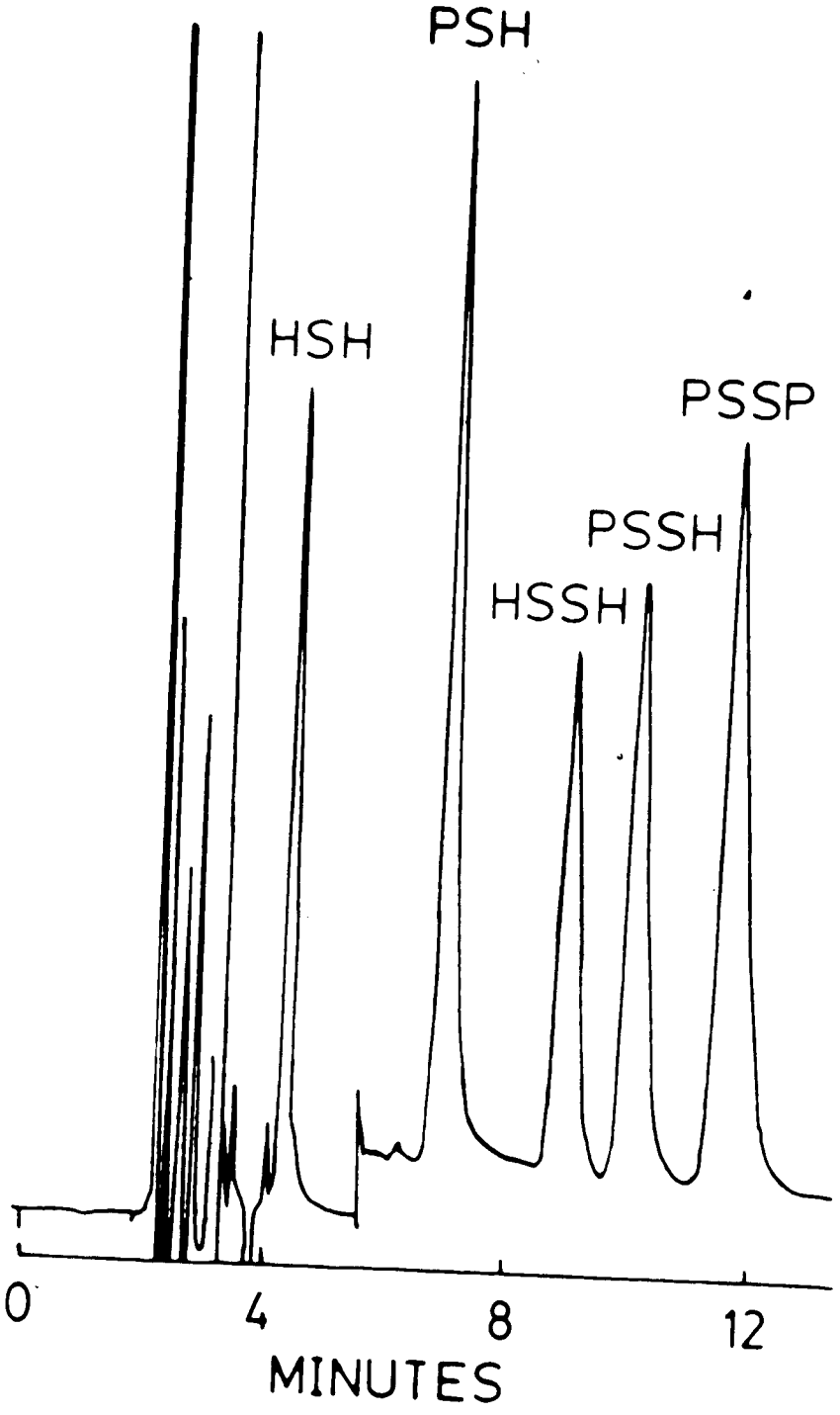

Figure 6.5. Chromatogram of a plasma sample spiked with a five-component mixture of 19.84 μM HSH, 19.72 μM PSH, 58.56 μM HSSH, 19.84 μM PSSH, and 494.00 μM PSSP. The mobile phase was a pH 3.0 phosphate buffer containing 0.34 mM sodium octyl sulphate. A flow rate of 1.0 mL/min. was used.

forms of homocysteine and penicillamine as well as the PSSH mixed disulfide were added to the treated plasma and urine. Injections of each solution were made and the recorded peak currents for each component were compared to calibration curves run on the same day.

Table 6.3 shows the results of the recovery study for penicillamine and homocysteine in plasma. The average percent recovery for 10 - 44 μM HSH was 104% while PSH covering the same range had an average recovery of 102%. Samples that were spiked with a second aliquot are marked in the table and appear immediately after the parent solution. For both HSH and PSH, the second increment resulted in an increased recovery.

In general, for a set of samples run on the same day, higher recoveries were seen for the samples of higher concentration. To illustrate this, note samples 5, 6 and 8 in Table 6.3. These three samples were run during one experiment and show a correlation between thiol concentration and percent recovery. Figure 6.6 shows a graph of the peak current versus the theoretical concentration for the homocysteine in these samples along with part of the calibration curve obtained from standard solutions prepared in buffer. The increased slope for the results from the plasma samples suggests that the plasma matrix increases the electrode response for the

Table 6.3. Recovery of homocysteine and penicillamine in spiked plasma samples. All concentrations are reported in μM units.

	Series[a]	[HSH] found	[HSH] spike	Percent Recovery	[PSH] found	[PSH] spike	Percent Recovery
1.	A	18.3 ± 0.2	19.8	92 ± 1	19.7 ± 0.2	20.6	96 ± 1
2.	A*	31.8 ± 0.4	29.8	107 ± 2	31.4 ± 0.5	30.9	101 ± 2
3.	B	10.9 ± 0.1	10.4	105 ± 1	13.4 ± 0.1	13.2	101 ± 1
4.	B*	23.0 ± 0.1	20.6	111 ± 1	27.0 ± 0.5	26.3	102 ± 2
5.	C	21.9 ± 0.9	19.8	111 ± 4	21.7 ± 0.8	22.9	95 ± 5
6.	C	12.3 ± 0.2	11.9	104 ± 2	12.3 ± 0.2	13.7	90 ± 2
7.	C*	37.6 ± 0.8	32.1	117 ± 2	40.5 ± 0.5	37.0	109 ± 2
8.	C	38.6 ± 0.3	31.7	122 ± 1	40.4 ± 0.7	36.6	110 ± 3
9.	D	11.6 ± 0.3	11.9	97 ± 2	13.1 ± 0.5	13.7	95 ± 3
10.	D*	18.4 ± 0.4	18.6	99 ± 2	22.4 ± 0.7	21.5	104 ± 3
11.	D	15.1 ± 0.6	15.8	95 ± 4	20.0 ± 0.4	18.3	110 ± 2
12.	E	26.5 ± 0.4	28.2	94 ± 3	26.9 ± 0.4	26.3	102 ± 3
13.	E*	41.7 ± 0.4	44.1	94 ± 2	42.3 ± 0.4	41.2	103 ± 2

[a]The series refers to samples run during the same experiment, ie. compared to the same series of calibration curves.

*Are runs of the preceeding sample that were spiked with a second aliquot of the mixture of thiols and disulfides.

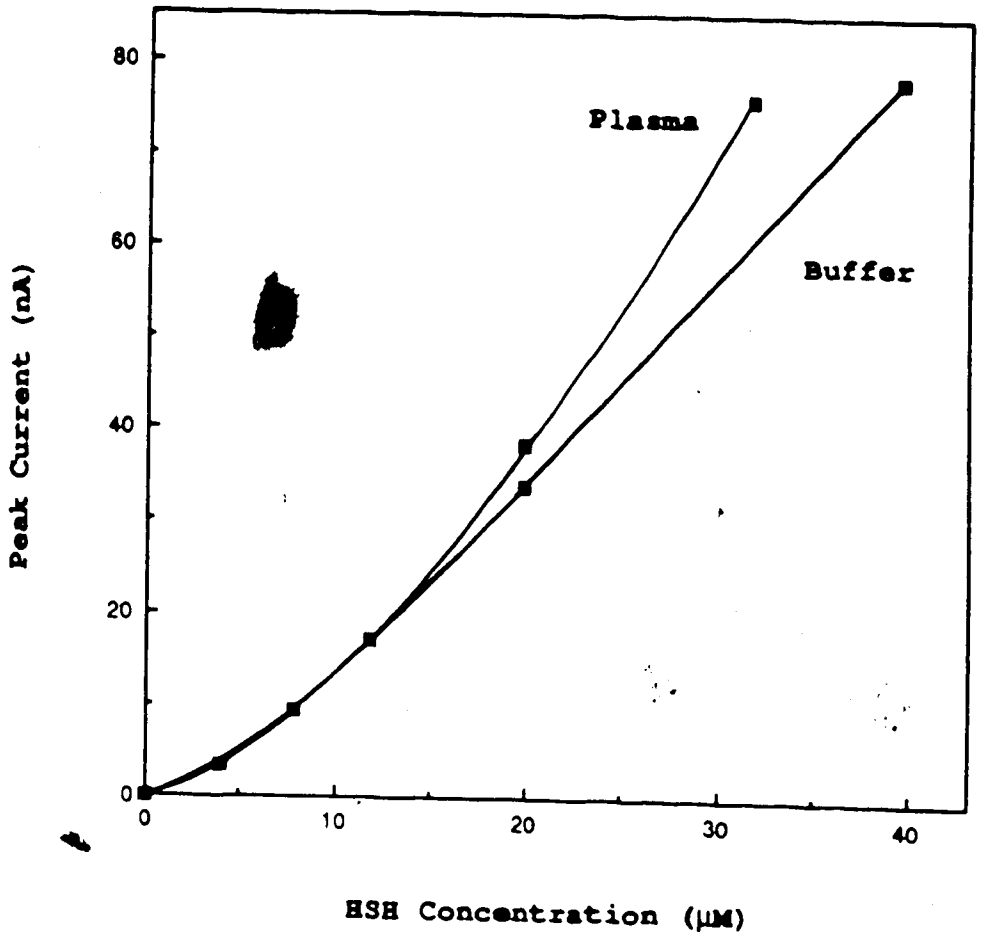

Figure 6.6. Comparison of calibration curves for HSH standards prepared in plasma with HSH standards prepared in buffer.

homocysteine. A similar trend was observed for penicillamine and is shown in Figure 6.7. The vertical dimension of the symbols used in these figures is representative of the standard deviation for the replicate measurements made at each concentration.

To correct for this matrix effect, calibration standards were prepared using plasma from which the proteins were precipitated and removed by filtration. Samples were prepared in an manner identical to the standards using plasma taken from a second individual. Samples 9 - 13 in the recovery tables for the plasma samples were measured against calibration solutions that were prepared in this manner. The average percent recoveries for both of these compounds using the plasma calibration standard curve did not appear to be significantly different from the average percentage found using the calibration curve from standards prepared in buffer. The recoveries of HSSH, PSSH and PSSP in plasma solutions are listed in Table 6.4. The matrix effect observed for the thiols was much less for homocystine and for the penicillamine-homocysteine mixed disulfide. However, significantly larger than theoretical recoveries were observed for the PSSP. Figures 6.8 to 6.10 show the calibration curves for HSSH, PSSH and PSSP standards prepared in plasma and in buffer. The difference in the slope for PSSP in plasma compared to that found for PSSP in

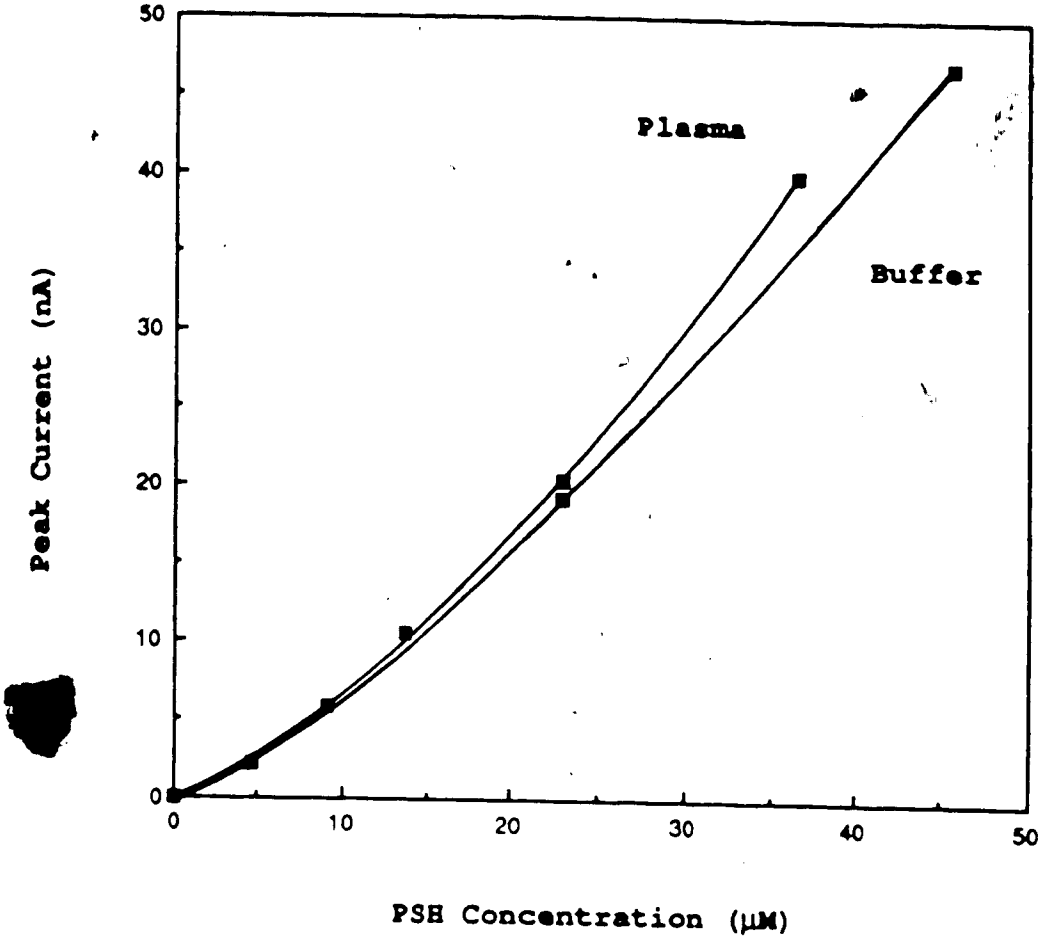

Figure 6.7. Comparison of calibration curves for PSH standards prepared in plasma with PSH standards prepared in buffer.

Table 6.4. Recovery of HSSH, PSSH and PSSP in spiked plasma samples. All concentrations are reported in μM units.

	Series[a]	[HSSH] found	[HSSH] spike	Percent Recovery	[PSSH] found	[PSSH] spike	Percent Recovery
1.	A	64 ± 1	59	109 ± 1	21.7 ± 0.5	19.8	109 ± 2
2.	A*	96 ± 1	88	109 ± 1	32.3 ± 0.3	29.8	108 ± 1
3.	B	11.3 ± 0.1	9.7	116 ± 1	12.0 ± 0.1	10.4	115 ± 3
4.	B*	22.0 ± 0.1	19.3	114 ± 1	24.0 ± 0.1	20.6	116 ± 1
5.	C	10.8 ± 0.3	10.3	105 ± 3	20.8 ± 0.4	19.8	105 ± 2
6.	C	6.5 ± 0.1	6.2	106 ± 1	12.6 ± 0.3	11.9	106 ± 2
7.	C*	17.6 ± 0.6	16.6	106 ± 3	34.3 ± 0.9	32.1	107 ± 3
8.	C	17.6 ± 0.5	16.4	107 ± 3	34.6 ± 0.5	31.7	109 ± 1
9.	D	6.5 ± 0.1	6.2	105 ± 1	13.2 ± 0.1	11.9	111 ± 1
10.	D*	10.0 ± 0.2	9.6	103 ± 2	20.9 ± 0.1	18.6	112 ± 3
11.	D	8.8 ± 0.1	8.2	107 ± 1	18.4 ± 0.1	15.8	116 ± 1
12.	E	22.3 ± 0.1	23.9	93 ± 1	27.0 ± 0.6	28.2	96 ± 4
13.	E*	34.9 ± 0.2	37.5	93 ± 1	41.9 ± 0.2	44.1	95 ± 1

	Series[a]	[PSSP] found	[PSSP] spike	Percent Recovery
1.	A	846 ± 11	494	171 ± 1
2.	A*	1200 ± 20	743	161 ± 1
3.	B	436 ± 12	286	152 ± 3
4.	B*	848 ± 5	569	149 ± 2
5.	C	599 ± 18	283	221 ± 3
6.	C	382 ± 14	170	225 ± 4
7.	C*	978 ± 11	459	213 ± 1
8.	C	999 ± 16	453	220 ± 2
9.	D	-----	0	-----
10.	D*	-----	0	-----
11.	D	-----	0	-----
12.	E	605 ± 7	567	107 ± 2
13.	E*	959 ± 1	888	108.0 ± 0.2

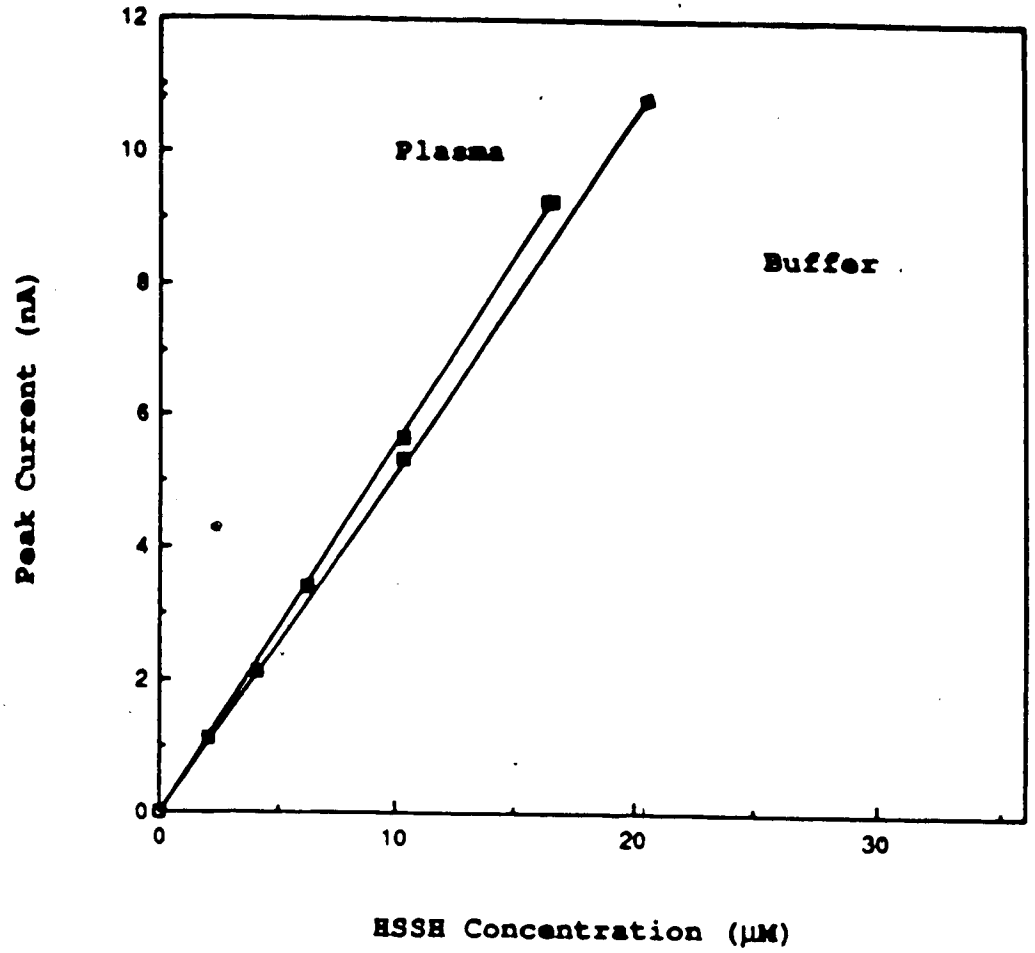

Figure 6.8. Comparison of calibration curves for HSSH standards prepared in plasma with HSSH standards prepared in buffer.

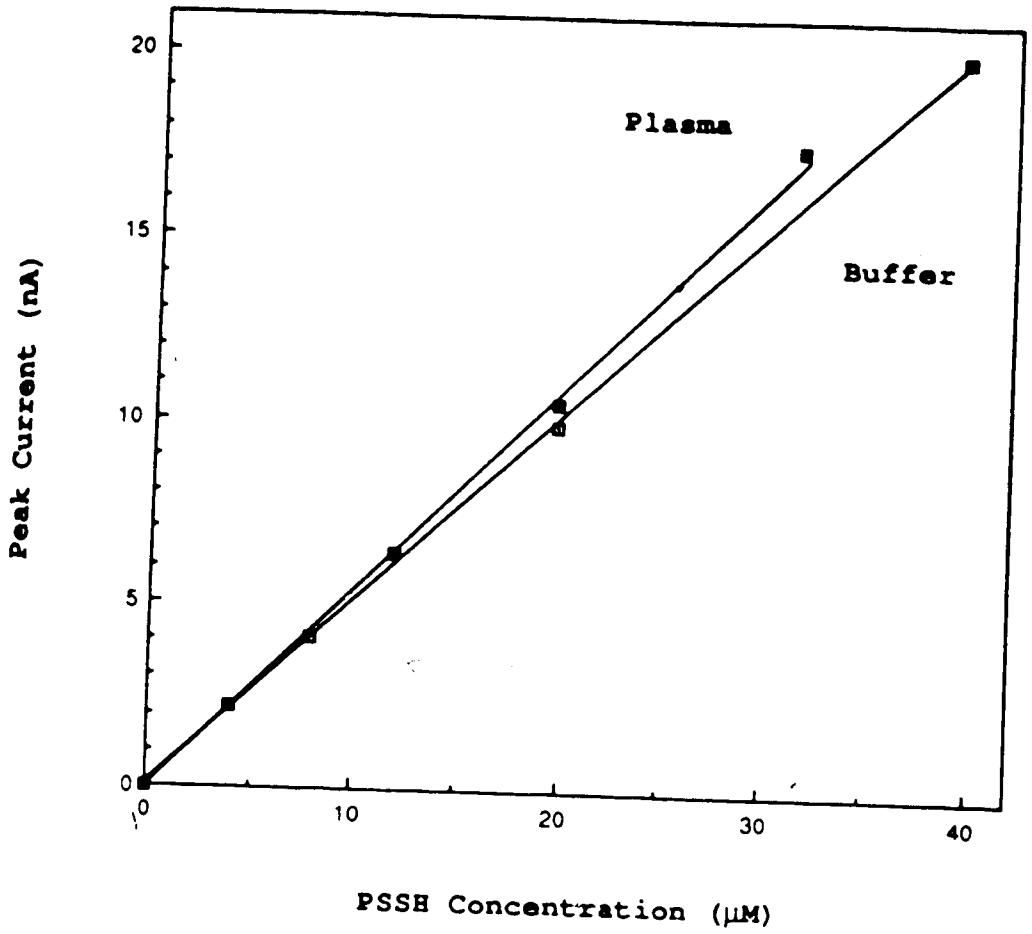

Figure 6.9. Comparison of calibration curves for PSSH standards prepared in plasma with PSSH standards prepared in buffer.

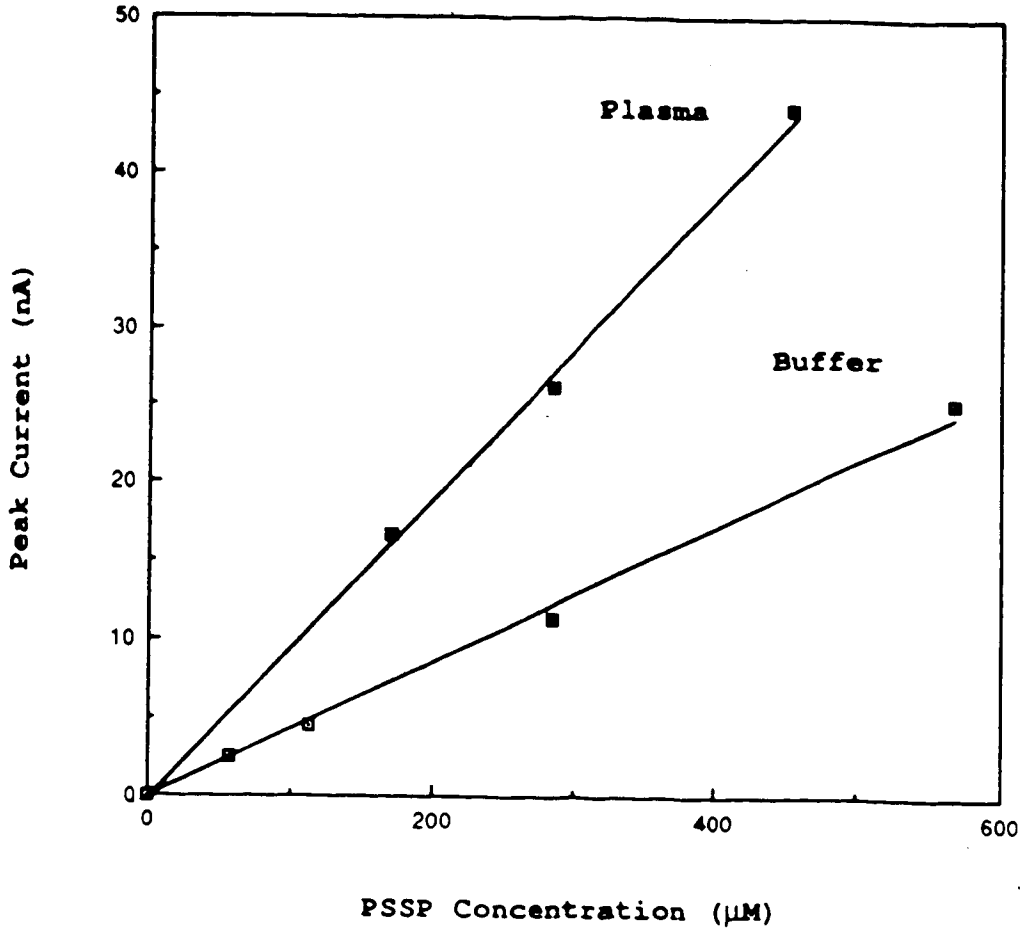

Figure 6.10. Comparison of calibration curves for PSSP standards prepared in plasma with PSSP standards prepared in buffer.

dramatically changed. Again, use of calibration standards prepared in plasma corrects for this matrix effect and the average percent recovery for the PSSP is 107% as seen by the last two entries in Table 6.4.

Similar recovery studies were performed for urine samples. Table 6.5 lists the percent recovery for homocysteine and penicillamine in urine. The average percent recovery for the range of 12 to 40 μM homocysteine was 106% while the average recovery for penicillamine in the same concentration range was 99%. Samples 8 and 9 were measured with respect to calibration curves prepared with plasma standards, but do not have recovery percentages that are significantly different from the net average.

Table 6.6 reports the recovery results for homocystine, penicillamine disulfide and penicillamine-homocysteine disulfide in urine. The average recovery for homocystine covering a concentration range of 6 - 160 μM was 103%. The recovery for 10 - 110 μM penicillamine-homocysteine disulfide was 107%. No significant change in the electrode sensitivity was observed for these two components in the urine samples. The penicillamine disulfide showed larger than theoretical recoveries for all but the last two samples listed in Table 6.6. The peak current versus the theoretical concentration for the PSSP in the urine samples was compared to the calibration results

Table 6.5. Recovery of homocysteine and penicillamine in spiked urine samples. All concentrations are reported in μM units.

	Series[a]	[HSH] found	[HSH] spike	Percent Recovery	[PSH] found	[PSH] spike	Percent Recovery
1.	A	24.0 ± 0.8	29.8	81 ± 3	17.0 ± 0.6	20.8	82 ± 4
2.	A	19.2 ± 0.7	14.8	129 ± 4	11.4 ± 0.2	10.4	110 ± 2
3.	A	25.9 ± 0.8	38.5	91 ± 3	27.3 ± 0.3	28.1	97 ± 1
4.	B	44.4 ± 0.8	38.5	115 ± 2	9.3 ± 0.2	9.6	96 ± 2
5.	C	40.5 ± 1.0	31.7	127 ± 3	40.0 ± 0.9	36.6	109 ± 2
6.	C	22.8 ± 0.9	19.8	115 ± 4	22.7 ± 0.4	22.9	99 ± 2
7.	C	11.2 ± 0.7	11.9	94 ± 6	12.9 ± 0.6	13.7	94 ± 5
8.	D	12.0 ± 0.1	11.9	101 ± 1	13.5 ± 0.1	13.7	99 ± 1
9.	D	20.2 ± 0.2	18.5	109 ± 1	22.5 ± 0.4	21.5	104 ± 2
Average				105%			102%

[a]The series refers to samples run during the same experiment, ie. compared to the same series of calibration curves.

Table 6.6. Recovery of HSSH, PSSH and PSSP in spiked urine samples. All concentrations are reported in μM units.

	Series[a]	[HSSH] found	[HSSH] spike	Percent Recovery	[PSSH] found	[PSSH] spike	Percent Recovery
1.	A	13.9 ± 0.6	10.9	105 ± 1	99 ± 1	87	113 ± 1
2.	A	56 ± 1	55	103 ± 1	48 ± 1	43	110 ± 1
3.	A	167 ± 1	162	103 ± 1	144 ± 2	129	111 ± 1
4.	B	19.0 ± 0.3	19.0	100 ± 1	39 ± 1	38	100 ± 2
5.	C	17.3 ± 0.2	16.4	105 ± 1	33.6 ± 0.3	31.6	106 ± 9
6.	C	10.8 ± 0.3	10.3	105 ± 1	20.6 ± 0.6	19.8	104 ± 3
7.	C	6.4 ± 0.1	6.2	104 ± 2	12.1 ± 0.3	11.9	102 ± 3
8.	D	6.4 ± 0.1	6.16	104 ± 1	12.4 ± 0.2	11.9	104 ± 2
9.	D	9.9 ± 0.1	9.6	102 ± 1	20.1 ± 0.1	18.5	109 ± 1

	Series[a]	[PSSP] found	[PSSP] spike	Percent Recovery
1.	A	672 ± 14	500	134 ± 2
2.	A	351 ± 21	250	140 ± 6
3.	A	882 ± 9	742	119 ± 1
4.	B	703 ± 17	567	124 ± 3
5.	C	965 ± 16	453	213 ± 2
6.	C	594 ± 31	283	210 ± 5
7.	C	356 ± 18	170	209 ± 5
8.	D	179 ± 14	170	105 ± 8
9.	D	275 ± 26	266	103 ± 9

[a]The series refers to samples run during the same experiment, ie. compared to the same series of calibration curves.

for standards made in buffer and is plotted in Figure 6.11. Again a distinct change in the electrode sensitivity was seen. Use of calibration solutions prepared in urine produced quantitative results for urine samples spiked with PSSP, as indicated by an average recovery of 104% for samples 8 and 9 in Table 6.6.

Further investigation of the matrix effect on the analysis of penicillamine metabolites was performed using a solution containing penicillamine, its symmetrical disulfide, the penicillamine-cysteine mixed disulfide, cysteine, and cystine. Calibration solutions were prepared in buffer and in pretreated urine. Figures 6.12 - 6.16 show the comparison of the calibration curves for all five components in urine and in buffer. The non-zero intercepts for the CSH and CSSC in the urine standards are due to endogenous CSH and CSSC. For all five components, increased calibration slopes were observed with the urine standards.

The results from the penicillamine/homocysteine and penicillamine/cysteine studies indicate that matching of the calibration matrix to the sample matrix is important. Use of standards prepared in buffer, although adequate for some components, is not recommended since measured quantities may be in error by as much as 100%, as was seen for the PSSP. The only inherent problem with using standards prepared in

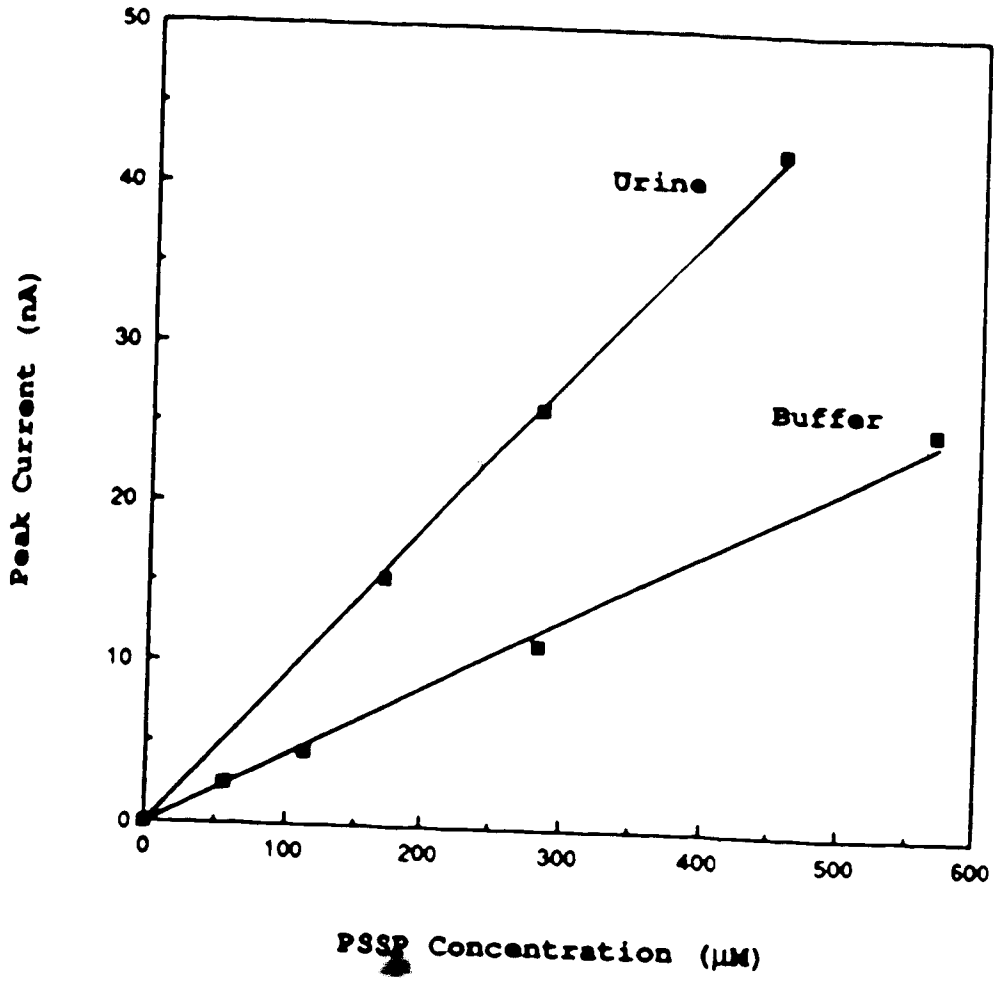

Figure 6.11. Comparison of the calibration curves for PSSP in urine with PSSP in buffer. The PSSP was added as one of five components resulting from the thiol-disulfide exchange reaction of PSH and HSSH.

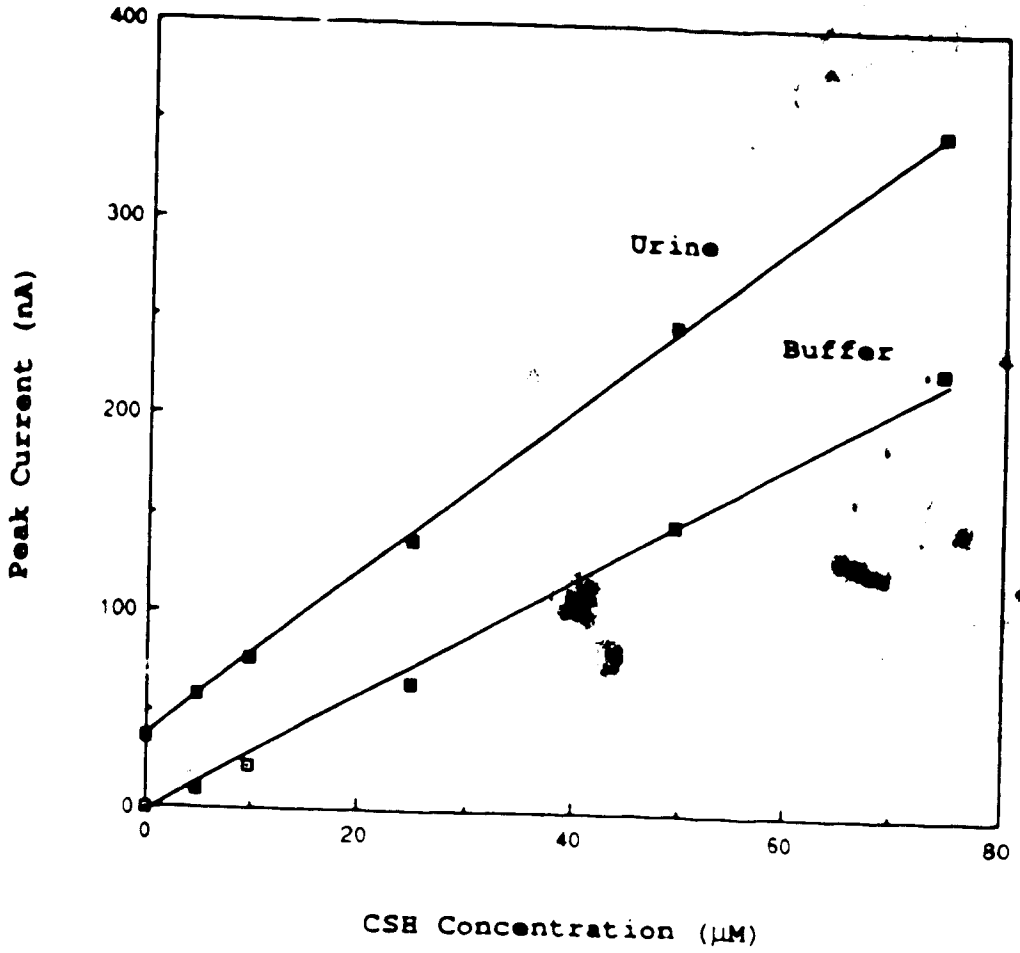

Figure 6.12. Comparison of calibration curves for CSH added to urine with CSH added to buffer. The non-zero intercept for the urine calibration curve is due to endogenous CSH. The CSH added was the result of a thiol-disulfide exchange reaction for PSH and CSSC.

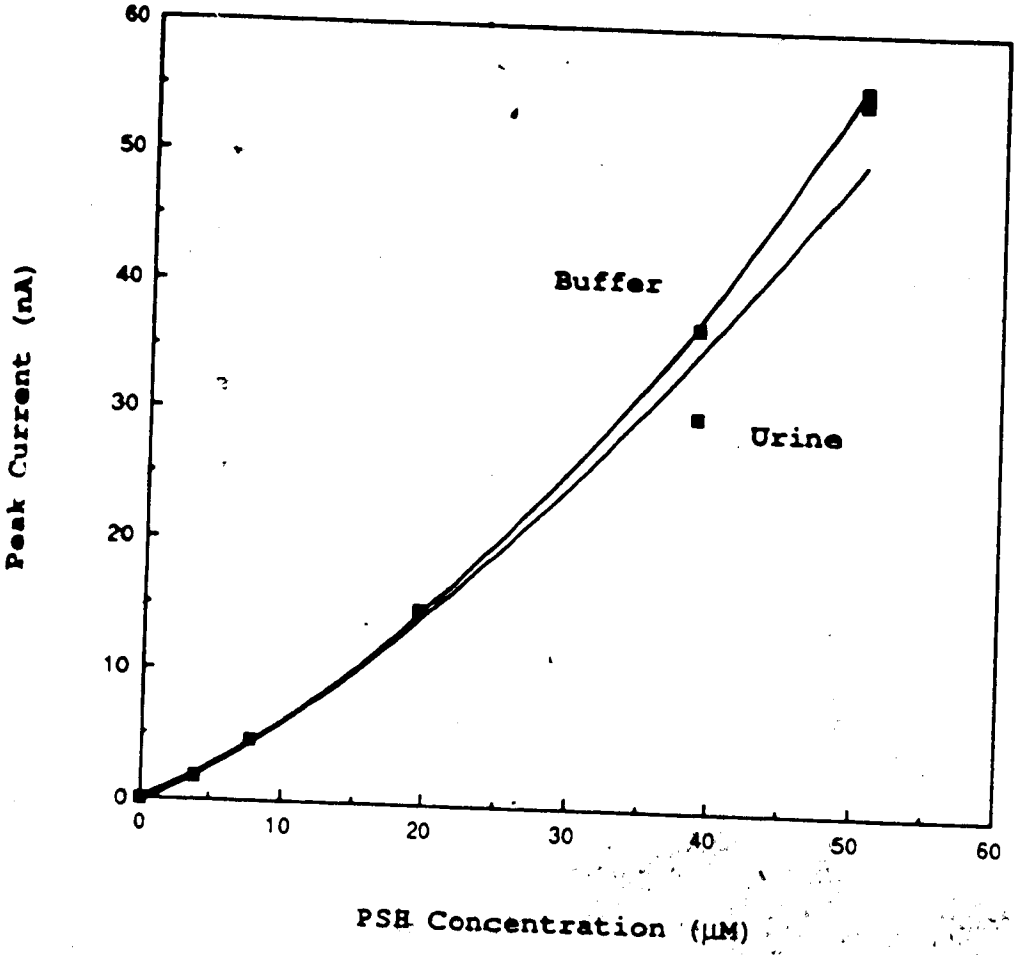

Figure 6.13. Comparison of calibration curves for PSH added to urine with PSH added to buffer. The PSH added was one of five components resulting from the exchange reaction for PSH and CSSC.

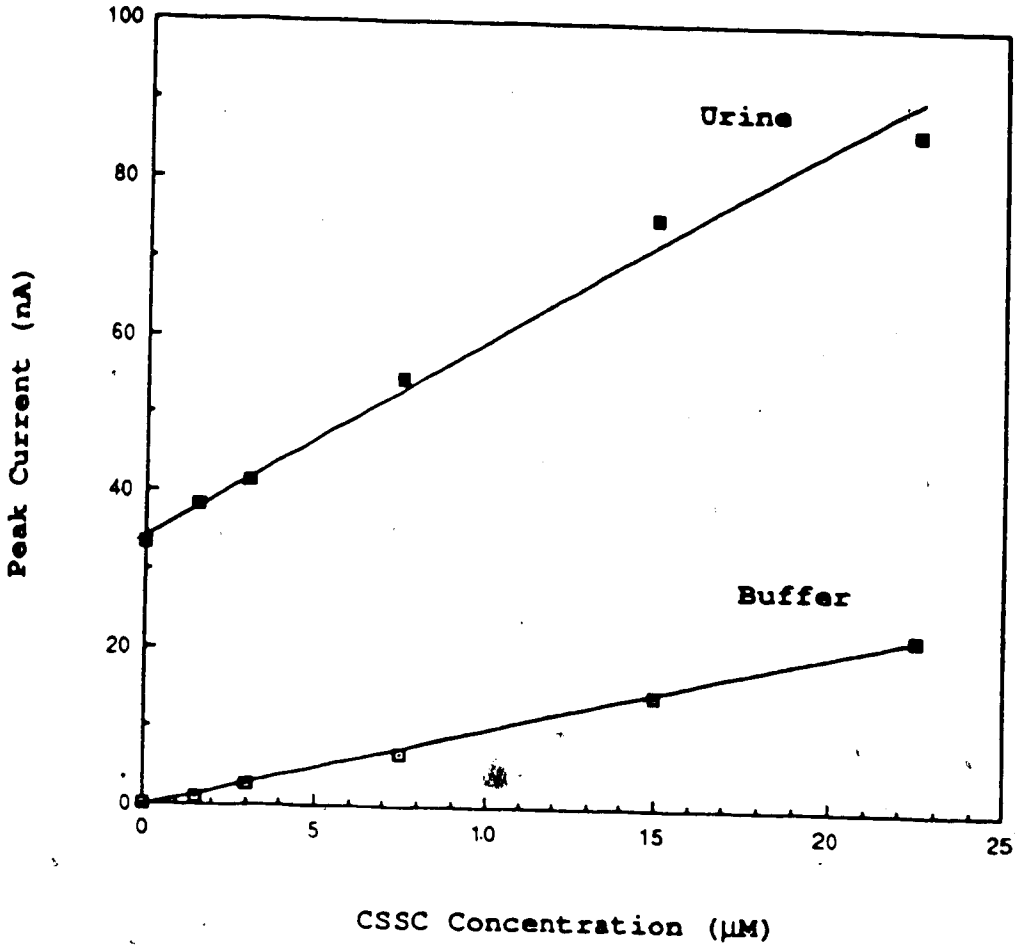

Figure 6.14. Comparison of calibration curves for CSSC mixed with urine to CSSC mixed with buffer. The non-zero intercept for the urine calibration curve is due to endogenous CSSC. The CSSC added was one of five components resulting from the exchange reaction for PSH and CSSC.

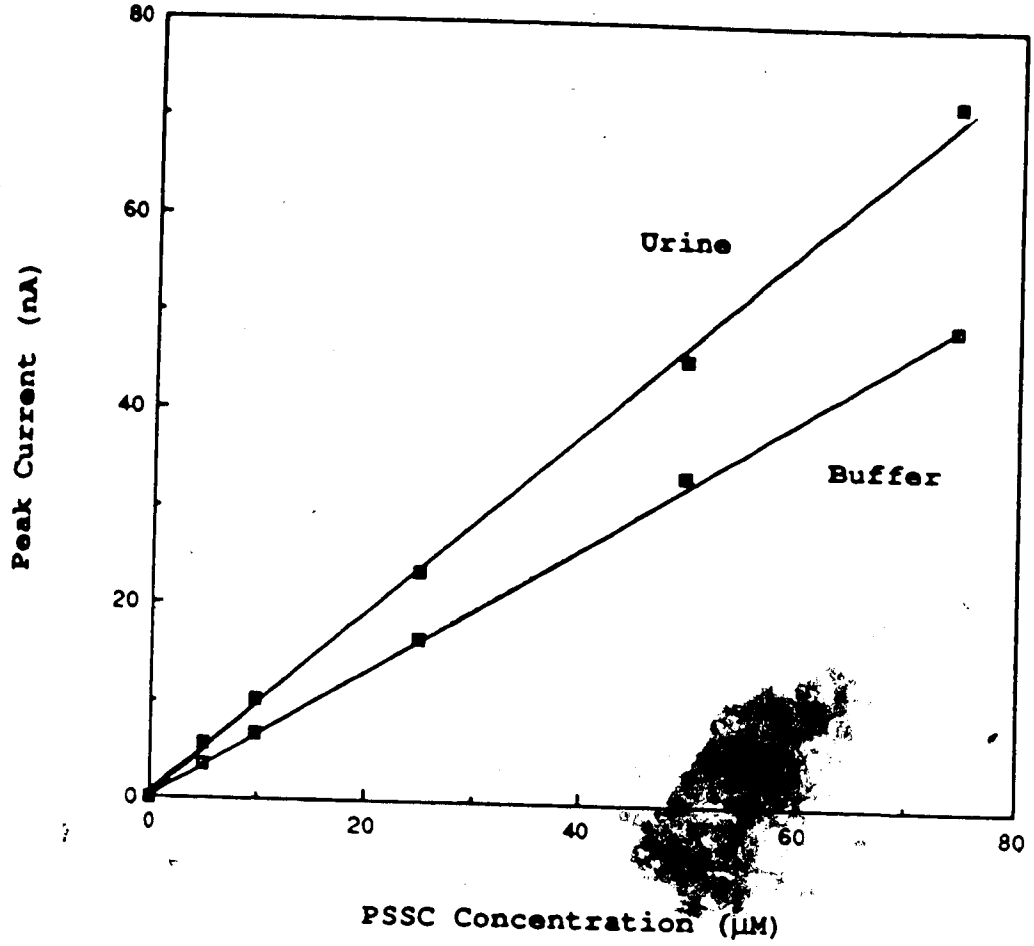

Figure 6.15. Comparison of calibration curves for PSSC added to urine with PSSC added to buffer. The PSSC added was one of five components resulting from the thiol-disulfide exchange reaction for PSH and CSSC.

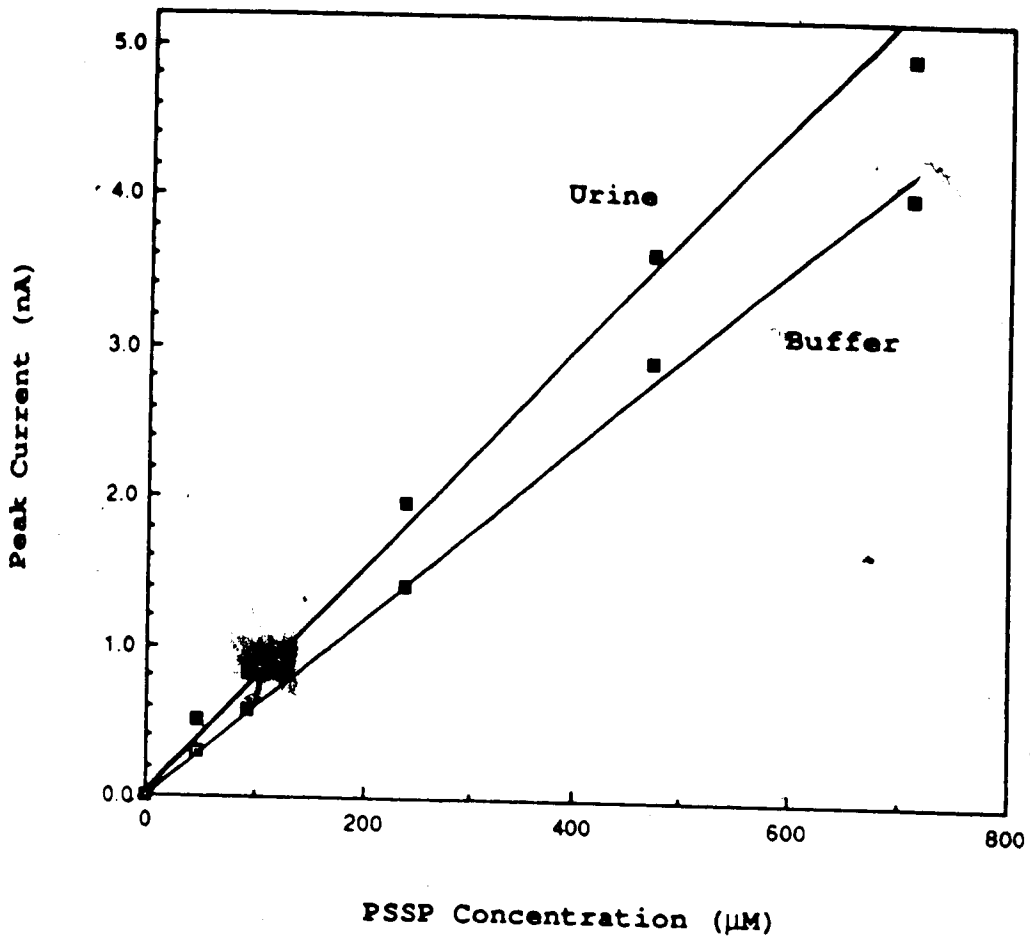

Figure 6.16. Comparison of calibration curves for PSSP standards prepared in urine with PSSP standards prepared in buffer. The PSSP added was one of five components resulting from the thiol-disulfide exchange reaction for PSH and CSSC.

urine is the increased baseline noise when analysing very low analyte concentrations.

E. Discussion

Although several chromatographic methods have been reported for thiol and disulfide analysis, only a few measure the various biological metabolites of the drug, penicillamine [42,50,53,131]. The HPLC-ED methods presented in this chapter provide quantitative determinations of this drug and its disulfide metabolites, PSSP and PSSH, in both urine and plasma matrices. Kang et al [42] measured penicillamine, homocysteine and their symmetrical and mixed disulfides as the carboxymethyl derivatives using an amino acid analyzer. Such measurements are time-consuming, and take several hours for a single chromatographic run. The average analysis time for samples containing homocysteine, homocystine, penicillamine, penicillamine disulfide, and the penicillamine-homocysteine mixed disulfide by HPLC-ED was only 16 minutes. By using calibration standards prepared in a matrix that is identical to the sample matrix, the results for HPLC-ED determinations were found to be quantitative as well as rapid.

Recently Sampson et al [131] have applied HPLC with electrochemical detection to the analysis of penicillamine and its penicillamine-cysteine mixed disulfide in urine

samples. Quantification of the urinary disulfides was performed by comparison with a single calibration standard. The authors reported that the calibrations of cystine and penicillamine-cysteine mixed disulfide were linear over the required assay concentration range and that this permitted quantitative comparison of sample signals to single calibration standards. No description of the composition of the standard was provided and no discussion on the possible problem of a matrix effect was addressed. In the work presented in this chapter calibration curves from standards prepared in buffer were linear but were not identical to the responses observed for standards prepared in plasma or urine. For the PSH/CSSC system in particular, each of the five compounds showed a difference in sensitivity for standards prepared in urine compared to standards made with buffer, even though all calibration curves were linear.

Comparisons of a sample signal to a single calibration standard reduces error that might arise from changes in the electrode sensitivity between the time a complete set of calibration standards are run and the analysis of the sample. However, the results of this study indicate that the possible influence of matrix conditions must be evaluated and an appropriate standard must be selected to ensure that the results will be quantitative and accurate.

CHAPTER VII

CONCLUSION

The primary objective of the research contained in this thesis has been the development of methodology for the determination of the therapeutic drug, penicillamine, and its disulfide metabolites in biological fluids. The diverse applications of penicillamine make it an important drug in medicine today. Its mode of action in the treatment of certain diseases, eg. Wilson's disease and cystinuria, is understood at the molecular level. However, little is known about its function in the treatment of rheumatoid arthritis or of its potential for the treatment of the Acquired Immune Deficiency Syndrome. As well, the adverse effects of the drug have not been fully characterised or understood. Part of this lack of knowledge stems from the absence of quantitative analytical methods for the determination of penicillamine and its metabolites at physiological levels in biological samples.

For some time it has been recognized that penicillamine can be metabolized by a thiol/disulfide exchange reaction to produce penicillamine mixed disulfides and/or the symmetrical penicillamine disulfide. Although the kinetics and equilibria of these reactions have been studied using ^{1}H

NMR, very few publications on the measurement of the metabolic disulfides in biological fluids have appeared. Previously, high performance liquid chromatography with electrochemical detection has been used for the analysis of several biologically significant thiols, including penicillamine. In this thesis, the method was extended to obtain direct electrochemical detection of the metabolic disulfides by the use of dual mercury-gold electrodes. The electrodes were used in the series configuration with the upstream electrode set at a potential of -1.100 volts vs. Ag/AgCl for the reduction of the disulfides while the downstream electrode was held at a potential of +0.150 volts vs Ag/AgCl for the detection of the thiols produced at the upstream electrode. The methods were developed for determining penicillamine and its major metabolites, together with endogenous thiols that would be present in biological specimens.

During the development of this methodology, the electrochemical behaviour of penicillamine, glutathione, cysteine, and homocysteine and their symmetrical disulfides at a dropping mercury electrode was investigated. As well, hydrodynamic voltammograms for penicillamine, glutathione, cysteine, and homocysteine and their symmetrical disulfides, and for penicillamine-cysteine, penicillamine-glutathione, and penicillamine-homocysteine mixed disulfides were

obtained using the dual mercury-gold electrochemical detector. No such information for the mixed disulfides has been reported before in the literature.

Methodology for the determination of penicillamine, glutathione, oxidized penicillamine, oxidized glutathione, and the penicillamine-glutathione mixed disulfide was presented in Chapter V. While obtaining calibration curves for glutathione and penicillamine, it was observed that although the curves were linear, there was a non-zero y-intercept which suggested that some of the thiol was not being detected at the downstream electrode. This was believed to be due to thiol adsorption onto the mercury of the upstream electrode. The problem was remedied by the addition of another SH-containing compound which would elute before the thiols of interest and be lost to the upstream electrode. Subsequent calibration curves for glutathione, penicillamine, oxidized glutathione, oxidized penicillamine and the penicillamine-glutathione mixed disulfide showed good linearity and had y-intercepts of zero.

Studies of the determination of penicillamine, glutathione, oxidized penicillamine, oxidized glutathione and penicillamine-glutathione mixed disulfide in blood plasma showed quantitative results for the glutathione-containing species, but the PSH recoveries were occasionally low while the PSSP recoveries were slightly high. Similar

results were obtained with the same mixture in urine, although the low recoveries appeared to depend on the concentration of penicillamine being analysed.

In the determination of penicillamine, homocysteine and their mixed and symmetrical disulfides described in Chapter VI, the matching of the matrix of the calibration standards to that of the sample medium was found to be a key factor for quantitative determinations. The recoveries of a mixture containing penicillamine, homocysteine, oxidized penicillamine, homocystine, and penicillamine-homocysteine mixed disulfide in urine and plasma samples were investigated. In these studies a high percent recovery for the symmetrical penicillamine disulfide was observed. Studies indicated that the increase in the electrode response was probably due to the matrix of the biological medium.

This assumption was further supported by the results of experiments performed with a set of calibration standards prepared in urine and in buffer which contained a mixture of oxidized and reduced penicillamine, cysteine, cystine, and the penicillamine-cysteine mixed disulfide. Each set of calibration standards was analysed by HPLC with electrochemical detection. For each component, larger slopes were observed for the calibration curves from standards prepared in urine over the ones made with buffer.

These results were similar to the findings for the penicillamine/homocystine system and supports the theory that the matrix of the solutions affects the electrode response.

The results of Chapters V and VI demonstrate the versatility of the HPLC-ED system for the determination of penicillamine and its metabolic disulfides. The various mobile phase parameters that control the retention characteristics of the thiols and disulfides provide the means by which the necessary separations can be achieved. The dual electrochemical detectors permit quantitative measurement for the simultaneous determination of thiols and disulfides. The HPLC-ED method was rapid and sensitive for the determination of penicillamine and its metabolic disulfides in biological samples.

BIBLIOGRAPHY

1. W.H. Wollaston, Ann. Chim. 76, 21 (1810).
2. W. Friedmann, Beitr. chem. physiol. Path. 2, 433; 3,1(1902).
3. E. Baumann, Hoppe-Seyler's Z. Physiol. Chem. 8, 299 (1884).
4. M.K. Gaitonde, Biochem. J. 104, 627 (1967).
5. P.C. Jocelyn, Biochemistry of the SH Group, Academic Press, (1972) p.165.
6. P.C. Jocelyn, Glutathione. Biochemistry Society Symposia, No. 17, E.M. Crook (ed.), London & New York, Academic Press (1959) p.17.
7. E.C. Moore, P. Reichart and L. Thelander, J. Biol. Chem. 239, 3445 (1964).
8. E. Racker, J. Biol. Chem., 217, 867 (1955).
9. S. Nagai and S. Black, J. Biol. Chem., 243, 1942.
10. G.C. Mills, J. Biol. Chem., 229, 189 (1957).
11. L.F. Chasseaud, Drug Metab. Rev., 2, 185 (1973).
12. L.A. Stocken, Biochem. J., 41, 358 (1947).
13. H.A. Braun, L.M. Lusky and H.O. Calvery, J. Pharm. Exp. Ther., 87, (S) 119 (1946).
14. M.A. Ondetti, B. Rubin and D.W. Cushman, Science, 196, 441 (1977).

15. D.W. Cushman, H.S. Cheung, E.F. Sabo and M.A. Ondetti, Prog. Cardiovasc. Dieg. 21, 176 (1978).

16. D.W. Cushman, H.S. Cheung, E.F. Sabo and M.A. Ondetti, Biochemistry, 16, 5484 (1977).

17 W.H. Lyle, J. Rheum., Suppl. 7, 96, (1981).

18. D. Perrett, J. Rheum., Suppl. 7, 41, (1981).

19. W.R. Kukovetz, E. Beubler, F. Kreuzig, A.J. Moritz, G. Nirnberger, L Werner-Breitenecker, J. Rheum., 10:1, 90, (1981).

20 A. Schuna, M.A. Osman, R.B. Patel, P.G. Welling, W.R. Sunstrom, J. Rheum. 10:1, 95, (1981).

21 T. A. Medsger, Jr., Arth. and Rheum. 30:7, 832, (1987).

22. Multicentre Trial Group, Lancet 2, 257, (1973). PSH/RA.

23. R.A. Keith, D.M.Otterness, A.J. Kerremans and R.M. Weinshilboum, Drug. Metab. Dispos. 13(6), 669, (1985).

24. G.W. Rafter, Biochem. Biophys. Res. Comm. 126(2), 867, (1985).

25. L.S. decherck, J. Dequeker, L. Francx and M. Demedts, Arth. Rheum. 30(6), 643, (1987).

26. E. Munthe, E. Kass and E. Jellum, J.Rheum., Suppl. 7, 14, (1981).

27. E.M. Veys, H. Mielants, G. Verbruggen, Clin. Exp. Rheum. 5, 111, (1987).

28. S.T. Dawes, T.P. Sheeran, P.D. Fowler and M.F. Bradforth, Clin. Exp. Rheum. 5, 151, (1987).

29. J.M. Walshe, Q. J. Med 22, 483, (1953).

30. J.M. Walshe, Am. J. Med., 21, 487, (1956).

31. Ref. 5, p.344.

32. H.K.Sachs, L.A. Blanksma, E.F. Murray, Peditrics, 46, 389 (1970).

33. S. Selanders, K. Cramer and L. Hallberg, Br. J. Ind. Med., 23:282 (1966).

34. R.G. Peterson, B.H. Rumack, J. Pediatr., 91, 661 (1977).

35. J.C. Crawhall, E.F. Scowen and R.W.E. Watts, Br. Med. J., 1, 588 (1963).

36. J.C. Crawhall, D. Lecav[illegible]er and D. Ryan, Biopharm. Drug Dispos. 1, 73, (1979).

37. J.C. Crawhall, J. Rheum., Suppl. 7, 100, (1981).

38. J.C. Crawhall, J. Lietman, J.A. Schneider, Am. J. Med. 44, 330 (1968).

39. I.M. Kolthoff, W. Stricks and R.C. Kapoor, J.A.C.S., 77, 4733 (1955).

40. Ref. 5, p.166.

41. D.C. Cusworth and C.E. Dent, Biochem. J. 111, 1P, (1969).

42. S. Kang, P.W.K. Wong and K. Curley, Pediatr. Res. 16, 370, (1982).

43. M. Totani, S. Shimizu, H. Yamada, T. Murachi, Biochem. Soc. Trans. 14(6), 1172, (1986).

44. J.O. Miner, P.M. Brooks and D.J. Birkett, in Immunogenetics in Rheumatology:Musculoskeletal Disease and D-Penicillamine, R.L Dawkins, F.T. Christiansen and P.J. Zilko (ed.), Excerpta Medica, Amsterdam, Oxford-Princeton, 1982 p.282 chapt 8.2

45. Chem. Abs. 1986 vol 104:141803s, P. Chandra and P.S. Sarin, Arzneim-Forsch., 36(2), 184, (1986).

46. D.R. Lecavalier and J.C. Crawhall, J. Rheum., Suppl. 7, 20, (1981).

47. M.P. Brigham, W.H. Stein and S. Moore, J. Clin. Invest: 39, 1633, (1960).

48. G.W. Frimpter and A. Bass, J. Chromatog. 7, 427, (1962).

49. G.W. Frimpter, J. Clin. Invest. 42, 1956, (1963).

50. J.W. Purdie, R.A. Gravelle and D.E. Hanafi, J. Chromatog., 38, 346, (1968).

51. J.W. Purdie and D.E. Hanafi, J. Chromatog. 59, 181, (1971).

52. J.C. Crawhall, C.J. Thompson and K.H. Bradley, Anal. Biochem., 14, 405, (1966).

53. B. Fowler and A.J. Robins, J. Chromatogr., 72, 105, (1972).

54. E. Beutler, O. Duron, B.M. Kelly, J. Lab. Clin. Med., 61, 882 (1963).

55. F. Tietze, Anal. Biochem., 27, 502 (1969).

56. P.L. Wendell, Biochem. J., 117, 661, (1970).

57. J. Roberts and N.S. Agar, Clin. Chim. Acta, 34, 475 (1971).

58. D. Beales, R. Finch, A.E.M. McLean, M. Smith, I.D. Wilson, J.Chromatogr. 226, 498 (1981).

59. J. Nishiyama and T. Kuninori, Anal. Biochem. 138, 95, (1984).

60. E.P. Lankmayr, K.W. Budna and K. Müller, J. Chromatog. Biomed. Appl. 222, 249, (1981).

61. T. Toyo'oka and K. Imai, J. Chromatog., 282, 495, (1983).

62. K. Mopper and D. Delmas, Anal. Chem. 56, 2557, (1984).

63. D.A. Keller and D.B. Menzel, Anal. Biochem. 151, 418, (1985).

64. C.E. Werkhoven-Goewie, W.M.A. Niessen, U.A.Th. Brinkman and R.W. Frei, J. Chromatog. 203, 165, (1981).

65. J.O. Miners, I. Fearnley, K.J. Smith, D.J. Birkett P.M. Brooks and M. W. Whitehouse, J. Chromatogr. 275, 89, (1983).

66. D.L. Rabenstein and R. Saetre, Anal. Chem. 49, 1036 (1977).

67. D.L. Rabenstein and R. Saetre, Clin. Chem. 24, 1140, (1978).

68. R. Saetre and D.L.Rabenstein, Anal. Biochem. 90, 684, (1978).

69. R. Saetre and D.L. Rabenstein, Anal. Chem. 50, 276, (1978).

70. P.T. Kissinger, "Electrochemical Detectors" in Liquid Chromatography Detectors, T.M. Vickrey (ed.), Chromatographic Science Series vol. 23, Marcel Dekker Inc., New York, 1983.

71. Y. Imai, S. Ito and K Fujita, J. Chromatog. Biomed. Appl. 420, 404, (1987).

72. M.K. Halbert, R.P. Baldwin, J. Chromatog. Biomed. Appl. 345, 43, (1985).

73. L.A. Allison and R.E. Shoup, Anal. Chem., 55, 8, (1983).

74. A.F. Stein, R.L. Dills and C.D. Klaassen, J. Chrom. Biomed. Appl. 381, 259, (1986).

75. J.P. Richie, Jr., C.A. Lang, Anal. Biochem. 163, 9, (1987).

76. R.F. Bergstrom, D.R. Kay and G.Wagner, J. Chromatog. Biomed. Appl. 222, 445, (1981).

77. D. Dupuy and S. Szabo, J. Liq. Chrom. 10, 107, (1987).

78. S.M. Lunte and P.T. Kissinger, J. Chromatogr., 317, 579 (1984).

79. S.M. Lunte and P.T. Kissinger, J. Liq. Chromatog. 8(4), 691, (1985).

80. O.H. Drummer, N. Christophidis, J.D. Horowitz and W.J. Louis, J.Chromatog. Biomed. Appl. 374, 251, (1986).

81. E.G. Demaster, F.N. Shirota, B. Redfern, D.J.W. Goon and H.T. Nagasawa, J. Chromatogr. Biomed. Applic. 308, 83 (1984).

82. D. Perrett, S.R. Rudge, J. Chromatog. 294, 380, (1984).

83. R. Saetre and D.L. Rabenstein, Agri. Food Chem. 26, 982, (1978).

84. G.L. Newton, R. Dorian and R.C. Fahey, Anal. Biochem., 114, 383 (1987).

85. M. Johansson and D. Westerlund, J. Chromatog., 385, 343, (1987).

86. R. Eggli and R. Asper, Anal. Chim. Acta, 101, 253 (1978).

87. Ref. 5, Chapter 4.

88. D.L.Rabenstein and Y. Theriault, Can. J. Chem., 62, 1672 (1984).

89. C.Voegtlin, J.M. Johnson and S.M. Rosenthal, J. Biol. Chem., 93, 435 (1931).

90. L. Eldjarn and A. Pihl, J. Biol. Chem., 225, 499 (1957).

91. J.C. Ellory and J.D. Young (ed.) Red Cell Membranes - A Methodological Approach, Academic Press, London, (1982).

92. J.D. Young and J.C. Ellory, in Membrane Transport in Red Cells, J.C. Ellory and V.L Lew (ed.), Academic Press, London/New York (1977).

93. D.E. Leyden and R.H. Cox "Analytical Applications of NMR" in Chemical Analysis, vol.48, John Wiley and Sons, New York/London/Sydney/Toronto (1977) p.68.

94. Y. Theriault, B.V. Cheesman, A.P.Arnold, D.L. Rabenstein, Can. J. Chem., 62, 1312 (1984).

95. S. Biffar, V. Greely and D. Tibbetts, J. Chromatogr., 318, 404, (1985).

96. M.A. Raggi, V. Cavrini and A.M. Di Pietra, J. Pharm. Sci. 71(12), 1384, (1982).

97. W. Kemula, Roczz. Chem., 26, 281 (1952).

98. B. Drake, Acta Chim. Scand. 4, 554 (1950).

99. P.T. Kissinger, C.J. Refeshauge, R. Dreiling and R.N. Adams, Anal. Lett. 6, 465 (1973).

100. F. Kreuzig and J. Frank, J. Chromatog., 218, 615, (1981).

101. A.M. Krstulovic, H. Colin and G.A. Guiochon, in "Advances in Chromatography" Giddings, Grushka, Cazes, and Brown (ed.) vol. 24, Marcel Dekker Inc., New York, (1984) pp.

102. W.A. MacCrehan and R.A. Durst, Anal. Chem., 50, 2108 (1978).

103. R.E. Shoup, "Minireview: RSH/RSSR Applications using the Dual Hg/Au Amperometric Detector", Current Separations, BAS Press, West Lafayette. (1987).

104. W.A. MacCrehan, R.A. Durst and J.M. Bellama, Anal. Lett., 10, 1175 (1977).

105. Bioanalytical Systems LC-4B Amperometric Detector Manual, West Lafayette

106. I.M. Kolthoff and C. Barnum, J.A.C.S., 62, 3061,(1940).

107. W. Stricks and I.M. Kolthoff, J.A.C.S., 74, 4646 (1952).

108. I.M. Kolthoff and C. Barnum, J.A.C.S., 63, 520 (1941).

109. I.M.Kolthoff, W. Stricks and N. Tanaka, J.A.C.S., 77, 5211, (1955).

110. D.B. Dahl, L.W. Selberg and P.F. Lott, Biochem. J., 31, 135 (1985).

111. W. Stricks and I.M. Kolthoff, Anal. Chem., 25, 1050, (1940).

112. I.M. Kolthoff, W. Stricks and N. Tanaka, J.A.C.S., 77, 5215, (1955).

113. Ref. 5, p.3.

114. D.H. Spackman, W.H. Stein and S. Moore, Anal. Chem., 30, 1185 (1958).

115. S. Moore, D.H. Spackman, and W.H. Stein, Anal. Chem., 30, 1190 (1958).

116. L.R. Snyder and J.J. Kirkland, "Introduction to Modern Liquid Chromatography, 2nd ed., (1979), p.427.

117. E.L. Johnson and R. Stevenson,. "Basic Liquid Chromatography, Varian Associates Inc., Palo Alto, (1978) p.38.

118. Ref. 116, p.52.

119. R.W Ross, J. Pharm. Sci. 61, 1979 (1972).

120. D.L. Ball, W.E. Harris and H.W. Habgood, Separation Science, 2, 81 (1967).

121. J.J. Kirkland, Analyst, 99, 859 (1974).

122. C. Horvath, W. Melander, I. Molnar, J. Chromatogr. 125, 129, (1976).

123. B.L. Karger, J.R. Gant, A. Hartkopf, P.H. Weiner, J. Chromatogr. 128, 65 (1976).

124. "Care and Use of Partisil Columns for HPLC", Whatman, #111-10/80.

125. R.S. Reid and D.L. Rabenstein, Can. J. Chem., 59, 1505 (1981).

126. Y. Theriault, Ph.D. Thesis, University of Alberta, 1985, Table 7.

127. Ref 116, p.579.

128. G.D. Fasman, "Handbook of Biochemistry and Molecular Biology" 3rd ed. Proteins-Volume 1, CRC Press, Cleveland, 1976, p.155.

129. M.T.W. Hearn (ed.) "Ion-Pair Chromatography, Theory, and Biological and Pharmaceutical Applications, Marcel Dekker Inc., N[redacted]k/Basel, 1985.

130. E. Jellum and S. Skrede, in "Penicillamine Research in Rheumatoid Disease", E. Munthe (ed.), Fabritius and Sonner, Oslo (1976) pp.68-79.

131. D.C. Sampson, P.M. Stewart and J.W. Hammond, Biomed. Chromatogr., 1 (1), 21, 1986.

132. Ref 5, p.11.

133. M.W. Wolowyk, R. Guy, D.L. Rabenstein, and J.C. Ellory, P. West Pharmcol. Soc., 28, 327 (1985).

134. J.D. Young, M.W. Wolowyk, S.M. Jones, J.C. Ellory, Biochem. J., 216, 349 (1983).

135. Ref. 5, p.248.

136. Ref. 5, pp. 163-173.